The University of Nottingham

UNITED KINGDOM · CHINA · MALAYSIA

Optimisation of Microparticle Formulations for IL-4 Delivery for Macrophage Modulation in Spinal Cord Injury

Jasmine Z Stening, BSc (Hons)

Thesis submitted to The University of Nottingham for the degree of Doctor of Philosophy (PhD)

January 2020

This thesis is dedicated to Dr Theo Stening.

Abstract

Spinal cord injury currently lacks treatment capable of restoring limb function and sensation. Current strategies, using pharmaceuticals and physiotherapy, focus on alleviating the high inflammatory environment triggered as a result of injury. These often result in adverse side effects and no rehabilitation. The discovery of macrophage phenotypes and their roles in inflammation within spinal cord injury has provided a new target for treatment development. Understanding macrophage behaviour and the roles of their sub-phenotypes has suggested a method for controlling inflammation by modulation towards a pro-immunoregulatory subgroup using cytokine interleukin 4 (IL-4). The hypothesis was that sustained delivery of IL-4 could modulate macrophage phenotype and provide resolution in the context of inflammation in spinal cord injury.

The use of microparticles is widely reported as a drug delivery method for controlled and sustained release in pharmaceutical strategies. The ability to tailor the release of proteins from microparticles by changing their composition ensures a specific release pattern can be obtained for specific applications. Poly(lactic-co-glycolic acid) and various release modifiers such as polaxamers F127 or P188 and triblock co-polymer were used to tailor microparticle release in this project.

IL-4 was encapsulated following the tailoring of microparticle release using a model protein. These particles were used to treat two cell macrophage models, THP-1 cells and immortalised bone marrow derived macrophage cells. The effects of exogenous IL-4 delivery and microparticle IL-4 delivery on macrophage modulation were compared, the aim being to modulate towards a pro-immunoregulatory subgroup.

The use of different microparticle formulations to obtain a database of release profiles was explored in this work, in order to obtain controlled and sustained protein release. From the microparticle formulations tested, 20 % *w/v* total polymer 40 % *w/w* TB4 85:15 PLGA was chosen as the optimal formulation to result in sustained delivery of a model protein, and this was replicated using IL-4. Difficulties in characterising a dynamic macrophage population *in vitro* are also highlighted in this work. The exogenous modulation of macrophage cells to specific subgroups was examined and compared with the results of microparticle induced modulation. The main findings were that the treatment of macrophage cell models with IL-4-containing microparticles resulted in a reduction of proinflammatory cell markers in a similar manner to the treatment with exogenous IL-4. These results also demonstrated the release of active IL-4 from polymeric microparticles. It is hoped that this approach will lead to a therapy targeting the inflammatory environment in spinal cord and in doing so aid repair and regeneration.

Publications and Presentations

Publications in Peer-Reviewed Journals

Hodgkinson, T, **Stening, JZ**, White, LJ, Shakesheff, KM, Hoyland, JA, Richardson, SM. Microparticles for controlled GDF6 delivery to direct ASC-based nucleus pulposus regeneration. Journal of Tissue Engineering and Regenerative Medicine. 2019;(8):11406-1417.

Published Conference Abstracts

Stening, JZ, Rose, FRAJ, White, LJ. Optimisation of microparticle formulations for cytokine delivery for macrophage modulation in spinal cord injury. eCM Online Periodical, TCES Conference Abstracts. 2018(4):108.

Stening, JZ, Rose, FRAJ, White, LJ. Optimisation of microparticle formulations for cytokine delivery for macrophage modulation in spinal cord injury. eCM Periodical, TERMIS EU Abstracts. 2019(3): 534.

Conference Presentations

- Tissue and Cell Engineering Society 2017, Manchester, UK
- Future Investigators in Regenerative Medicine 2017, Girona, Spain
- UK and Ireland Controlled Release Society 2018, Belfast, UK
- Tissue and Cell Engineering Society 2018, Keele, UK
- Future Investigators in Regenerative Medicine 2018, Girona, Spain
- Centre for Biomolecular Science Symposium 2019, Nottingham, UK
- TERMIS 2019, Rhodes, Greece
- Tissue and Cell Engineering Society and UK Society for Biomaterials Joint Conference 2019, Nottingham, UK

Acknowledgements

I would like to begin by thanking my Grandpa, Dr Theo Stening, for being my inspiration and role model on this journey, and for always supporting and encouraging me throughout my years in education. Without his support I would not have completed this work and I am honoured to follow in his footsteps as the next Dr Stening. This thesis is dedicated to him.

I am grateful for the invaluable support and encouragement from my family and friends, especially my parents who have always been there for me but particularly throughout the ups and downs of this PhD. I don't know where I would be today without their unwavering support. I would particularly like to thank Lydia, Victoria, Mat, John and Lauren for encouraging me over the three years.

I would like to thank all the members of the Regenerative Medicine and Cellular Therapies group at the University of Nottingham who have helped and guided me through this project. I would particularly like to thank the members of Lisa White's group for their advice and moral support, and for putting up with my many breakdowns in the lab. A special acknowledgement for the International foundation for Research in Paraplegia, (Grant no. P155) and the University of Nottingham for funding this project.

A special thanks to Teresa Marshall, Ann Williams, Omar Qutachi, Marta Alvarez Paino, Hosam Abu Award, Vincenzo Taresco, Lia Blokpoel Ferreras and Mathew Hollingworth for training and advice on techniques and methods. I am grateful to Dr Andrew Bennett for the provision of iBMDM cells, and Dr Omar Qutachi and Dr I-Ning Lee for manufacture of triblock polymers.

Table of Contents

List of Figures

Figure 3.2: Schematic showing the structure of **(A)** Lysozyme made up of 147 amino acids folded into alpha helices and beta pleated sheets with mass of 16,239Da; and **(B)** IL-4 made up of 153 amino acids folded into alpha helices and beta pleated sheets with mass of 17,492 Da.

Figure 3.3: Morphology (left hand column) and size distributions (right hand column) from 20 % *w/v* total polymer microparticles from 50:50 PLGA with different percentages of F127 containing water or HSA:lysozyme.

Figure 3.4: Morphology and size distribution from 20 % *w/v* total polymer microparticles from 85:15 PLGA with different percentages of F127 containing water or HSA:lysozyme.

Figure 3.5: Morphology and size distribution from 20 % *w/v* total polymer microparticles from 50:50 PLGA with different percentages of P188 containing water or HSA:lysozyme.

Figure 3.6: Morphology and size distribution from 20 % *w/v* total polymer microparticles from 85:15 PLGA with different percentages of P188 containing water or HSA:lysozyme.

Figure 3.7*:* Cumulative protein release (μg/mg particles) from microparticles fabricated from PLGA and release modifiers F127 (A, B) and P188 (C, D) where coloured symbols are consistent for proportion of modifier included.

Figure 4.1: Morphology and size distribution of particles formed from 50:50 PLGA with different percentages of total polymer, containing water only.

Figure 7.3: Morphology and size distribution of 20 % *w/v* total polymer particles formed from 50:50 PLGA with different percentages of P188, blank and containing HSA:lysozyme.

Figure 7.4: Morphology and size distribution of 20 % *w/v* total polymer particles formed from 85:15 PLGA with different percentages of P188, blank and containing HSA:lysozyme.

Figure 7.5: Cumulative percentage protein release (%) from 20 % *w/v* total polymer particles from 50:50 or 85:15 PLGA with different percentages of F127 or P188.

Figure 7.6: Nuclear magnetic resonance spectrum for in-house made release modifiers: TB1, TB2, TB3, TB4 and DB1.

Figure 7.7: Morphology and size distribution of 50:50 PLGA microparticles with different total polymer and TB percentage containing water or HSA:lysozyme.

Figure 7.8: Cumulative percentage protein release (%) from different total polymer percentage particles from 50:50 or 85:15 PLGA with different percentages of TB2.

Figure 7.9: Morphology and size distribution of 20 % *w/v* total polymer particles from 50:50 PLGA with different percentages of TB1 containing water or HSA:lysosyme.

Figure 7.10: Morphology and size distribution of 20 % *w/v* total polymer particles from 85:15 PLGA with different percentages of TB1 containing water or HSA:lysozyme.

List of Tables

85:15 PLGA with different percentages of TB1. **(iv)** 20 % *w/v* total polymer percentage 50:50 and 85:15 with different percentages of TB4.

Table 4.6: Combined daily protein release (μg/mg particles) for 20 % *w/v* total polymer with 85:15 40 % *w/w* TB4 comparison between HSA:Lysozyme and HSA:IL-4 loaded particles.

Table 4.7: Estimated IL-4 release based on daily total release from BCA assay in comparison to actual IL-4 per day calculated using IL-4 ELISA for 7 days.

Table 5.1: Exogenous IL-4 treatment concentrations used for $M_{(IL-4)}$ exogenous reference based on BCA assay results

List of Abbreviations

BCA	Bicinchoninic acid
BHT	Butylated hydroxytoluene
bmMSC	Bone-marrow derived mesenchymal stem cells
CSF	Cerebrospinal fluid
Da	Daltons
DB-P	PLGA-PEG diblock synthesised from polymers
$dCDCl_3$	Deuterated chloroform
DCM	Dichloromethane
DMSO	Dimethyl sulfoxide
DNA	Deoxyribonucleic acid
DPSC	Dental pulp stem cells
ECM	Extracellular matrix
EDTA	Ethylenediaminetetraacetic acid
ELISA	Enzyme-linked immunosorbent assay
FBS	Fetal bovine serum
FDA	Food and Drug Administration
F127	Poloxamer F127
g	gram
GFAP	Glial fibrillary acidic protein
GM-CSF	Granulocyte-macrophage colony-stimulating factor
GNDF	Glial cell line derived neurotrophic growth factor
GPC	Gas permeation chromatography
HEPES	(4-(2-hydroxyethyl)-1-piperazineethanesulfonic acid)
HSA	Human serum albumin
iBMDM	Immortalised bone-marrow derived macrophage

IFN	Interferon
IL-1ra	Interleukin 1 receptor antagonist
IL-4	Interleukin-4
IL-10	Interleukin-10
IL-13	Interleukin-13
iPSCs	Induced pluripotent stem cells
IV	Intravenous
L	Litre
LPS	Lipopolysaccharides
LxA4	Lipoxin A4
M	Molar
M-CSF	Macrophage colony-stimulating factor
ml	millilitre
mg	milligram
MSCs	Mesenchymal stem cells
MW	Molecular weight
NaOH	Sodium hydroxide
nM	nanoMolar
NMR	Nuclear magnetic resonance
NSAIDs	Non-steroidal anti-inflammatory drugs
NSCs	Neural stem cells
NSPCs	Neural stem progenitor cells
PBS	Phosphate buffer saline
PEG	Polyethylene glycol
PEO	Polyethylene oxide
PLGA	Poly(lactic-co-glycolic acid)
PMA	Phorbol myristate acetate

PPO	Polypropylene oxide
PVA	Polyvinal alcohol
P188	Poloxamer 188
RNA	Ribonucleic acid
RPM	Revolutions per minute
RPMI	Roswell Park Memorial Institute
RSA	Rat serum albumin
RT	Reverse transcriptase
RvD1	Resolvin
SCAP	Stem cells form the apical papilla
SCI	Spinal cord injury
SD	Standard deviation
SDS	Sodium dodecyl sulphate
SEM	Scanning electron microscope
SHED	Stem cells from human exfoliated deciduous teeth
TEA	Triethanolamine
TB-M	PLGA-PEG-PLGA triblock synthesised from monomers
TB-P	PLGA-PEG-PLGA triblock synthesised from polymers
THF	Tetrahydrofuran
Th1	T helper 1 cells of the adaptive immune system
Th2	T helper 2 cells of the adaptive immune system
TMB	Tetramethylbenzidine
TMS	Tetramethylsilane
qPCR	Quantitative polymerase chain reaction
µl	microlitre
µg	microgram
µm	micrometer

v/v	Volume by volume
w/w	Weight by weight
w/v	Weight by volume

Chapter 1: Introduction

1.1 Spinal Cord Injury

1.1.1 ***Causes***

The main application for this project was in spinal cord injury (SCI), a detrimental and devastating condition, with many causes resulting in central nervous system damage and a prolific immune response at the site of injury. SCI has a high morbidity and mortality rate (Shende and Subedi, 2017) and can lead to loss of motor and sensory capabilities in individuals of all ages. There are multiple causes of SCI including motor accidents, combat, sport, and falls as summarised in Figure 1.1. Injuries as a result of an accident or fall are referred to as 'traumatic' whereas injury as a result of disease or infection are referred to as 'non-traumatic' (NHS and Board, 2013). The causes of SCI can be categorised into four main groups: (i) compression injury, (ii) contusion injury, (iii) laceration injury and (iv) solid core lesions (McCreedy and Sakiyama-Elbert, 2012; Silva *et al.*, 2014; Tuladhar *et al.*, 2015; Führmann, Anandakumaran and Shoichet, 2017). Alongside other causes, motor accidents have remained the leading cause for SCI for the past four decades accounting for nearly half of all cases (McCreedy and Sakiyama-Elbert, 2012; Silva *et al.*, 2014; Tuladhar *et al.*, 2015).

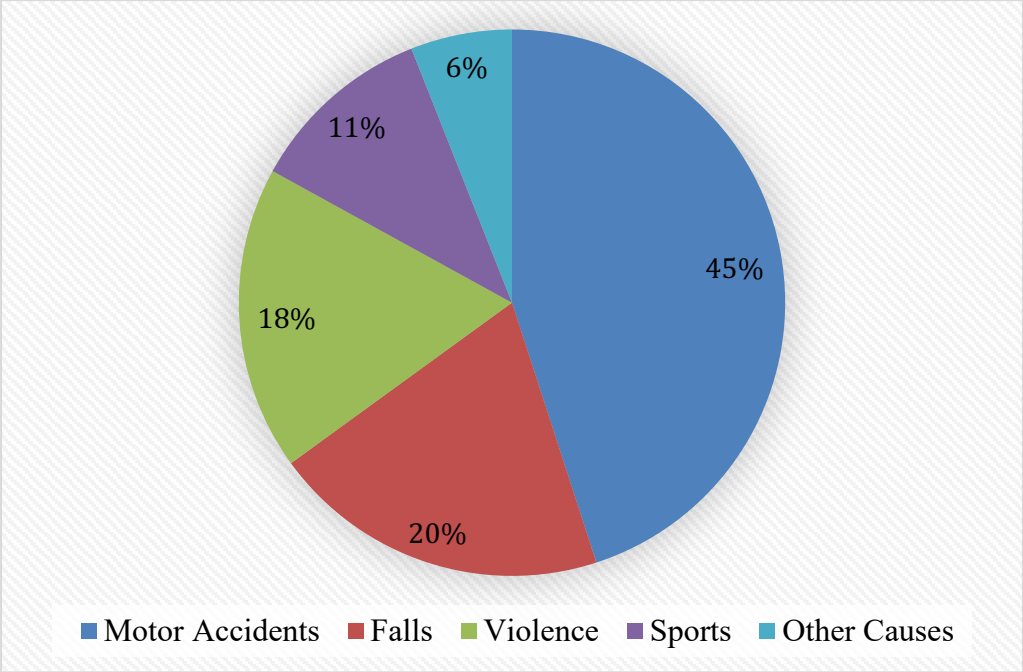

Figure 1.1: Schematic of SCI causes worldwide. (Adapted from Branco *et al.,* 2007).

All forms of spinal cord injury ultimately result in dysfunctions related to inadequate replacement of cells and nerve axonal connections by the central nervous system (CNS) and glial scarring (Wang *et al.*, 2014a; Hilton *et al.,* 2016a; Führmann *et al.*, 2017). The full extent of locomotive or sensory deficits as a result of SCI depends on the level, type and extent of the injury, although most patients suffer lifelong disabilities (Mothe and Tator, 2012; Tuladhar *et al.*, 2015). SCI can be classified as acute (within several days of injury), subacute (one- or two-weeks post-injury) or chronic (four or more weeks post-injury). Recovery has been shown to be more promising when treated in the subacute stage (Mothe and Tator, 2012). It is thought that this is due to the well-known limited capacity of the CNS for self-repair in comparison to injuries elsewhere (Mothe and Tator, 2012; Tuladhar *et al.*, 2015). Despite the spinal cord being

responsible for transfer of information to and from the brain, the impact of SCI is not limited to neurological deficits and can also affect function of other organs such as the bladder, kidneys, and have a detrimental impact on the entire body (Silva *et al.*, 2014).

1.1.2 ***Epidemiology of spinal cord injury***

With no current cure for SCI, it is important to consider the epidemiology of the disease (Ning *et al.*, 2011). SCI is not restricted to a certain age or people demographic. However, certain age groups and professions have a higher risk of SCI, for example the elderly or combat soldiers. In 2009, Baumann *et al* reported 11,000 new cases of SCI annually in the United States (Baumann *et al.*, 2009) and in 2012 Mothe and Tator reported 12,000 new cases per year (Mothe and Tator, 2012). The global incidence in 2017 was stated to be 40 - 80 persons in one million (Shende and Subedi, 2017) with increasing incidence due to non-traumatic causes. Survival in the case of SCI depends on the extent of the injury but can range from 10 – 28 years with the more severe paraplegia cases having lower survival rates compared to incomplete paraplegia or small spinal lesions (Kurtzke, 1977). It is suggested that males are affected five times as often as females, with 80 % of incidence occurring in males (Shende and Subedi, 2017) and with maximal ages at risk between 15 and 34. However, there is also a second age peak for SCI incidence in older adults mainly as a result of falls (Kurtzke, 1977; Mothe and Tator, 2012). According to Shende and Subedi, the age for peak incidence increased from 29 years in the 1970s to 42 years in 2017 (Shende and Subedi, 2017). This may be attributed to the average life

expectancy increasing. However the hospital stay time decreased from 24 days to 11 over this time frame (Shende and Subedi, 2017).

1.1.3 ***Pathophysiology of spinal cord injury***

In order to understand the pathophysiology of SCI it is important to understand the anatomical and physiological aspects of the bundle of tissues that make up the cord. The spinal cord consists of both grey and white matter in a similar manner to the brain (Tuladhar *et al.*, 2015). The grey matter contains glial cell bodies including astrocytes and non-myelinating oligodendrocytes, motor neurons, interneurons and non-myelinated axons (Tuladhar *et al.*, 2015). In contrast, the surrounding white matter contained myelinated axons and glial cell projections but no cell bodies (Tuladhar *et al.*, 2015). As shown in Figure 1.2.

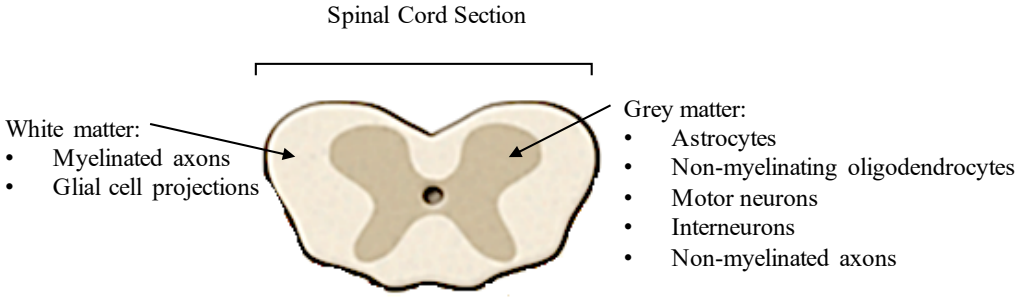

Figure 1.2 : A schematic to show the anatomical bundle of cells and tissues making up the spinal cord (Tuladhar *et al.*, 2015).

SCI can be separated into two physical phases: the primary phase consisting of the initial impact, and secondary phase consisting of cascade cellular responses (Shende and Subedi, 2017). The physical mechanisms involved in the initial trauma include laceration, acute stretching and sudden acceleration-deceleration injuries (Baptiste and Fehlings, 2006). Due to the physical injury in the primary phase there are repercussive effects on upper and lower motor neurons extending away from the injury site affecting respiration, cardiac outputs, vascular tones and sensory functions (Shende and Subedi, 2017). The initial trauma in the primary phase of injury causes axon shearing, blood vessel rupture and cell death mainly affecting the spinal cord white matter (Sadler, 2011; McCreedy and Sakiyama-Elbert, 2012; Mothe and Tator, 2012; Tuladhar *et al.*, 2015; Hilton *et al.*, 2016b; Viswanath *et al.*, 2017).

The secondary phase of SCI, occurring in the hours to days after injury, is characterised by an immune response. This spreads from the injury site with glial scar formation in combination with bleeding, apoptosis, excitotoxicity, ischemia and free radical production (Beck *et al.*, 2010; Wang *et al.*, 2014). These can all ultimately result in cell death and can also cause further damage to the surrounding cells and tissues. Although all of these effects lead to further demyelination of remaining axons in the white matter, interpreting the exact impacts are difficult due to the enzymatic and biochemical cascades initiated as part of injury (Popovich *et al.*, 2002; Mothe and Tator, 2012; Wang *et al.*, 2014a; Silva *et al.*, 2014; Dumont *et al*, 2015; Tuladhar *et al.*, 2015; Hilton *et al*, 2016b; Führmann *et al.*, 2017; Shende and Subedi, 2017a, 2017b; Viswanath *et al.*, 2017). Arguably it is the inflammation which causes SCI to become a chronic

injury, due to the ongoing cascades of proinflammatory factors and lack of inflammatory resolution. This secondary phase leads can last from weeks to years' post-injury, preventing healing and becoming more debilitating on the patient (Shende and Subedi, 2017). A summary of SCI pathophysiology and primary and secondary phase mechanisms are displayed in Figure 1.3 and Figure 1.4.

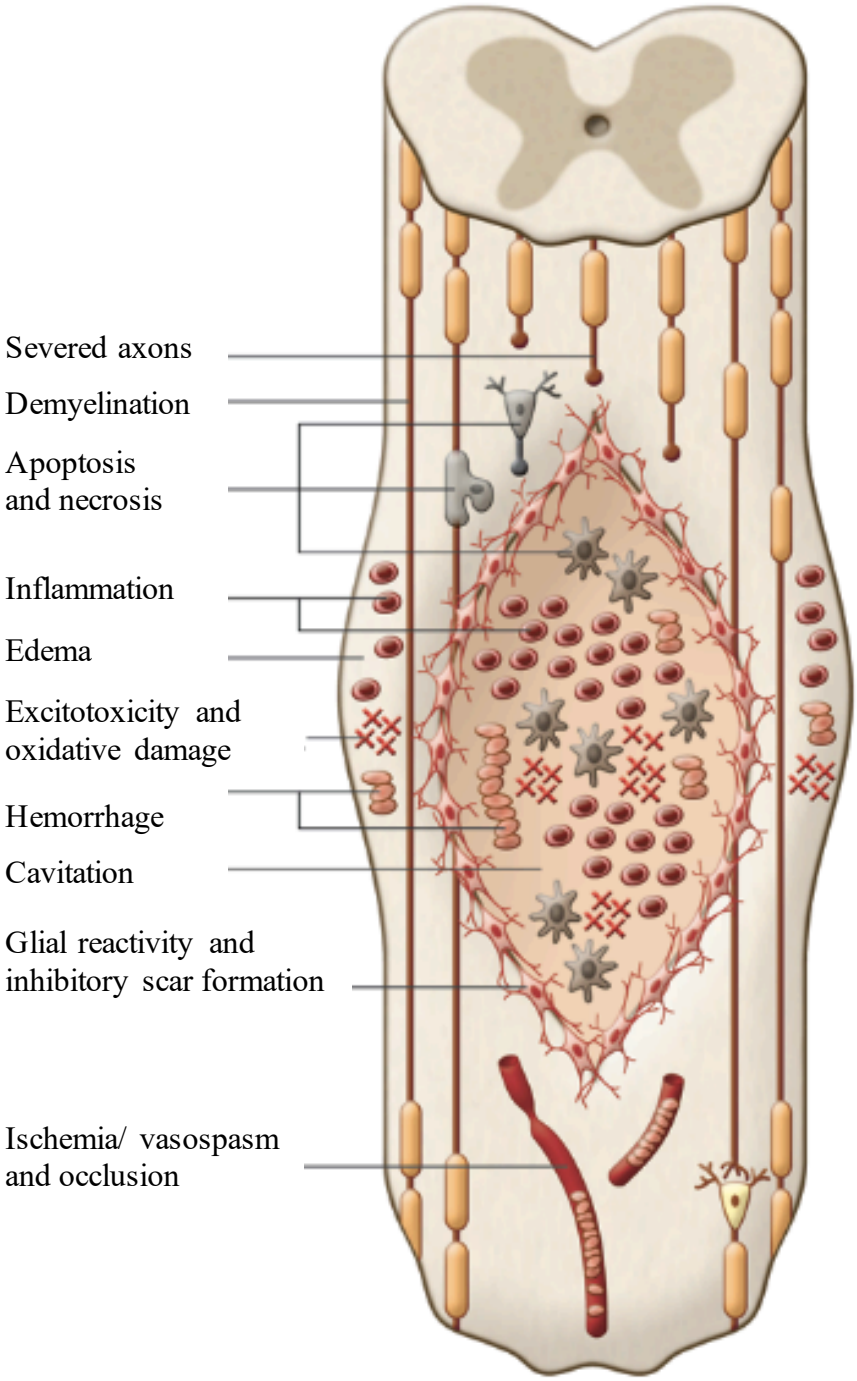

Figure 1.3: Schematic displaying the pathophysiology of SCI. The diagram shows the physiology of primary and secondary SCI including edema, haemorrhage, inflammation, apoptosis, necrosis, excitotoxicity, lipid peroxidation, electrolyte imbalance, ischemia/vasospasm and blood vessel occlusion (Reproduced from Mothe and Tator, 2012).

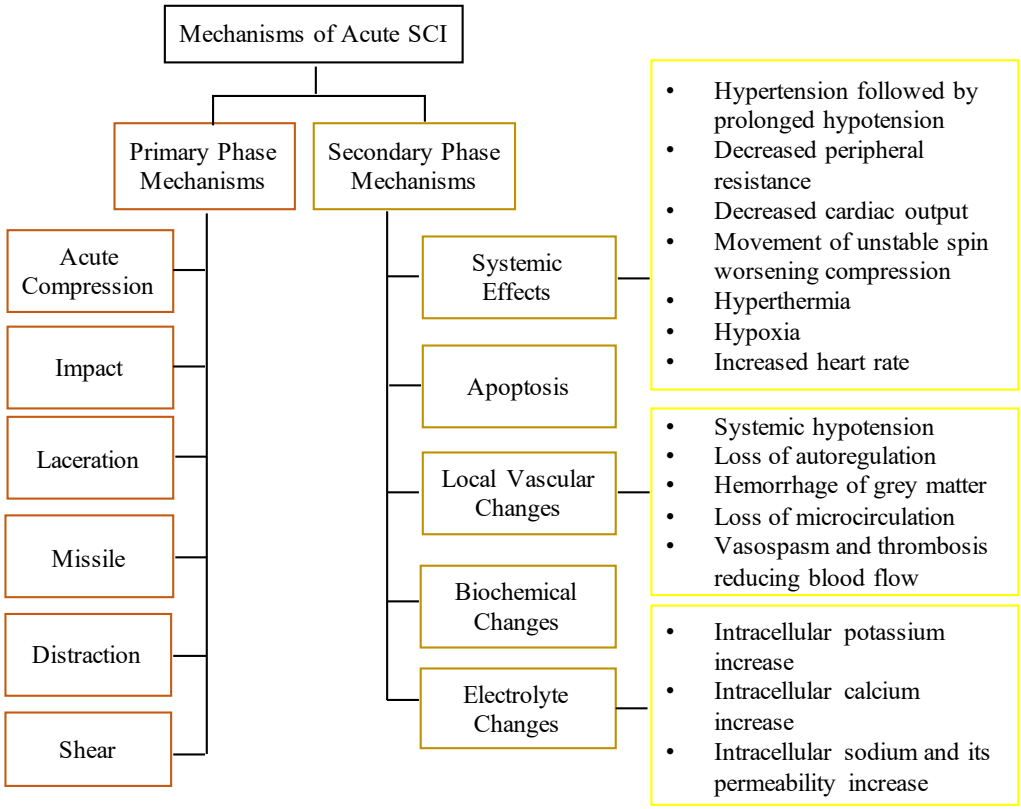

Figure 1.4: Schematic showing the effects of primary and secondary phase mechanisms in acute SCI (Adapted from Shende and Subedi, 2017a).

1.1.4 Cellular response to SCI

One result of traumatic SCI is the dynamic and diverse cellular response both to primary and secondary stages of injury. Recent developments have shown that the cellular response to SCI can be detrimental to recovery (Plemel *et al*, 2014; Silva *et al.*, 2014; Shende and Subedi, 2017b) and needs to be taken into consideration in the design of new treatments. Examination of the secondary phase of SCI has suggested that damage is propagated by high levels of proinflammatory cytokines as well as reactive oxygen species (Hilton *et al*,

2016b). Cytokines such as TNFα, IL-1β, iNOS, IL-12, IL-23 and IL-6 have all been shown to cause further inflammatory responses (Sierra-Filardi *et al.*, 2011; Bao *et al.*, 2018). Recent developments have shown that the highly inflammatory environment around spinal cord injury sites following trauma is detrimental to recovery (Plemel *et al*, 2014; Silva *et al.*, 2014; Shende and Subedi, 2017b).

An influx of neutophils is the first immune cell response to injury along with leukocytes and macrophages which are able to penetrate the CNS at the damaged site (Tuladhar *et al.*, 2015). It is here that the immune cells act to remove debris caused by the accident, either foreign bodies, dead or damaged cells (Tuladhar *et al.*, 2015). This process is essential for removal of any infection causing debris which may cause further damage. However, the immune response cells produce neurotoxic enzymes and free radicals as part of this process, causing further cell death and demyelination (Miron, 2013; Tuladhar *et al.*, 2015). Resident microglia in the spinal cord are also activated as a result of injury and act to protect surrounding tissue by formation of a glial scar for isolation of the injury site. This unfortunately provides a chemical and physical barrier to regeneration and is partly responsible for the lack of spinal cord self-repair (Tuladhar *et al.*, 2015). Discovery of multiple macrophage subgroups such as proinflammatory and immunoregulatory has enabled the SCI immune response to be studied more extensively and further the understanding of the role of inflammation in SCI (Barros *et al.*, 2013; Miron, 2013; Das *et al.*, 2015; Chistiakov *et al.*, 2017).

1.2 The Role of Macrophages in Spinal Cord Injury

1.2.1 General macrophage overview

Macrophages exist within the blood stream as circulating macrophages able to be recruited to various tissues depending on biochemical signals, or as tissue resident macrophages which remain at the site only activate when required. Macrophages are active cells of the immune system with many roles depending on the physiological scenario including tissue destructive roles versus reconstructive, immunostimulatory roles versus immunosuppressive, and proinflammatory roles versus immunoregulatory (Duluc *et al.*, 2007; Alvarez *et al.*, 2016).

Macrophages originate from bone marrow progenitor cells as monocytes and either enter circulation to form macrophages or infiltrate into tissues to become resident macrophages (Das *et al.*, 2015). Circulating monocytes are recruited to the injury site by pro-inflammatory cytokines, for example tumour necrosis factor (TNFα) and interleukin 1 (IL-1), where they differentiate into macrophages (Alvarez *et al.*, 2016). Once differentiated these cells become key mediators of inflammation and removal of foreign bodies though the means of phagocytosis, macrophages also regulate other cell types important in tissue healing such as fibroblasts, osteoblasts, endothelial cells and keratinocytes (Das *et al.*, 2015; Alvarez *et al.*, 2016). Some of these tissue specific macrophage functions are summarised in Table 1.1.

Table 1.1: A summary of the various tissue specific functions of macrophages *in vivo* (Adapted from Das *et al.*, 2015).

Tissue/ Organ	Cell Type	Functions
Wound	Wound Macrophage	Scavenging, phagocytosis, efferocytosis, antigen presentation, promotion of repair, extracellular signalling and angiogenesis
Central Nervous System (CNS)	Microglial Cells	Scavenging, phagocytosis, cytotoxicity, antigen presenting, synaptic stripping, promotion of repair and extracellular signalling
Lungs	Alveolar Macrophages	Efferocytosis, phagocytosis, surfactant homeostasis
Connective Tissue	Histiocytes	Phagocytosis and antigen presentation
Liver	Kupffer Cells	Endocytic activity against blood-borne materials and host defence
Bone	Osteoclasts	Bone resorption

A correctly regulated macrophage response to injury is crucial in preventing infection by the clearing of dead tissues and cells via phagocytosis, and regulating formation and repair of new tissues (Spiller and Koh, 2017). This is an integral role undertaken by all macrophage cells from wound macrophages

to osteoclasts as indicated in Table 1.1. These functions are integral to maintain tissue and organ health and prevent damage. Dysregulation of macrophage activity can be a prominent factor in chronic tissue degeneration post-injury (Spiller and Koh, 2017) and this is evident in the case of SCI.

A population of pro-inflammatory macrophages, referred to broadly as M1 henceforth, has been suggested to increase inflammation through release of pro-inflammatory cytokines which are elevated in SCI (day 1-5) (Schwartz, 2010; Antonios *et al.*, 2013; Guo *et al.*, 2013; Minardi *et al.*, 2016). These M1 macrophages play an important role in the removal of debris after injury, and also encourage immune system attack on foreign organisms by cell dysfunction or apoptosis (Meda *et al.*, 1995; Popovich *et al.*, 1999, 2002; Majed, 2006; Letellier *et al.*, 2010; Murray *et al.*, 2014; Chistiakov *et al.*, 2017). The M1 population can be characterised by production of high levels of IL-12, IL-13, IL-1β, TNF-α and IL-6, all of which contribute to inflammation (Antonios *et al.*, 2013; Chanput *et al.*, 2013; Galdiero and Mantovani, 2015; Chistiakov *et al.*, 2017). M1 macrophages are also thought to be potent killers of microorganisms and tumour cells (Duluc *et al.*, 2007; Schwartz, 2010; Antonios *et al.*, 2013; Guo *et al.*, 2013; Minardi *et al.*, 2016). The presence of a large unresolved M1 population after initial injury creates an unsuitable environment for cell repair, cause further damage and can be detrimental to recovery (Meda *et al.*, 1995; Popovich *et al.*, 1999, 2002; Majed, 2006; Shechter *et al.*, 2009; Letellier *et al.*, 2010; Miron, 2013; Murray *et al.*, 2014). The functions and characteristic cytokines for M1 macrophages are summarised in Table 1.2.

Table 1.2: A summary of the characteristic cytokines and cell functions associated with specific macrophage subpopulations.

Cell Subpopulation	Characteristic Cytokines	Main Cellular Functions
M1	IL-12, IL-13, IL-1β, TNF-α, IL-6	Remove debris Attack foreign organisms
M2	IL-4, IL-10, Il-13, IL-33, activin a	Reduce inflammation Initiate Th2 response

A population of pro-immunoregulatory macrophages, referred to as M2 henceforth, has been shown to have regenerative roles and activate a T helper 2 (Th2) response (Barros *et al.*, 2013; Chanput *et al.*, 2013; Miron, 2013; Murray *et al.*, 2014; Chistiakov *et al.*, 2017; Park *et al.*, 2017). These M2 are characterised by down regulation of pro-inflammatory cytokine production and up regulation of IL-10 production. These are shown to reduce inflammation and trigger the Th2 response (Meda *et al.*, 1995; Popovich *et al.*, 1999, 2002; Majed, 2006; Nair *et al.*, 2006; Letellier *et al.*, 2010; Antonios *et al.*, 2013; Yang *et al.*, 2013; Galdiero and Mantovani, 2015; Chistiakov *et al.*, 2017). The M2 subgroup can be further divided into at least three groups, M2a, M2b and M2c, induced by IL-4/ IL-13, TLR agonists, and IL-10 respectively (Wolf *et al.*, 2014; Soldano *et al.*, 2016; Park *et al.*, 2017). Various growth factors have roles in macrophage modulation, particularly IL-4, IL-10, IL-13, IL-33, and Activin A (Bomstein *et al.*, 2003; Schwartz *et al.*, 2006; Qin, 2012; Yang *et al.*, 2013; Galdiero and

Mantovani, 2015; Molina *et al.*, 2015; Minardi *et al.*, 2016; Soldano *et al.*, 2016; Chistiakov *et al.*, 2017). It has been suggested that M1 macrophages could be modulated towards an M2 phenotype using growth factors to provide a more suitable regenerative environment (Martinez and Gordon, 2014).

1.2.2 Pro-inflammatory and pro-immunoregulatory macrophage phenotypes in SCI

The discovery of multiple macrophage subgroups such as pro-inflammatory and pro-immunoregulatory has encouraged a different outlook on the study of the SCI immune response (Popovich *et al.*, 1999; Duluc *et al.*, 2007; Barros *et al.*, 2013; Miron, 2013; Alvarez *et al.*, 2016). The current understanding is that macrophage resolution exists as a spectrum between two extreme phenotypes of M1 and M2 (Alvarez *et al.*, 2016). M2 macrophages express different genes to those by M1 with up-regulation of Arginase 1 (Arg-1) and IL-10, and down-regulation of IL-6, TNF-α and nitric oxide synthase (iNOS) (Das *et al.*, 2015). An overview of macrophage polarisation and the time scale over which polarisation occurs is shown in Figure 1.5.

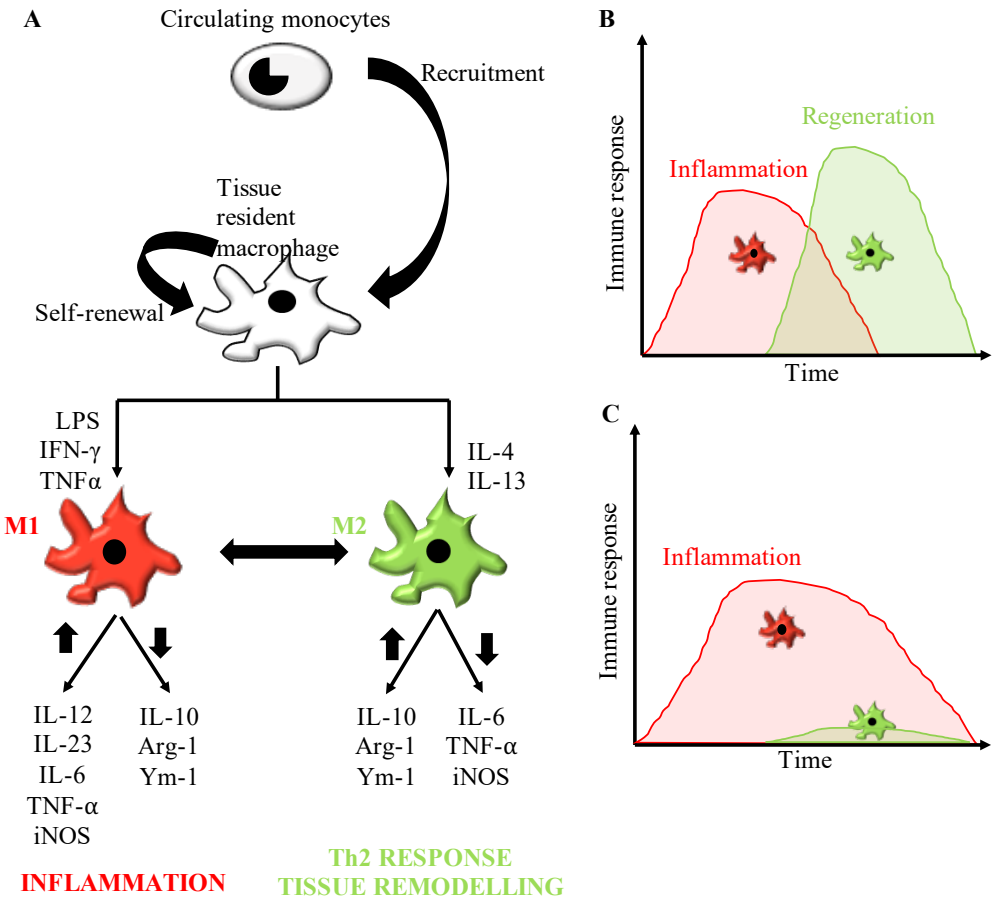

Figure 1.5: (A) A schematic showing the journey from circulating monocyte to macrophage phenotype according to most prevalent nomenclature. **(B)** The time scale over which macrophage phenotype ratio switches from M1 dominated to M2 dominated and the resulting immune response in injuries where inflammation is resolved. **(C)** The macrophage phenotype ratio of M1 to M2 and the resulting immune response in spinal cord injuries. (Adapted from Das *et al.*, 2015; Alvarez *et al.*, 2016).

As shown in Figure 1.5 (B) for most injuries the population of macrophages present changes over time with an initial population of M1 giving way to an M2

population. The natural injury healing process for general injuries consists of four phases characterised by a 3-5 day lag followed by; haemostasis, inflammation, proliferation and remodelling (Kotwal and Chien, 2017). This system ensures that any foreign organisms or debris are removed by the M1 macrophages first before promotion of repair and regeneration by M2 macrophages which in turn reduces the inflammatory environment. However, in SCI this switch does not occur (Figure 1.5 (C) and a large unresolved M1 population remain after initial injury. This creates an unsuitable environment for cell repair, causes further damage and is detrimental to recovery (Meda *et al.*, 1995; Popovich *et al.*, 1999, 2002; Majed, 2006; Shechter *et al.*, 2009; Letellier *et al.*, 2010; Miron, 2013).

1.2.3 Control of inflammation

Controlling inflammation in SCI requires a consideration of both the beneficial and damaging roles of macrophages. For example, complete immunosuppression would prevent the removal of cell and foreign debris, leading to further injury or infections and further damage to the injury site (Minardi *et al.*, 2016b). The highly inflammatory environment of SCI itself causes much damage through the production of free reactive species and neurotoxic cytokines as a result of macrophage phagocytosis. Finding a balance between the optimal inflammation period for removal of debris without further damaging the site and preventing repair is a major challenge for SCI treatments. One aim of future treatments for SCI is the resolution of inflammation as occurs in natural healing (Alvarez *et al.*, 2016). It is hoped that this process can be

enhanced and encouraged in injuries such as SCI where resolution does not occur.

1.2.4 Macrophage modulation

It is desirable to exercise control over the balance of M1 and M2 macrophages in order to obtain a smooth transition from an inflammatory environment to an environment more suitable to healing. This is the case particularly for SCI in which there is an unresolved population of proinflammatory macrophages (Alvarez *et al.*, 2016). Altering this dynamic balance requires careful consideration to properly exploit the environment in therapeutic applications. However, recent studies have demonstrated that doing so can support endogenous healing and tissue regeneration (Alvarez *et al.*, 2016). In order to facilitate healing with both M1 and M2 macrophages (Alvarez *et al.*, 2016), 1-3 days is usually required in general injuries for the recruitment of M1 populations and removal of debris or foreign organisms followed by resolution to M2 (Kotwal and Chien, 2017).

Various growth factors have been shown to have roles in macrophage modulation, particularly IL-4, IL-10, IL-13, IL-33, and activin a as shown in Table 1.3 (Bomstein *et al.*, 2003; Schwartz *et al.*, 2006; Duluc *et al.*, 2007; Qin, 2012; Yang *et al.*, 2013; Galdiero and Mantovani, 2015; Molina *et al.*, 2015; Rőszer, 2015; Minardi *et al.*, 2016; Soldano *et al.*, 2016).

Table 1.3: Macrophage modulation growth factors (Adapted from Duluc *et al.*, 2007; Rőszer, 2015).

	M1	**M2a**	**M2b**	**M2c**	**M2d**
Stimulation	IFN-γ LPS GM-CSF	IL-4 IL-13 Activin a	ICs IL-1R	IL-10 TGF-β	IL-6 LIF Adenosine

Thus, it has been suggested that a population predominantly made up of M1 macrophages could be modulated to give rise to a more predominantly M2 population using growth factors (Martinez and Gordon, 2014). Ultimately, this has the potential to provide a more suitable regenerative environment (Martinez and Gordon, 2014). When stimulated using growth factors in *in vitro* or *in vivo* studies, the macrophage populations can be referred to by their stimulation factor, for example an M1 population could be $M_{(LPS,\ IFN\gamma)}$ or an M2 population could be $M_{(IL\text{-}4)}$.

Human Interleukin 4 (IL-4) has been shown to modulate macrophage phenotype from a proinflammatory phenotype to a proimmunoregulatory phenotype (Mantovani *et al.*, 2014; Galdiero and Mantovani, 2015; Alvarez *et al.*, 2016; Arora *et al.*, 2017). IL-4 has main roles in cell signalling but has been shown to have effects on the polarisation of macrophage cells alongside various other factors including IL-13 and macrophage colony-stimulating factor (M-CSF)

(Mantovani *et al.*, 2014; Murray *et al.*, 2014; Galdiero and Mantovani, 2015; Alvarez *et al.*, 2016; Arora *et al.*, 2017).

1.3 Current Spinal Cord Injury Treatments

1.3.1 SCI management

In spinal cord injury, the complex structure and vascular system of the CNS and its protective barriers such as the blood-cerebral spinal fluid barrier, results in an environment that is biochemically and immunologically isolated from the body making regenerative strategies difficult (Kim *et al.*, 2012; Tuladhar *et al.*, 2015). Any drugs or cells are required to cross the tight epithelial junctions present in the CNS and render oral, intravenous and intramuscular delivery obsolete (Tuladhar *et al.*, 2015).

Current treatments for SCI are very limited and focus on reducing inflammation through the use of immunosuppressive drugs (McCreedy and Sakiyama-Elbert, 2012), stabilisation of the injury site and prevention of secondary complications (Mothe and Tator, 2012). However these have many side effects and low recovery rates (Bomstein *et al.*, 2003; Baumann *et al.*, 2009; Kang *et al*, 2010; Silva *et al.*, 2014). Most treatments depend on the time at which the patient is seen, the exact location of the injury on the spinal cord and the causation of the injury (NHS and Board, 2013). The general consensus is that the earlier the patient is treated the more effective the treatment (NHS and Board, 2013; Silva

et al., 2014), however, no immunosuppressive drug treatments have resulted in full functional limb control.

Current therapeutic strategies following SCI focus on physiotherapy for limb function as well as psychotherapy to aid the patient in coping with difficulties associated with loss of limb function and feeling (Tuladhar *et al.*, 2015). Particular focus is made on the effects of the injury on the function of the bladder and bowel, depending on where the injury occurred to improve quality of life and encourage rehabilitation (Silva *et al.*, 2014). Unfortunately, there are very few biomolecular treatments available on the market for treatment of CNS damage (Tuladhar *et al.*, 2015). However, many drug and molecule therapies are being investigated for this purpose and are summarised in Table 1.4.

Table 1.4: A summary of tested CNS therapies and an overview of the research outcomes.

Therapeutic Agent	SCI Model/ Human	Overall Outcomes	Mechanism of Action	References
Methylpr-ednisolone	Cat	Improved functional recovery with high dose – not universally accepted. Decreased free radical production.	Reduction of free radical production and lipid peroxidation.	(Hall and Braughler, 1981, 1982)
	Human	High rates of neurological recovery when treated within 8 hours of injury. High infection rates.		(Bracken *et al.*, 1990)
	Rat	High mortality and morbidity with adverse side effects.		(Cerqueira *et al.*, 2013)
	Rat	High mortality and morbidity with adverse side effects.		(Short, 2000; Short, El Masry and Jones, 2000)
Ibuprofen	Rat/ Mouse	Behavioural and histological improvements. Controversial high dosing.	Inhibition of downstream RhoA signalling.	(Fu, Hue and Li, 2007)
	Rat	Promoted axonal sprouting. High dose required		(Wang *et al.*, 2009)

Indomethacin	Rabbits	Reduction in tissue damage. Behaviour and function not assessed.	Decreased action of phospholipase.	(Pantović *et al.*, 2005)
	Rat	Reduced microglia and astrocytes at injury site. Behaviour and function not assessed.		(Schwab *et al.*, 2004)
Atorvastatin	Rat	Reduction in inflammatory cytokine expression.	Inhibition of Rho signalling.	(Pannu *et al.*, 2005, 2007)
Minocycline	Mice	Improved axonal regrowth and recovery. Improved function.	Inhibition of caspase-1, caspase-3, nitric oxide synthase and matrix metalloproteinases.	(Wells, 2003)
	Rat	Reduced cavitation, necrosis and gliosis.		(Festoff *et al.*, 2006)
	Rat	Reduced pro-inflammatory cytokine production.		(Stirling *et al.*, 2004)
	Rat	Functional improvements.		(Teng *et al.*, 2004)
	Rat	Unable to obtain functional improvements.		(Lee *et al.*, 2010)
	Rat	Unable to obtain functional improvements.		(Pinzon *et al.*, 2008)
	Rat	Unable to obtain functional improvements.		(Saganová *et al.*, 2008)

The gold standard treatment for spinal cord in many countries is methylprednisolone, a corticosteroid anti-inflammatory agent, and is currently the only therapeutic available for SCI. Despite its use, methylprednisolone has been reported to cause many life threatening side effects including infections, wound-related complications, gastrointestinal haemorrhages, sepsis, pneumonia and in some cases death (AANS and CNS, 2002; Silva *et al.*, 2014). Due to the high mortality and morbidity associated with methylprednisolone use, many clinicians warn against its use and some centres have stopped its administration entirely (Mothe and Tator, 2012; Silva *et al.*, 2014; Tuladhar *et al.*, 2015). The drug was found to maintain the spinal cord-blood barrier, inhibit lipid peroxidation and endorphin release, and also to limit the inflammatory response as shown in Table 1.4 (Hall and Braughler, 1981, 1982; Bracken *et al.*, 1990; Tator, 1998; Silva *et al.*, 2014). Hall and Braughler showed that high doses of methylprednisolone in spinal cord injury cat models reduced lipid peroxidation and free radical production and interaction with nerve cell membranes, therefore reducing further damage to the injured area (Hall and Braughler, 1981, 1982). Despite the efficacy of its use shown by Hall and Braughler in 1981 and 1982, follow up studies showed that the dosage required to produce similar effects in humans as seen in animal models would be fatal (Short, 2000; Short, El Masry and Jones, 2000; AANS and CNS, 2002; Silva *et al.*, 2014). Some studies investigated new approaches for the sustained delivery of methylprednisolone, aiming to reduce the need for high dose injections (Cerqueira *et al.*, 2013), however as yet there is no such method. Bracken *et al* undertook a study using SCI patients in a double-blind placebo controlled trial which showed improved function when patients were treated within 8 hours of injury as a result of

reduction in lipid peroxidation, however there was high levels of infection and mortality observed (Bracken *et al.*, 1990). The clinical studies undertaken to assess the use of methylprednisolone as a treatment strategy for spinal cord injury are further discussed in section 1.3.2.

The main understanding of why methylprednisolone was more effective in rodent models surrounds its ability to inhibit the inflammatory response as well as reducing production of free radicals through limit of lipid peroxidation. As discussed previously the immune response is particularly important in the prevention of infection by removal or microorganisms, foreign objects and cell/ tissue debris. Therefore targeting the inflammatory response must be approached carefully in the design of a therapeutic in order to prevent worsening the injury (Kim *et al.,* 2012; Tuladhar *et al.*, 2015).

Ibuprofen, a commonly used non-steroidal anti-inflammatory drug (NSAID) was tested for its use as an inflammation control method in spinal cord injury. Studies by Fu *et al,* and Wang *et al* showed that administering ibuprofen at days 3 and 7 post-injury resulted in behavioural improvements in rodent models (Fu, Hue and Li, 2007; Wang *et al.*, 2009). The findings were that ibuprofen acted by inhibiting the downstream signalling of RhoA, a GTPase with important cell-signalling roles including production of reactive oxygen species, and recruitment of neutrophils or leukocytes (Knaus, 2000; Fu, Hue and Li, 2007). The behavioural improvements were thought to have resulted from reduced cell death and protein degradation as a result of reactive oxygen species production

(Fu, Hue and Li, 2007). Despite this positive outcome, the upscale dosage to a human was too high and could be toxic. This research did however, highlight the importance of timing and response intensity in treating SCI, which was further supported by Butovsky *et al* and Shaked *et al* (Shaked *et al.*, 2004; Butovsky *et al.*, 2005). Ibuprofen was also tested alongside another NSAID, indomethacin by Pantovic *et al* and Schwab *et al* who demonstrated a reduction in tissue damage due to a reduction of phospholipase action and therefore reduced breakdown of cell membranes and less free fatty acids (Winkler *et al.*, 1993; Schwab *et al.*, 2004; Pantović *et al.*, 2005). These studies did not however show functional improvements after treatment with indomethacin.

Atorvastatin, more commonly known for its use in lowering cholesterol, was tested on rat models in 2005, and 2007 by Pannu *et al* as a method for inflammation control. Its administration was shown to reduce the expression of inflammatory cytokines through the inhibition of Rho signalling and subsequently reactive oxygen species production (Pannu *et al.*, 2007). However further testing is required to assess functional recovery.

Some neuroprotective agents have been investigated for use in SCI treatment including a sodium channel blocker, riluzole and an antibiotic with anti-inflammatory properties, minocycline (Mothe and Tator, 2012). Minocycline, an antibiotic more commonly used to treat pneumonia or acne amongst other bacterial infections, was shown by various research studies to improve axonal regrowth and improve functional recovery in rodent models (Wells, 2003;

Stirling *et al.*, 2004; Teng *et al.*, 2004; Festoff *et al.*, 2006). The use of minocycline was found to inhibit the expression and activity of various pathways and enzymes which result in tissue injury, production of inflammatory cytokines, production of free radical species and proteinase activation (Wells, 2003). Inhibition of caspase-1 and caspase-3 by minocycline is thought to reduce the production of inflammatory cytokines such as IL-1 and cell apoptosis in a similar way to the inhibition of nitric oxide synthase and therefore nitric oxide production (Wells, 2003; Festoff *et al.*, 2006). Another role of minocycline is the inhibition of matrix metalloproteinases which prevents the breakdown of cell membranes and therefore tissue damage (Wells, 2003). Despite these effects resulting in less tissue damage and a more suitable environment for repair and recovery, many of the minocycline studies were unable to result in functional improvements in SCI rodent models (Pinzon *et al.*, 2008; Saganová *et al.*, 2008; Lee *et al.*, 2010).

Unfortunately, due to the extent and dynamicity of SCI, the treatments explored in Table 1.4 and in this section (section 1.3.2) are not thought to be sufficient for functional recovery alone (Mothe and Tator, 2012). Despite this, some studies have been explored in human trials and these are discussed in section 1.3.2.

1.3.2 Clinical studies for SCI treatment

In the recent decades extensive research has been carried out with the attempt to find promising new therapies for spinal cord injuries, some of which were taken forward into clinical trials, however none of these revealed robust efficacy enough to be widely accepted as clinical treatments (Hawryluk *et al.*, 2008). Arguably the most controversial treatment currently used is that of methylprednisolone as discussed in section 1.3.1 and Table 1.6. This treatment was tested in multiple clinical trials (phase I, II and III) and the neuroprotective effects were deemed to outweigh the potential side effects (Hawryluk *et al.*, 2008). In a trial conducted by Bracken *et al* in 1990 (NASCIS I), the administration of methylprednisolone to SCI patients did not result in significant neurological improvements and did result in increased rates of infection, haemorrhage, pulmonary embolism, poor wound healing and in some cases death (Bracken *et al.*, 1985). Despite the negative results from this trial, previous animal studies had suggested larger dosage would be required for human treatment (Braughler and Hall, 1984). Further trials were conducted in 1990 (NASCIS II) using greater dosage of methylprednisolone, these found that some neurological benefits could be obtained if drug was administered within 8 hours of the injury, however the side effects were still present (Bracken *et al.*, 1990; Bracken, 2001). In a third study (NASCIS III), improvements in neurological functions were found after methylprednisolone administration for 24 hours between 3 – 8 hours after injury or 48 hours after post 8 hours after injury

(Bracken *et al.*, 1997, 1998). Various other trials confirmed these results and methylprednisolone is currently used as a treatment despite the potential side effects due to a lack of alternatives (Otani *et al.*, 1994; Pointillart *et al.*, 2000; Hawryluk *et al.*, 2008).

Due to the side effects from methylprednisolone treatment, alternative treatments have been investigated using cells and cytokines rather than steroids. A particularly interesting clinical study for SCI treatment was undertaken by Yoon *et al* using bone-marrow derived stem cells (MSCs) and granulocyte macrophage colony stimulating factor (GM-CSF), however no significant functional improvements were observed (Yoon *et al.*, 2007). This study used 35 human complete spinal cord injury patients in a phase I/II open-labelled and non-randomised study where MSCs were injected directly into the injury site at different times after injury and a control group was treated with decompression and fusion surgery (Yoon *et al.*, 2007). Following treatment either within 14 days of injury, between 14 days and 8 weeks, or after 8 weeks post-injury, the patients underwent neurological assessments, electrophysiological monitoring and magnetic resonance imaging. The reported results after 4 months were an enlarged spinal cord with no lesions, cysts, haemorrhage or infection, however no significant functional improvement (Yoon *et al.*, 2007). This lack of improvement may have been the result of the hostile inflammatory environment preventing survival of the introduced MSCs.

As well as the pharmacological strategies for SCI treatment, various surgical trials have been undertaken, especially in the use of decompression of the spinal cord (Hawryluk *et al.*, 2008). Work started by Fehlings in 2003 followed on from the discovery that decompression in animal models led to neurological benefits and suggested that decompression of the human spinal cord within 24 hours of injury led to a beneficial effect (Fehlings and Perrin, 2005). This practice is carried out as a treatment currently, however, it is difficult to get the patient to surgery in time for treatment and is therefore not effective. Other surgical strategies towards SCI have been investigated and some are summarised in a review by Hawryluk *et al,* including the use of oscillating field stimulation and hypothermia as treatment options (Hawryluk *et al.*, 2008). The overall consensus is that no current treatments are able to restore function and feeling following spinal cord injury. The following section discusses some regenerative strategies that have been investigated as an alternative for SCI treatment.

1.3.3 Regenerative strategies for SCI repair

Regenerative strategies can be defined as a therapy or system for targeting a certain damaged tissue or organ in order to repair the damage and return it to normal function. Not all strategies are successful, but many can promote repair and therefore prevent further damage. Further challenges the injury poses on regenerative strategies include cell death, demyelination, glial scarring and a growth-inhibitory environment (Kim *et al.*, 2012). Despite this, some cell

replacement treatments have been trialled using cellular transplantation alone, or with biomaterials or drugs in animal models (Tuladhar *et al.*, 2015), those discussed are summarised in Table 1.5.

Table 1.5: A summary of studies for regenerative strategies for SCI/ CNS in literature.

Strategy	SCI Model	Overall Outcomes	References
Peripheral nerve grafts	Rat	Promotion of axon regrowth and regeneration.	(Richardson, McGuinness and Aguayo, 1980; Bregman and Reier, 1986)
Stem cell transplants	*In vitro*	Differentiation of DPSCs to active neurons.	(Király *et al.*, 2009)
	Human	Functional improvements after BMSC implantation.	(Sykova *et al.*, 2006; Yoon *et al.*, 2007)
PLGA scaffold and neural SCs	Rat	Reduction in glial scar formation. Improved functional recovery.	(Teng *et al.*, 2002)
PEG micelles	Rat	Reduction in spinal cord lesion. Attenuated macrophage response.	(Shi and Borgens, 1999)

Cell therapies were explored in the 1970s by Richardson *et al* who used peripheral nerve grafts to promote CNS axon regeneration (Richardson, McGuinness and Aguayo, 1980), and by Bregman *et al* who showed fetal spinal cord grafts supported axon regrowth (Bregman and Reier, 1986). Richardson *et al* were unable to show axonal sprouting when using peripheral nerve grafts in the CNS of rat models with transected spinal cords, the grafts which consisted of myelinated and nonmyelinated axons ensheathed in Schwann cells also resulted in the development of cysts after transplantation (Richardson, McGuinness and Aguayo, 1980). The suggestion was that the harsh environment at the injury site was unsuitable for axonal regeneration (Richardson, McGuinness and Aguayo, 1980). However, Bregman and Reier showed in 1986, that the transplant of fetal spinal cord grafts could encourage the projection of neurons from the cord to the transplant (Bregman and Reier, 1986). The results of this study in rats suggested that the use of fetal spinal cords provided trophic substances that prevented retrograde cell death of immature neurons and essentially acted as a surrogate for cell growth (Bregman and Reier, 1986). It is therefore evident that under the correct environmental conditions it is possible to encourage the repair and regeneration of the spinal cord after injury.

The implantation of stem cells has also been suggested as a strategy to replace and repair cells after injury due to their ability to differentiate to new cell types (Kim, Cooke and Shoichet, 2012). An advantage of the use of stem cells is their ability to continually proliferate and generate new cells for differentiation, thereby providing new cells to replace those lost or damaged in the injury (Mothe and Tator, 2012). Some specific cell types suggested to have

applications in SCI include dental stem cells such as stem cells from the apical papilla (SCAP), dental pulp stem cells (DPSCs) and stem cells from human exfoliated deciduous teeth (SHED) (Bakopoulou and About, 2016). One particular study by Király *et al* showed that *in vitro* DPSCs could be differentiated with the activation of protein kinase C and treatment with neurotrophin-3 and dibutyryl cyclic AMP to result in active neurons with neuronal morphology and expressing neuronal markers (Király *et al.*, 2009). Thus, showing the potential for use of these stem cells in encouraging neuronal growth with applications in CNS repair.

Other important cell types considered for transplantation are mesenchymal stem cells (MSCs) such as bone marrow-derived stromal cells (BMSCs), neural stem/progenitor cells (NSPCs) and induced pluripotent stem cells (iPSCs) (Mothe and Tator, 2012; Martens *et al.*, 2013). Cells transplanted face many challenges, importantly survival in the hostile environment created by the immune response in the secondary phase of SCI. It is thought that cell transplantation could ameliorate some of the cascades caused by the secondary phase of injury and in this way offer neuroprotection (Mothe and Tator, 2012). Various studies have been undertaken using BMSCs with mixed results. In work by Sykova *et al* and Yoon *et al* the interspinal dose of BMSCs resulted in neurological improvements for subacute SCI but not in chronic cases (Sykova *et al.*, 2006; Yoon *et al.*, 2007). Both studies reported no adverse side effects or complications (Sykova *et al.*, 2006; Yoon *et al.*, 2007).

Another challenge faced is the delivery method of cells to the site of injury without causing more damage to the delicate white matter within the spinal cord. Some investigation has been done into the use of injectable hydrogels or microparticles rather than intravenous injection to the injury site (Kim, Cooke and Shoichet, 2012; Tuladhar *et al.*, 2015). The use of biomaterials in the delivery of stem cells is suggested to improve cell survival and enhance their ability to differentiate and integrate with host cells (Kim, Cooke and Shoichet, 2012). Teng *et al* explored the use of a PLGA scaffold in combination with neural stem cells (NSCs) (Teng *et al.*, 2002). This approach was shown to reduce the formation of glial scars and improve functional recovery. Shi and Borgens showed in 1999, that PEG micelles could reduce the volume of the lesion at the injury site in SCI and attenuate the macrophage response, although further studies were required to assess the functional recovery (Shi and Borgens, 1999; Silva *et al.*, 2014).

The incorporation of various research in drug delivery, stem cell delivery, and tissue regeneration may be required in order to effectively treat such a complex and delicate environment. As SCI has so many contributing factors preventing repair and recovery, it is likely that a multifaceted approach is required (Silva *et al.*, 2014)

1.3.4 Current macrophage targeted therapeutic research in CNS

There are many reported cases of exogenously modulated macrophages for different applications and different injuries using different methods for macrophage activation or deactivation, as shown in Table 1.6.

Table 1.6: A summary of the macrophage targeted therapeutic strategies in the context of SCI.

Therapeutic Agent	Model	Overall Outcomes	References
Anti TNFα	Rat – SCI model	Inhibition of the inflammatory response.	(Esposito and Cuzzocrea, 2011)
	Rat – SCI model	Reduction in apoptotic cells. Reduction in nitric oxide production.	(Lee *et al.*, 2000)
	Rat – SCI model	Reduction in number of macrophages at injury site.	(Mabon *et al.*, 2000)
IL-10	Rat – SCI model	Decreased TNFα production in CNS. Lesion volume reduced.	(Bethea *et al.*, 1999)
	Mouse – T helper response model	Decreased Th1 response.	(McGuirk *et al.*, 2002)
IL-10	Mouse – Autoimmune model	Enhanced functional recovery in SCI.	(Cottrez *et al.*, 2000)

IFNγ and IL-4	*In vitro* – primary human macrophages	Modulation from M1 dominant to M2 dominant population.	(Spiller *et al.*, 2015)
	Rat – SCI model	Up-regulation of anti-inflammatory cytokines.	(Lima *et al.*, 2017)
LxA4 and RvD1	Mouse – air-pouch model	Reduction in pro-inflammatory cytokines.	(Vasconcelos *et al.*, 2015)
Transplantation of activated macrophages	Rat – SCI model	Improved function. Clinically significant motor recovery.	(Rapalino *et al.*, 1998)
Proinflammatory factors	Rat – SCI model	Reduced functional movement. Increased reactive oxygen species. Reduced tissue survival.	(Popovich *et al.*, 2002)

One strategy is the blockage of TNFα as an inducer to M1 and a prominent proinflammatory factor (Horiuchi *et al.*, 2010; Brenner, Blaser and Mak, 2015). In recent studies, the use of anti-TNFα neutralising antibodies shifted the M1-M2 balance towards M2 in a mouse model for rheumatoid arthritis (RA) and resulted in accelerated wound healing, although not technically a CNS model, RA is characterised by chronic inflammation and therefore has similarities to SCI (Taylor and Feldmann, 2009). Commonly this strategy has been used in the treatment of autoimmune diseases such as RA and many formulations are

available commercially including monoclonal antibodies (e.g. infliximab, adalimumab and golimumab), antibody fragments (e.g. certolizumab pegol), or fusion recombinant proteins (e.g. Etanercept) (Taylor and Feldmann, 2009). Esposito *et al* (2011) also showed that neutralising TNFα with antibodies, soluble receptors or recombinant TNF binding proteins had an effect on the inflammatory response in SCI rat models as shown in Table 1.6 , suggesting a similar effect to that in RA (Esposito and Cuzzocrea, 2011). Despite these outcomes, an anti-TNFα strategy has not been used in clinical trials for spinal cord injury, this may be linked to the need for an active immune response for prevention of infection and removal of debris.

Another strategy is the manipulation of local cytokine concentrations to modulate the macrophage phenotype (Alvarez *et al.*, 2016). Work by Carvalho *et al* showed that IL-10 was effective in reducing inflammation in animal models when incorporated in a dextrin nanogel matrix (Carvalho *et al.*, 2010). A similar effect was seen by McGuirk *et al* (2002) and Cottrez *et al* (2000) where IL-10 reduced the Th1 response in murine models. Bethea *et al* (1999) also used IL-10 to target the macrophage response and showed a reduction in TNFα production in SCI as well as enhanced functional recovery.

Spiller *et al* (2015) used a similar strategy to release IFNγ and IL-4 from a decellularised bone matrix which trigged polarisation from an M1 dominant to M2 dominant phenotype. Lima *et al* (2017) also showed the beneficial effects of IL-4 with up regulation of anti-inflammatory cytokines following IL-4

treatment of SCI rat models. The use of lipid mediators lipoxin (LxA4) and resolvin (RvD1) were demonstrated by Vasconcelos *et al* to shift M1 to M2 and decrease production of several pro-inflammatory cytokines (Vasconcelos *et al.*, 2015). Further work showed that loading RvD1 onto a porous scaffold also produced a immunoregulatory effect on the macrophage population (Vasconcelos *et al.*, 2015). These studies all confirm that the control of the macrophage population has an effect on inflammation and therefore on the chance of repair and regeneration at an injury site.

Rapalino *et al* showed, in 1998, that the transection and transplantation of activated macrophages had a positive effect on limb function following transection of the spinal cord in rat models. This study showed that 3 out of 8 rat models gained improved motor function in their limbs to a significant extent and the treatment stimulated tissue repair (Rapalino *et al.*, 1998). The implantation of autologous macrophage cells to the transected cord appeared to stimulate re-growth and reconnection of spinal tracts across the lesion site as well as stimulating growth of white matter as a result of the growth-permissive environment from the activated macrophage treatment (Rapalino *et al.*, 1998). This particular study by Rapalino *et al* was the first study using autologous cells targeted at CNS self-repair rather than use of non-autologous tissues such as peripheral nerve grafts, non-autologous cells or foreign molecules (Rapalino *et al.*, 1998). In a contrasting study, by Popovich *et al* in 2002, the activation of intrinsic macrophages at the site of SCI by injection of proinflammatory factors showed reduction in limb function in rat models and also tissue survival (Popovich *et al.*, 2002). This suggesting that the macrophage response is of high

importance to the recovery of the spinal cord following injury. Work by Minardi *et al* showed IL-4 could be released from a biomimetic scaffold and have an *in vitro* effect on the response of macrophage cells (Minardi *et al.*, 2016). Other work by Pajarinen *et al* showed this effect could also be seen when IL-4 was delivered using an osmotic pump system, where drug was pushed through a semipermeable membrane on contact with water (Pajarinen *et al.*, 2015). In both these studies the activity of the protein remained intact post-release, as demonstrated by the positive effect on the macrophage cells (Pajarinen *et al.*, 2015; Minardi *et al.*, 2016).

1.4 Microparticle Use for Drug Delivery

1.4.1 A brief overview of biomaterials and microparticles

Biomaterials are substances engineered to take a form which can be used with components of living systems for a therapeutic or diagnostic procedure in human or veterinary medicine (Williams, 2009). They can be naturally derived or synthetic materials with a diverse range of physical and chemical properties leading to a wide range of applications (Kim *et al.*, 2012). The majority of biomaterials are bioresorbable polymers to ensure the materials only exist temporarily in the body (Chew *et al.,* 2017). Natural biomaterials such as alginate and collagen, are advantageous due to their inherent roles in biological systems and biologic recognition. (Chew *et al.*, 2017). However, synthetic biomaterials provide more consistent and tuneable properties (Atala, 2012; Kim *et al.*, 2012). Acellular tissue matrices are also used, for example bladder

submucosa and small-intestine submucosa (Atala, 2012). These acellular tissues are high in collagen and are prepared by removal of cellular components from the tissues to produce an extracellular matrix (Atala, 2012). Tissues such as these have been shown to support cell growth and tissue regeneration (Atala, 2012). However due to the tissue and processing methods the material properties can be unpredictable and not reproducible. The most commonly used synthetic biomaterials are poly(glycolide) (PGA), poly(lactide) (PLA) and poly(lactic-co-glycolic acid) (PLGA) (Atala, 2012; Kim *et al.*, 2012; Huang *et al.*, 2013). These are advantageous due to large scale reproducibility with controllable properties, easy processing, biodegradability, biocompatibility, degradation rate and microstructure (Atala, 2012; Rambhia and Ma, 2015; Mir *et al.*, 2017a). These synthetic materials have been approved by the Food and Drug Administration (FDA) and European Medicine Agency for multiple applications in humans including repair of the liver, trachea, heart, blood vessels and kidney (Atala, 2012), as they are degraded to nontoxic metabolites which can be naturally eliminated from the body through metabolic pathways (Atala, 2012; Chew *et al.*, 2017; Mir *et al.*, 2017a). For cell-based strategies, biomaterials provide a three-dimensional (3D) structure for cells to form new structures and can act as an anchor to natural tissues (Atala, 2012; Rambhia and Ma, 2015). For drug-delivery strategies, biomaterials can protect the drug from the harsh environment and ensure localised delivery as well as increasing bioavailability and decreasing drug dosage (Rambhia and Ma, 2015).

Different forms of biomaterials can be used for different applications, these include scaffolds, hydrogels and microparticles (O'Brien, 2011). Microparticles

are spherical biomaterials of varying sizes and properties in which drugs, DNA, RNA, protein, vaccines or cells can be encapsulated and released from within (Chew *et al.*, 2017). Microparticles are often combined with scaffolds or hydrogels to ensure localised delivery to a certain site, reduce the chance of migration, protect the drug and to reduce frequency and dosage (Lee and Yeo, 2015; Rambhia and Ma, 2015; Chew *et al.*, 2017). Encapsulated drugs can be released from within polymeric microparticles on contact with an aqueous environment through different methods including; polymer erosion, diffusion through the polymer matrix, diffusion through water-filled pores and via osmotic pumping as illustrated in Figure 1.6. The encapsulation and release of a drug from within a microparticle sphere largely depends on the size, structure, isoelectric point and mass of the drug. For this reason, each microparticle delivery system has to be tailored to the specific drug and application.

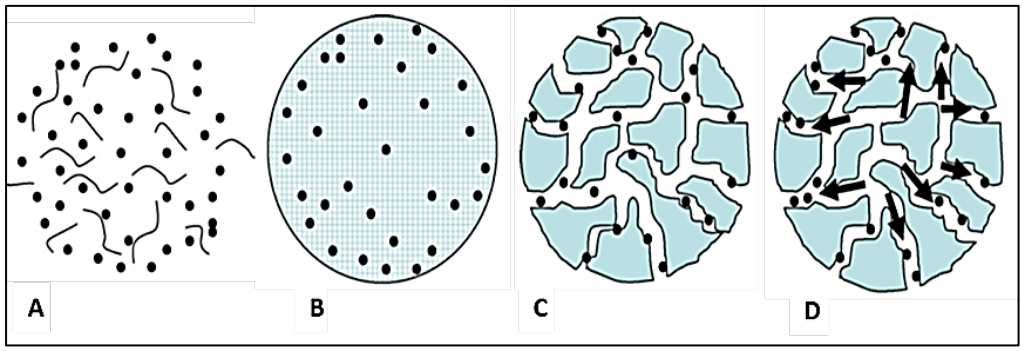

Figure 1.6: An illustration showing the various methods of drug release from microparticles. (**A**) Polymer erosion; (**B**) Diffusion through a polymer matrix; (**C**) Diffusion through water-filled pores; (**D**) Osmotic pumping. (Adapted from Fredenberg *et al.*, 2011).

The main reason for controlling the release kinetics from drug delivering MPs is to maintain the drug concentration within the therapeutic window (Lee and Yeo, 2015). It is therefore important to tailor it to each specific drug and application. Typically, a zero-order controlled release system is desirable with an initial burst release and continued release within the therapeutic window, unlike multiple dose drugs where the drug concentration oscillates above and below the therapeutic window as illustrated in Figure 1.7 (Lee and Yeo, 2015).

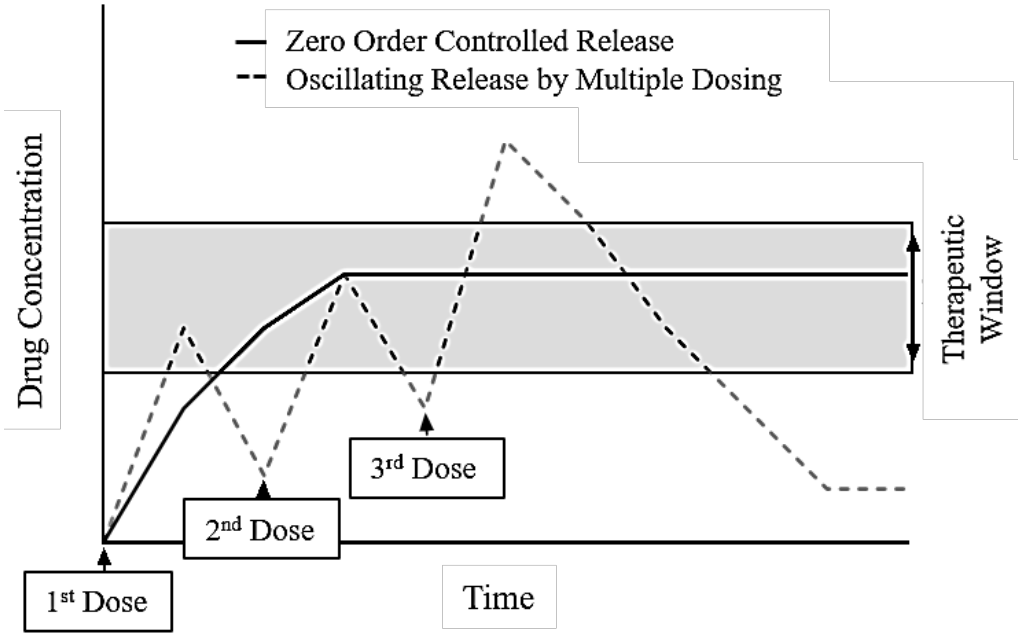

Figure 1.7: Drug concentration profile comparison between zero-order controlled release (solid line) and oscillating release by multiple dosing (dashed line) showing the drug therapeutic window where the drug is most effective without displaying toxicity. (Adapted from Lee and Yeo, 2015).

1.4.2 Use of microparticles in regenerative medicine and significance of controlled release

Microparticles have many uses in regenerative medicine and are commonly used for cross-disciplinary controlled release applications (Rambhia and Ma, 2015). Their applications include drug delivery for cancer treatments, control of infection or inflammation, regeneration of tissue, and also cell delivery (Rambhia and Ma, 2015). Some of the main advantages of the use of microparticles for drug delivery are the reduction of toxicity and side effects, and the increase of therapeutic efficacy (Han *et al.*, 2016). They also provide a more targeted system than previously-used intravenous (IV) injection of drugs (Lee and Yeo, 2015). Microparticles also offer a system to improve patient's adherence to regimen by reducing the dose and frequency of administration (Lee and Yeo, 2015). This system relies particularly on controlled release of a known drug concentration over time, for example, one single microparticle dose may release the same amount of drug as daily IV injections.

Microparticles and nanoparticles have already been investigated for use in various cancer therapies to target drugs to tumour sites. They show high permeability and therapeutic efficacy in the tumour and low toxicity in the surrounding tissue (Acharya and Sahoo, 2011; Maeda, 2012; Maeda *et al.*, 2013). Due to these characteristics, microparticles have many potentials uses in the field of regenerative medicine, with the ability to tailor particles to each use, tissue and drug.

1.4.3 Current general microparticle drug delivery treatments

Although microparticles have not yet been used for the delivery of IL-4 with the application of modulating the immune environment in SCI, they have been well studied and documented for other drug delivery techniques both in preclinical and clinical settings.

1.4.3.1 Preclinical microparticle delivery studies

Various preclinical microparticle drug delivery treatments investigated in *in vitro* studies and preclinical trials are discussed forthwith. One particular use for microparticles is in delivery vehicles for cancer treatments, both in chemotherapies and radiotherapies (Vilos and Velasquez, 2012; Batty *et al.*, 2018). In preclinical studies, Zhao *et al* used mouse models to show the delivery of oxaliplatin within PEG-PLGA particles to result in decreased pancreatic cancer cells and reduced tumour mass (Zhao *et al.*, 2016). Various other treatments have been tested using microparticles for chemotherapies in preclinical animal studies (He *et al.*, 2016) or radiotherapy in *in vitro* cell studies and *in vivo* animal studies (Min *et al.*, 2017) to reduce the side effects and dose requirements.

Treatments for leukaemia and melanoma have been approved by the FDA using IFN-α and IL-12 where microparticle delivery protects the proteins from degradation and in doing so increases treatment half-life (Lee and Margolin, 2011; Maciejko, Smalley and Goldman, 2017). Menei *et al* also showed delivery of chemotherapeutic agent 5-fluorouracil within microparticles to reduce

malignant gliomas in preclinical rat models and reduce therapy associated side effects as well as clinical studies described further in section 1.4.3.1 (Menei and Benoit, 2003; Menei *et al.*, 2004).

Microparticles have also been used as drug delivery methods in studies for other treatments besides cancer. Formiga *et al* showed in 2010 that the sustained release of VEGF from PLGA microparticles could reduce myocardial infarction in rat models (Formiga *et al.*, 2010). The use of microparticles have also been studied for the delivery of vaccines in order to produce long-term immune response and preserve the vaccine structure with increased safety, these include Vibrio cholerae in preclinical rat models (Año *et al.*, 2011), Pseudomonas aeruginosa *in vitro* study (Taranejoo *et al.*, 2011), and Bordetella pertussis in preclinical mouse models (Garlapati *et al.*, 2011).

One therapeutic tested using microparticles as a drug delivery system and used in animal trials by Mundargi *et al,* was the use of PLGA microparticles for insulin delivery for diabetes (Emami *et al.*, 2009; Cozar-Bernal *et al.*, 2011; Mundargi, Rangaswamy and Aminabhavi, 2011). This treatment involved the development of insulin particles for oral administration with the view of increasing safety for the patients (Emami *et al.*, 2009; Cozar-Bernal *et al.*, 2011; Mundargi, Rangaswamy and Aminabhavi, 2011).

1.4.3.2 Clinical microparticle delivery studies

Various clinical microparticle delivery systems and approved treatments are discussed forthwith. One particular microparticle delivery therapy is Lupron Depot®, which was developed originally in 1977 for prostate cancer treatment and FDA approved in 1989 following trials (Langer and Folkman, 1976; Chaubal, 2002; Anselmo and Mitragotri, 2014). The therapy consisted of leuprolide encapsulated within PLGA microparticles and due to controlled release, no longer required daily injections of leuprolide alone improving compliance and convenience for patients (Langer and Folkman, 1976; Chaubal, 2002; Anselmo and Mitragotri, 2014). A similar delivery system, Nutropin Depot® was also approved for delivery of recombinant growth hormone as a treatment for paediatric growth hormone deficiency following clinical trials showing growth improvement using two monthly doses in comparison to previous multiple weekly injections (Jiang et al., 2005; Johnson et al., 1996; Jordan et al., 2010). Many other treatments have been investigated for use with microparticle delivery systems to reduce inconvenience for patients as well as improve drug efficacy. Further examples of FDA approved microparticle therapies include Risperdal® Consta®, Vivitrol® and Bydureon®, for treatment of schizophrenia, alcohol/ opioid dependence, and type 2 diabetes respectively (Anselmo and Mitragotri, 2014). As described previously, Menei *et al* used 5-fluorouracil within microparticles to reduce malignant gliomas in a phase I pilot study on newly diagnosed glioblastoma patients and showed reduction in malignant gliomas (Menei and Benoit, 2003). Similar studies have been carried

out for peritoneal and ovarian cancers with promising results in patients (Armstrong and Brady, 2006; Zeimet *et al.*, 2009; Lu *et al.*, 2010).

Although only a small number of microparticle treatments have been discussed here, the studies undertaken with applications other than SCI hold valuable information in the suitability of microparticles for controlled and sustained release of drugs and can therefore provide insight for the development of new treatments.

1.4.4 Use of microparticles in central nervous system diseases

Due to the complexity of the central nervous system, treatments are difficult mainly due to the need to cross the blood-brain barrier. A number of strategies use biomaterials for CNS related treatments including electrospun scaffolds, nanofiber mats, injectable scaffolds and solid scaffolds (Lowry *et al.*, 2012; Yao *et al.*, 2013; Ren *et al.*, 2014; Chrapusta *et al.*, 2015; Johnson *et al.*, 2018; Liu *et al.*, 2018). Nano or microparticles have also been used previously to enable drug delivery of drugs that are too large or insoluble to cross the blood-brain barrier (Chen *et al.*, 2019).

The use of nanoparticles for SCI treatment has been explored with the focus on limiting monocyte infiltration into the injury site and therefore reducing

inflammation (Jeong *et al.*, 2017). Jeong *et al* demonstrated that synthetic nanoparticles could be taken up by blood-borne monocytes and result in the monocytes no longer moving to the sites of infection in mice with spinal cord injury, limiting the inflammation at injury site (Jeong *et al.*, 2017). In another study, Gwak and Wang encapsulated plasmid DNA in chitosan-MP nanoparticles and demonstrated reduced apoptosis and inflammation at the injury site (Wang *et al.*, 2008; Gwak *et al.*, 2016). Tan *et al* showed that microparticles could be used for sustained release of an exoenzyme, TAT-C3 and subsequently reduce glial scar formation and apoptosis in CNS injury (Tan *et al.*, 2007) suggesting cross-application in spinal cord injury. A similar study by Ren *et al* used PLGA nanoparticles to deliver flavopiridol and inhibit astrocyte growth and inflammation in CNS injury (Ren *et al.*, 2014). This method improved the motor recovery of animal models with induced spinal cord injury and could therefore have human applications also (Ren *et al.*, 2014). One other study that showed potential for SCI intervention was the delivery of Sonic Hedgehog proteins (Shh) by microparticles, which resulted in significant functional improvement in mouse models with induced SCI (Lowry *et al.*, 2012). All these studies suggest that the delivery of various factors to the spinal cord after injury can significantly improve functional outcome.

1.5 Overall hypothesis and aims

The overall hypothesis for this project was that sustained delivery of IL-4 could modulate macrophage phenotype and provide resolution in the context of

inflammation in SCI. This hypothesis was broken into three sub-hypotheses as follows:

1. IL-4 in the context of SCI can modulate macrophage phenotype to resolve a chronic pro-inflammatory environment to a pro-immunoregulatory environment to aid repair and regeneration.
2. Sustained delivery of IL-4 would be required to have an impact on macrophage populations in order to enable control over the dynamic macrophage population and ensure resolution of a pro-inflammatory environment.
3. Microparticles would provide a suitable method for sustained delivery of IL-4 due to the ability to tailor the release kinetics to a specific profile.

The specific aims were as follows:

- To establish a macrophage cell model using THP-1 cells as a cell line replicating human macrophages and murine immortalised bone-marrow derived macrophage (iBMDM) cells *in vitro*.
- Exogenously differentiate and modulate these cells to $M_{(LPS,\ IFN\gamma)}$ and $M_{(IL\text{-}4)}$ subgroups using cytokines.
- Determine the cell tolerance when grown in contact with microparticles.
- To optimise the production of PLGA microparticles for sustained drug delivery, using various release modifying methods to obtain a database of release kinetics for HSA and a model protein, lysozyme.
- To use this database to choose a microparticle formulation most suited to controlled sustained release of protein and therefore most suited to the application.

- To encapsulate IL-4 in the chosen microparticle formulation and assess release kinetics.
- To use microparticles containing IL-4 to treat differentiated THP-1 and iBMDM cells and determine their macrophage-modulating ability *in vitro*.

1.5.1 Specific microparticle objectives

In order to achieve controlled and sustained delivery the objectives were to assess the impact of different process variables. The variables to microparticle formulations explored were:

1. Variations of the lactide:glycolide ratio.
2. Variations of the total polymer percentage and therefore different thicknesses of particle surface.
3. Polaxamers F127 and P188 addition in different quantities; evaluated at 10 %, 20 %, 30 % and 40 % *w/w* of total polymer.
4. Addition of a triblock (PLGA-PEG-PLGA) copolymer at 10 %, 20 % and 30 % *w/w* of total polymer.

A database of microparticle formulations was developed in order to determine the formulation most suitable for the controlled and sustained release of IL-4 as per the project hypothesis.

1.5.2 Specific macrophage model objectives

The aim was to establish culture of a human THP-1 cell line and murine immortalised bone-marrow derived macrophage (iBMDM) model for future use alongside microparticles.

Specifically, the objectives were to:

1. Establish a robust cell culture method suitable for cell culture with microparticles.
2. Determine if THP-1 cells and iBMDMs could be exogenously differentiated with cytokines to produce cells expressing markers of human/ murine $M_{(LPS,\ IFN\gamma)}$ and $M_{(IL\text{-}4)}$ macrophages.
3. Determine if differentiated cells could be cultured alongside microparticles without affecting their growth.
4. Use microparticles containing IL-4 to treat the cells and compare their differentiation ability to that of exogenous IL-4.

Chapter 2: Materials and Methods

This chapter details the experimental methodologies used throughout this research. Many methods are utilised in multiple research chapters and are the basis of different experiments performed. All assays and other protocols are described. Specific experimental designs are included in each results chapter.

2.1 General Polymer and Microparticle Methods

2.1.1 Triblock/ diblock copolymer synthesis and characterisation

Synthesis of the triblock copolymer poly(lactic-co-glycolic acid)-polyethylene glycol-poly(lactic-co-glycolic acid) (PLGA-PEG-PLGA) was achieved by two methods: first from the lactide and glycolide monomers, and second from the PLGA polymer. Diblock (PLGA-PEG) was formed from the PLGA polymer.

The triblock from monomer was prepared in-house by Dr Omar Qutachi and Dr I-Ning Lee using the following method. Briefly, PEG (5.5575 g, 1500 Da, Sigma-Aldrich, Dorset, UK) and stannous octoate (0.075 g, Sigma-Aldrich, Dorset, UK) were heated to 45°C in a reaction vessel under nitrogen with or without vacuum until the PEG reached a molten state. The sample was dried under nitrogen for 1 hour before addition of DL-lactide (7.5 g, Lancaster synthesis, UK) and glycolide (2.5 g, PURAC, Netherlands). The reaction was left to proceed for 8-24 hours at 110-150°C. The vessel was removed from heat

and polymer dissolved in cold water (5-8°C). The solution was then heated to 80°C and supernatant removed to leave precipitated polymer. Precipitation was repeated before lyophilisation to remove residual water (Zentner *et al.*, 2001; Chen *et al.*, 2005). The viscous semi-solid triblock polymer was then stored at -20°C.

For the copolymers synthesised from polymer, the polymers were weighed (triblock 1:2, diblock 1:1) and dissolved in DCM overnight. Polymer was then precipitated out in chilled methanol and dialysed for 2-3 days before lyophilisation under vacuum to remove residual water and stored at -20°C. The exact conditions used for the in-house synthesised polymers are shown in Chapter 4, Table 4.1.

Nuclear Magnetic Resonance (NMR) analysis of copolymers was undertaken using deuterated chloroform ($dCDCl_3$) (Bruker 400 Spectrometer). Briefly, 5 mg of dried polymer was dissolved in $dCDCl_3$, analysed using 1H-NMR and data was processed using MestReNova software. A tetramethylsilane (TMS) signal was taken as the zero chemical shift the composition of the copolymer was determined by integrating the peaks for each monomer. The molecular weight and polydispersity of the copolymers were determined using Gel Permeation Chromatography (GPC) (Shimadzu, Japan) with refractometer detection by Dr Vincenzo Taresco, Dr Pratik Gurnani and Catherine Vasey. Briefly, 5 mg of dried polymer was dissolved in either chloroform ($CDCl_3$) or tetrahydrofuran (THF) and filtered into GPC vial before analysis. Samples were run with two Agilent PL gel mixed D columns heated to 30°C with THF + 2 % *v/v* triethanolamine (TEA) (57653380, Sigma-Aldrich, Dorset, UK) + 0.01 % *v/v* butylated hydroxytoluene (BHT) (329749182, Sigma-Aldrich, Dorset, UK) at a flow rate of 1 mL/min.

2.1.2 Microparticle preparation by double emulsion

Microparticles were prepared using 50:50 PLGA (lactide:glycolide 50:50 DLG 4.5A 59 kDa, Surmodics, Birmingham, USA). Particles were also made with 85:15 PLGA (85:15 DLG 4A 56 kDa, Surmodics, Birmingham, USA). One of three copolymer release modifiers was used in addition to PLGA: an in-house made PLGA-PEG-PLGA triblock or a commercially sourced F127 poloxamer, $C_3H_6OC_2H_4O$ (MFCD00082049, Sigma-Aldrich, Dorset, UK) or P188 poloxamer, $C_8H_{18}O_3$ (P188, Merck, Germany) at 10 %, 20 %, 30 % or 40 %

w/w. The specific microparticle formulations are shown in Table 2.1. Particles were fabricated with 20 % *w/v* total polymer to solvent ratio. The triblock formulations were also fabricated at 10 % *w/v* total polymer to create thin surfaced particles, and a single batch was made at 15 % *w/v* total polymer for 50:50.

Table 2.1: Table of microparticle formulations used in biomaterial design. TB*;* Triblock, F127/ P188; poloxamer copolymers

Polymer	Modifier	Polymer: Modifier Ratio (% *w/w*)	Microparticle Batch
50:50 PLGA	No Modifier	100:0	50:50 0 %
	TB1/ TB2/ TB4 F127 / P188	90:10	50:50 10 % TB 50:50 10 % F127
		80:20	50:50 20 % TB 50:50 20 % F127 50:50 20 % P188
		70:30	50:50 30 % TB 50:50 30 % F127
		60:40	50:50 40 % P188
85:15 PLGA	No Modifier	100:0	85:15 0 %
	TB1/ TB2/ TB4 F127/ P188	90:10	85:15 10 % TB 85:15 10 % F127
		80:20	85:15 20 % TB 85:15 20 % F127 85:15 20 % P188
		70:30	85:15 30 % TB 85:15 30 % F127
		60:40	85:15 40 % P188

Prior to microparticle preparation, polyvinyl alcohol (PVA, molecular weight: 13,000-23,000 Da, 87-89 % *w/v* hydrolysed, Sigma-Aldrich, Dorset, UK) (3±0.03 g) was dissolved in distilled water (1000±10 ml) and stirred at 300 rpm overnight to produce 0.3 % *w/v* PVA solution. The PVA solution was filtered through a 0.2 µm Nalgene filter and stored at room temperature. In order to create particles of differing surface thickness by using different total polymer concentrations (10 %, 15 % and 20 % *w/v* total polymer) different masses of polymer (500 mg, 750 mg, and 1 g polymer respectively), were dissolved in 5 ml DCM (Fisher Scientific UK Lts, Loughborough, UK) in a 25 ml PTFE screw top vial. For blank particles, 100 µl of distilled water was added to the polymer/ DCM solution to create a primary emulsion. For microparticles containing protein, 10 mg total protein (9 mg HSA/ 1 mg Lysozyme or 9.5 mg HSA/ 0.5 mg IL-4) in 100 µl distilled water was added to the polymer/ DCM solution. The primary emulsion was then homogenised for 2 minutes at 4000 rpm. The primary emulsion was poured into a 250 ml beaker containing 200±5 ml PVA solution as the second emulsion and homogenised at 9000 rpm for 2 minutes. The beaker was left stirring (300 rpm) for 4 hours to ensure DCM evaporation. Microparticles were then washed six times in deionised H_2O and centrifuged at 2200 g for 3 minutes between each wash. Following this, the particles were lyophilised in a freeze-dryer (ModulyoD-230, ThermoFisher) for 24 hours before storage at -20°C as described previously (White *et al.*, 2013). This process is illustrated in Figure 2.1.

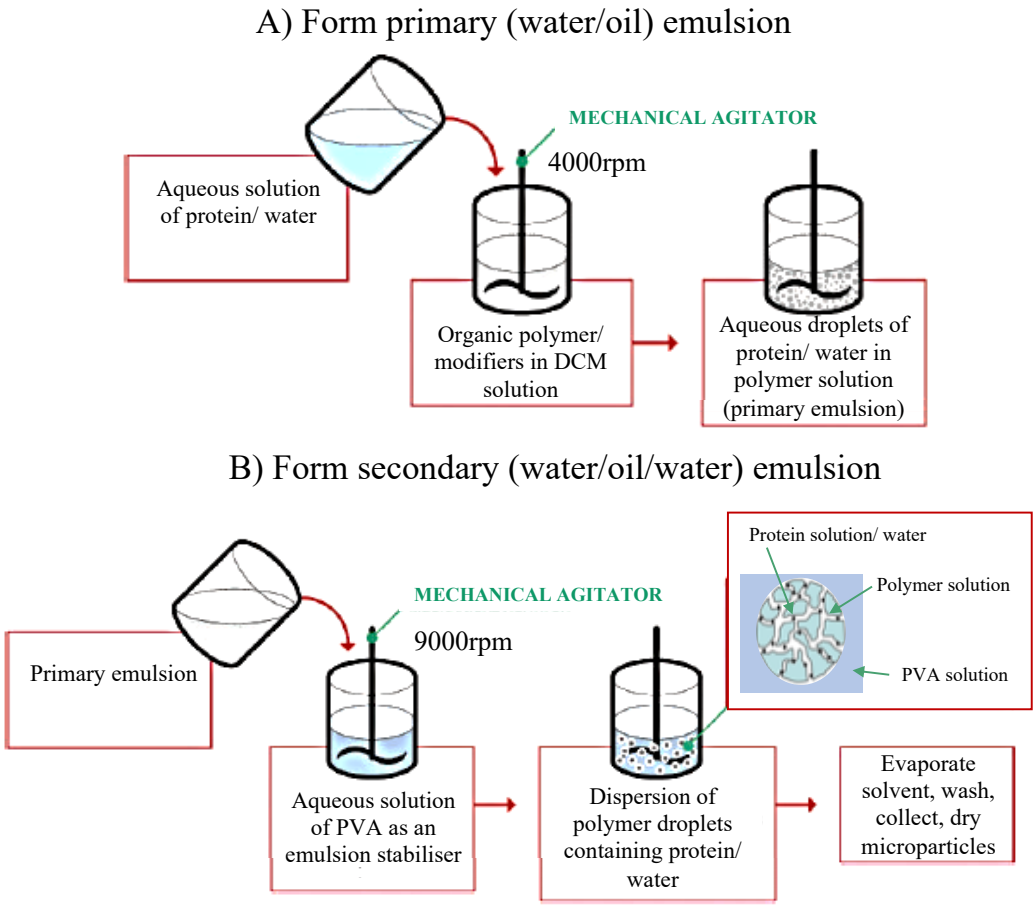

Figure 2.1: A schematic to show the double emulsion water in oil in water emulsion technique used for microparticle production. First emulsion step **(A)** to generate primary water in oil emulsion and second step **(B)** to form secondary water in oil in water emulsion. (Adapted from Chau *et al*, 2008).

Addition of 100 µl water was replaced by 100 µl concentrated protein solution for loaded particles. Protein solution was made using model protein lysozyme from chicken egg white and HSA (both Sigma-Aldrich, Dorset, UK) (10 mg: 90 mg in 1 ml dH_2O/ 10 mg: 90 mg in 2 ml dH_2O) at 100 mg/ml concentration for thick particles and 50 mg/ml concentration for thin particles. Lysozyme was selected as a suitable model for IL-4 due to similarities between isoelectric

points (lysozyme: 9.00, IL-4: 9.17) and molecular weights (lysozyme: 14 kD, IL-4: 17 kD). Encapsulation in combination with albumins has been shown to improve protein stability and encapsulation, as described previously (White *et al.*, 2013).

2.1.3 Microparticle characterisation by laser diffraction and scanning electron microscopy

Particle size distribution was assessed using laser diffraction (Coulter LS230, Beckman Coulter, UK). Briefly, particles were suspended in water to obtain 8-13 % *v/v* obscuration with agitation to prevent particle settling. The volume percentage at different channel diameters was detected in triplicate through laser diffraction to determine particle diameter. The mean particle diameter for each batch was calculated and the overall size distribution plotted as volume percentage against channel diameter.

The microparticle surface morphologies were analysed following gold splutter coating (Blazers SCD 030 gold splutter coater, Blazers, Liechtenstein) of a thin layer of particles adhered to an adhesive stub at 25 mA for 70 seconds. Coated particles were imaged using a JOEL 6060LV or JEOL 6490LV scanning electron microscope (SEM) (JEOL, Welwyn Garden City, UK) with voltage set to 10-25 kV depending on sample charging and working distance of 10 -15 mm.

2.1.4 Microparticle encapsulation efficiency and release study comparison

2.1.4.1 Encapsulation efficiency

Encapsulation efficiency was measured using a micro bicinchoninic acid (BCA) assay (Fisher Scientific UK Lts, Loughborough, UK). 10 mg of microparticles were dissolved in 750 µl dimethyl sulphoxide (DMSO, Sigma-Aldrich, Dorset, UK) at room temperature, followed by the addition of 2150 µl of 0.02 % *w/v* sodium dodecyl sulphate (SDS, Sigma-Aldrich, Dorset, UK) in 0.2 M sodium hydroxide (NaOH, Sigma-Aldrich, Dorset, UK) and 1 hr incubation at 37°C. A standard curve of protein in DMSO/SDS/NaOH was prepared using a serial dilution from 40 µg/ml. BCA reagent was made by mixing reagents A, B and C in a 25:24:1 ratio as per manufacturer guidelines (protein detection range: 200-1000 µg/ml). The sample/ standard (150 µl) and BCA working reagent (150 µl) were mixed and incubated at 37°C for 2 hrs (White *et al.*, 2013). The absorbance was read at 562 nm using a plate reader (Infinite M200, Tecan UK Ltd., Reading, UK) to determine total protein content. The encapsulation efficiency was calculated by subtracting the absorbance readings from the blank particles (containing water only) from the absorbance readings of the same microparticle formulation containing HSA:lysozyme/ HSA:IL-4. A percentage of total encapsulated protein was calculated using the following equation: ((amount of protein (µg))/ (mass of microparticles x 10))/ 100. The standard deviations (SD) were calculated between repeats.

2.1.4.2 Protein release: BCA assay and enzyme-linked immunosorbent assay (ELISA)

Triplicate aliquots (n3) of 25 mg of microparticles from each batch were suspended in 1.5 ml PBS and incubated on a rocker (Gyrotwister, Fisher Scientific UK Ltd) at 37°C. At different time intervals, samples were removed from the rocker, centrifuged for 30 seconds and supernatants were removed and replaced with fresh PBS. Supernatants were stored at -20°C prior to analysis with a micro BCA assay. A standard curve of protein in PBS was prepared using a serial dilution from 40-0.625 µg/ml, PBS alone was used as a blank (0 µg/ml). 150 µl of either collected sample or prepared standard and 150 µl BCA working reagent were mixed and incubated at 37°C for 2 hrs (White *et al.*, 2013). The absorbance was read at 562 nm using a plate reader (Infinite M200, Tecan UK Ltd., Reading, UK) to determine total protein content. The protein release kinetics were calculated as cumulative µg/mg particles as well as cumulative % total protein. Both of these calculations were adjusted to account for the specific encapsulation efficiency for each microparticle formulation using the following equations respectively:

((total protein (µg/mg))/actual mass of particles (encapsulation efficiency x 250)) x 100

((percentage release (% *w/w*))/actual mass of particles (encapsulation efficiency x 250)) x 100

The standard deviations were calculated between n3 triplicates and displayed as cumulative SD.

An IL-4 ELISA (BMS225, Invitrogen, UK) (detection range 7.8 - 500 pg/ml) was used to determine the exact concentration of IL-4 released from the IL-4 containing microparticles. Briefly, microwell strips were washed twice using wash buffer. Standards were prepared from 500 - 7.8 pg/ml in assay buffer. 100 µl standards were added to standard wells and 100 µl assay buffer was added as a blank (0 pg/ml). 50 µl assay buffer and 50 µl samples were added to sample wells, followed by 50 µl biotin-conjugate to all wells. Plate was sealed and incubated for 2 hrs on a microplate shaker at room temperature. Wells were aspirated and washed 3 x with wash buffer before 1 hr incubation in 100 µl streptavidin-HRP at room temperature. Wash step was repeated 3 x followed by 10 min incubation in 100 µl TMB substrate solution at room temperature in the dark. Following this, 100 µl stop solution was added to all wells and absorbance was read immediately at 450 nm. Standards were made as per manufacture guidelines and absorbance values were corrected for blank standard reading.

2.2 Cell Culture Methods

A list of general cell culture consumables used for routine cell work and experimental work is shown in Table 2.2.

Table 2.2: General cell culture consumables.

Consumable	Manufacturer
Universal tube (20 ml)	Starstedt
Tissue culture flasks (75 cm^2 and 175 cm^2)	Nunc, Fisher Scientific
Tissue culture treated 12-well plates	Falcon, Becton Dickinson
Cryovials, sterile pipettes, pipette tips (1 ml, 200 µl, 20 µl and 10 µl), 0.22 µm filters and 1.5 ml Eppendorf tubes	Fisher Scientific
Improved Neubauer haemocytometer	Scientific Laboratory Supplies
Trypsin-EDTA (0.05 % *v/v*) (Product number: 11590626)	Gibco, Fisher Scientific
Phosphate buffered saline (PBS)	Fisher Scientific
Phorbol 12-myristate 13-acetate (PMA)	Sigma-Aldrich
Lipopolysaccharides (LPS)	Sigma-Aldrich,
Interferon gamma (IFN-y)	ThermoFischer
Granulocyte-macrophage colony-stimulating factor (GM-CSF)/ Macrophage colony-stimulating factor (M-CSF)	Sigma-Aldrich
Interleukin 4 (IL-4)	Preprotech,

2.2.1 THP-1 cell culture optimisation and exogenous differentiation to macrophage cells

Human peripheral blood monocyte cells (THP-1, ATCC® TIB-202TM, ATCC, Middlesex, UK) (passages 2 and 10) were cultured as described by Huleihel *et al* (49) at 37°C and 5 % CO_2 in RPMI-1640 medium modified with HEPES, L-glutamine and phenol red. This medium was supplemented with 10 % (*v/v)* foetal bovine serum, 1 % (*v/v)* penicillin and streptomycin and ß-mercaptoethanol (0.05 mM) to make complete medium until they reached 1 million cells/ml. The complete medium recipe is shown below in Table 2.3.

Table 2.3: Complete RPMI-1640 medium used for THP-1 cell culture.

Product	Concentration	Supplier
RPMI-1640 medium with HEPES, L-glutamine and phenol red	N/A	Gibco, 52400025
Foetal bovine serum	10 % *v/v*	Sigma-Aldrich, F9665
Penicillin and Streptomycin	1 % *v/v*	Gibco, 15070063
ß-Mercaptoethanol	0.05 mM	Sigma-Aldrich, MFCD00004890

For THP-1 differentiation into macrophage cells, the cells were cultured in tissue culture treated plates for 24 hours in complete medium supplemented with 50 ng/ml phorbol 12-myristate 13-acetate (PMA) followed by one wash in supplemented media and a further 48 hours incubation in medium only. For differentiation into M1/ M2 the cells were then cultured with medium containing the respective cytokines for 72 hours. For M1: 100 ng/ml lipopolysaccharide (LPS) and 20 ng/ml interferon-γ (IFN-γ), and 50 ng/ml granulocyte-macrophage colony-stimulating factor (GM-CSF); For M2: 20 ng/ml interleukin-4 (IL-4), and 50 ng/ml macrophage colony-stimulating factor (M-CSF). For population doubling, cell standard curve and optimal seeding density see appendix. Following differentiation, the cells were analysed using enzyme-linked immunosorbent assay (ELISA) and qualitative polymerase chain reaction assay (qPCR) for characterisation of the cell subgroups described below.

2.2.2 Murine immortalised bone-marrow derived macrophage (iBMDM) culture and exogenous polarisation to macrophage subgroups

An established line of murine immortalised bone-marrow derived macrophage cells were kindly provided by Dr Andrew Bennett, University of Nottingham. Briefly, these cells were isolated from the femur of C3H Heston mice (contain mutation in toll-like receptor 4 gene) as described by Gandino and Varesio, and were supplied as immortalised for experimentation (Gandino and Varesio, 1990).

The cells were cultured at 37°C and 5 % CO2 in RPMI-1640 medium modified with HEPES, L-glutamine and phenol red. This medium was supplemented with 10 % (*v/v)* foetal bovine serum, 1 % (*v/v)* penicillin and streptomycin and ß-mercaptoethanol (0.05 mM) to make complete medium until they reached 80-90 % confluence. The complete medium recipe is shown in Table 4. To passage cells they were washed with PBS before treated for 5 minutes with 5 ml trypsin-EDTA at 37°C. The trypsin was neutralised with 10 ml media before centrifugation of cell suspension at 350 g for 5 minutes. The supernatant was aspirated, and cells resuspended in 5 ml media. A haemocytometer was used to count the cells before resuspension in flask or plate for further culture or experimental set up.

For modulation of macrophage populations, the iBMDM cells were cultured in tissue culture treated plates for 24 hours in complete medium supplemented with the respective cytokines for 72 hrs. For M1 the cytokines and concentrations were 100 ng/ml LPS and 20 ng/ml IFN-γ, and 50 ng/ml granulocyte-macrophage colony-stimulating factor (GM-CSF) and for M2 20 ng/ml IL-4, and 50 ng/ml macrophage colony-stimulating factor (M-CSF) were used. Following treatment, the cells were analysed using ELISAs for characterisation of the cell subgroups, as described in section 2.2.4.

2.2.3 Addition of microparticles to THP-1/ iBMDM for polarisation to macrophage subgroups

THP-1 cells were cultured as described in section 2.2.1 and seeded at 500,000 in tissue culture treated 12-well plates. The cells were then differentiated using PMA as described in section 2.2.1 for 24 hrs, before a 48 hr rest in fresh media. 1 mg of microparticles were weighed and soaked in 1.5 ml media (no9 supplements) on a rocker (60 rpm) at 37°C for 24 hrs. Following this, the particles were centrifuged and supernatant was discarded. They were resuspended in fresh complete media to be added to the cell containing plate. The cells were then incubated with specific cytokines stated above or 1 mg IL-4 containing microparticles either in transwells (indirect) (665610, Greiner, UK) or direct contact with the cells. Blank, water containing microparticles were also added to separate wells with direct contact to the cells as a further control.

iBMDM cells were cultured as described in section 2.2.2 and seeded at 100,000 in tissue culture treated 12-well plates. The cells were then incubated with cytokines and microparticles as for the THP-1 cells. Experimental set up is summarised in Table 2.5. Exogenously treated M2 control was treated daily with IL-4 for a direct comparison to the IL-4 released from the microparticles. The exact concentrations were calculated based on the release data obtained from the microparticle release study. These exact concentrations are shown in Table 2.4. Supernatants were harvested at days 3 and 7 and analysed using various methods for characterisation of the cell subgroups including enzyme-linked immunosorbent assay (ELISA) and qualitative polymerase chain reaction assay

(qPCR), methods described in section 2.2.4. Exogenous IL-4 treatment concentrations used for $M_{(IL-4)}$ exogenous reference based on calculations in Chapter 4.

Table 2.4: Microparticle induced THP-1/ iBMDM polarisation to macrophage subgroups experimental set up following PMA treatment. Cytokine concentration the same on each treatment unless stated otherwise.

Cell Subpopulation	**Cytokines & Concentration (ng/ml)**	**Treatment Day & Concentration IL-4 (ng/ml)**		**Microparticles**
M0	Media only	N/A		N/A
$M_{(LPS, IFN\gamma)}$ Reference	LPS (100), IFNy (20), GM-CSF (50)	N/A		N/A
$M_{(IL-4)}$ Reference	M-CSF (50)	N/A		N/A
	IL-4 (various)	**1**	25.65	
		2	22.90	
		3	13.79	
		4	4.46	
		5	6.47	
		6	7.17	
M0	Media only	N/A		IL-4 MPs (in transwells)
M0	Media only	N/A		IL-4 MPs (direct contact)
M0	Media only	N/A		Blank MPs (direct contact)

2.2.4 Enzyme-linked immunosorbent assay cell analysis

Following cell culture as described in section 2.2.3, the cell media was removed, centrifuged at 250 g for 5 minutes before frozen in fresh eppendorfs at -20°C. The samples were then analysed using an enzyme-linked immunosorbent assay (ELISA) to determine the presence of macrophage phenotypes. For THP-1 cells, human TNF-α (EH3TNFA, Invitrogen, UK) was used as a marker for $M_{(LPS, IFN\gamma)}$ and human IL-1receptor antagonist (IL-1ra) (CHC1183, Invitrogen, UK) a as a marker for $M_{(IL\text{-}4)}$. For iBMDM cells, murine TNF-α (10272923, Fischer Scientific, UK) was used for $M_{(LPS, IFN\gamma)}$ and murine IL-10 (BMS614INST, Invitrogen, UK) as a marker for $M_{(IL\text{-}4)}$.

The TNFα concentration in the cell media was measured using a commercial ELISA kit (minimum detection 2 pg/ml, BD) following the manufacturer's instructions. Briefly, 50 µl of ELISA diluent was added with 100 µl sample/ standard (500 - 7.8 pg/ml) to plate and incubated at room temperature for 2 hrs on microplate shaker. The well contents were aspirated and washed 5 x using manufacture provided wash buffer, before incubation for 1 hr with 100 µl working detector. Wash steps were repeated 7 x before incubation in the dark for 30 minutes with 100 µl TMB one-step substrate reagent. Following incubation, 50 µl stop solution was added to the wells and absorbance read at 450 nm.

The IL-1ra concentration was measured using a commercial ELISA kit (minimum detection 4 pg/ml, Invitrogen) following manufacturer's instructions. Briefly, 100 µl of incubation buffer was added with 100 µl sample/ standard (2000-31.2 pg/ml) to plate and incubated with 50 µl biotin conjugate at room temperature for 2 hrs on microplate shaker. The well contents were aspirated and washed 3 x using manufacture provided wash buffer, before incubation for 1 hr with 100 µl diluted streptavidin-HRP. Wash steps were repeated 4 x before incubation in the dark for 30 minutes with 100 µl chromogenic solution. Following incubation, 100 µl stop solution was added to the wells and absorbance read at 450 nm.

The concentration of IL-10 was assessed for the experiments using iBMDM cells using the manufacturer's instructions (minimum detection 5.28 pg/ml, Invitrogen). Briefly, 150 µl distilled water was added to standard wells to generate a serial dilution of standards from 2500 - 39.1 pg/ml. 100 µl distilled water added to sample wells along with 50 µl sample. Plate was sealed and incubated for 3 hrs at room temperature on a microplate shaker. Wells were aspirated and washed 4 x before incubation with 100 µl TMB substrate for 10 minutes at room temperature. Stop solution (100 µl) was added to all wells and absorbance was read immediately at 450 nm.

All ELISA standards were made as per manufacture guidelines and absorbance values were corrected for blank standard reading.

2.2.5 Cell gene expression kinetics by real-time qPCR

Following cell culture as described in section 2.2.3, cells were treated with 200 µl trypsin for 10 minutes at 37 °C and transferred into eppendorfs. They were then centrifuged at 250 g for 5 minutes before removal of liquid and resuspension in 300 µl RLT buffer. The cell pellets in RLT buffer were stored at -80 °C prior to analysis with real-time qPCR to determine gene expression of specific cell markers. The total RNA was extracted using RNeasy mini kit (Qiagen, USA) according to manufacturer's instructions with an RNase-free DNase (Qiagen) treatment at room temperature for 15 min. The resulting RNA was quantified using a Nanodrop (Labtech, UK). Following extraction, the RNA was used to synthesise complementary DNA (cDNA) using SuperScript III First-Strand Synthesis SuperMix (Invitrogen, UK) according to manufacturer's instructions. In brief, 1 µl of 10 mM dNTP and 1 µl of random hexamer (250 ng/µl) were mixed with 11 µl of nuclease-free water (Sigma-Aldrich, UK). The reaction mix was then transferred to a thermocycler (PX2) and incubated at 65°C for 5 min to allow denaturation followed by quenching on ice for 1 min. Reaction Master Mix consisting of 4 µl of first strand buffer, 1 µl DTT, 1 µl RNase-OUT and 1 µl superscript III enzyme was prepared and added to the reaction mix. A final volume of 20 µl sample was incubated in the thermo-cycler for 10 min at 25°C then 50 min at 50°C and finally the reaction was ended by heating for 5 min at 80°C. The synthesised cDNA was mixed with Taqman master mix and specific gene primers (ThermoFisher Scientific, UK) in a 20 µl reaction volume. The specific gene primers used are displayed in Table 2.5.

Table 2.5: Specific gene primers and their working concentrations. All purchased from ThermoFisher Scientific.

Gene Name	Accession Number	Species	Cell Target
MMP-9	Hs0095752	Human	Pan-macrophage marker
TNF-α	Hs00174128	Human	$M_{(LPS,\ IFN\gamma)}$
MRC1	Hs00267207_m1	Human	$M_{(IL\text{-}4)}$
ACTβ	Hs01060665	Human	Housekeeping Gene

The mix was pre-heated at 95°C for 90 seconds, followed by PCR for 40 cycles, denaturing temperature of 95°C for 10 seconds, annealing temperature of 58°C for 10 seconds, and elongation temperature of 72°C for 15 seconds, and finally elongation temperature of 72°C for 2 min. Actin-β (ACTβ) was chosen as a housekeeping gene because it has been shown to be stably expressed in both THP-1 monocytes and macrophages (Maeß *et al.*, 2010). Obtained Ct values for target genes were corrected against the housekeeping gene Ct and relative quantification was calculated as fold change compared to M0.

2.2.6 Statistical Analysis

Throughout the experiments described in this research one-way ANOVAs were used to analyse the experimental datasets with Tukey's multiple comparisons test. Significance was defined by $p<0.05$.

Chapter 3: Microparticles fabrication with commercial release modifiers as a method to obtain a controlled drug delivery system

3.1 Introduction

The overall aim was to develop a microparticle system for the controlled release of IL-4. Microparticles were chosen as the delivery method for this project due to the ability to modulate their release. Controlled and sustained release kinetics were desired to enable daily release of IL-4 and therefore a single dose required for a patient when used as a therapy. The idea behind the hypothesis was to reduce the need for daily injections of intravenous IL-4 and have a single injection of IL-4-containing microparticles. This would be more cost effective and less of a burden on the patient. The specific aim for this chapter was to determine if a commercially purchased release modifier could result in a microparticle formulation with a suitable release profile for sustained controlled release of lysozyme as a model protein for IL-4.

The specific microparticle objectives explored in this chapter, as described in Chapter 1, were modification to microparticle formulation by:

1. Variations of the lactide:glycolide ratio.
2. Addition of polaxamers F127 or P188 in different quantities, these were evaluated at 10 %, 20 %, 30 % and 40 % (*w/w)* of total polymer.

This chapter shows the comparison of release kinetics from microparticles made with different percentages of F127 and P188 using both 50:50 and 85:15 PLGA. Commercially purchased modifiers were chosen due to their low polydispersity and lack of batch-to-batch variation in properties. F127 and P188 were chosen specifically due to their non-toxicity (Wang *et al.*, 2016) and the hypothesis they could modulate release from PLGA microparticles by increasing the particle hydrophilicity (Leo *et al.*, 2006; Ma and Song, 2006; Parajó, *et al.*, 2010; Gujral *et al.*, 2013).

Poly(lactic-co-glycolic acid) was chosen as the main polymer for microparticle manufacture in this project due to its tailorable release properties, and biodegradability as well as its well documented use in literature (Atala, 2012; Kim *et al.*, 2012; Huang *et al.*, 2013; Rambhia and Ma, 2015; Mir *et al.*, 2017b) Drug release occurs over different time scales depending on the polymer and drug used. For example, PLGA 85:15 takes longer to degrade than PLGA 50:50, due to less hydrophilicity and would therefore release at a slower rate via polymer degradation. A large or hydrophobic drug may take longer to release as less suited to move through polymer pores or undergo release via osmosis (Fredenberg *et al.*, 2011). However, many applications require delivery at a faster or slower rate and via certain kinetics, for example a fast burst release at day 1 or prolonged release over 50 days. Here microparticles have an advantage over other methods of delivery, such as scaffolds, hydrogels or intravenous delivery. Microparticles can be formulated and tailored to particular release kinetics and applied in a single dose rather than multiple which is often required for intravenous delivery. The desired release kinetics for this project were a

small burst release at day 1 followed by continuous sustained release. The use of microparticles formulated from PLGA alone was hypothesised to not enable sufficient protein release between days 1 and 14 due to the slow degrading polymer, and for this reason a modifier was included. The addition of various release modifiers to obtain controlled sustained release have been explored in literature, including the use of a PLGA-PEG-PLGA triblock and polaxamers (Chen *et al.*, 2005; Tran *et al.*, 2012; White *et al.*, 2013). These modifiers act by increasing the hydrophilicity of the polymer and therefore increasing the speed of release via water filled pores and osmotic pumping, in this manner the release is decoupled from the degradation of the polymer. Alternative commercially purchased release modifiers were explored prior to triblock due to the desire to reduce processing and batch variation, in particular polaxamers F127 and P188. These modifiers were chosen as they were non-cytotoxic and expected to increase particle hydrophilicity in a similar way to triblock due to the multiple hydroxyl groups in the polymer structure. The expectation was that increasing percentages of F127 or P188 in the microparticle formulation would result in faster release due to osmosis or through water filled channels in the particle structure. F127 and P188 were also expected to have less batch-to-batch variation due to commercial purchasing and therefore have an advantage over the in-house synthesised triblock. The chemical structure of F127 and P188 are shown in Figure 3.1.

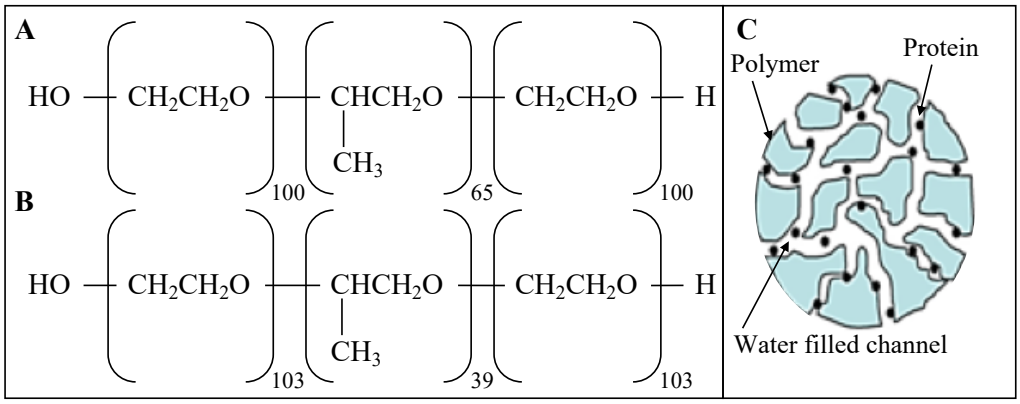

Figure 3.1: Chemical structure for polaxamers (**A**) F127 and (**B**) P188. (**C**) Microparticle structure showing water filled channels. (Adapted from Fredenberg *et al.*, 2011).

Polaxamers F127 (Figure 3.1 A) and P188 (Figure 3.1 B) have many uses as biomaterials, mainly due to their thermoresponsive properties, however there is very little work exploring their use as a microparticle release modifier (Wang *et al.*, 2016). Despite the lack of literature, Wang *et al* showed work using F127 to obtain sustained release of a drug from PLGA microparticles by decoupling release from the polymer degradation and encouraging release via osmosis and through pores or channels in the particle structure. The hypothesis was that the F127 or P188 polymer would homogenously disperse between the PLGA structure with hydrophilic areas creating channels throughout the structure and the outside surface of the particle with hydrophobic areas on the inside. A schematic of the microparticle structure is shown in Figure 3.1 C. Parajo *et al*

displayed a similar finding to that shown by Wang *et* al with P188, where addition of the release modifier increased the speed of release suggesting that F127 and P188 could be used for this project to obtain sustained release (Parajó *et al.*, 2010; Wang *et al.*, 2016). The hypothesis was that the use of polaxamers F127 or P188 would provide a similar release pattern with PLGA microparticles to that shown in literature with a PLGA-PEG-PLGA triblock (White *et al.*, 2013) and could therefore be used as a commercially purchased alternative.

A model protein was chosen in place of IL-4 during the optimisation stages of this project due to the cost of IL-4. Lysozyme from chicken egg white was chosen as a suitable model as it had a similar isoelectric point (Lysozyme: 11.35, IL-4: 9.17) and molecular weight to IL-4 (Lysozyme: 16.2kDa, IL-4: 17.5kDa) (*UniProtKB - P00698 (LYSC-CHICK)*, 1986; *UniProtKB - P05112 (IL4_HUMAN)*, 1987). It was therefore assumed that the model protein would behave in a similar manner once encapsulated and when released from the microparticles. Other work, particularly by White *et al* have shown lysozyme release from PLGA microparticles and provides a basis for the microparticle formulations used for optimisation in this project (White *et al.*, 2013). Figure 3.2 shows the protein structure of lysozyme and IL-4.

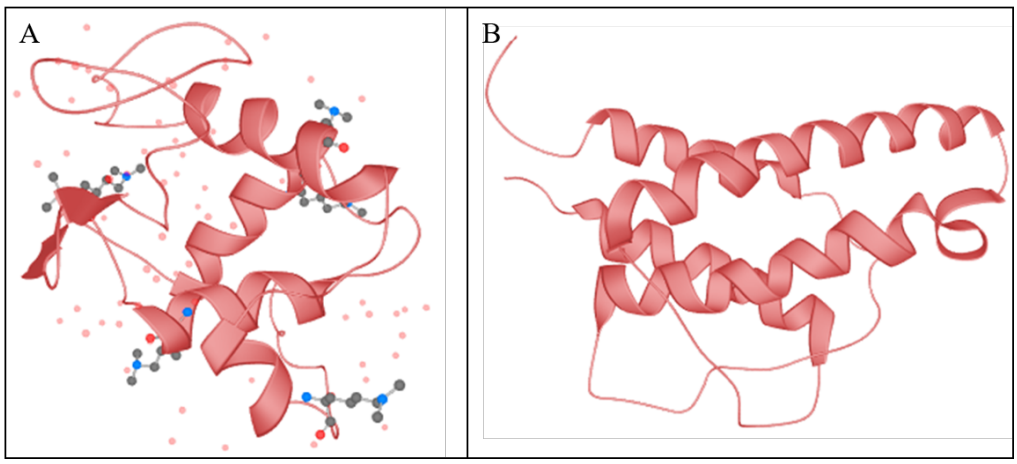

Figure 3.2: Schematic showing the structure of **(A)** Lysozyme made up of 147 amino acids folded into alpha helices and beta pleated sheets with mass of 16,239Da; and **(B)** IL-4 made up of 153 amino acids folded into alpha helices and beta pleated sheets with mass of 17,492 Da. Adapted from UniProt.org (*UniProtKB - P00698 (LYSC-CHICK)*, 1986) (*UniProtKB - P05112 (IL4_HUMAN)*, 1987).

3.2 Experimental Design

3.2.1 Microparticle preparation by double emulsion and characterisation

Microparticles were prepared as described in section 2.1.2 using 50:50 lactide to glycolide ratio PLGA or 85:15 lactide to glycolide ratio PLGA and a copolymer release modifier consisting of poloxamer F127 10 %, 20 % or 30 % *w/w* or poloxamer P188 20 % or 40 % *w/w*. The specific microparticle formulations discussed in this chapter are shown in Table 3.1 and were fabricated at 20 % *w/v* total polymer. Microparticles were characterised using SEM for surface morphology and laser diffraction for the size distribution as detailed in section 2.1.3.

TABLE 3.1: Microparticle formulations containing commercial release modifiers used in biomaterial experimental design.

Modifier	**Formulation (% *w/w*)**
No Modifier	50:50 0 %
F127	50:50 10 % F127
	50:50 20 % F127
	50:50 30 % F127
P188	50:50 20 % P188
	50:50 40 % P188
No Modifier	85:15 0 %
F127	85:15 10 % F127
	85:15 20 % F127
	85:15 30 % F127
P188	85:15 20 % P188
	85:15 40 % P188

3.2.2 Microparticle encapsulation efficiency and release study comparison

Encapsulation efficiency and protein release was measured using a micro BCA assay as described in section 2.1.4.1. A human IL-4 ELISA was also used to assess the concentration of IL-4 in release supernatant following release study on IL-4 batches as described in section 2.1.4.2.

3.3 Results

3.3.1 Release modifier characterisation: molecular weight and polydispersity comparison between F127 and P188

The polymer dispersity of F127 and P188 were determined using gel permeation chromatography (GPC), as described in section 2.1.1, as a measure of the distribution of the molecular mass in a polymer sample with a dispersity of 1 indicating a monodisperse polymer chain and to determine the polymer molecular weight as described in section 2.1.1. The results are shown in Table 3.2.

Table 3.4: Gel permeation chromatography results for F127 and P188 release modifiers.

	M_W (Da)	Polymer Dispersity
F127	240432	2.72129
P188	12426	1.05985

The polymer dispersity was much greater for F127 than for P188, but as these were commercially purchased polymers the values were considered to be standardised due to commercial large batch processing. The molecular weight was also higher for F127 at 24 kDa compared to 12 kDa for P188.

3.3.2 Microparticle characterisation: particle morphology and size distribution comparison between F127 and P188 formulations

PLGA microparticles containing encapsulated HSA:lysozyme were produced using the double emulsion method described in section 2.1.2. The particles were then characterisation using scanning electron microscopy and coulter sizing analysis. The SEM images, sizing distributions and average particle diameters are shown in Figures 3.3 - 3.6 for representative microparticle formulations at 20 % (*w/v)* total polymer. Images and size distributions for all F127 and P188 batches can be found in the supplementary data, section 7.1.1.

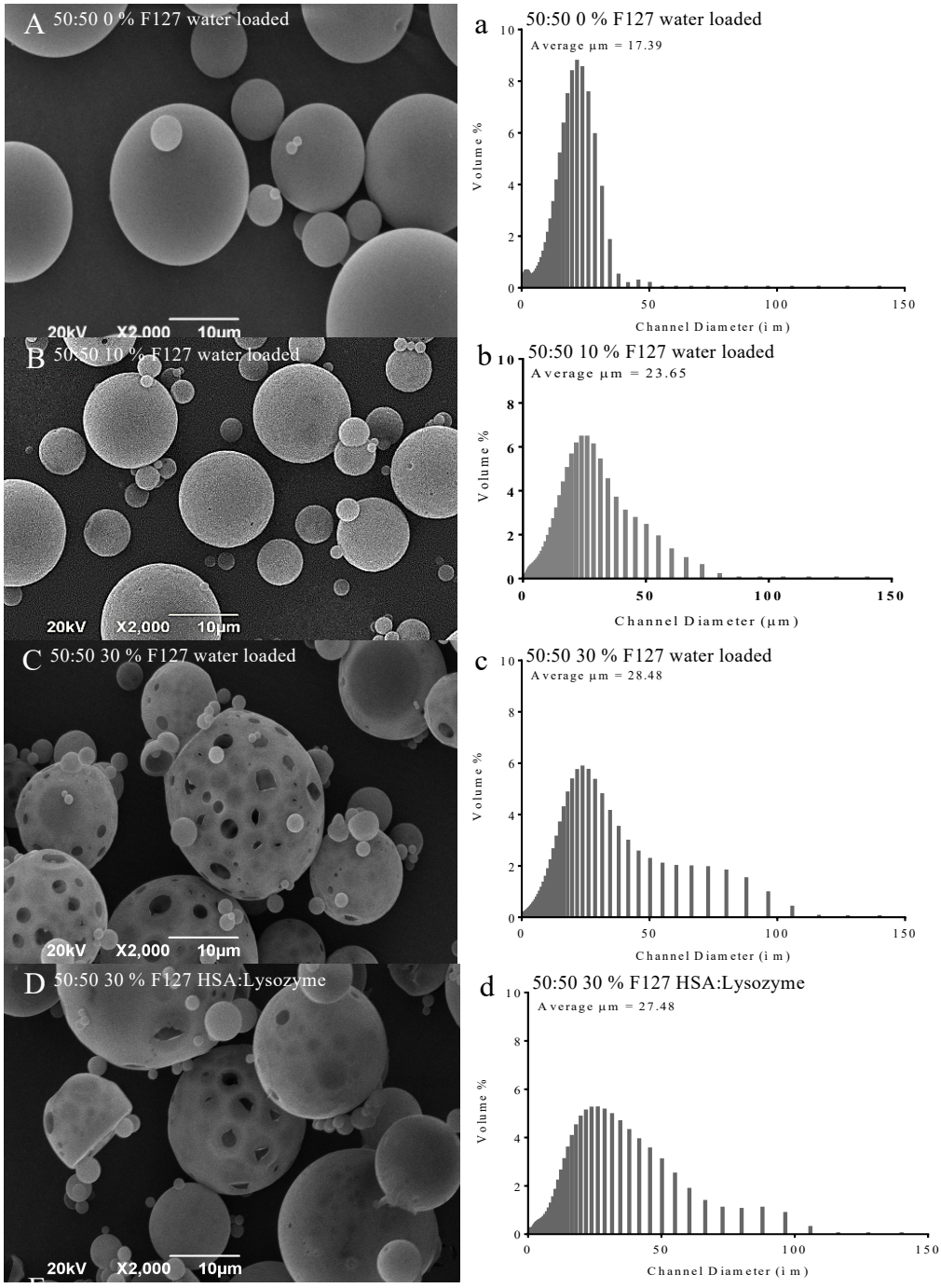

Figure 3.3: Morphology (left hand column) and size distributions (right hand column) from 20 % (*w/v)* total polymer microparticles from 50:50 PLGA with different percentages of F127 containing water or HSA:lysozyme. **(A/ a)** 0 % *w/w* F127, water loaded, **(B/ b)** 10 % *w/w* F127, water loaded, **(C/ c)** 30 % *w/w* F127, water loaded, **(D/ d)** 30 % *w/w* F127, HSA:Lysozyme.

The particles manufactured with F127 by the double emulsion method displayed similar morphology to those in literature made without F127 (Leo *et al.*, 2006), they were smooth surfaced and spherical. The particles shown in Figure 3.3 were of similar sizing, between 15 - 28 μm diameters, although in comparison of Figure 3.3 a and b it appeared that the addition of F127 resulted in increased size. The addition of F127 also appeared to increase the average size and broaden the size distribution, with average μm diameter for 0 % *w/w* F127 17.39 μm and for 30 % *w/w* F127 28.48 μm (Figure 3.3 a and c). It has also been shown in Figure 3.3 that the addition of F127 broadened the size distribution, where the bell curve distribution shown for 0 % *w/w* F127 (Figure 3.3 a) was narrower than the distribution shown for 10 and 30 % *w/w* F127 both with and without HSA:lysozyme (Figure 3.3 b, c, and d).

There appeared to be a direct correlation between F127 and the presence of particle pores, where those with increasing percentages of F127 appeared to be increasingly porous as seen in the SEM images for 0, 10 and 30 % *w/w* F127 in Figure 3.3 A, B and C. The 0 % *w/w* F127 microparticles displayed minimal to no pores as expected, in comparison to 30 % *w/w* F127 which was porous as seen in Figure 3.3 A and C. The particles also appeared to be less stable when manufactured with F127 at all percentages, with some particles collapsed or less spherical than those manufactured without F127 (Figure 3.3 C and D). The addition of HSA:lysozyme did not appear to effect the morphology or size distribution of the particles as can be seen in a comparison of Figure 3.3 C, D and c, d.

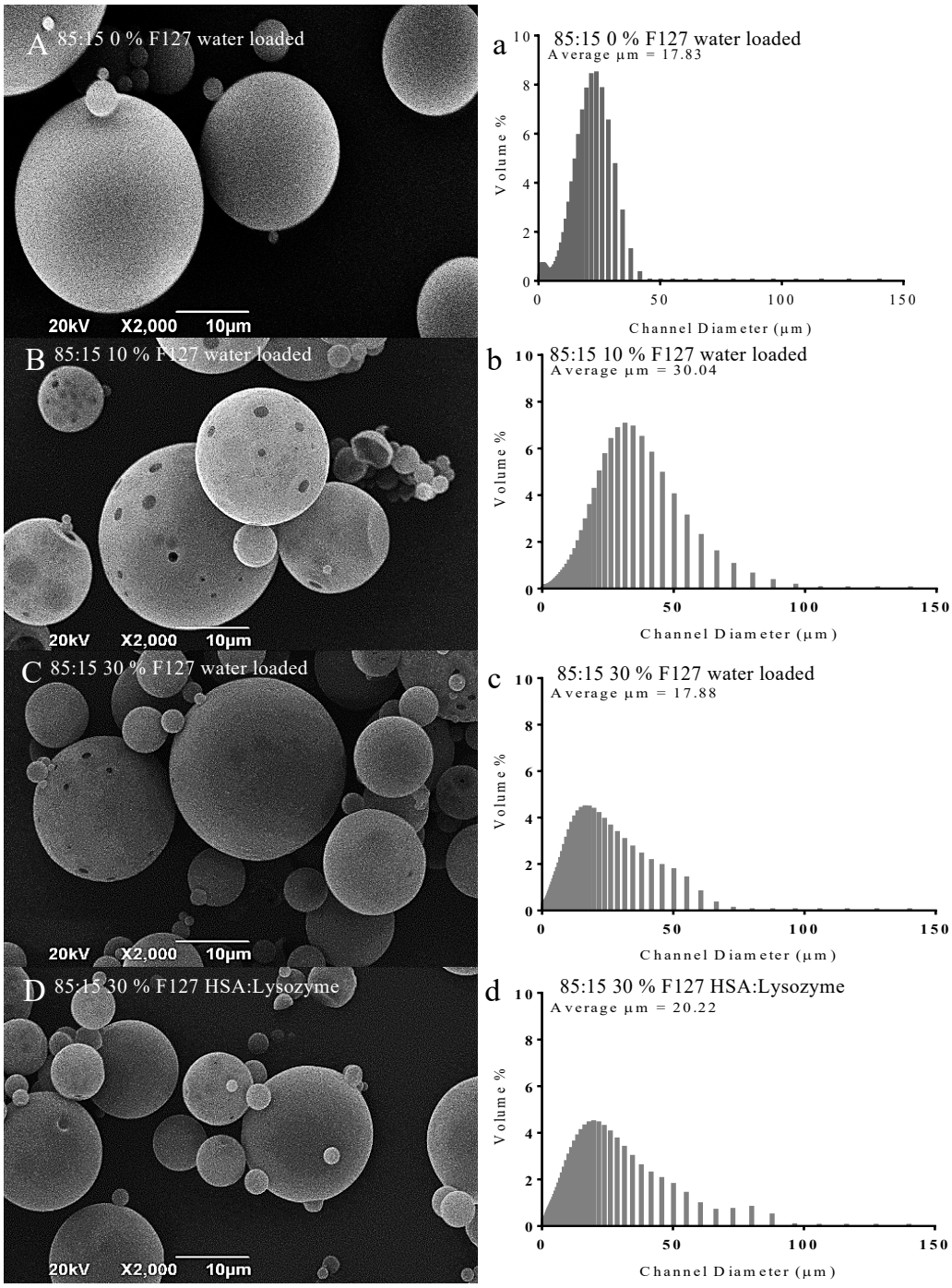

Figure 3.4: Morphology and size distribution from 20 % (*w/v)* total polymer microparticles from 85:15 PLGA with different percentages of F127 containing water or HSA:lysozyme. **(A/ a)** 0 % *w/w* F127, water loaded, **(B/ b)** 10 % *w/w* F127, water loaded, **(C/ c)** 30 % *w/w* F127, water loaded, **(D/ d)** 30 % *w/w* F127, HSA:Lysozyme.

In a comparison of polymer lactide to glycolide ratios, the effect of F127 on the microparticle morphology did not appear to differ between 50:50 and 85:15 PLGA as shown in Figures 3.3 and 3.4. The effect of lactide to glycolide ratio on the size distribution was also minimal, with average μm diameter for 50:50 PLGA 0 % *w/w*, 17.83 μm (Figure 3.3 a) and for 85:15 PLGA 0 % *w/w*, 17.88 μm (Figure 3.4 a). The addition of F127 appeared to have less effect on the morphology of the particles manufactured from 85:15 PLGA. From Figure 3.4, the addition of F127, particularly 10 % *w/w* (Figure 3.4 B) resulted in porous particles. However, these particles were not as porous as was seen in Figure 3.3 B for the particles made from 50:50 PLGA. The effect of F127 on the particle size distribution for 85:15 PLGA was similar to that shown in Figure 3.3 for 50:50 PLGA. The addition of 10 % *w/w* F127 resulted in larger particles compared to 20 % and 30 % *w/w* with an average particle diameter of 17.88 – 30.04 μm, but the broadening of the size distribution was similar to that seen with 50:50 PLGA. As seen in both Figure 3.3 D, d and Figure 3.4 D, d, the addition of HSA:lysozyme to the particles did not appear to have an effect on the surface morphology or the size distribution.

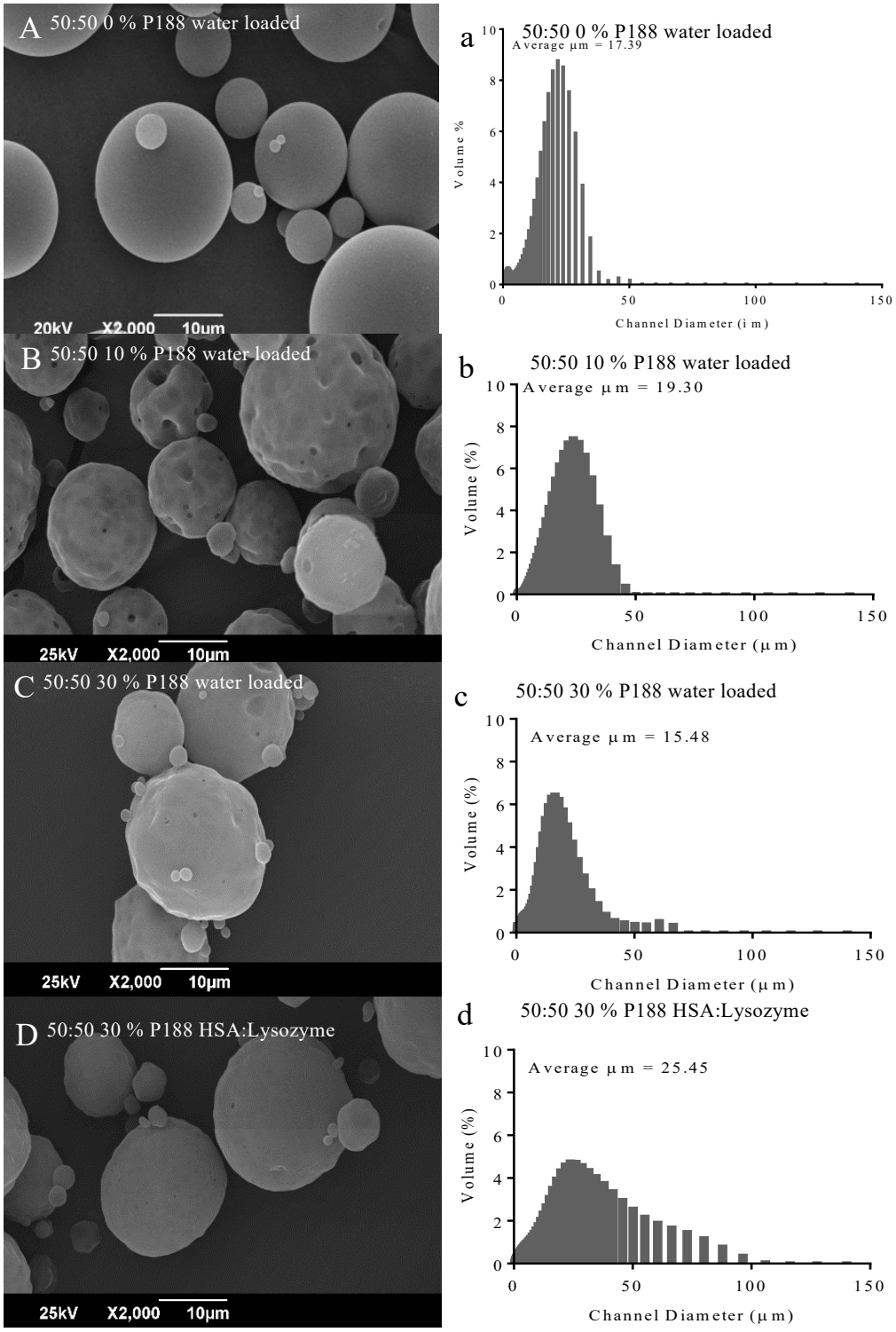

Figure 3.5: Morphology and size distribution from 20 % (*w/v)* total polymer microparticles from 50:50 PLGA with different percentages of P188 containing water or HSA:lysozyme. **(A/ a)** 0 % *w/w* P188, water loaded, **(B/ b)** 10 % *w/w*

P188, water loaded, **(C/ c)** 30 % *w/w* P188, water loaded, **(D/ d)** 30 % *w/w* P188, HSA:Lysozyme.

The particles manufactured using P188 displayed similar morphology to those made without P188 as shown in Figure 3.5, however the morphology appeared more irregular with some particles more disk shaped rather than spherical. The addition of P188 appeared to result in particles with dimpled surfaces and pores, as can be seen particularly in Figure 3.5 B. The particles containing P188 were also not a spherical in shape as those without P188 (Figure 3.5 A). P188 did not however, appear to affect the particle size distribution with the average diameter of 0 % *w/w* P188 20.94 µm and 10 % *w/w* P188 19.30 µm. The addition of HSA:lysozyme did not appear to have an effect on the particle surface morphology as can be seen in a comparison of Figure 3.5 C and D. The particle batch containing HSA:lysozyme did appear to have a broader size distribution than those containing water (Figure 3.5 D).

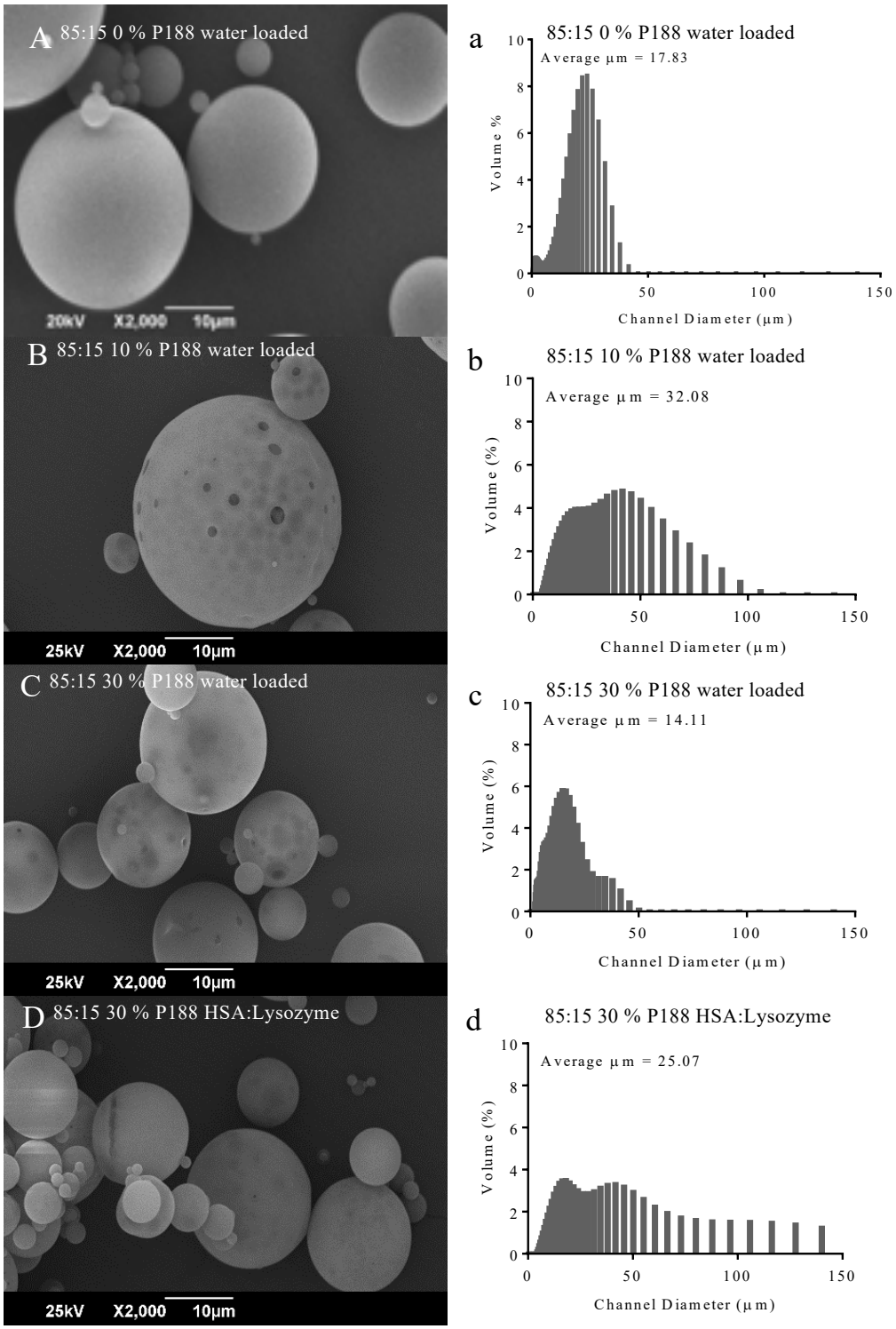

Figure 3.6: Morphology and size distribution from 20 % (*w/v)* total polymer microparticles from 85:15 PLGA with different percentages of P188 containing water or HSA:lysozyme. **(A/ a)** 0 % *w/w* P188, water loaded, **(B/ b)** 10 % *w/w*

P188, water loaded, **(C/ c)** 30 % *w/w* P188, water loaded, **(D/ d)** 30 % *w/w* P188, HSA:Lysozyme.

The particles made with 85:15 shown in Figure 3.6 appeared to have a smoother surface than those made with 50:50 PLGA shown in Figures 3.5. The particles shown in Figure 3.6 more closely resemble the particles made with F127 (Figure 3.3 and 3.4). The particles made with P188 were of similar average size to those made with the equivalent percentages of F127, however the size distribution was broader for the particles containing P188 as can be seen in a comparison of Figures 3.3 – 3.6. As was seen in Figure 3.5 for the particles made with 50:50 PLGA, the addition of P188 to 85:15 PLGA resulted in irregular or porous particle surfaces, as can be seen particularly in Figure 3.6 B for 10 % *w/w* P188. The particles containing P188 also appeared to have a dimpled surface, although not as irregular as those seen in Figure 3.5 for 50:50 PLGA. As seen for the particle formulations previously discussed with F127, the addition of HSA:lysozyme did not have an effect on the morphology or the average particle diameter when used with P188 for 85:15 PLGA, shown in Figure 3.6 d. However, the addition of HSA:lysozyme did result in a much broader size distribution and an increased size from 14 to 25 μm (Figure 3.6 d), in a similar manner to that shown for 50:50 PLGA in Figure 3.5 d.

3.3.3 Microparticle encapsulation efficiency and protein release: comparison of the effect of F127 and P188 on microparticle protein encapsulation and release kinetics

The encapsulation efficiency and release profiles of the microparticles were determined using a micro BCA protein activity assay as described in section 2.1.3. Encapsulation efficiency results are displayed in Table 3.3 where blank particles contain H_2O and loaded particles contain 10 mg/ml HSA:lysozyme. As described in section 2.1.3, the encapsulation efficiency was calculated by subtracting the absorbance readings from the blank particles from the absorbance readings of the same microparticle formulation containing protein to account for background readings. A percentage of total encapsulated protein was then calculated using the following equation: ((amount of protein (μg))/(mass of microparticles x 10))/ 100. The standard deviations (SD) were calculated between triplicates.

Table 3.3: Average size (µm) and encapsulation efficiency (% *w/w*) of microparticles fabricated from PLGA and release modifiers F127 and P188 (± indicates standard deviation from triplicates).

PLGA	Release Modifier		Blank/ Protein	Average Size (µm)	Average Encapsulation Efficiency (%*w/w*)
	Type	Percentage (% *w/w*)			
50:50	-	0	Blank	20.94 ± 9.29	-
			Protein	23.51 ± 9.33	68.80 ± 5.76
50:50	F127	10	Blank	23.65 ± 12.02	-
			Protein	29.14 ± 13.49	23.03 ± 2.14
50:50	F127	20	Blank	27.23 ± 17.80	-
			Protein	32.38 ± 21.47	21.89 ± 4.03
50:50	F127	30	Blank	28.48 ± 21.41	-
			Protein	27.48 ± 20.00	49.96 ± 6.15
85:15	-	0	Blank	22.95 ± 9.58	-
			Protein	23.03 ± 8.44	78.03 ± 7.12
85:15	F127	10	Blank	30.04 ± 17.05	-
			Protein	27.38 ± 16.10	18.90 ± 2.48
85:15	F127	20	Blank	20.25 ± 10.35	-
			Protein	17.18 ± 10.66	29.41 ± 2.78
85:15	F127	30	Blank	17.88 ± 14.07	-
			Protein	20.22 ± 16.91	19.45 ± 1.34
50:50	P188	20	Blank	19.30 ± 9.89	-
			Protein	24.76 ± 13.10	33.50 ± 4.78
50:50	P188	40	Blank	15.48 ± 11.04	-
			Protein	25.45 ± 20.06	104.00 ± 9.89
85:15	P188	20	Blank	32.08 ± 20.99	-
			Protein	18.92 ± 13.97	65.15 ± 6.88
85:15	P188	40	Blank	14.11 ± 9.04	-
			Protein	25.07 ± 14.77	20.22 ± 3.67

The results displayed in Table 3.3 suggested that the addition of F127 did not significantly change the encapsulation efficiency, however a lower efficiency was seen for the 85:15 microparticle batches in comparison with the 50:50, especially for the 10 % *w/w* and 30 % *w/w* F127 formulations. This difference could be attributed to inter-operator variability or could also be explained by the increased porosity of the 85:15 microparticle batches as can been seen in the SEM images in Figure 3.4 (C). The encapsulation efficiencies for particles containing F127 were lower than that seen for particles manufactured from the same PLGA without F127 with the exception of 30 % *w/w*. There was some variation in average size between different batches of microparticle however, there did not appear to be a correlation between addition of F127 or protein and the average size, despite the standard deviation. The encapsulation efficiencies shown in Table 3.3 for particles containing P188 was higher than those seen for F127, especially for the particles manufactured from 85:15. This could be due to the increased amount of pores seen in the particle surface of those made with F127 and therefore the leakage of protein through pores on contact with an aqueous solution, for example in the washing step of manufacture. As was seen for the particles made with F127 there did not appear to be a correlation between average size and addition of P188 or protein.

The cumulative protein release was compared from the different microparticle formulations in order to determine the effect of F127 and P188 on protein release with the aim of identifying a formulation with sustained and controlled release. Protein release results are displayed as cumulative percentage release for

particles made from 20 % (*w/v)* total polymer with different percentages of F127 or P188 with 50:50 PLGA and 85:15 PLGA shown in Figure 3.7. Cumulative µg protein/mg particles data can be found in supplementary data, section 7.1.1 for each microparticle formulation.

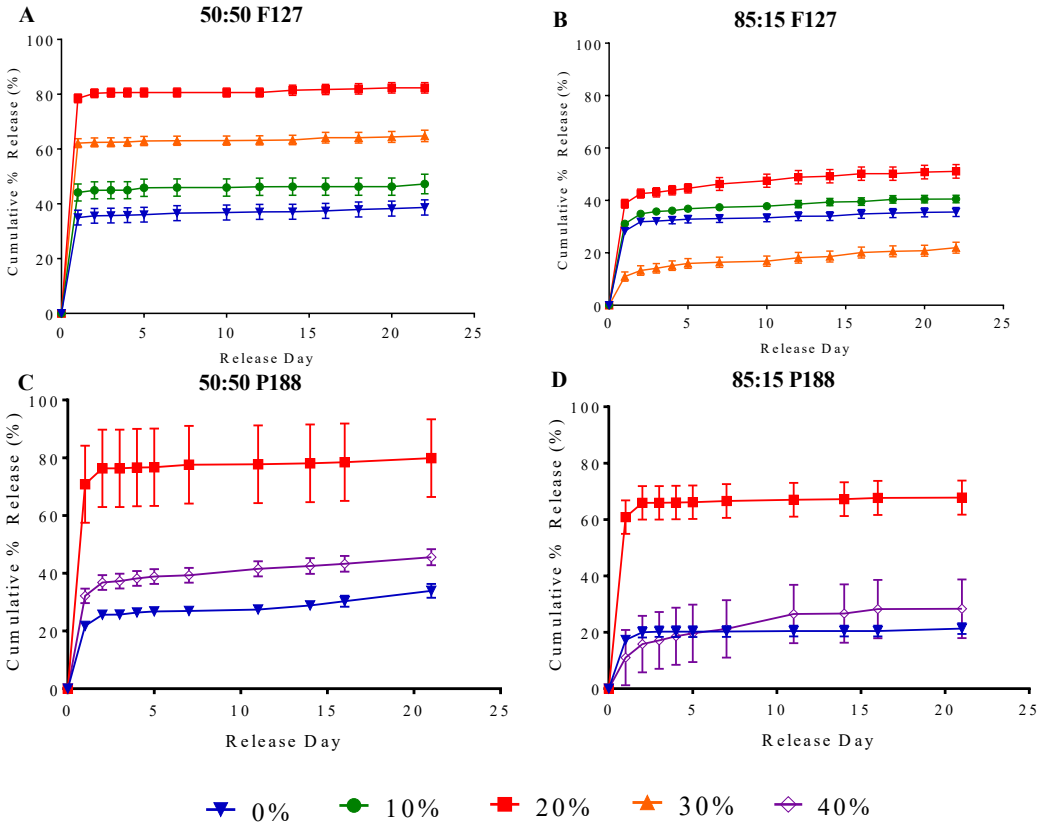

Figure 3.7*:* Cumulative percentage release (% *w/v*) from microparticles fabricated from PLGA and release modifiers F127 (A, B) and P188 (C, D) where coloured symbols are consistent for proportion of modifier included. **(A)** 50:50 PLGA polymer microparticles with 0, 10, 20 and 30 % *w/w* F127, **(B)** 85:15 PLGA polymer microparticles with 0, 10, 20 and 30 % *w/w* F127, **(C)** 50:50 PLGA polymer microparticles with 0, 20 and 40 % *w/w* P188, **(D)** 85:15 PLGA polymer microparticles with 0, 20 and 40 % *w/w* P188**.** All formulations**:** (N1,

n3). Results have been adjusted to account for the encapsulation efficiency. Error bars represent cumulative standard deviation calculated from triplicates.

As can be seen in Figure 3.7 A, the addition of F127 to particles made with 50:50 PLGA did have an effect on the cumulative protein release, especially the initial burst release at day 1. Unexpectedly, the formulation containing 20 % *w/w* F127 resulted in the fastest burst release, followed by 30 % *w/w* and 10 % *w/w*, with 0 % *w/w* showing the slowest release as expected. The subsequent release after day 1 was minimal for all formulations and therefore none of these could be considered a sustained release profile. In comparison, in the formulations with 85:15 (Figure 3.7 B), the effect was less evident for the 50:50 formulations. As can be seen in Figure 3.7 B, the addition of F127 did affect the protein release in a different manner to that seen in Figure 3.7 A for 50:50 PLGA. The initial burst release was less for the 85:15 formulations and showed more controlled protein release post-day 1 unlike the release shown for 50:50 PLGA. As seen for 50:50 PLGA, 20 % *w/w* F127 resulted in the biggest burst release at day 1, but unexpectedly 30 % *w/w* resulted in the slowest release and was slower than the 0 % *w/w* formulation. The 30 % *w/w* formulation displayed a release profile most similar to sustained release, however only reached 20 % *w/v* total protein release after 22 days and was therefore too slow to be considered for this project.

As can be seen in Figure 3.7 C, the addition of P188 to 50:50 PLGA had a similar effect to that seen in Figure 3.7 A for F127. The initial burst release was increased, with 20 % *w/w* P188 resulting in the biggest burst release followed

by 40 % *w/w*. Despite this, the 40 % *w/w* P188 formulation displayed more sustained release than 20 % *w/w* following the initial burst, it was not however much more release than seen for the 0 % *w/w* formulation and followed the same release trend. A similar effect was seen in Figure 3.7 D for P188 use with 85:15 PLGA, where 20 % *w/w* P188 resulted in the largest burst release but little subsequent release. The 40 % *w/w* formulation displayed the release profile most similar to controlled sustained release, with a small burst release at day 1 followed by increasing release up to day 22. However, as was seen in Figure 3.7 B for 30 % *w/w* F127, the release from 40 % *w/w* P188 resulted in around 20 % (*w/v*) total polymer release after 22 days and was therefore too slow to be considered for this application.

In order to make a direct comparison of the initial burst release of each particle formulation, the daily protein release was compiled to show initial burst release at day 1 shown in Table 3.4.

Table 3.4: Combined daily protein release (µg/mg particles) for 50:50 and 85:15 PLGA with different percentages of F127 and P188. Results have been adjusted for the specific encapsulation efficiency for each formulation (Modifier % *w/w)*.

Days	Average daily release HSA/Lysozyme (µg/mg)							
	50:50 PLGA				85:15 PLGA			
	0 % F127	10 % F127	20 % F127	30 % F127	0 % F127	10 % F127	20 % F127	30 % F127
1	3.50	4.41	7.85	6.22	3.13	3.12	3.87	1.09
Days	**50:50 PLGA**				**85:15 PLGA**			
	0 % P188	**20 % P188**		**40 % P188**	**0 % P188**	**20 % P188**		**40 % P188**
1	3.50	7.08		3.21	3.13	6.08		1.10

As shown in Table 3.4, the addition of F127 resulted in increased burst release at day 1 for 50:50 PLGA formulations. The largest burst release was seen for 20 % *w/w* F127, at 7.85 µg/mg compared to 3.50 µg/mg for 0 % *w/w* F127. Unexpectedly, 30 % *w/w* F127 showed a smaller burst release at 6.22 µg/mg than 20 % *w/w* F127. A similar trend was seen for 85:15 PLGA, where 20 % *w/w* F127 resulted in the largest burst release of 3.87 µg/mg compared to 1.09 µg/mg for 30 % *w/w* F127. The effect of F127 was not as great on the particles made with 85:15 PLGA, where initial release from 10 % *w/w* and 20 % *w/w* F127 was 3.12 and 3.87 µg/mg respectively compared to 3.13 µg/mg for 0 % *w/w* F127.

A similar trend to that of F127 was seen for P188, where 20 % *w/w* P188 showed the greatest burst release for both 50:50 and 85:15 PLGA, at 7.08 and 6.08 μg/mg compared to 3.50 and 3.13 μg/mg for 0 % *w/w* P188 respectively. The formulation resulting in release closest to sustained release was 85:15 40 % *w/w* P188 which continued to release protein between days 11-20 as can be seen in Figure 3.7.

3.4 Discussion

When comparing the NMR and GPC results for the commercially purchased F127 and P188, the higher molecular weight of F127 suggested it may have a greater effect on the particle composition due to the interaction of the polymers. Due to the low polydispersity of F127, the expectation was little batch-to-batch variation between microparticles using F127. The variation in molecular weights between P188 and F127 may contribute to different release modifying properties, however this needed to be confirmed with a release study.

In general, the microparticles made from PLGA were smooth, spherical and uniform in morphology as shown for the 0 % *w/w* formulations in this chapter and shown in literature for 85:15 PLGA and 50:50 PLGA microparticles (Vij *et al.*, 2010; Kirby *et al.*, 2011; White *et al.*, 2013; Abu-Awwad *et al.,* 2017). However, this was not the case for the particles containing F127 or P188 as seen in this chapter. The particles containing F127 or P188 were increasingly porous with increasing percentages of copolymer. This could be attributed to the

copolymer increasing the hydrophilicity of the particles and the formation of more water filled pores and channels resulting in a less stable structure and less rigidity (Gujral *et al.*, 2013; Wang *et al.*, 2016). This was similar to work by Leo *et al* who showed the internal structure of PLA/F127 microparticles to have increased channels as well as dimpled surface morphology (Leo *et al.*, 2006). The suggestion is that the increased hydrophilicity of the polymers within the microparticle structure would lead to misaligned structures and therefore less stability, in addition the hydrophilic areas would assemble together to form the pores and channels with the hydrophobic areas assembling to form the structure of the particle (Figure 3.1 C). From these findings it can be stated that the addition of F127 or P188 did result in pores in microparticle surface and less stability in structure. It is therefore assumed that the F127 increased the hydrophilicity of the particles as expected generating more water filled channels and subsequently sped up protein release.

The particles fabricated using P188 had a more dimpled and less smooth surface morphology in a similar manner to that shown by Ma *et al* when using P188 alongside poly ε-caprolactone in microparticle formation (Ma and Song, 2006). This could mean that the addition of P188 resulted in reduced particle stability and structure in a similar manner to F127. The particles containing P188 were less porous than those made with F127, suggesting less hydrophilicity of the polymer and therefore the particles. The particles were similar to the spherical, non-porous particles shown by Parajo *et al* when using P188 alongside PLGA (Parajó *et al.*, 2010). The broad size distribution seen for the particles containing P188 may have been an effect of the morphological irregularities, with more

unstable particles breaking or being damaged in processing and therefore not resulting in a diameter reading when analysed using laser diffraction. The size distribution data was supported by the SEM images where smaller particles can be seen amongst larger ones, attributing to the size distribution bell curve. The particles fabricated using F127 in this chapter resemble the size of those manufactured by Leo *et al* using PLA and F127, with average particle diameters between 20 – 50 µm (Leo *et al.*, 2006).

The increase in pores and therefore water filled channels in the particle formulations containing F127 could have resulted in leaching of the protein during the manufacturing process and therefore a lower encapsulation efficiency than that seen for the particles made without modifiers. The encapsulation efficiencies for these particles was lower than reported for PLGA alone batches which is concerning for the release profiles. It was expected that less protein encapsulated would influence the release kinetics, as an optimisation step the release curves were adjusted to account for the exact encapsulation efficiency for each formulation. The addition of P188 did not significantly change the encapsulation efficiency however, the increase in P188 percentage for particles made with 85:15 PLGA did appear to reduce efficiency with 85:15 40 % *w/w* P188 only achieving 20 % *w/w* efficiency. This contradicts reports in literature where 80-90 % *w/w* encapsulation efficiency was reported with the use of P188 by Ma and Song, however as PLGA was not the main polymer in that work it is difficult to make a comparison (Ma and Song, 2006). Due to this the release graphs were adjusted for the actual protein encapsulated calculated from the individual encapsulation efficiencies. There was not a significant difference in

encapsulation efficiency between particles made with 50:50 or 85:15 PLGA with P188 as was seen for F127, although they were lower than those reported for particles made with a PLGA-PEG-PLGA triblock as a release modifier (Vij *et al.*, 2010; Kirby *et al.*, 2011; White *et al.*, 2013; Abu-Awwad *et al.*, 2017).

When considering the release profiles shown in this chapter, in comparison to PLGA alone the F127 did not result in controlled and sustained release over 20 days. However, the addition of F127 did dramatically increase the initial burst release at day 1. This is not surprising as the SEM images show that the particles containing F127 were more porous than those without F127. Interestingly, different percentages of F127 appeared to have different effects on the particles made with 50:50 PLGA and those made with 85:15 PLGA. Despite this, for both 50:50 and 85:15, the initial burst and total overall cumulative release was less for the 30 % *w/w* F127 than for the 20 % *w/w*. This contradicts work by Wang *et al* who showed a sustained release profile from PEG-F127 microparticles, although the difference may be due to release of a different protein, exenatide, and the use of PEG alongside the PLGA (Wang *et al.*, 2016). Wang *et al* also showed that the addition of F127 slowed polymer degradation which may explain the slow release of lysozyme seen in this study (Wang *et al.*, 2016). This does not support the data shown by Wang *et al*, where 20 % *w/w* F127 showed sustained release when used with PEG, however, the difference in polymer and drug encapsulated may have attributed to this effect (Wang *et al.*, 2016). Leo *et al* reported similar when using F127 alongside PLA, showing sustained release of BSA using an F127 thermo-responsive gel (Leo *et al.*, 2006), thus suggesting

that sustained release can be obtained using F127 as a release modifier. However, the data shown in this chapter suggests that the addition of F127 modifies the initial burst release from PLGA particles to varying extents but does not continue to modify release post-day 1 and is therefore does not provide controlled and sustained release. It also suggests that the addition of F127 had more effect on the 50:50 PLGA formulations than on the 85:15 PLGA formulations, this may be due to the faster degradation rate of 50:50 PLGA than 85:15 (Ye *et al.*, 2010).

The addition of P188 to PLGA microparticles did not result in controlled and sustained release over 20 days in a similar way to that seen for F127. The initial burst release was increased at day 1, especially for the 50:50 formulations where the increase in P188 percentage correlated to an increase in μg protein/mg particles on day 1. The exception was for 40 % *w/w* P188 which had a lower burst release than that seen for 20 % *w/w* P188. As was seen for the F127 formulations, the addition of P188 appeared to have a greater effect on the release kinetics in the 50:50 formulations than in the 85:15. As stated previously, this may be due to the slower degradation rate of 85:15 PLGA due to it being less hydrophilic than 50:50 PLGA, as the effect may be seen later than the 21 days analysed. The only batch containing P188 which showed continuous release after day 1 was 85:15 40 % *w/w* P188. These findings did not support work done by Parajo *et al*, who managed to obtain a zero order release curve from PLGA-P188 particles over 25 days, however the release of a different protein, SHA-22-2, may have had an effect (Parajó *et al.*, 2010). Ma and Song also reported sustained release using P188 as a release modifier for poly ε-

caprolactone using similar sized particles to those reported in this chapter (18-24 μm), however releasing paclitaxel over 60 days (Ma and Song, 2006). These studies highlight that P188 and F127 may have use as microparticle release modifiers but were not found suitable in this project for the sustained release of HSA:lysozyme from particles approximately 20 μm in diameter.

3.5 Conclusions

To conclude, the addition of F127 to PLGA microparticles did have a small effect on the morphology and release kinetics in comparison to PLGA particles with 0 % *w/w* release modifier. Although F127 did increase the initial burst release it did not promote the same effect as seen in literature by Wang *et al* (Parajó *et al.*, 2010; Wang *et al.*, 2016). Therefore, F127 did not help to obtain controlled sustained release as was the aim for this chapter. It is possible this was due to an interaction between the polymer and the encapsulated HSA:Lysozyme preventing release. It is also possible that F127 is not a sufficient release modifier at 10, 20 or 30 % *w/w* and a higher percentage is required to increase particle hydrophilicity enough to speed up release. However, Wang *et al* used 20 % *w/w* F127 and were able to establish a controlled mechanism of release.

Increasing percentages of P188 led to increasingly irregular particle morphologies, that were however, less porous in comparison to F127

microparticles. An increase in initial burst release was observed with the particles containing P188, especially those made with 50:50 PLGA in a similar way to seen with F127. However, the subsequent release after day 1 was negligible and therefore not a controlled sustained release profile. Both F127, and P188 were found to be an unsuitable release modifiers used with 50:50 or 85:15 PLGA for the release of HSA:lysozyme in this study.

Due to the findings shown in this chapter it became apparent that the use of a PLGA-PEG-PLGA triblock (TB) or other release modifying techniques had to be investigated (Kirby *et al.*, 2011; White *et al.*, 2013; Chen *et al.*, 2017) in order to find a release profile showing sustained and controlled release for use with IL-4 as per the hypothesis for this project.

Chapter 4: Microparticles using a triblock modifier as a controlled drug delivery system

4.1 Introduction

The aim for this chapter was to obtain a database of microparticle formulations providing different release kinetics in order to select a formulation more suitable for sustained continuous release of lysozyme. Following the formulation choice, the aim was to repeat the microparticle manufacture with HSA:IL-4 in place of the model protein lysozyme and compare release kinetics. It was hoped that a delivery system for IL-4 could be developed to prevent the need for multiple treatments or injections, reducing cost and patient inconvenience, therefore the sustained release profile was desirable.

As explored throughout Chapter 3, microparticle release kinetics can be modified by: (i) varying polymers; (ii) addition of release modifiers and (iii) changing size or porosity of the microparticles (Moisés Alvarez *et al.*, 2016). New methods of release modulation were required as the use of F127 and P188 as modifiers in chapter 3 did not provide a suitable profile due to lack of controlled sustained release.

Specific microparticle objectives 1, 2 and 3 were explored in this chapter. As described in section 1.5.3 these were to modify microparticle formulation using:

1. Variations of the lactide:glycolide ratio.

2. Variations of the total polymer percentage and therefore different thickness of particle surface.
3. Addition of a triblock (PLGA-PEG-PLGA) copolymer at 10 %, 20 %, 30 % and 40 % *w/w* of total polymer.

The purpose of these modifications to the particle formulation was to decouple the protein release from the natural degradation of the polymer and result in faster and controlled release.

The specific aims for this chapter were to manufacture, characterise and analyse microparticles containing an in-house synthesised PLGA-PEG-PLGA triblock release modifier for controlled drug delivery. Additionally, this chapter provided an opportunity to explore the batch-to-batch variations between individual batches of triblock. It also shows a comparison between particles manufactured from different percentage total polymer and therefore different surface thickness as an additional method for controlling protein release. Lysozyme was chosen as a model protein for IL-4 due to its similar isoelectric point and molecular weight and was used throughout the optimisation of microparticle formulations.

The use of PLGA-PEG-PLGA as a release modifier in microparticles has been widely documented (Chen *et al.*, 2005; Makadia and Siegel, 2011; White *et al.*, 2013). White *et al* showed that increasing percentage of PLGA-PEG-PLGA increased the release of lysozyme with more sustained release than seen for PLGA alone (White *et al.*, 2013). However, many inconsistencies have been observed between batches of PLGA-PEG-PLGA triblock as an in-house

synthesised polymer as described (Chen *et al.*, 2005, 2017; Tran *et al.*, 2012; White *et al.*, 2013). Due to this batch-to-batch variation multiple batches were made for comparison to each other as well as to those documented in literature. When in contact with water, PLGA biodegrades through the breakdown of ester bonds between its components (Makadia and Siegel, 2011). The incorporation of PEG into the polymer modifies the release kinetics of microparticles by increasing their hydrophilicity and uncoupling release from the degradation of the polymer (Chen *et al.*, 2005). Due to this, the incorporation of greater percentages of triblock was expected to result in faster release via osmotic pumping and through water filled channels as described in section 1.4.1 (Figure 1.6). The decision was made to test multiple percentages in order to develop a database of release profiles to choose an optimal formulation from. As well as the addition of triblock, the percentage total polymer was explored as an alternative way to modulate release. The incorporation of a lower percentage of total polymer, although not reported in literature, was expected to result in particles of thinner surface and therefore faster releasing due to less surface to degrade as well as less area for proteins to release through. As explored through Chapter 3, the use of different lactide to glycolide ratios in PLGA was expected to affect the protein release, with the 85:15 PLGA degrading at a slower rate and therefore resulting in slower release than for particles formed with 50:50 PLGA. The presence of more lactide is reported to make the polymer more hydrophobic and therefore slow the breakdown of ester bonds and subsequently biodegradation (Makadia and Siegel, 2011), this is the reason that PLGA 85:15 degrades at a slower rate than the more hydrophilic 50:50. The desired release kinetics were a small burst release at day 1 followed by continuous sustained

release of HSA:lysozyme and following the choice of a suitable particle formulation, continuous sustained release of HSA:IL-4.

4.2 Experimental Design

4.2.1 Triblock/ diblock copolymer synthesis and characterisation

In-house synthesis of the triblock copolymer (PLGA-PEG-PLGA) was achieved by two methods: first from the lactide and glycolide monomers, and second from a PLGA polymer. Diblock (PLGA-PEG) was also formed from the PLGA polymer. The synthesis methods are described in detail in section 2.1.1. The exact conditions used for the in-house synthesised polymer batches are shown in Table 4.1.

Table 4.1: Table of release modifier polymer formulations used in biomaterial design. TB: PLGA-PEG-PLGA Triblock. DB: PLGA-PEG Diblock.

Name	Polymer Source	Reaction Conditions	
		Time (hrs)	Environment
TB1	Lactide and glycolide monomers	24	Vacuum
TB2	Lactide and glycolide monomers	22	Nitrogen
TB3	PLGA and PEG polymers	24	Nitrogen
TB4	Lactide and glycolide monomers	5	Nitrogen
DB1	PLGA and PEG polymers	24	Nitrogen

The polydispersity index (PDI) and molecular weight (MW) of the copolymers was determined as described in section 2.1.1.

4.2.2 Microparticle preparation by double emulsion and microparticle characterisation

Microparticles were prepared, as described in section 2.1.2, using 50:50 lactide:glycolide PLGA or 85:15 lactide:glycolide PLGA and a copolymer release modifier. The release modifier used was PLGA-PEG-PLGA triblock from polymers at 10 %, 20 %, 30 % or 40 % *w/w*. The specific microparticle formulations described in this chapter are shown in Table 4.2 and were fabricated for l0 %, 15 % or 20 % *w/v* total polymer. The 10 % (*w/v)* total polymer particle batches were only fabricated with 50:50 PLGA. Exact formulations of TB batches can be found in Table 4.2. Microparticles were characterised using SEM for surface morphology and laser diffraction for the size distribution as detailed in section 2.1.3.

Table 4.2: Microparticle formulations containing in-house release modifiers used in biomaterial experimental design. TB refers to a PLGA-PEG-PLGA triblock.

Total Polymer (%*w/v*)	Formulation
10	50:50 0 %
	50:50 10 % TB2
	50:50 20 % TB2
	50:50 30 % TB2
15	50:50 0 %
20	50:50 0 %
	50:50 10 % TB1
	50:50 20 % TB1
	50:50 30 % TB1
	50:50 20 % TB4
	50:50 40 % TB4
	85:15 0 %
	85:15 10 % TB1
	85:15 20 % TB1
	85:15 30 % TB1
	85:15 20 % TB4
	85:15 40 % TB4*$^{IL\text{-}4}$

4.2.3 Microparticle encapsulation efficiency and release study comparison

Encapsulation efficiency and protein release was measured using a micro BCA assay as described in section 2.1.4.1. A human IL-4 ELISA was also used to assess the concentration of IL-4 in release supernatant following release study on IL-4 batches as described in section 2.1.4.2.

4.3 Results

4.3.1 Release modifier characterisation: molecular weight and polydispersity comparison between different triblock formulations

The characterisation of in-house synthesised copolymers, as described in section 4.2.1 was undertaken with NMR and GPC and the results are shown in Table 4.3. NMR spectra can be found in the supplementary data, Figure 7.6.

Table 4.3: Nuclear magnetic resonance [a] and gel permeation chromatography [b] results for PLGA-PEG-PLGA/ PLGA-PEG copolymers.

Nomenclature	Polymer Source	M_W [a]	PDI [b]
TB1	Monomer	5452	1.159
TB2	Monomer	2300	1.213
TB3	Polymer	7523	1.894
TB4	Monomer	6405	1.145
DB1	Polymer	5742	1.156

The molecular weight for the synthesised copolymer batches ranged from 2300 to 7523 which suggests there will be differences in the polymer properties. The polydispersity ranged from 1.145 to 1.894. Due to its limited use in literature, diblock was not explored as a release modifier in this project. The decision was made to continue microparticle production using triblock from monomer due to a lower PDI of 1.159 in comparison to 1.894 for triblock from polymer. TB3

was not used due to the high polydispersity and assumed variation in polymer properties. TB1, TB2 and TB4 were used in particle manufacture due to low polydispersity and similar molecular weights.

4.3.2 Microparticle characterisation: particle morphology and size distribution comparison between formulations made with different triblocks

PLGA microparticles containing encapsulated HSA:lysozyme were produced using the double emulsion method before characterisation using scanning electron microscopy and coulter sizing analysis. The SEM images, sizing distribution and average size are shown in Figure 4.1 and Figure 4.2 for different microparticle formulations.

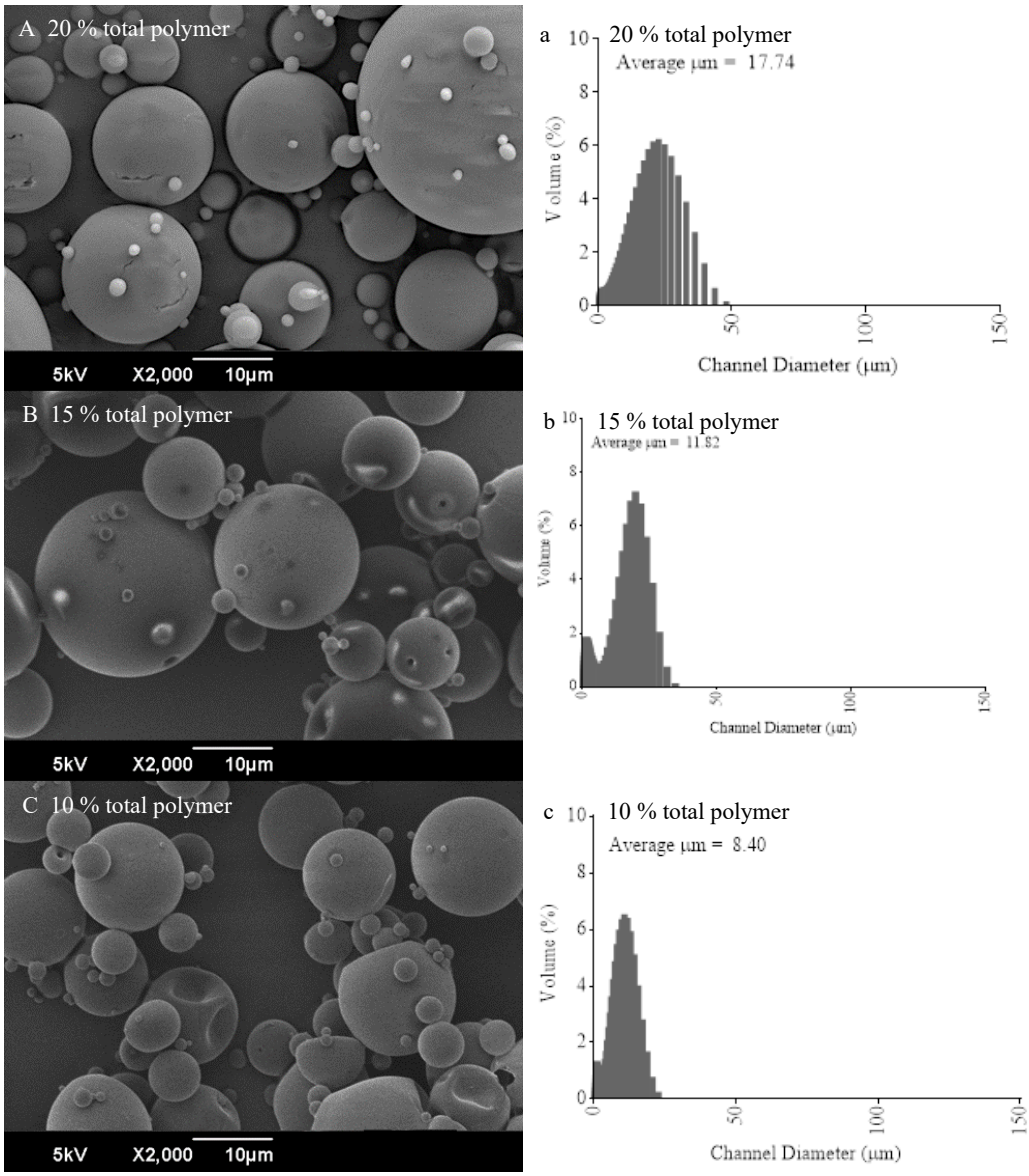

Figure 4.1: Morphology and size distribution of particles formed from 50:50 PLGA with different percentages of total polymer, containing water only. Formulation: **(A/ a)** 20 % *w/v* total polymer, **(B/ b)** 15 % *w/v* total polymer, **(C/ c)** 10 % *w/v* total polymer. Magnification at x2000.

There was minimal difference in the morphology of particles fabricated from 20 %, 15 % and 10 % *w/v* total polymer, although, particles fabricated from 10 % total polymer did appear to have more irregular shaped particles. The size distribution for each formulation showed a similar trend with bell curve distribution, with a lower total polymer percentage leading to a smaller average particle size. The particles made with 20 %, 15 % and 10 % *w/v* total polymer had average sizes of 17.74 μm, 11.82 μm and 8.40 μm respectively (Figure 4.1 a, b, c). This may be due to the lack of structural integrity for the 10 % *w/v* total polymer batches and the collapse of particles as can be seen in the SEM image (Figure 4.1. C).

Due to widely reported use, 20 % *w/v* total polymer was used for further microparticle optimisation. A comparison was made between morphology and size distribution of particles made from 50:50 PLGA and 85:15 PLGA. A further comparison was made between water loaded or blank particles and those encapsulating HSA:lysozyme. The addition of a PLGA-PEG-PLGA triblock release modifier was also explored for the effect on morphology and size distribution. These results are shown in Figure 4.2.

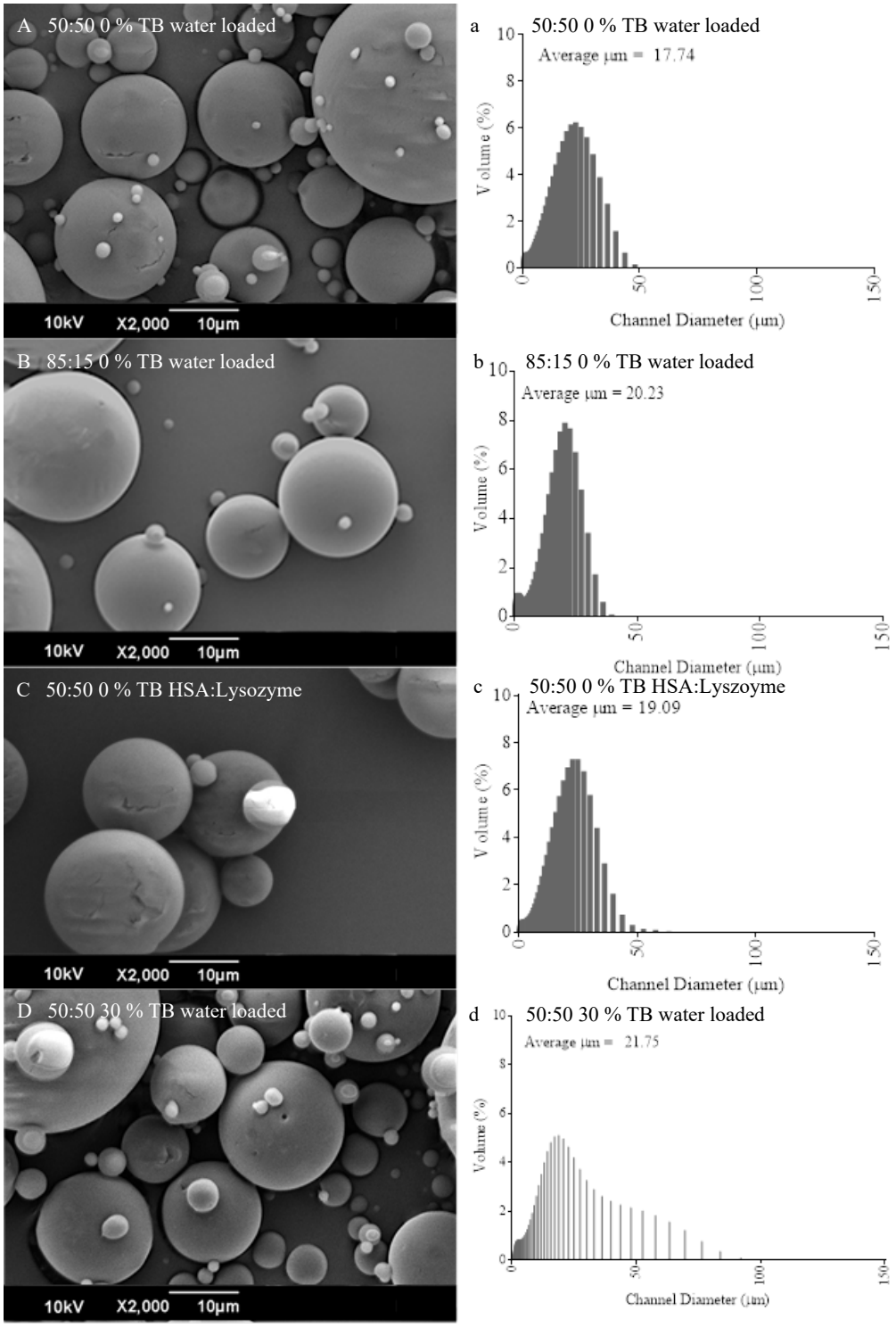

Figure 4.2: Morphology and size distribution of 20 % *w/v* total polymer particles formed from 50:50 or 85:15 PLGA with different percentages of triblock, blank and containing protein. Formulations: **(A/ a)** 50:50 PLGA, 0 %

w/w triblock, water loaded, **(B/ b)** 85:15 PLGA, 0 % *w/w* triblock, water loaded, **(C/ c)** 50:50 PLGA, 0 % *w/w* triblock, HSA:Lysozyme loaded, **(D/ d)** 50:50 PLGA, 30 % *w/w* TB2, water loaded.

There was minimal difference between the surface morphology of microparticles made using 50:50 PLGA (Figure 4.2 A) and 85:15 PLGA (Figure 4.2 B) with both producing spherical non-porous particles. There was also no significant difference between the size distribution with microparticles made from 50:50 and 85:15 PLGA, both showing a bell curve distribution with average sizes around 20 μm in diameter (Figure 4.2 a and b). Addition of HSA:lysozyme also did not have an effect on the microparticle morphology or on the size distribution making for direct comparisons between loaded and blank particles (Figure 4.2 C, A and c, a).

The addition of triblock as a release modifier also did not appear to have an effect on the surface morphology with particles remaining spherical and non-porous on the addition of 30 % *w/w* TB (Figure 4.2 D). The addition of triblock did however result in a broader particle size distribution, confirmed by results shown in supplementary data, which could be attributed to the polydispersity of the triblock polymer shown in Table 4.2, where the incorporation of TB with varying polydispersity may have affected the particle size, however this has not been reported previously.

4.3.3 Microparticle encapsulation efficiency and protein release: comparison of the batch-to-batch variation of triblock and the effect it has on protein encapsulation and release kinetics

The encapsulation efficiency and release profiles of the microparticles were determined using a micro BCA protein activity assay. Protein release results are displayed as cumulative percentage release (% protein *w/*w to particles). Cumulative μg protein/ mg particles release data can be found in Supplementary Data (Figures 7.5, 7.8, 7.13 and Figure 7.14). Encapsulation efficiency results are displayed in Table 4.4 and protein release results in Figure 4.3 as cumulative percentage release (% *w/w*).

Table 4.4: Average particle size (μm) and encapsulation efficiency (% *w/w*) for particles formed from 50:50 or 85:15 PLGA with different total polymer percentages and addition of modifiers. TB refers to PLGA-PEG-PLGA triblock. All particles contain HSA:Lysozyme except where * indicates HSA:IL-4 and ± standard deviation from triplicates.

PLGA	Percentage Total Polymer (% *w/v* TP)	Modifier		Average Size (μm)	Average Encapsulation Efficiency (% *w/w*)
		Type	Percentage (% *w/w*)		
50:50	10	-	0	14.43 ± 5.32	41.75 ± 2.93
85:15	10	-	0	17.65 ± 14.12	45.20 ± 1.79
50:50	15	-	0	15.65 ± 8.92	25.58 ± 2.07
50:50	10	TB2	10	8.69 ± 7.21	66.42 ± 3.23
50:50	10	TB2	20	9.57 ± 5.78	92.79 ± 1.33
50:50	10	TB2	30	14.56 ± 10.05	82.86 ± 1.21
50:50	20	-	0	19.09 ± 7.67	72.06 ± 12.35
50:50	20	TB1	10	17.66 ± 12.64	81.73 ± 0.27
50:50	20	TB1	20	21.30 ± 10.98	63.59 ± 5.30
50:50	20	TB1	30	20.17 ± 17.81	49.93 ± 13.36
85:15	20	-	0	22.64 ± 11.64	53.88 ± 32.62
85:15	20	TB1	10	31.75 ± 10.45	73.80 ± 3.26
85:15	20	TB1	20	18.30 ± 12.24	50.52 ± 2.40
85:15	20	TB1	30	24.77 ± 15.66	51.39 ± 4.98
85:15	20	-	0	24.58 ± 9.07	77.29 ± 6.53
85:15	20	TB4	20	20.30 ± 17.67	61.06 ± 9.47
85:15	20	TB4	40	21.95 ± 8.08	59.26 ± 5.36
85:15*	20	TB4	40	17.69 ± 10.08	68.50 ± 1.12

The encapsulation efficiencies for the particles ranged from 25.58 % for the 15 % *w/v* total polymer 50:50 batch to 92.79 % for the 10 % *w/v* total polymer 50:50 20 % *w/w* TB1 batch. Changing the lactide to glycolide ratio and addition of triblock did not significantly change the encapsulation efficiency of HSA:lysozyme. However, the encapsulation efficiencies for particles made using 15 % *w/v* or 10 % *w/v* total polymer were much lower with 10 % *w/v* TP 50:50 0 % *w/w* TB1 at 41.75 % and 15 % *w/v* TP 50:50 0 % *w/w* TB1 at 25.58 %. This suggests that decreasing the total polymer percentage reduced the encapsulation efficiency. However, in the case of 20 % *w/v* total polymer, the addition of TB did not affect the encapsulation efficiency with little difference observed between particles containing 10, 20 and 30 % *w/w* TB for both 50:50 and 85:15 PLGA. It is also important to consider the large standard deviation for the size distribution which can also be seen in the size distribution graphs (Figure 4.1 and 4.2) showing a large size range of particles which may have an effect on the release kinetics of the particles with smaller particles thought to release at a faster rate from larger particles.

The release kinetics for each microparticle batch manufactured were adjusted to account for the specific encapsulation efficiencies in order to generate an accurate comparison between batches. The protein release (cumulative percentage release) kinetics are displayed in Figure 4.3 and Figure 4.4.

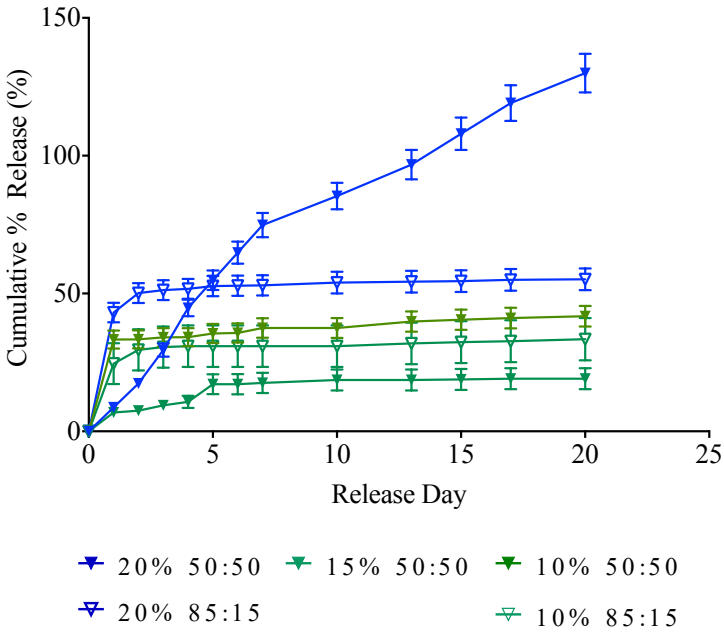

Figure 4.3: Cumulative percentage release (% *w/w*) for particles formed from 50:50 or 85:15 PLGA with 20 and 10 % *w/v* total polymer and 50:50 PLGA with 15 % *w/v* total polymer all with 0 % *w/w* triblock. (N1, n3). Error bars represent cumulative standard deviation. Adjusted for encapsulation efficiencies.

The particles made with 10 % *w/v* or 15 % *w/v* total polymer showed accelerated release of HSA:lysozyme with a small burst release at day 1 followed by minimal protein release on the subsequent days as can be seen in Figure 4.3. The overall maximum protein release for these particles was 40 % of the total encapsulated, seen in Figure 4.3. When compared to 20 % *w/v* TP 50:50 the 10 % *w/v* and 15 % *w/v* TP showed accelerated release at day 1, however, in the case of 20 % *w/v* TP 85:15 it showed accelerated release compared to 10 % *w/v* TP. The 20 % *w/v* 50:50 PLGA formulation resulted in the most sustained release with a small release at day 1 followed by continued release up till day 20 as can be seen in Figure 4.3, however results show the percentage release to be

greater than 100 % suggesting a degree of error resulting from the use of multiple batches of particles as well as BCA assays for analysis of encapsulation efficiency and protein release. Therefore, it is more useful to look at the trend of release rather than the exact percentage release, which shows sustained release, due to this the 20 % *w/v* total polymer formulations were further investigated as can be found in Chapter 4. From the findings in Figure 4.3, the 10 % *w/v* and 15 % *w/v* total polymer particles were unsuitable for a controlled release application. Despite this, the 10 % *w/v* TP 50:50 microparticles were used to test the effect of PLGA-PEG-PLGA triblock to determine if a sustained release could be obtained after day 1 and results are shown in Figure 4.4.

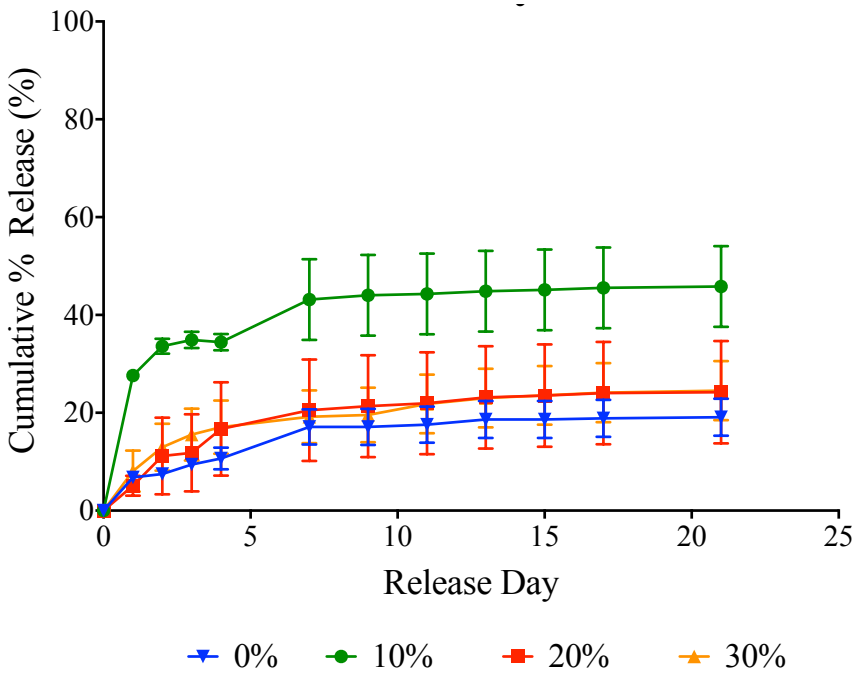

Figure 4.4: Cumulative percentage release (% *w/w*) for particles formed from 10 % *w/v* total polymer 50:50 PLGA with 0 %, 10 %, 20 % and 30 % *w/w* TB2. (N2, n3). Error bars represent cumulative standard deviation. Adjusted for encapsulation efficiencies.

From Figure 4.4 it can be seen that the addition of 10, 20 and 30 % *w/w* TB did have an effect, although not as expected. When used with 10 % *w/v* TP, 10 % *w/w* TB batch showed a greater burst release followed by continued release up to day 7, however the ongoing release was minimal. The effect of 20 and 30 % *w/w* TB was expected to be greater than that of 10 % *w/w* due to greater hydrophilicity of the particles, nevertheless as evident from Figure 4.4 they displayed release kinetics comparable to that of 0 % *w/w* TB.

From the results shown in Figure 4.3, the 20 % *w/v* total polymer particles appeared to show more sustained and controlled release than the 15 % *w/v* or 10 % *w/v* total polymer. The addition of triblock (Figure 4.4) to 10 % *w/v* total polymer particles did not result in sustained release of protein. Therefore, the use of triblock as a release modifier was tested with 20 % *w/v* total polymer particles fabricated from 50:50 PLGA and 85:15 PLGA and the release results are shown in Figure 4.5.

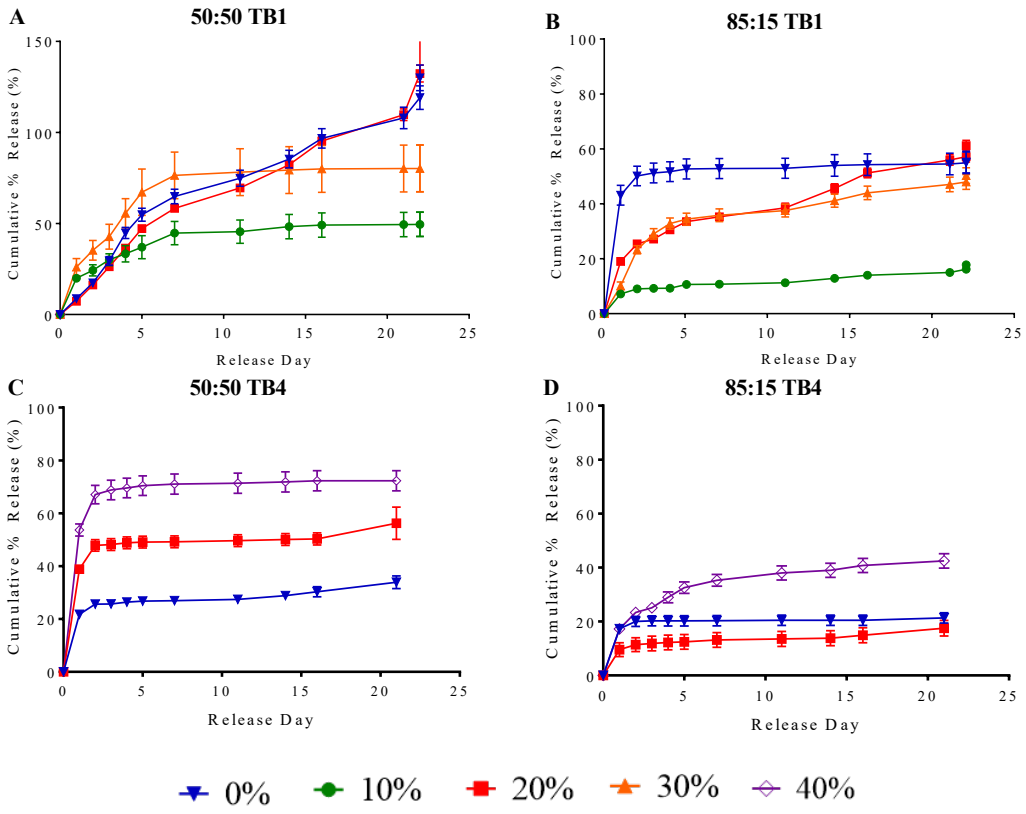

Figure 4.5: Cumulative percentage release (% *w/w*) for particles formed from 50:50 (A, C) or 85:15 (B, D) PLGA with different total polymer percentages and addition of modifiers where coloured symbols are consistent for proportion of modifier included. **(A)** 20 % *w/v* total 50:50 PLGA with 0 %, 10 %, 20 % and 30 % *w/w* TB1. (N3, n3), **(B)** 20 % *w/v* total 85:15 PLGA with 0 %, 10 %, 20 % and 30 % *w/w* TB1 (N1, n3), **(C)** 20 % *w/v* total 50:50 PLGA with 0 %, 20 % and 40 % *w/w* TB4 (N1, n3), **(D)** 20 % *w/v* total 85:15 PLGA with 0 %, 20 % and 40 % *w/w* TB4 (N1, n3). Error bars represent cumulative standard deviation. Adjusted for encapsulation efficiencies.

An increased initial burst release was seen in particles made with 50:50 PLGA as shown in Figure 4.5 A. On addition of TB to particles made from 85:15 PLGA the release was slower but more controlled and sustained with a less sharp burst release than that seen for 0 % *w/w* (Figure 4.5 B). Sustained release of HSA:lysozyme was obtained using 50:50 with 0 % *w/w* TB1 and 20 % *w/w*TB1 (Figure 4.5 A) when adjusted for the encapsulation efficiency for each formulation.

30 % *w/w* TB displayed quicker release than the 20 % *w/w* TB in the particles made with 50:50 PLGA (Figure 4.5 A). In contradiction to this when used with 85:15 PLGA, the 0 % *w/w* TB particles had a quicker rate of release compared to 10 %, 20 % and 30 % *w/w* (Figure 4.5 B). The 30 % *w/w* TB 50:50 batch did display quickest release however not as sustained and controlled as that for 20 % *w/w* TB. A similar trend was seen for 85:15 PLGA, however the release from TB particles was slower than for the 0 % *w/w* TB, with the exception of 20 % *w/w* TB which showed accelerated release after day 13.

Due to inconsistencies in triblock batches the microparticles were manufactured using a newly synthesised triblock (TB4) as described earlier in this chapter. From Figure 4.5 C and D it can be seen that TB4 had different effects to that seen for the previous triblock formulation (TB1). TB4 had a greater effect on the 50:50 PLGA batches as seen before, however, there was a greater difference between the 20 % and 0 % *w/w* TB. The effect of TB4 at 40 % *w/w* was also tested to determine if the 30 % *w/w* was not great enough to observe an effect

on the protein release. A much larger burst release of 5.37 µg/mg was seen for 50:50 PLGA 40 % *w/w* TB, however there was very minimal release post-day one. These results suggest that TB4 did not have as great a modifying effect on the release kinetics as TB1 and was unable to obtain sustained release when used with 50:50 PLGA. Like to like formulations using TB1 and TB4 resulted in different release kinetics, for example, where 50:50 20 % *w/w* TB1 was able to produce sustained release (Figure 4.5 A) 50:50 20 % *w/w* TB4 did not result in a sustained release profile (Figure 4.5 C). A similar result was seen for 85:15 where 20 % *w/w* TB1 looked most promising (Figure 4.5 B) but 20 % *w/w* TB4 showed very minimal release (Figure 4.5 D).

The daily protein release for each formulation has been compiled to show initial burst release at day 1 in µg/mg particles in Table 4.5, in order to compare the burst release between formulations.

Table 4.5: Initial protein release at day 1 (μg/mg particles) for **(i)** Different total polymer (TP) percentages with 50:50 and 85:15 PLGA and 0 % *w/w* TB. **(ii)** 10 % *w/v* total polymer percentage 50:50 and 85:15 PLGA with different percentages of TB2. **(iii)** 20 % *w/v* total polymer percentage 50:50 and 85:15 PLGA with different percentages of TB1. **(iv)** 20 % *w/v* total polymer percentage 50:50 and 85:15 with different percentages of TB4. All values have been adjusted for encapsulation efficiency. TB: PLGA-PEG-PLGA triblock.

Average initial release HSA/Lysozyme at day 1 (μg/mg)			
(i) Comparison of total polymer percentage with 0 % *w/w* TB			
20 % TP 50:50	**15 % TP 50:50**	**10 % TP 50:50**	**10 % TP 85:15**
0.09	3.33	0.68	2.46

(ii) 10 % *w/v* total polymer comparison of percentages (*w/w*) of TB2			
50:50 PLGA			
0 % TB2	**10 % TB2**	**20 % TB2**	**30 % TB2**
0.68	2.76	0.51	0.81

(iii) Comparison of lactide to glycolide ratio with percentages (*w/w*) of TB1							
50:50 PLGA				**85:15 PLGA**			
0 % TB1	**10 % TB1**	**20 % TB1**	**30 % TB1**	**0 % TB1**	**10 % TB1**	**20 % TB1**	**30 % TB1**
0.09	1.99	0.01	2.60	1.73	0.72	1.90	1.01

(iv) Comparison of lactide to glycolide ratios with percentages (*w/w)* of TB4					
50:50 PLGA			**85:15 PLGA**		
0 % TB4	**20 % TB4**	**40 % TB4**	**0 % TB4**	**20 % TB4**	**40 % TB4**
0.09	3.89	5.37	1.73	0.96	1.72

The reduction in total polymer percentage appeared to increase the initial burst release, with 15 % *w/v* TP releasing 3.33 µg/mg and 20 % TP 0.09 with 50:50 PLGA. However, the 10 % *w/v* TP only released 0.68 µg/mg at day 1, this may be due to breakdown of the particle surface structure due to the presence of less polymer. The particles fabricated using 15 % *w/v* TP displayed the fastest release, as can be seen in Figure 4.4 A, with 4.19 µg/mg released between days 11 and 22, compared to less than 1 µg/mg for all other batches. The expectation was that more TB would result in faster release due to the increased hydrophilicity of the particles, however, 30 % *w/w* TB released 0.81 µg/mg on day 1 compared to 2.76 µg/mg by 10 % *w/w* TB.

In a comparison of lactide to glycolide ratio in 20 % *w/v* TP particles, a similar result was seen to that of 10 % *w/v* TP particles. For 0 % *w/w* TB, the 85:15 PLGA particles had a faster burst release of 4.31 µg/mg compared to 0.09 µg/mg for 50:50 PLGA, this may be due to the slower breakdown of the polymer. As was seen in the 10 % *w/v* TP particles, the addition of 10 % *w/w* TB to 50:50

PLGA particles resulted in a faster burst release than 20 % *w/w* TB which was unexpected, however 30 % *w/w* TB did result in the fastest burst release. For the particles made from 85:15 PLGA, addition of 20 % *w/w* TB resulted in faster release than 10 % *w/w* and 30 % *w/w*.

In a comparison of lactide to glycolide ratio using TB4, increasing percentages of TB resulted in faster release, with 40 % *w/w* TB4 releasing 5.37 µg/mg at day 1 and 0 % *w/w* TB4 releasing 2.18 µg/mg. Although 40 % *w/w* TB4 did result in faster release than 20 % *w/w* in the 85:15 PLGA particles, it was similar to the release seen for 0 % *w/w* TB4. Despite this, the particles showing the most sustained release over the 22 day study, was the 20 % *w/v* TP, 85:15 PLGA, 40 % *w/w* TB4 formulation, where a significant amount of protein was released at each time point.

Due to the sustained controlled release observed for 20 % *w/v* TP 85:15 PLGA 40 % *w/w* TB4, this formulation was chosen as optimal for the application and repeat batches of microparticles were manufactured to confirm this decision.

4.3.4: Optimum microparticle formulation confirmation and comparison between lysozyme and IL-4 release

To further validate this decision, new microparticle batches were fabricated with either water, HSA:lysozyme or HSA:IL-4 and morphology and size distribution are shown in Figure 4.6.

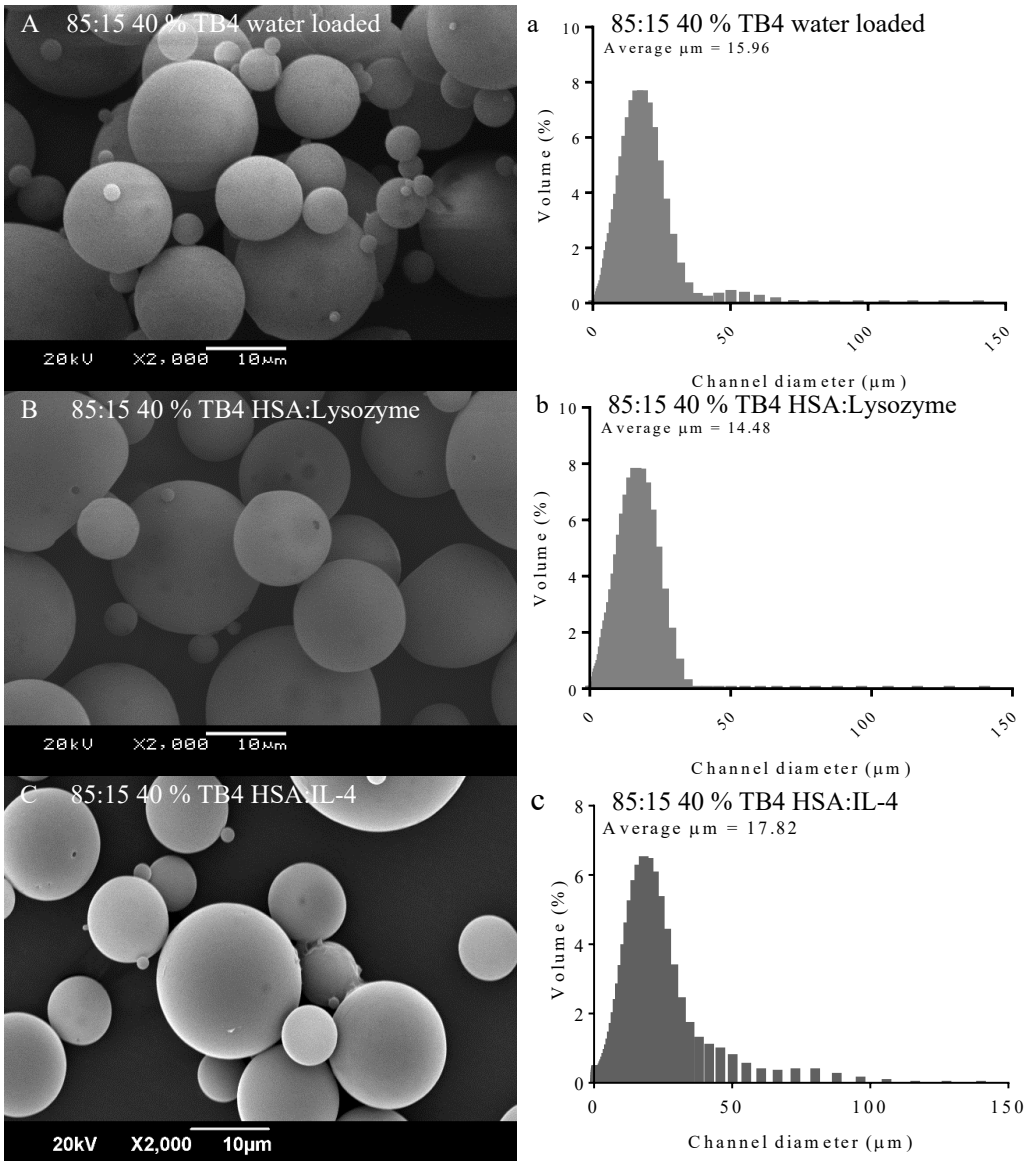

Figure 4.6: Morphology and size distribution of 20 % *w/v* total polymer particles formed from 85:15 PLGA and 40 % *w/w* TB4 containing water, lysozyme or IL-4. Formulation: **(A/ a)** water loaded; **(B/ b)** HSA:lysozyme loaded; **(C/ c)** HSA:IL-4 loaded. Magnification at x2,000.

The microparticles fabricated at 20 % *w/v* total polymer 85:15 PLGA 40 % *w/w* TB4 showed similar morphology seen for previous batches, where all particles were spherical and non-porous with a bell curve size distribution (Figure 4.6 A, a). The average size was slightly smaller than seen for 20 % *w/v* total polymer formulations previously but still displayed a similar size distribution. As seen for batches discussed previously and the morphology and size was not affected by the addition of HSA:lysozyme or HSA: IL-4 (Figure 4.6 B, C and b, c).

A release study was carried out on the microparticles to compare the effect of TB4 on the release of HSA:lysozyme to that of HSA:IL-4, cumulative release results adjusted for encapsulation efficiency are shown in Figure 4.7 and daily results in Table 4.5. The model protein, lysozyme was assumed to behave in a similar manner to IL-4 upon release from the microparticles. However, due to it being a different protein, the results of the release kinetics were also tested with the IL-4 protein. The exact IL-4 release kinetics were determined using an IL-4 ELISA to assess the amount of active protein released rather than the total protein including carrier (HSA), this data is also displayed in Figure 4.7.

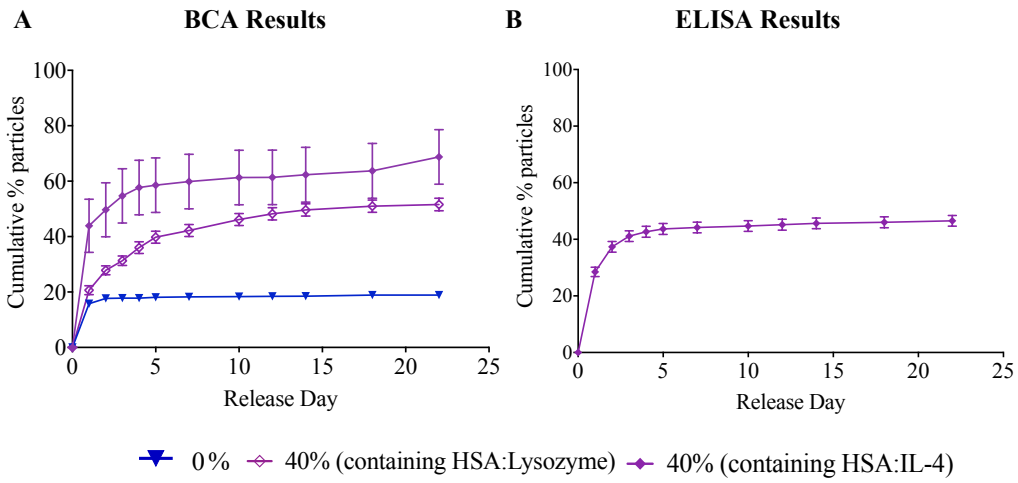

Figure 4.7*:* Cumulative percentage release (% *w/w*) from 20 % *w/v* total 85:15 PLGA polymer with different percentages of TB4 containing lysozyme or IL-4. **(A)** BCA determined: 40 % *w/w* TB4 containing HSA:lysozyme (◊), 0 % *w/w* TB4 containing HSA:lysozyme (▽) (N3, n3) and containing HSA:IL-4 (♦) (N3, n3). **(B)** ELISA determined: 40 % *w/w* TB4 containing human IL-4 (♦) (N1, n2). Error bars represent cumulative standard deviation.

The microparticles fabricated with 85:15 40 % *w/w* TB4 containing HSA:Lysozyme did result in controlled and sustained release over the 22 day study, especially in comparison to 85:15 0 % *w/w* TB4 which resulted in a small burst release followed by no release (Figure 4.7 A). A similar trend was seen for the release of HSA:IL-4 where a burst release was seen at day 1 followed by sustained release over 22 days with an increase in protein release seen at day 18. However, the burst release was greater for HSA:IL-4 release than for HSA:lysozyme, and resulted in more cumulative protein at the end of the study on day 22 (Figure 4.7 A). When analysed using an ELISA for IL-4

concentration (Figure 4.7 B), the IL-4 release showed a small burst release at day 1, followed by sustained release up to day 4 in a similar trend to that seen in Figure 4.7 A. However, from day 5 to 22 very little IL-4 was detected in the release analysis. The combined daily total protein release for the batches shown in Figure 4.7 A and B are summarised in Table 4.6 for a direct comparison of protein (μg/mg particles) over the days studied.

Table 4.6: Combined daily protein release (μg/mg particles) for 20 % total polymer with 85:15 40 % *w/w* TB4 comparison between HSA:Lysozyme and HSA:IL-4 loaded particles. All values have been adjusted for encapsulation efficiency. TB: PLGA-PEG-PLGA triblock (refer to Table 4.1 for exact formulations).

Days	**Optimisation of 20 % (*w/v*) total polymer 85:15 PLGA 40 % *w/w* TB4 for HSA:Lysozyme and HSA:IL-4**		
	HSA:Lysozyme		**HSA:IL-4**
	0 % TB4	**40 % TB4**	**40 % TB4**
1	1.58	2.07	4.03
2-5	0.23	1.91	1.34
6-10	0.03	0.64	0.27
11-22	0.09	0.66	0.75

Calculations were made using the encapsulation efficiency to determine the total protein, HSA:IL-4 content (protein encapsulated at 10 % (*w/w)* of polymer). The percentage of IL-4 alone encapsulated was calculated based on the ratio of HSA to IL-4 encapsulated (0.5:9.5), and the results are shown in Table 4.7.

Table 4.7: Estimated IL-4 release based on daily total release from BCA assay in comparison to actual IL-4 per day calculated using IL-4 ELISA for 7 days. All data adjusted to ng protein per mg particles per day of release.

Release Day	Total Protein (ng/mg)	Estimated IL-4 (ng/mg)	Actual IL-4 (ng/mg)
1	4030	201.42	127.83
2	510	25.65	17.02
3	460	22.90	4.83
4	280	13.79	1.21
5	90	4.46	2.19
6	130	6.47	0.36
7	140	7.17	0.15

Table 4.7 suggests that the actual IL-4 in the release supernatant was not as much as estimated from the known protein encapsulated in the manufacture of the particles. The estimated concentration of IL-4 at day 1 was 201.42 ng/ml based

on 5 % of the total protein released (4030 ng/ml), however the concentration of IL-4 detected by ELISA was 127.83 ng/ml which is approximately 3.172 % of the total protein. A similar result is seen over the next 6 days as can be seen in Table 4.6, with the actual concentration of IL-4 much lower than the estimated value.

4.4 Discussion

A similar PLGA-PEG-PLGA triblock was used by White *et al* and was shown to successfully modulate protein release from 50 – 100 µm PLGA microparticles but had not been used with smaller microparticles (White *et al.*, 2013). However, as the triblock was manufactured in house, the polydispersity and molecular weight varied between batches, it was important to test multiple batches in this study as well as choose a polymer with a low polydispersity in order to reduce variation between microparticle batch properties. The results suggested that when manufactured from the polymers, the triblock had more polydispersity and therefore a manufacturing method from monomers was chosen. Although diblock had a low polydispersity, there are no known reports of a PLGA-PEG diblock as a release modifier. Therefore, the triblock from monomer batches (TB1, TB3 and TB4) were chosen for use in microparticle manufacture.

The results in this chapter show that the encapsulation efficiency for the particle batches range from 26 % to 92 % *w/w*. This has a large impact on the use of

microparticles as a drug delivery system as in some cases the majority of the encapsulated protein is lost during manufacture. When using an expensive drug, it is important that it is not wasted in the encapsulation as this would make the system unnecessarily expensive and possibly not viable as a treatment method. Reported encapsulation efficiencies for the double emulsion manufacturing method range from 42 % to 100 % *w/w* for 20 % *w/v* total polymer PLGA particles, but little is reported using lower polymer percentages (Crotts and Park, 1998; Chen *et al.*, 2001; Kirby *et al.*, 2011; White *et al.*, 2013). Due to this, comparisons can only be made to the 20 % *w/v* total polymer particles, both reported in literature and in this study.

It is not surprising that there is variation in the encapsulation efficiencies between batches of particles due to the polydispersity of the polymer and the difference in particle size. Encapsulation alongside HSA has been shown to improve efficiency as well as protein bioactivity (Sah, 1999; Srinivasan *et al.*, 2005; Ye *et al*, 2010; He *et al.*, 2011). The addition of HSA as a carrier protein binds to the active protein and not only protects it from degradation but the larger combined protein is less likely to be lost in the manufacturing method, due to its size and mass as well as a larger surface area to interact with the polymer. The addition of protein during the single emulsion stage in manufacture leads to its contact with the organic solvent which can lead to precipitation or uneven distribution of the protein within the particles; addition of a serum albumin prevents this by protecting the protein from the organic interphase (Sah, 1999). The use of a water in oil in water method also requires a solvent evaporation stage in which highly water soluble proteins can become unstable when

encapsulated without a carrier protein (Srinivasan *et al.*, 2005). Work by He *et al,* also showed that using HSA as a carrier for rhEPO in microparticles prevented protein denaturation and aggregation (He *et al.*, 2011), and Srinivasan *et al* showed the same using rat serum albumin (RSA) as a carrier for lysozyme (Srinivasan *et al.*, 2005). The protection of the active protein is not only important during the manufacturing stage but also throughout its release, where the degradation of the polymer can lead to increased pH within the particle resulting in free radical production and acid induced protein denaturation (Srinivasan *et al.*, 2005).

Traditionally, proteins were required to be injected to patients multiple times to maintain efficacy, the use of drug delivery systems such as microparticles eliminates the need for this, however it is important that the active protein remains active throughout its release from the particle (Ye, Kim and Park, 2010). This is where carrier proteins such as HSA, BSA or RSA are of most importance as they protect the active protein from the acidic environment upon polymer degradation, enabling long-term release of a bioactive protein (Ye, Kim and Park, 2010). For this project, the protection of the protein at the manufacturing stage, during primary emulsion, solvent evaporation, lyophilisation and storage, was more important as the addition of release modifiers decoupled release from the degradation of polymer.

When particles were manufactured using different total polymer percentage, the resulting particles appeared spherical and uniform in shape, with minimal pores.

This is similar to reported microparticles using PLGA at 20 % *w/v* total polymer (White *et al.*, 2013; Abu-Awwad *et al.,* 2017), however there are no known reports using 10 or 15 % *w/v* total polymer so a comparison cannot currently be made. The results showed more collapsed particles for the 10 % *w/v* total polymer fabrication, suggesting that the surface integrity is not strong enough at that percentage to support a spherical structure or that there is not enough polymer to disperse around the larger protein droplets during manufacture resulting in smaller microparticles. Despite this, the size distribution for 10, 15 and 20 % *w/v* total polymer remained in a bell curve as similar to that seen in literature for PLGA microparticles manufactured using the double emulsion technique (Vij *et al.*, 2010; Kirby *et al.*, 2011; White *et al.*, 2013). The bell curve distribution was seen by Abu-Awwad *et al,* Vij *et al,* Kirby *et al,* and White *et al,* for particles made from PLGA with average particle diameter ranging from 40 – 97 μm and containing GET protein, C57BL6, BMP-2 and HSA:BMP- respectively, thus showing even with different sized particles the distribution trend remained the same (Vij *et al.*, 2010; Kirby *et al.*, 2011; White *et al.*, 2013; Abu-Awwad *et al.* , 2017). Changing the total polymer percentage and therefore the particle surface thickness did not appear to affect the surface morphology, but a lower total polymer percentage did result in smaller average particle diameters although not a significant difference from the 20 % *w/v* total polymer particles.

When analysing the release kinetics of the different particle batches, the effect of changing the particle surface thickness, changing lactide to glycolide ratio, and addition of PLGA-PEG-PLGA triblock were compared in order to generate

a release kinetics database from which to choose an optimal formulation for the sustained delivery of IL-4 as stated in the hypothesis for this study. It was expected that by using a lower total polymer percentage, the particles would have faster release due to less polymer to breakdown or less channels for the protein to move through. However, when using 10 or 15 % *w/v* total polymer, very little release was seen, and 20 % *w/v* total polymer released the most protein. This may be due to complex interactions of the polymers at the lower percentages or due to altered release kinetics as a result of lower encapsulation efficiency, where the protein was either washed off the particle surface upon aqueous contact or remained within the particle for longer than the 22 day study. Even with the addition of a PLGA-PEG-PLGA triblock to the 10 % *w/v* total polymer 50:50 particles, a sustained release pattern could not be obtained. The addition of the triblock did reduce the initial burst release and sustained release was seen for 6 days, however the cumulative release was very small and resulted in only 45 % *w/w* total release after 22 days. As there are no known reports of particles using 10 or 15 % *w/v* total polymer used for protein delivery, a comparison could only be made to 20 % *w/v* total polymer particles. These release kinetics are similar to those seen by Kirby *et al*, for 85:15 10 % *w/w* TB with BMP-2 (2). However, the release was too slow over the 20 day period for the sustained release aimed for. These microparticles were found not to be suitable for a controlled sustained release profile.

Particles fabricated using 20 % *w/v* total polymer with the addition of triblock, using both 50:50 and 85:15 PLGA displayed morphology similar to reported in literature. (Kirby *et al.*, 2011; White *et al.*, 2013; Han *et al.*, 2016). These were

all spherical and non-porous, with some size variation, although the particles manufactured during this project were smaller than those reported in literature, around 15 – 50 μm rather than 50 – 100 μm as reported by White *et al* and Kirby *et al* (Kirby *et al.*, 2011; White *et al.*, 2013). The addition of triblock or protein did not change the particle morphology. This was expected as the main polymer used in triblock manufacture, PLGA was the same as used for the particles and therefore no reason to affect the particle structure. The addition of triblock did however broaden the size distribution of the particles, suggesting there to be a larger range of particle sizes. This may be due to particles sticking together following the manufacturing process or interacting with the surface of neighbouring particles and appearing as one larger particle. Despite the broader size distribution, the particles were still within the same size range. The broader size distribution could provide an advantage by changing the release profile due to smaller particles releasing at a faster rate than larger ones.

When analysing the use of TB2 as a release modifier with 50:50 and 85:15 PLGA using 20 % *w/v* total polymer, the expectation was that faster release would be obtained from increasing the triblock percentage due to increasing hydrophilicity and particle interaction with an aqueous phase. However, this was not shown in this chapter where 10 % *w/w* TB resulted in faster release than 20 % *w/w*, this may be a result of discrepancies between batches of in-house made polymers. Slightly different results were seen for TB4, which highlights the property variation between the in-house synthesised copolymers. For both 50:50 and 85:15 PLGA, the 40 % *w/w* TB4 formulation resulted in the fastest release as expected, however the release was only sustained in the 85:15 formulation

suggesting that TB4 had a larger impact on the 85:15 PLGA. The difference in the effect of the different triblock batches on 50:50 and 85:15 PLGA highlights that the release kinetics can easily be modified and tailored to specific requirements, however, with each triblock batch resulting in a different effect, all must be batch tested for result confirmation.

From the results shown in this chapter, the particle formulation showing protein release most suited to the continuous release required for IL-4 delivery was 20 % *w/v* total polymer, 85:15 PLGA, 40 % *w/w* TB4. This gave in the region of 50 % *w/w* release of total protein over 14 days in a similar manner to results published by White *et al* when using 85:15 PLGA and 30 % *w/w* PLGA-PEG-PLGA triblock in particles averaging with 90 μm diameter and manufactured using a double emulsion method as used in this project (White *et al.*, 2013). A comparable trend was seen in work by Kirby *et al* where sustained release of BMP-2 was achieved from particles, averaging 97 μm in diameter, over 14 days when using 85:15 PLGA with 10 % *w/w* PLGA-PEG-PLGA triblock after manufacture with the double emulsion method (Kirby *et al.*, 2011). Although both the particles made by White *et al* and Kirby *et al* used the same double emulsion manufacture method as used in this project and similar polymers, the microparticles were larger averaging over 90 μm compared to 20 μm as seen in this project. Many other sustained release profiles have been reported for the release of various proteins using different particle formulations. For example, Vij *et al* reported sustained release of C57BL6 for inflammation control from PLGA-PEG nanoparticles of 120 nm in average diameter over 7 days (Vij *et al.*, 2010). This formulation would have been too small for the encapsulation of

HSA:IL-4 so was not tested for application in this project, however, it does highlight the need for sustained release profiles and the complexity of control for specific drugs and applications. The use of porous particles was not suitable for this project due to the potential loss of expensive protein and the fast release over 10 days. The use of porous particles for sustained release was also used by Hombreiro-Perez *et al,* for the release of Propranolol HCI and Nifedipine, however the release was only reported over 10 hours and was much faster than required for this project where 14 day release was the aim (Hombreiro-Pérez *et al.*, 2003). When comparing the release profiles reported in literature and those reported in this project the particle formulation selected 20 % *w/v* total polymer, 85:15 PLGA, 40 % *w/w* TB4 as it resulted in particles which showed continued release over all days tested and were therefore be considered as a sustained release mechanism.

The BCA analysis of total protein content was compared between release of HSA:lysozyme and HSA:IL-4 from the chosen microparticle formulation, 20 % *w/v* total polymer 85:15 PLGA 40 % *w/w* TB4. The use of lysozyme as a model protein was chosen due to its similar molecular weight and isoelectric point to IL-4 and this is reflected in the consistency of the release profiles confirming the choice of model protein for this project. The IL-4 batches showed a greater burst release than those containing HSA:lysozyme with continuous and sustained release over the 20 day study. In comparison to the particles made without TB4 there was more release in days 2-20 for both lysozyme and IL-4 batches. The increased initial burst seen at day 1 for the IL-4 batches may be a result of the encapsulation of a greater amount of HSA to IL-4, however the

overall total protein content remained the same. As the BCA analysis determined the total protein released, a human IL-4 ELISA was used to assess IL-4 concentration within the total protein content. The results showed that the concentration of IL-4 released per day was not comparable to the percentage total protein encapsulated. This implies that of the total protein release, the sustained release is mostly a result of HSA and not of IL-4. A burst release was still observed at day 1 and a small amount of daily IL-4 release seen up to day 3, however very minimal release thereafter. This could be due to loss of protein activity on encapsulation, storage or release, however the HSA was used as a carrier protein in order to protect the protein from denaturation (Ye *et al.*, 2010).

4.5 Conclusions

In this chapter, the optimisation of microparticle formulations for controlled and sustained release have been explored using different lactide to glycolide ratios, different percentage total polymer, and addition of different batches of PLGA-PEG-PLGA triblock. The objective was to develop a suitable formulation for the sustained release of IL-4 to be subsequently used for macrophage modulation as stated in the hypothesis.

A controlled release delivery system was developed using PLGA microparticles with incorporation of PLGA-PEG-PLGA triblock enabling a controlled release profile over 22 days. The incorporation of triblock allowed release to be decoupled from polymer degradation and therefore be quicker than with

polymer alone (Tran *et al.*, 2012; White *et al.*, 2013). However, an in-house triblock synthesised from PLGA and PEG polymers displayed high polydispersity and as a result, triblock synthesised from lactide and glycolide monomers was better suited to particle fabrication. The formulation showing the most promising release results for the delivery of IL-4 was 20 % *w/v* total polymer using 85:15 PLGA and 40 % *w/w* PLGA-PEG-PLGA triblock (TB4).

The release kinetics for the chosen formulation with HSA:lysozyme were comparable to those of HSA:IL-4 as expected. However, when analysed for the IL-4 content, IL-4 release was only sustained up to day 3 and release thereafter was minimal. Due to this, further optimisation would be required to obtain sustained release of IL-4 over a longer time period.

There is currently no reported use of PLGA microparticles as a delivery system for IL-4 and therefore this work, especially the optimisation discussed in this chapter has novelty and may provide a new therapeutic focus for spinal cord injury in particular. The microparticle formulations explored in this chapter may also be compared or tailored to other applications with the incorporation of different proteins.

Chapter 5: In vitro macrophage cellular response to exogenous delivered cytokines

5.1 Introduction

The aim of this project was to promote modulation of M1 to M2 using IL-4 which is a naturally produced cytokine and in doing so reduce the inflammatory environment in SCI. These IL-4 stimulated macrophages will be referred to as $M_{(IL\text{-}4)}$ and those stimulated towards an M1-like population referred to as $M_{(LPS/IFN\gamma)}$.

The dynamic nature of a population of macrophages means that the ratio of M1 and M2 cells naturally changes depending on the signals within any site of injury (Shiratori *et al.*, 2017). For most impact injuries, at injury occurrence the proportion of M1 is high but naturally switches to M2 after time to aid repair after the removal of any debris or invading organisms (Arora *et al.*, 2017). However, as discussed in section 1.2.1, this is not the case in spinal cord injury where the proportion of M1 remains high (Duluc *et al.*, 2007) resulting in chronic inflammation (Guo *et al.*, 2013). This creates a microenvironment which is unsuitable for repair and often causes more damage. The chronic inflammatory environment can result in cell apoptosis and glial scar formation which hinders axonal regrowth and myelination (Wang *et al.*, 2014).

Some work has shown that reducing the chronic inflammatory environment in SCI has provided a promising therapeutic approach for treatment (Bao *et al.*,

2018). Delivery of cytokines to influence the macrophage population via microparticles would provide a robust delivery method where the protein could be protected from degradation by the polymer particle and by carrier proteins. Microparticles could also be tailored for a specific protein release kinetic profile enabling continuous release. Using a continuous release delivery system would ensure that minimal treatments are required for the patient, reducing discomfort and cost. For these reasons, microparticles were chosen as the delivery system for IL-4.

In order to test if the presence of IL-4 could influence the macrophage population and therefore the inflammatory environment, two different cell models were established. THP-1 cells were used as when differentiated they resemble human macrophage cells and are well documented as an *in vitro* cell model for macrophages (Reiner, 2009; Chanput *et al.*, 2010, 2013; Spencer *et al.*, 2010; Chanput *et al.*, 2014; Bosshart and Heinzelmann, 2016; Alvarez *et al.*, 2016; Vishwakarma *et al.*, 2016; Huleihel *et al.*, 2017; Forrester *et al.*, 2018). These cells were isolated from the blood of an infant with acute monocytic leukaemia (Qin, 2012). THP-1 cells provide a cell line model for assessment of macrophage regulation and function and were also chosen because they have a simple culture process (Qin, 2012). The second cell model established used murine immortalised bone-marrow derived macrophages (iBMDMs), although non-human, they provide a further model to test the modulation ability of IL-4 containing microparticles and as a comparison to the THP-1 cells. The iBMDM cells were isolated from mice and unlike the THP-1 cells did not require further treatment to become macrophage cells, therefore provided a more natural

macrophage model. Other cell models considered were the use of primary isolated human and murine monocytes, however, due to the complex isolation process THP-1 and iBMDM cells were chosen as sufficient models.

The aims for this chapter were to establish a robust in vitro macrophage cell model to determine the efficacy of IL-4 released from the microparticles discussed in section 4.4. Although literature has shown that a macrophage population can be influenced by cytokines (Huleihel *et al.*, 2017), including IL-4, currently none have been delivered via a microparticle delivery system. The aim was to determine if microparticle delivered IL-4 was as effective as exogenous IL-4 in obtaining an $M_{(IL\text{-}4)}$ population, or in reducing the presence of inflammatory markers. This draws on the overall hypothesis for this project that sustained delivery of IL-4 could modulate macrophage phenotype and provide resolution from an $M_{(LPS/IFN\gamma)}$ predominant population to an $M_{(IL\text{-}4)}$ predominant population in the context of the inflammatory environment in SCI.

Microparticles, although widely used as drug delivery systems, have not been used as a vehicle specifically for IL-4 delivery and therefore it was unknown how the IL-4 protein would behave upon release. However, the use of microparticles for the delivery of similar growth factors such as VEGF (Qutachi *et al.*, 2013) have been explored and IL-4 was hypothesised to behave in a similar manner upon encapsulation and release. To test this, optimisation of the particle release kinetics was explored throughout Chapters 3 and 4 leading to an optimal formulation of 85:15 PLGA with 40 % *w/w* TB4. The release of IL-4

was tested in comparison to the model protein used, lysozyme. Particles were formulated, as described in section 4.3.4 in order to encapsulate sufficient IL-4 for cell treatment without exceeding therapeutic dose.

In order to test the efficacy of microparticle delivered IL-4 the cell models were first treated with exogenously delivered IL-4 and tested for markers specific to macrophage subpopulations. The intention was to use the cell models to mimic the macrophage environment found in spinal cord injury and suggest a method for modulation toward a pro-immunoregulatory subpopulation as stated in the overall hypothesis. This chapter also covers the treatment of the established cell models with the IL-4 loaded microparticles, in order to determine if microparticles can be used as a drug delivery system for IL-4 and influence the polarisation of macrophage cells to an immunoregulatory subgroup, $M_{(IL\text{-}4)}$. Both cell models, THP-1 and iBMDM were treated with IL-4 microparticles over a 7 day period, with analysis at days 3 and 7 to compare to exogenous IL-4 treatment. The time periods were chosen as they represented the time over which the macrophage population changes naturally (Mantovani *et al.*, 2014; Murray *et al.*, 2014), this was also the time over which the microparticles were optimised to release IL-4. Two time points were used for analysis to assess how the population changed over time dependent on cytokine treatment. The effect of microparticle mediated treatment was evaluated using microparticles with direct cell contact and with indirect contact, this was to ensure that any observed effect was a result of the delivered IL-4 and not the microparticle surface materials. An enhanced proinflammatory response was expected to occur with direct contact to the microparticles due to the macrophage response to foreign

bodies. However, PLGA was chosen as the microparticle material due to its biocompatibility and ability to be broken down into natural metabolites.

Specifically, the objectives explored in this chapter are as follows:

1. Establish robust cell culture methods suitable for cell culture with microparticles.
2. Determine if THP-1 cells and iBMDMs could be exogenously differentiated with cytokines to produce cells expressing markers of human/ murine $M_{(LPS/IFN\gamma)}$ and $M_{(IL\text{-}4)}$ macrophages.
3. Determine if differentiated cells could be cultured alongside microparticles without affecting their growth.
4. Use microparticles containing IL-4 to treat the cells and compare their differentiation ability to that of exogenous IL-4.

5.2 Experimental Design

5.2.1 THP-1 cell culture optimisation

THP-1 cell culture was optimised in order to create a robust and reproducible culture method which could be used for exogenous differentiation experiments and for use alongside microparticles. Population doubling and optimal seeding density were assessed to determine the normal culture behaviour of the THP-1 cells without the influence of external factors such as cytokines or microparticles. Cells were cultured as described in section 2.2.1 and

differentiated with PMA for 24 hours to change from monocytes in suspension to adherent macrophage cells, broadly reflecting an M0 population (Shiratori *et al.*, 2017). The exact optimisation methods are described in Supplementary data 7.2.1 and the results are shown in the Supplementary Data including optimal seeding density (Figure 7.15) and population doubling (Figure 7.16 A) with and without microparticles. THP-1 cells were used between passages 2 - 10 as recommended by the manufacturer, ATCC, to provide cells with characteristics and functions most similar to that of macrophages *in vivo*.

5.2.2 iBMDM cell culture

An established line of murine iBMDM cells were kindly provided by Dr Andrew Bennett for this work and therefore extensive optimisation of culture methods was not required. Cells were cultured as described in section 2.2.2. Population doubling results are shown in the Supplementary Data (Figure 7.16 B). Once culture was established cells were used for exogenous differentiation experiments, between passages 16 - 20 because cells were provided at passage 14.

5.2.3 Exogenous treatment of THP-1/ iBMDM cells in vitro

Known differentiation factors were used to polarise M0 to an $M_{(LPS/IFN\gamma)}$ population (Huleihel *et al.*, 2017), these were LPS, IFNγ and GM-CSF, to provide a proinflammatory macrophage population. IL-4 and M-CSF were used to polarise M0 to an $M_{(IL\text{-}4)}$ population to provide a proimmunoregulatory

population. The hypothesis was that the resulting macrophage populations could be characterised using protein and gene expression markers to determine the effect of IL-4 treatment.

THP-1 cells were treated with PMA (50 ng/ml) for 24 hours as described in section 2.2.1, to differentiate from monocytes in suspension to adherent macrophage or M0 cells. The cells were then rested in fresh medium for 48 hours. The differentiated macrophage cells were then exogenously polarised towards an $M_{(LPS/IFN\gamma)}$ and $M_{(IL\text{-}4)}$ population using LPS (100 ng/ml), IFNγ (20 ng/ml), GM-CSF (50 ng/ml) or IL-4 (20 ng/ml), M-CSF (50 ng/ml) respectively for 72 hours. The medium and cell pellet were collected following treatment as described in section 2.2.1 and used for ELISA or qPCR analysis.

iBMDM cells were also exogenously polarised towards an $M_{(LPS/IFN\gamma)}$ and $M_{(IL\text{-}4)}$ population using LPS (100 ng/ml), IFNγ (20 ng/ml), GM-CSF (50 ng/ml) or IL-4 (20 ng/ml), M-CSF (50 ng/ml) respectively for 72 hours as described in section 2.2.2. As for the THP-1 cell model, the medium was collected following treatment as described in section 2.2.2 and used for ELISA protein analysis.

The cell populations were assessed using ELISA and qPCR analysis, all undertaken using methods described in section 2.2.4. Figure 5.1 shows an overview of experimental design for the exogenous treatment of the cells.

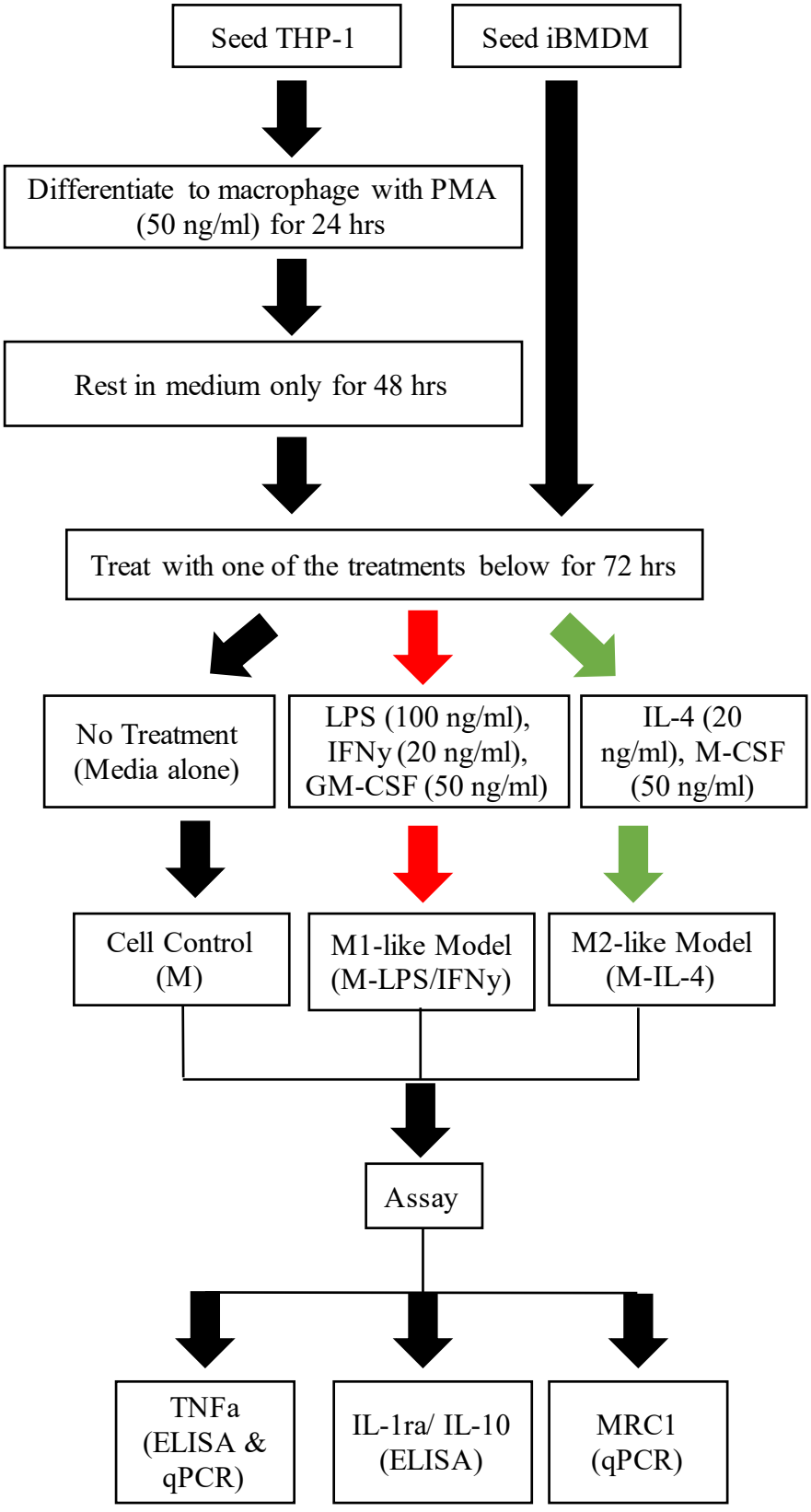

Figure 5.1: An overview of experimental design showing the exogenous treatment of THP-1 and iBMDM cells to different macrophage subpopulations.

5.2.4 Microparticle treatment of THP-1 and iBMDM cells

The hypothesis was that IL-4 treatment via microparticle delivery would result in the reduction of proinflammatory cell markers and increase in proimmunoregulatory cell markers as with the treatment with exogenous IL-4. The cell models were also treated with exogenous LPS, IFNγ, and GM-CSF for a comparison to a known $M_{(LPS/IFN\gamma)}$ population as well as to a non-treated control population. A comparison was also made between the effect of IL-4 microparticles and blank (water) microparticles to ensure the resulting effect was an outcome of the IL-4 and not interaction between cells and the microparticle materials. To further test if the effects were a result of the materials, microparticles were added to the cell population either with direct contact to the cell surface or indirect contact in a transwell for an additional comparison.

THP-1 cells were cultured and differentiated to M0 using PMA (50 ng/ml) for 24 hours as described in section 2.2.1. iBMDM were cultured as described in section 2.2.2. Microparticles, either blank or containing HSA:IL-4 were soaked in media for 24 hours prior to addition to cells to remove the burst release which would result in release of too high a concentration of IL-4. The microparticles were added alongside cytokines for control cell populations as described in section 2.2.3, Table 2.5. Briefly, there were six different conditions as follows: i) Media only, ii) LPS (100 ng/ml), IFNγ (20 ng/ml), GM-CSF (50 ng/ml), (iii) IL-4 (20 ng/ml), M-CSF (50 ng/ml), (iv) microparticles containing IL-4 with

direct contact (1 mg), (v) microparticles containing IL-4 with in direct contact (1 mg), (vi) microparticles containing water with direct contact (1 mg).

On daily intervals the $M_{(IL-4)}$ exogenous reference was treated with the concentration of IL-4 estimated to be released from the microparticles to ensure a direct comparison to the daily IL-4 estimated to be released from the microparticles. See Table 5.1 for exact IL-4 concentrations, these were calculated from the daily HSA:IL-4 release measured via BCA assay in section 4.3.4 (Table 4.6) using the encapsulation efficiency to determine the total protein content and percentage of IL-4 calculated based on the ratio of HSA to IL-4 encapsulated. The microparticles were soaked for 24 hours prior to use for treatment therefore day 1 of cell treatment refers to day 2 of protein release in Table 4.6.

Table 5.1: Exogenous IL-4 treatment concentrations used for $M_{(IL-4)}$ exogenous reference based on BCA assay results

Day of Cell Treatment	Estimated IL-4 Per Day (ng/mg)
1	25.65
2	22.90
3	13.79
4	4.46
5	6.47
6	7.17

The cell supernatants were taken from each condition at days 3 and 7 to determine the changes in cell population over time and assessed using ELISAs to determine the cell population.

An overview of the experimental design for microparticle treatment of THP-1 and iBMDM cells is shown in Figure 5.2.

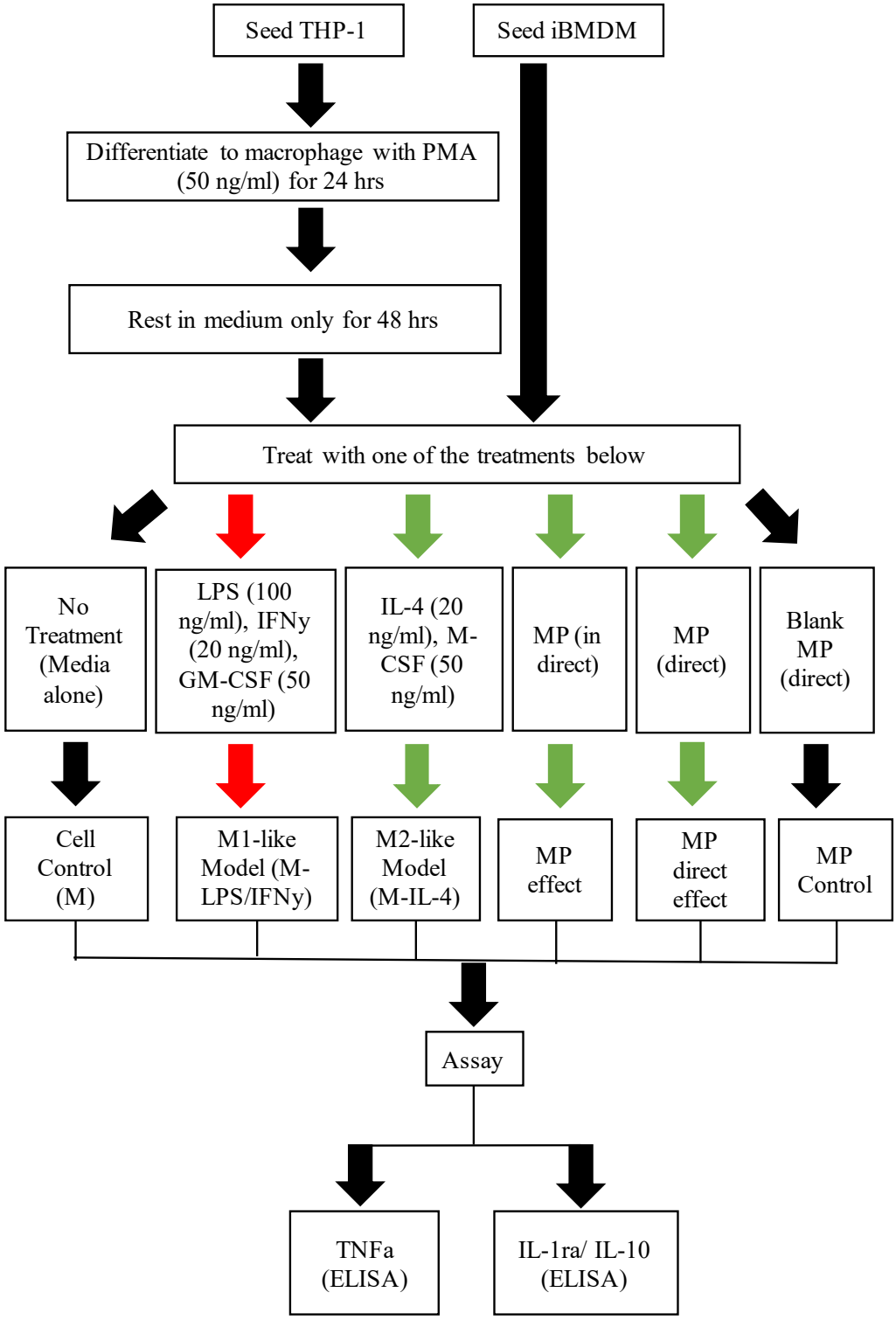

Figure 5.2: An overview of the experimental design for treatment of THP-1 and iBMDM cells with microparticles.

5.2.5 Enzyme-linked immunosorbent assay (ELISA) for macrophage population characterisation

Various markers have been reported for macrophage populations (Park *et al.*, 2007; Parsrinen *et al.*, 2015; Tu *et al.*, 2015; Minardi *et al.*, 2016; Huleihel *et al.*, 2017). TNFα was chosen as a marker for an $M_{(LPS/IFN\gamma)}$ population due to widely reported use (Park *et al.*, 2007; Huleihel *et al.*, 2017) and ease of detection in cell supernatants. IL-1ra and IL-10 were chosen as markers for an $M_{(IL\text{-}4)}$ population due to reported use (Parsrinen *et al.*, 2015; Huleihel *et al.*, 2017), however these were not as easily detected in cell supernatants. The TNFα, IL-1ra and IL-10 concentration in the cell media was measured using commercial ELISA kits following the manufacturer's instructions, as described in section 2.2.4. The proportion of each marker was compared for each condition, using the non-treated or M0 population as a cell control and blank microparticles as a microparticle control.

5.3 Results

5.3.1 Determination of macrophage population through enzyme-linked immunosorbent assay (ELISA) analysis following exogenous cytokine treatment

An ELISA was used on cell medium post-differentiation study as described in section 2.2.4 to determine the cell morphology using known markers for each cell type. This was undertaken to compare the effect of cytokine treatment on the macrophage population. The expectation was that the cells treated with LPS and IFNγ would result in a proinflammatory population and therefore secrete a

greater proportion of an inflammation marker, TNFα, and similarly for IL-4 treated resulting in a pro-immunoregulatory population. This study was undertaken to ensure that exogenous cytokines had the desired effect on the macrophage population before testing a microparticle cytokine delivery system. The results are shown in Figures 5.3 and 5.4.

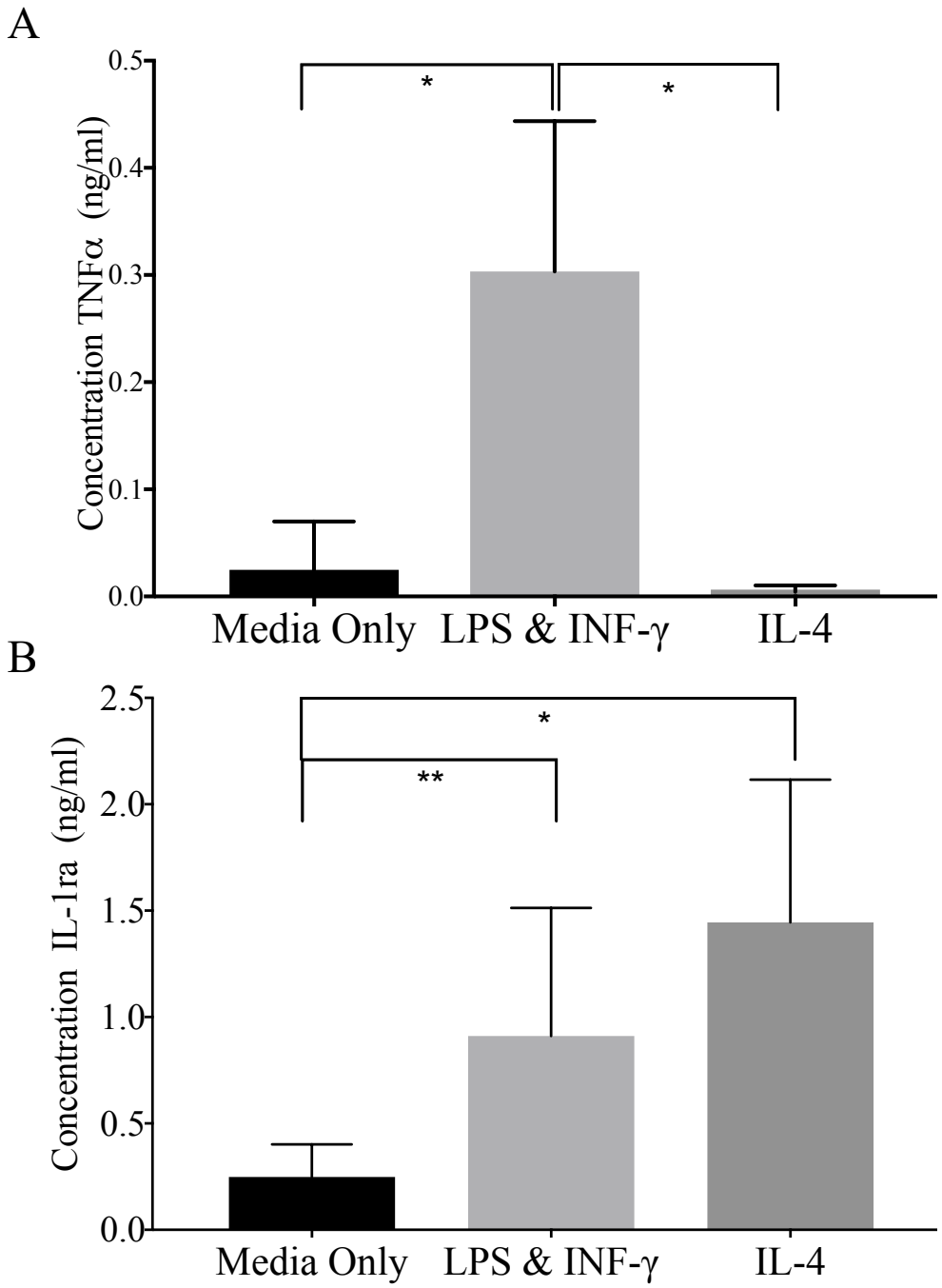

Figure 5.3: Enzyme-linked immunosorbent assay (ELISA) analysis of LPS, IFNγ, GM-CSF and IL-4, M-CSF exogenously treated THP-1 cells. **(A)** Human TNFa detection for $M_{(LPS/IFN\gamma)}$ cells and **(B)** human IL-1ra detection for $M_{(IL\text{-}4)}$ cells. Cell treatments were: PMA (50 ng/ml for 24 hrs) for M0 (THP-1 only); 72 hrs LPS (100 ng/ml), IFNγ (20 ng/ml) and GM-CSF (50 ng/ml) for $M_{(LPS/IFN\gamma)}$;

72 hrs IL-4 (20 ng/ml) and M-CSF (50 ng/ml) for $M_{(IL-4)}$. Significance was determined using one-way ANOVA with Tukey's multiple comparisons test and significance was defined by * p value <0.05. (N3, n3).

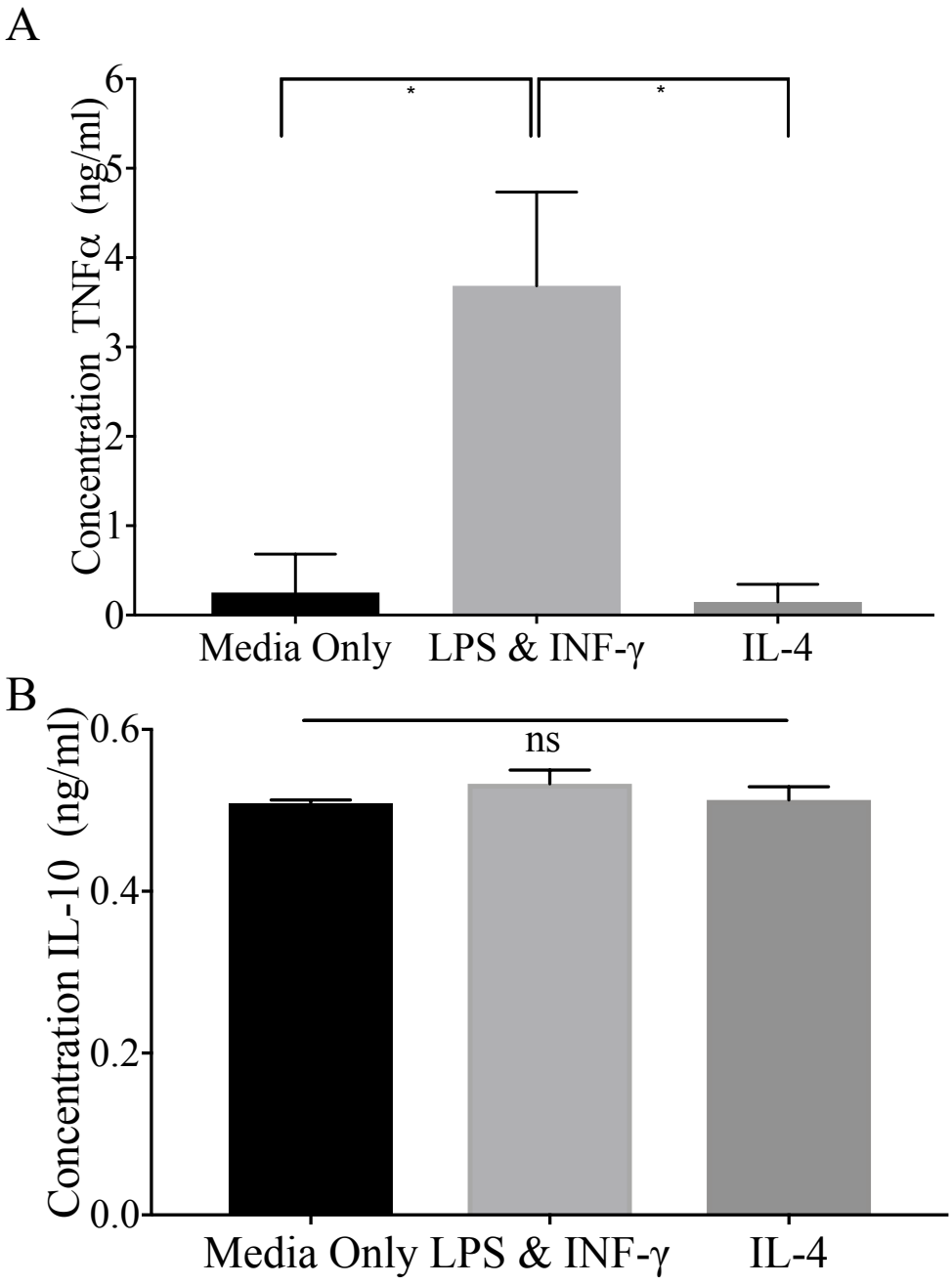

Figure 5.4: Enzyme-linked immunosorbent assay (ELISA) analysis of LPS, IFNγ, GM-CSF and IL-4, M-CSF exogenously treated iBMDM cells. **(A)**

Mouse TNFa detection for $M_{(LPS/IFN\gamma)}$ cells and **(B)** mouse IL-10 detection for $M_{(IL\text{-}4)}$ cells. Cell treatments were: PMA (50 ng/ml for 24 hrs) for M0 (THP-1 only); 72 hrs LPS (100 ng/ml), IFNγ (20 ng/ml) and GM-CSF (50 ng/ml) for $M_{(LPS/IFN\gamma)}$; 72 hrs IL-4 (20 ng/ml) and M-CSF (50 ng/ml) for $M_{(IL\text{-}4)}$. Significance was determined using one-way ANOVA with Tukey's multiple comparisons test and significance was defined by * p value <0.05. (N3, n3).

The results shown in Figure 5.3 A and Figure 5.4 A suggest that treatment of both cell types with LPS and IFN-γ result in a higher concentration of TNFα than for cells treated with IL-4 and control M0 cells. For the THP-1 cell model, treatment with IL-4 is suggested to increase the concentration of IL-1ra in comparison to non-treated and LPS, INFγ treated cells (Figure 5.3 B). However, no significant difference was seen in concentration of a second anti-inflammation marker, IL-10 for the iBMDM cell model (Figure 5.4 B).

As the microparticle delivery system was designed for continuous and sustained release of IL-4, the effect of exogenous daily treatment was also tested. Data was compiled for daily treatment with IL-4 and a single treatment at day 1. The compiled data is shown in Figure 5.5.

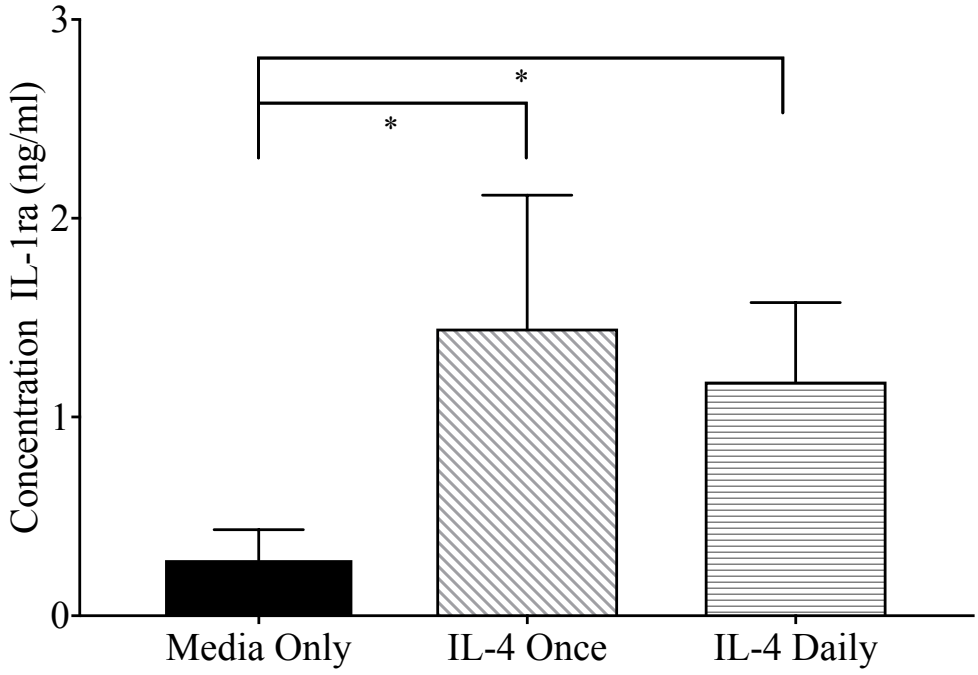

Figure 5.5: Concentration of IL-1ra comparison after 3 days between THP-1 cells treated once with IL-4 and treated daily with IL-4. (N2, n2). Error bars represent standard deviation. Significance was determined using one-way ANOVA with Tukey's multiple comparisons test and significance was defined by * $p<0.05$.

Figure 5.5 shows that there was no significant difference between the daily treatment of the THP-1 cell model with IL-4 and the single treatment with IL-4 when comparing IL-1ra concentration. There was a significant difference between both IL-4 treatments and the M0 cell control. Therefore, both established cell models could be used to test the effect of microparticle delivered IL-4 in comparison to exogenous delivered IL-4 and a non-treated M0 population.

5.3.2 Determination of macrophage population through real-time quantitative polymerase chain reaction (qPCR) analysis

Real-Time qPCR was used following the exogenous differentiation study (section 5.2.3) to determine the differentiated THP-1 cell population using known gene markers. These markers were chosen due to their reported use in literature (Huleihel *et al.*, 2017). MMP9 was used as a pan-macrophage model for THP-1 cells, TNFα as an $M_{(LPS/IFN\gamma)}$ marker and MRC1 as an $M_{(IL\text{-}4)}$ marker. The results are shown in Figure 5.6.

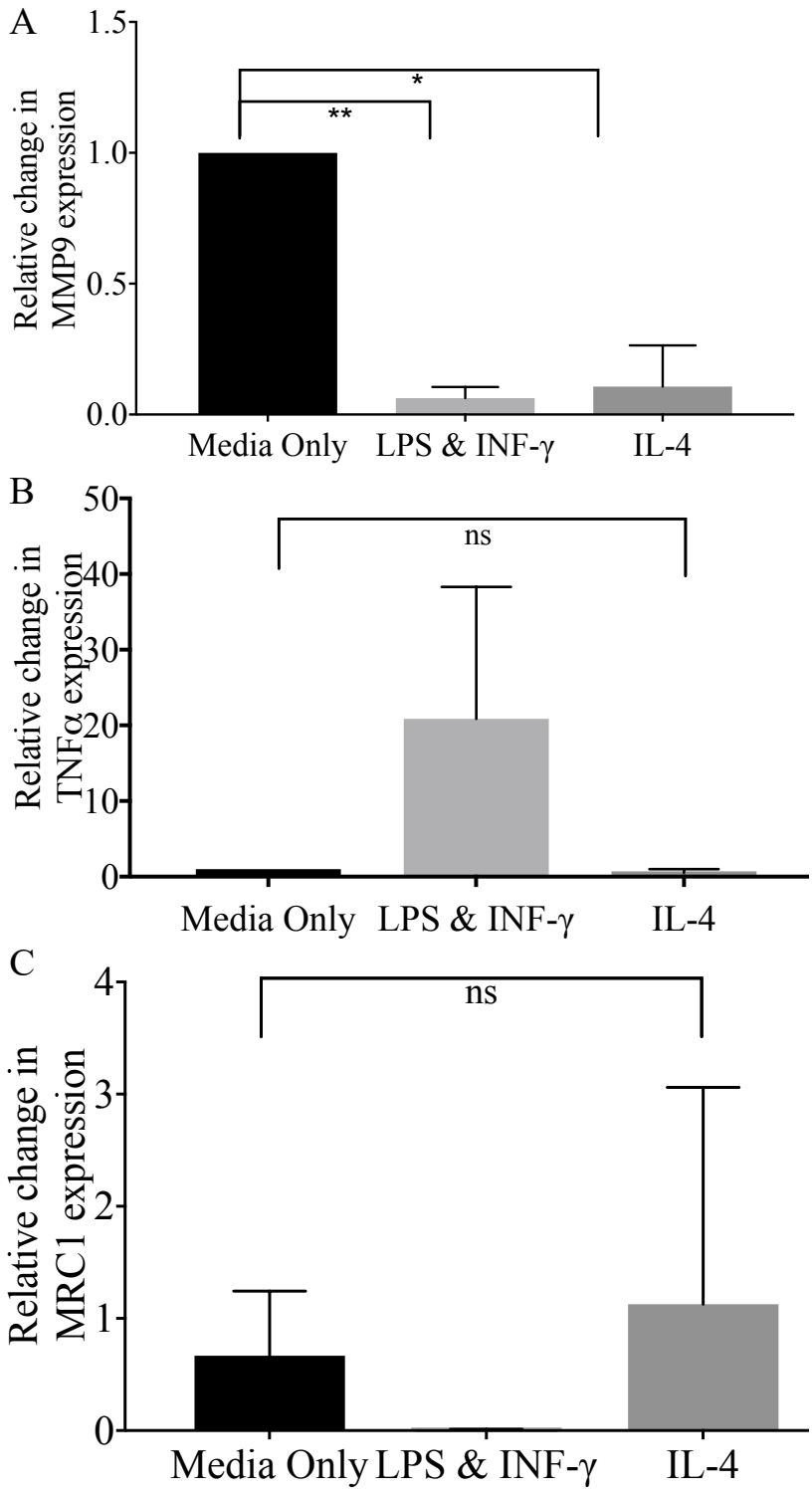

Figure 5.6: Quantitative polymerase chain reaction (qPCR) for **(A)** human MMP9, **(B)** human TNFα, and **(C)** human MRC1 expression in exogenously differentiated THP-1 cells. Cell treatments were: PMA (50 ng/ml for 24 hrs) for M0; 72 hrs LPS (100 ng/ml), IFNγ (20 ng/ml) and GM-CSF (50 ng/ml) for

$M_{(LPS/IFN\gamma)}$; 72 hrs IL-4 (20 ng/ml) and M-CSF (50 ng/ml) for $M_{(IL-4)}$. Significance was determined using one-way ANOVA with Tukey's multiple comparisons test and significance was defined by * p value <0.05 (N2, n3).

The results shown in Figure 5.6 A show that differentiation of THP-1 cells from monocytes in suspension to adherent macrophage cells with PMA results in increased expression of a pan-macrophage marker, MMP-9 as expected for a mixed macrophage population. Similarly, to the ELISA results shown in Figure 5.3 A, Figure 5.6 B suggests that treatment of the THP-1 cell model with LPS and IFN-γ results in increased gene expression of TNFα. However, the treatment with IL-4 did not result in a significant difference in MRC1 gene expression (Figure 5.6 C) which was unexpected for an $M_{(IL-4)}$ macrophage population.

5.3.3 Determination of macrophage population through enzyme-linked immunosorbent assay (ELISA) analysis following microparticle treatment

An ELISA was used to determine the cell population following microparticle treatment (section 5.2.4) using known markers for each cell type. TNF-α and IL-1ra/ IL-10 were used for $M_{(LPS/IFN\gamma)}$ and $M_{(IL-4)}$ cells respectively, chosen due to their reported use in literature. Non-treated macrophage cells were used as a comparative cell control and blank microparticles were used as a microparticle control. The microparticles were also added with direct or indirect contact to the cells to ensure any effect was a result of the delivered IL-4 rather than the cellular contact to the microparticle surface. The results are shown in Figures 5.7 and 5.8.

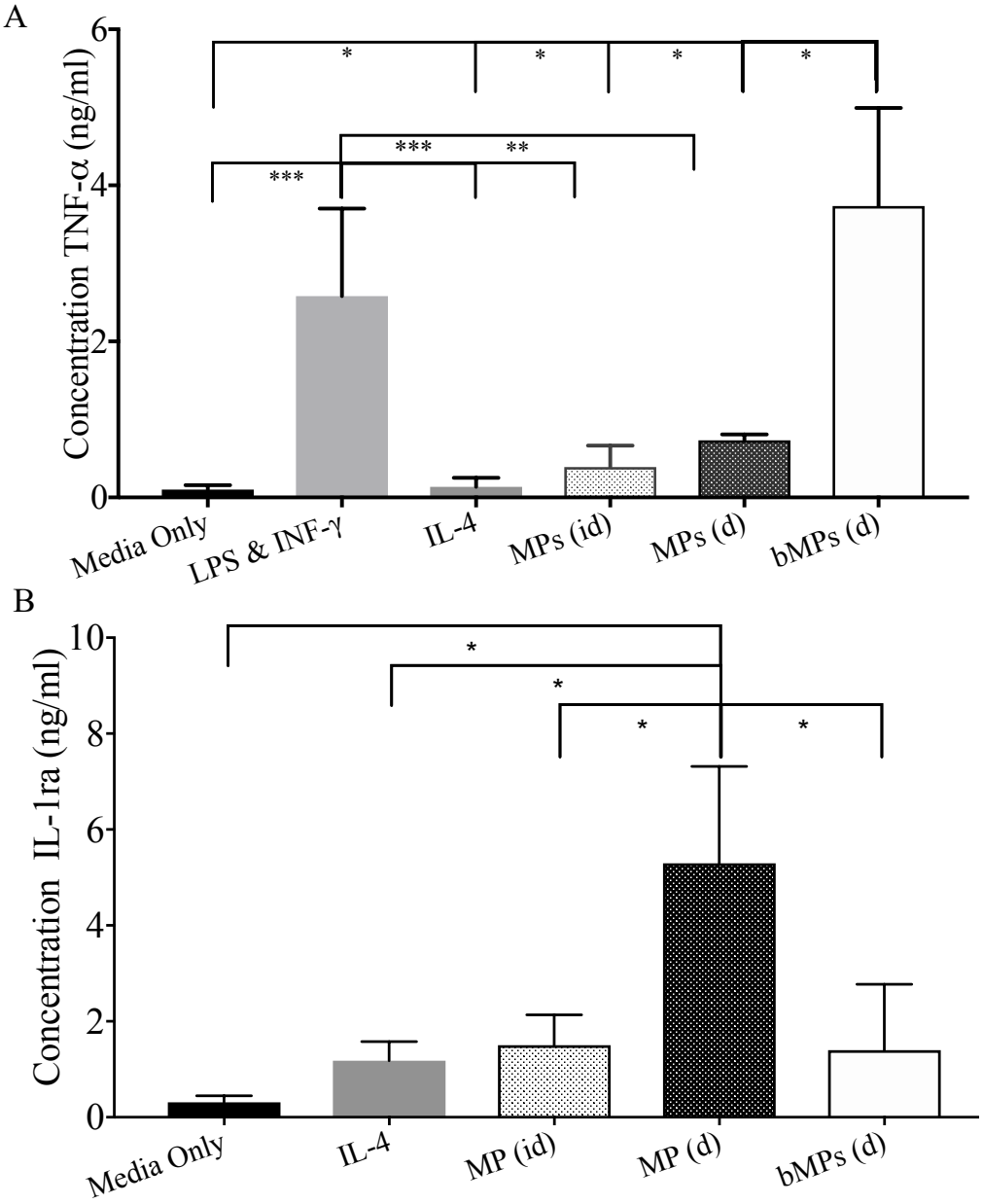

Figure 5.7: THP-1 macrophage characterisation post 3 day treatment with microparticle delivered IL-4. Concentration of **(A)** human TNFα as a $M_{(LPS/IFN\gamma)}$ marker and **(B)** human IL-1ra an anti-inflammatory marker for THP-1 cells. Cell treatments were: PMA (50 ng/ml for 24 hrs) for M0 (Media only), 72 hrs LPS (100 ng/ml), IFNγ (20 ng/ml) and GM-CSF (50 ng/ml) for $M_{(LPS/IFN\gamma)}$; 72 hrs IL-4 (20 ng/ml) and M-CSF (50 ng/ml) for $M_{(IL-4)}$. Cells either had direct contact to the cells (d) or in direct (id) where microparticles were suspended in a transwell

and blank MPs (bMPs) contained water only. (N2, n2). Error bars represent standard deviation. Significance was determined using one-way ANOVA with Tukey's multiple comparisons test and significance was defined by * $p < 0.05$.

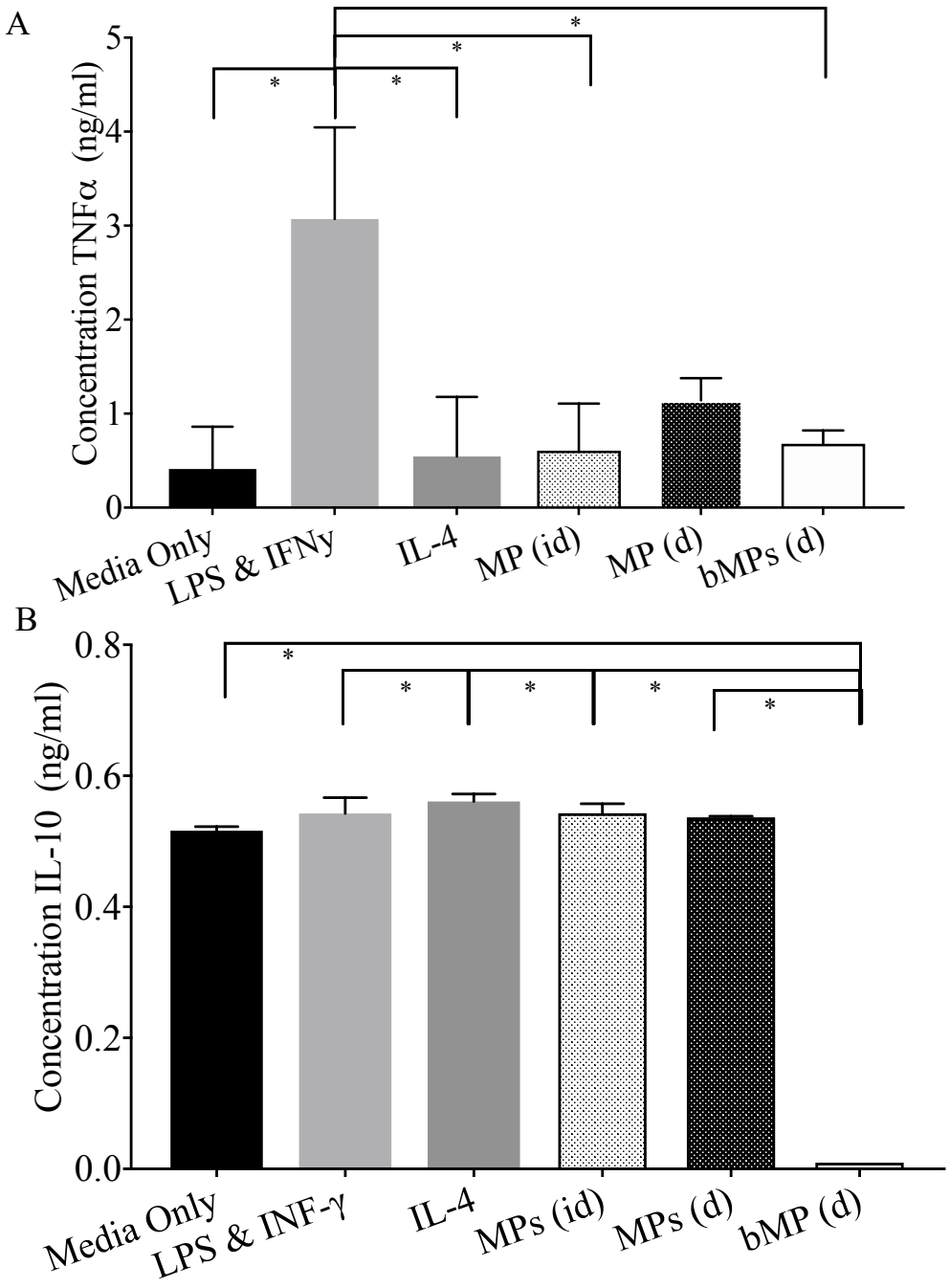

Figure 5.8: iBMDM cell characterisation post 3 day treatment with microparticle delivered IL-4. Concentration of **(A)** murine TNFα as an $M_{(LPS/IFN\gamma)}$ marker and **(B)** murine IL-10 as an $M_{(IL-4)}$ marker. Cell treatments were: 72 hrs LPS (100 ng/ml), IFNγ (20 ng/ml) and GM-CSF (50 ng/ml) for $M_{(LPS/IFN\gamma)}$; 72 hrs IL-4 (20 ng/ml) and M-CSF (50 ng/ml) for $M_{(IL-4)}$. Cells either

had direct contact to the cells (d) or in direct (id) where microparticles were suspended in a transwells and blank MPs (bMPs) contained water only. (N2, n2). Error bars represent standard deviation. Significance was determined using one-way ANOVA with Tukey's multiple comparisons test and significance was defined by * $p < 0.05$.

The results in Figure 5.7 A suggest that treatment of the THP-1 cell model with IL-4 containing microparticles resulted in a lower concentration of TNFα in comparison to the exogenous LPS and IFNγ treated cells. However, there was no significant difference between the TNFα concentration secreted by the media only cell control and the IL-4 treated cells. A similar result was seen in Figure 5.8 A for the iBMDM cell model, where IL-4 treated cells, both exogenous and microparticle delivered, secreted less TNFα than the LPS and IFNγ treated cells. As for the THP-1 cells, no significant difference was observed between the TNFα concentrations for media only treated iBMDM cells and IL-4 treated. For both cell models there was also no significant difference between the TNFα concentration for microparticle treatment and exogenous IL-4 treatment. Figure 5.7 B shows that the treatment with microparticles with direct cellular contact resulted in a higher concentration of IL-1ra for the THP-1 cell model. However, when analysing IL-10 for the iBMDM cell model, no significant difference was seen between the exogenous IL-4, microparticle treatments or M0 media only control.

Figure 5.7 A shows that treatment with blank (water containing) microparticles resulted in a higher concentration of TNFα in comparison to IL-4 microparticles, LPS, IFNγ treated cells and M0 control for the THP-1 cell model. The concentration of IL-1ra was reduced for the blank microparticle treatment, especially in comparison with IL-4 microparticles with direct cellular contact (Figure 5.7 B). When comparing the effect of blank and IL-4 microparticle treatments on the iBMDM cell model, no significant difference was seen between TNFα concentrations as shown in Figure 5.8 A. However, the concentration of IL-10 was significantly less for the blank microparticles in comparison to both IL-4 microparticle treatments and the M0 media only control (Figure 5.8 B). This confirmed that the IL-4 release was affecting the cells rather than the PLGA microparticle surface.

In order to gain more understanding of microparticle use for delivery of IL-4 on the macrophage population, TNFα, IL-1ra and IL-10 ELISAs were carried out at day 7 and results are shown in Figures 5.9 and 5.10. Due to the lack of significant difference between blank microparticles and cell control, the difference between microparticles with indirect contact and direct contact were the focus for the 7 day study. This was to determine if prolonged contact of the cells with microparticles had a different effect than seen at day 3 in comparison to the exogenously treated cells and microparticles with in direct contact.

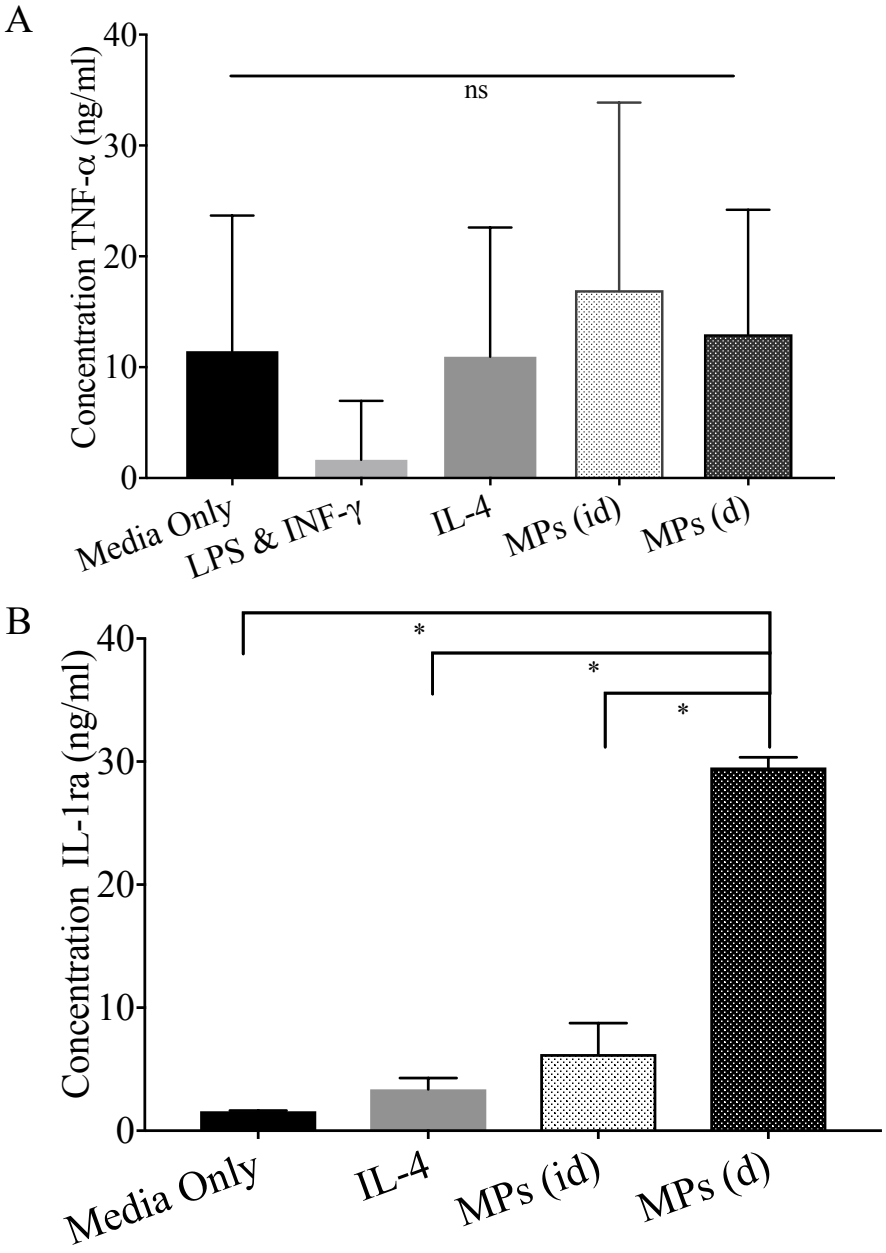

Figure 5.9: THP-1 macrophage characterisation post 7 day treatment with microparticle delivered IL-4. Concentration of **(A)** human TNFα as a $M_{(LPS/IFN\gamma)}$ marker and **(B)** human IL-1ra an $M_{(IL-4)}$ marker. Cell treatments were: PMA (50 ng/ml for 24 hrs) for M0 (Media only); 72 hrs LPS (100 ng/ml), IFNγ (20 ng/ml) and GM-CSF (50 ng/ml) for $M_{(LPS/IFN\gamma)}$; 72 hrs IL-4 (20 ng/ml) and M-CSF (50 ng/ml) for $M_{(IL-4)}$. (N2, n2). Error bars represent standard deviation. Significance

was determined using one-way ANOVA with Tukey's multiple comparisons test and significance was defined by * $p < 0.05$.

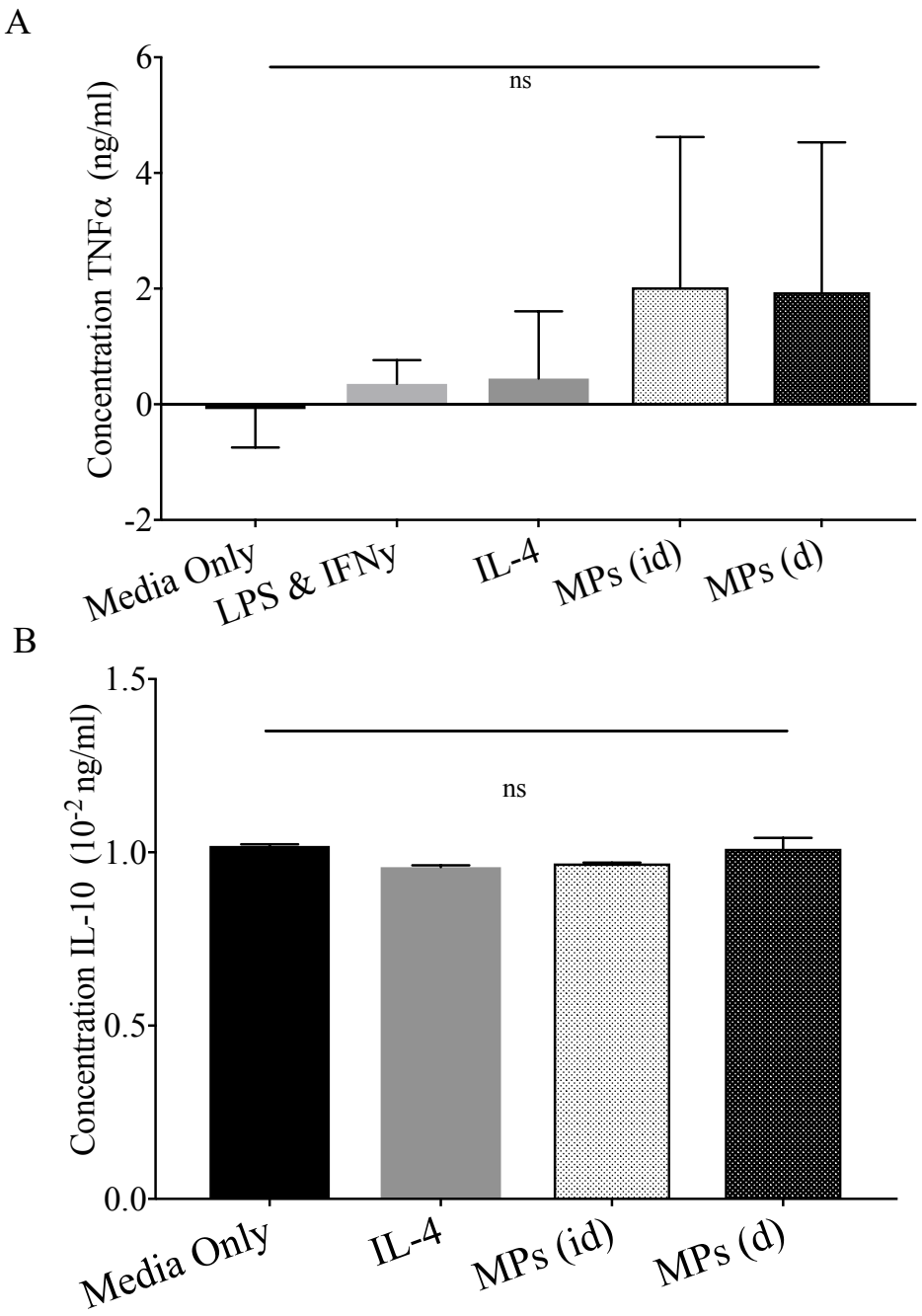

Figure 5.10: iBMDM cell characterisation post 7 day treatment with microparticle delivered IL-4. Concentration of **(A)** murine TNFα as an $M_{(LPS/IFN\gamma)}$ marker and **(B)** murine IL-10 as an $M_{(IL\text{-}4)}$ marker. Cell treatments

were: 72 hrs LPS (100 ng/ml), IFNγ (20 ng/ml) and GM-CSF (50 ng/ml) for $M_{(LPS/IFN\gamma)}$; 72 hrs IL-4 (20 ng/ml) and M-CSF (50 ng/ml) for $M_{(IL\text{-}4)}$. (N2, n2). Error bars represent standard deviation. Significance was determined using one-way ANOVA with Tukey's multiple comparisons test and significance was defined by * $p < 0.05$.

From the results shown in Figure 5.9 A, there was no significant difference in TNFα concentration after 7 days treatment for the THP-1 cell model. This could be a result of the dynamic population which changes over time, a continuous treatment of LPS, IFNγ may be required to see a difference in TNFα concentration at day 7. A similar result was shown for the iBMDM cell model, where no significant difference was seen for TNFα concentration (Figure 5.10 A). Post 7 day treatment, IL-4 microparticles with direct cellular contact did result in a higher IL-1ra concentration for the THP-1 cell model in comparison to microparticles indirectly, exogenous IL-4 and the M0 cell control (Figure 5.9 A). However, when tested with the iBMDM model no significant difference was seen between the microparticle treated, exogenous treated and media only control for IL-10 concentration after 7 days (Figure 5.10 C).

5.4 Discussion

Both THP-1 and iBMDM cell models were used in population doubling experiments, as shown in Supplementary Data (Figure 7.16), where cell growth was monitored with and without microparticles. The data showed that culturing the cells with microparticles did not affect the cell growth and the cells could therefore be used as a model for microparticle IL-4 treatment.

The ELISA results shown in Figure 5.2 A suggested that the cells treated with LPS, IFNγ and GM-CSF had a higher proportion of TNFα than those treated with PMA only or with IL-4 and M-CSF. These results are consistent with an $M_{(LPS/IFN\gamma)}$ population and suggest that the exogenous treatment with these three factors can influence macrophage polarisation from an M0 state to M1-like. Further tests could have been carried out to confirm this, including analysing the concentration of other markers such as; IL-1β, IL-6, IL-12 or IL-23 (Duluc *et al.*, 2007; Rőszer, 2015), or the use of immunostaining or western blot analysis. The proportion of IL-1ra was greater in the cells treated with IL-4 and M-CSF as shown in Figure 5.2 C, which is indicative of an $M_{(IL-4)}$ population. Although the proportion of IL-1ra was also notably higher in $M_{(LPS/IFN\gamma)}$ than M0 which could suggest a mixed population of macrophage types (Galdiero and Mantovani, 2015). Further analysis of markers such as TGFβ or IL-10 could have been used to indicate an $M_{(IL-4)}$ population (Duluc *et al.*, 2007; Rőszer, 2015).

Following on from these results, the THP-1 cells were further characterised using qPCR to confirm these findings and also to determine if an $M_{(IL-4)}$ population could be further distinguished or if a more defined population could be achieved. After treatment with PMA, the THP-1 cells expressed a large amount of the chosen housekeeping gene, MMP9 as expected for a population of macrophage cells (Figure 5.3 A). However, the expression of MMP9 was not high for the cells that were further differentiated with LPS, IFNγ or IL-4, suggesting that the pan-macrophage marker is not as apparent once macrophage cells are polarised to an $M_{(LPS/IFN\gamma)}$ and $M_{(IL-4)}$ state. It is possible that the expression of a different factor, such as CD86 or CD163 (Duluc *et al.*, 2007; Rőszer, 2015) down regulated the expression of MMP9 (Pannu *et al.*, 2007). A distinctive population of $M_{(LPS/IFN\gamma)}$ cells were seen when polarised with LPS & IFNγ with high TNFα expression (Figure 5.3 B), this was similar to results seen in literature (Chanput *et al.*, 2013; Vogel *et al.*, 2014; Huleihel *et al.*, 2017). There was very little expression of TNFα from the M0 and $M_{(IL-4)}$ treated populations as expected, however not a significant difference which may indicate a mixed population characteristic of the dynamic macrophage nature and the spectrum of activation states (Vogel *et al.*, 2014; Rőszer, 2015). This was particularly explored in a review by Tardito *et al* and showed that in many studies there was no significant difference between $M_{(IL-4)}$ markers and $M_{(LPS/IFN\gamma)}$ markers following stimulation, concluding there to be mixed $M_{(LPS/IFN\gamma)}$ and $M_{(IL-4)}$ populations (Tardito *et al.*, 2019). However, other studies by Huleihel *et al* have obtained appealingly distinctive $M_{(IL-4)}$ populations using IL-4 stimulation, when comparing phagocytosis the IL-4 treated cells expressed lower percentage change in intensity indicative of an $M_{(IL-4)}$ population (Huleihel

et al., 2017). This study by Huleihel *et al* also looked at immunostaining markers and showed lower intensity staining for TNFα and higher intensity for TGM2 and CD206, although not quantitative this still indicates a positive $M_{(IL-4)}$ population (Huleihel *et al.*, 2017). These studies suggest that despite the presence of mixed macrophage populations, $M_{(IL-4)}$ cell markers can be analysed and observed.

A similar situation was seen when analysing MRC1 expression as a $M_{(LPS/IFN\gamma)}$ and $M_{(IL-4)}$ population marker. The proportion of MRC1 for the IL-4 treated or $M_{(IL-4)}$ cells was greater than for the other treatments but not significantly different (Figure 5.3 C), suggestive of a mixed population. Despite this, the presence of MRC1 did indicate a IL-4 stimulated or $M_{(IL-4)}$ environment (Minardi *et al.*, 2016a). The lack of TNFα expression for the IL-4 treated cells is a positive indication of lack of proinflammatory macrophages, so although the MRC1 results are not significant, it is implied that the population is vastly reduced in $M_{(LPS/IFN\gamma)}$ and macrophages.

It is possible that the lack of difference between expression of TNFα and MRC1 in different cell treatments was due to the time of analysis. Samples were collected after 3 days treatment, at which the point of gene upregulation may have been missed. Further studies to analyse the gene expression at day 1 and day 2 post treatment would be interesting in comparison to day 3. Due to the lack of significant data obtained for gene expression analysis by qPCR, protein expression by ELISA analysis was focussed on in the following studies.

In a similar way to the THP-1 cells, the iBMDM cells secreted more TNFα post-treatment with LPS, IFNγ and GM-CSF (Figure 5.2 B) as expected for an $M_{(LPS/IFN\gamma)}$ population and as is reported in literature as a marker for a proinflammatory state (Spencer *et al.*, 2010; Barros *et al.*, 2013; Mantovani *et al.*, 2013; Genin *et al.*, 2015; Shiratori *et al.*, 2017; Tedesco *et al.*, 2018). Also, in a comparable way to the differentiated THP-1 cells, the non-treated or M0 cells and IL-4, M-CSF treated cells did not express large amounts of TNFα which could be attributed to a non-inflammatory or proimmunoregulatory population, however further investigation was required to confirm this. As shown in Figure 5.2 D, the IL-4, M-CSF treated cells expressed IL-10 as expected for a proimmunoregulatory environment, however there were also high expression for the LPS, IFNγ and GM-CSF treated cells. Both this data and the IL-1ra results for the THP-1 cells (Figure 5.2 C) highlight the difficulty in categorically defining an $M_{(IL-4)}$ cell population which has also been seen in (Porcheray *et al.*, 2005; Jaguin *et al.*, 2013; Vogel *et al.*, 2014). Part of this difficulty arises from the extremely dynamic macrophage cell environment, which is able to change quickly upon stimulation within the immune system as reported in literature (Murray *et al.*, 2014; Vogel *et al.*, 2014).

As implied by Vogel *et al,* there are no markers completely distinctive or specific to an $M_{(LPS/IFN\gamma)}$ and $M_{(IL-4)}$ population of macrophages (Vogel *et al.*, 2014). Unfortunately, the results shown for $M_{(IL-4)}$ marker ELISAs in iBMDM cells did not provide sufficient data to show a separate $M_{(IL-4)}$ population from

an $M_{(LPS/IFN\gamma)}$ population. The iBMDM cells were not analysed with qPCR due to lack of significance seen at day 3 for the THP-1s and due to lack of protein expression seen in ELISA analysis. Although, qPCR has been used in literature as a characterisation method for THP-1 cell models (Genin *et al.*, 2015; Huleihel *et al.*, 2017), it has not been well used for iBMDM cells.

Post-3 day treatment with microparticle delivered IL-4, both in direct contact and indirect contact with cells resulted in reduced TNFα for both THP-1 cells and iBMDM cells, especially in comparison to $M_{(LPS/IFN\gamma)}$. Interestingly there was a greater amount of TNFα production for the cells in direct contact with the microparticles. This could be due to a slight inflammatory response of the cells in contact with the biomaterial; however, this value was lower than the LPS, IFNγ treated population. The exogenous treatment results in this experiment confirmed that the addition of LPS and IFNγ resulted in a highly inflammatory environment. There was no significant difference between the TNFα expressions for the exogenous IL-4 treated cells and those treated with IL-4 delivered via microparticles. This indicates that it is possible to deliver active IL-4 from PLGA microparticles and not result in increased secretion of inflammatory markers, also to obtain a similar effect to the exogenous IL-4 treated cells.

The analysis of $M_{(IL\text{-}4)}$ population markers proved more difficult, as was seen for the exogenously treated cells. However, when treated with microparticles containing IL-4, there was a significant increase in IL-1ra for the THP-1 cells,

especially when the particles were in direct contact. A greater production was also seen for the microparticles in transwell than those treated exogenously although not a significant difference. Further repeats would be required to confirm this statement. Despite this, the results obtained gave a positive indication of the effect of microparticle delivered IL-4 on modulating macrophage phenotype towards a less inflammatory state. The data obtained for the iBMDM treated cells was less conclusive, with IL-10 concentration used as a marker for an $M_{(IL-4)}$ population. As such a minute amount of IL-10 was produced in all treated cells, it is difficult to assess the exact effect of the microparticles on the cell population. A further analysis of a different marker, such as CD206 may be required in order to determine this (Nakajima *et al.*, 2012; Wolf *et al.*, 2014; Minardi *et al.*, 2016).

A comparison was made between microparticles containing IL-4 and blank microparticles (bMPs) containing water, to determine if the difference in macrophage markers. When tested with the THP-1 cell model the culture with direct contact with bMPs appeared to produce significantly more TNFα after 3 days in culture. This suggests that the resulting reduction of inflammatory cytokines was a consequence of the IL-4 treatment rather than the contact with the microparticle surface. This was also confirmed when IL-1ra was used as a marker for proimmunoregulatory macrophages. Here it was seen that the microparticles containing IL-4 in direct contact with the cells resulted in a greater production of IL-1ra in comparison to those containing water. Interestingly, there was minimal difference between the IL-1ra production when IL-4 MPs were not in direct contact with the cells and the blank MPs. This

suggests that the IL-4 was unable to have the desired effect when released through a transwell. However, it is important to recognise that the cell models used *in vitro* were static and had no influence from other cells or external factors as would be the case *in vivo*, therefore although these results give an indication, verification *in vivo* is required.

When comparing the effect of MPs on iBMDM cells there was no significant difference between the TNFα concentration following culture with IL-4 MPs and bMPs. Therefore, it is difficult to confirm if the reduction in TNFα seen in Figure 5.8 (A) was a result of IL-4 or the MP surface. Very little IL-10 was seen after 3 days in culture for the bMPs. This suggests that the effect seen for the IL-4 MPs was a result of IL-4 release and not an external factor such as the microparticle surface interaction with the cells. However, the media treated cell control also expressed large amounts of IL-10 in contrast to what is seen in literature for macrophage controls (Minardi *et al.*, 2016) where controls expressed little to no IL-10 compared to IL-4 treated cells. Due to this, again it is difficult to determine the exact effects of the IL-4 MPs in this cell model after 3 days culture. Due to the novelty of MP treatment for IL-4 delivery to macrophage cells it is difficult to confirm using literature the effects of these studies.

It must also be taken into consideration that the cells treated with microparticles were subjected to IL-4 daily. Typically the *in vitro* cultures used a single day treatment of IL-4 so, in order to make a direct comparison between the

exogenous treated cells and the cells treated as a result of daily IL-4 released from microparticles, the exogenous treatment was made daily using the concentration of IL-4 estimated to be released from the particles. The results suggest that a continual treatment of IL-4 had an effect on the production of IL-1ra however, no significant difference to the effect of one treatment at day 1. Although, this study was only carried out until day 3, the effect of a daily treatment may be prolonged over a longer study. This requires further investigation. It is also important to consider that in an in vitro setting the population of cells is relatively static, whereas in an in vivo setting the population of macrophages would be continually recruited from the immune system and it may therefore be beneficial to have continuous treatment (Qin, 2012).

Following a 7 day culture with cytokines or MPs, ELISAs were carried out for each cell model. When MPs were used with THP-1 cells, there was no significant difference in concentration of TNFα after 7 days culture. This implies the presence of a dynamic changing population of macrophage cells which is changing over time and resulting a different population at day 7 than at day 3. As shown in the release curves in section 4.3.4 (Figure 4.5), IL-4 was not released at a significant rate after day 4 and therefore the effect on cells post-day 4 was not expected to mimic that of day 3. However, when analysing the concentration of IL-1ra, the microparticles in direct contact with the cells resulted in a significantly higher proportion of IL-1ra in comparison to cell control, exogenous treatment and indirect contact. This suggests that despite the assumption there was little IL-4 release following day 4, the MPs are still having

a proimmunoregulatory effect on the cells. This may be a result of the breakdown and metabolism of PLGA components into lactic acid and glycosides so the particles are not recognised as a threat to the immune system.

The same analysis was carried out on the iBMDM cell model, for both TNFα and IL-10 markers, but no significant difference was seen for the different conditions. This confirms data shown in Figures 5.8 and 5.10, where iBMDM cell characterisation of an $M_{(IL-4)}$ population was difficult to define. Limited literature explores the effect of IL-4 over a 7 day period as most studies look at the first 24 - 72 hrs post-treatment and therefore there were no expectations of the results. Huleihel *et al* showed that bone marrow derived macrophages could be used as a macrophage model for differentiation, however only treated for 24 hours (Huleihel *et al.*, 2017). Minardi *et al* also showed that bone marrow derived macrophages could be affected by the delivery of IL-4, but only assessed the effect up to 72 hrs (Minardi *et al.*, 2016). One study by Pajarinen *et al* looked at the effect of osmotic pump delivered IL-4 up to 4 weeks and found the concentration of $M_{(LPS/IFN\gamma)}$ markers to be unchanged over time and the concentration of $M_{(IL-4)}$ markers to increase over the 4 week period (Pajarinen *et al.*, 2015). Due to this, further optimisation and investigation was required to determine the long-term differentiation effects of these IL-4 containing microparticles on the THP-1 and iBMDM cell models established.

5.5 Conclusions

The results in this chapter highlight the difficulty in characterising a dynamic proimmunoregulatory population of macrophages, which has been discussed in literature and subsequently highlights the lack of macrophage model representation *in vitro* (Murray *et al.*, 2014; Vogel *et al.*, 2014; Huleihel *et al.*, 2017). The markers used for an $M_{(LPS/IFN\gamma)}$ population were much more easily detected then those for an $M_{(IL\text{-}4)}$ population and therefore this population was more able to be identified. This suggests that rather than focusing on analysing markers for a predominately $M_{(IL\text{-}4)}$ population, it may be more effective to look at the decrease in proinflammatory markers as an alternative. Using current understandings of macrophage modulation (Arora *et al.*, 2017), it has been demonstrated in this chapter than the treatment of both THP-1 cells and iBMDM with exogenous IL-4 does result in a reduction of inflammatory markers and is likely due to the reduction of $M_{(LPS/IFN\gamma)}$ macrophages.

In comparison to the exogenous treatment of the cell models with IL-4 shown in this chapter, the treatment with IL-4 containing microparticles did appear to have an effect on the modulation of macrophage cells, especially for the THP-1 cell model. When analysing TNFα as a marker for $M_{(LPS/IFN\gamma)}$ the concentration of TNFα was reduced in the IL-4 treated cells in comparison to the $M_{(LPS/IFN\gamma)}$ control. An increase in IL-1ra, as a marker for $M_{(IL\text{-}4)}$, was also seen upon treatment with IL-4 containing microparticles. The effects were more defined when the cells had direct contact with the microparticles, suggesting that the effect of IL-4 was hindered when released through a transwell.

A similar effect was seen for the iBMDM cell model when testing for TNFα secretion. Treatment with IL-4 containing microparticles resulted in a similar effect to the treatment of exogenous IL-4, where the concentration of TNFα was reduced in the IL-4 treated cells in comparison to the LPS, IFNγ treated or $M_{(LPS/IFN\gamma)}$ control. Unlike for the THP-1 cells, when IL-10 was used as a marker for an $M_{(IL-4)}$ population little difference was seen between the IL-4 treated cells, both exogenous and microparticle delivered, and the M0 media only control. Further optimisation may be required to fully test the effects of these particles on this cell model, testing further markers and using alternative analysis methods such as immunostaining, western blot analysis or qPCR.

The results shown after 7 days treatment with IL-4 microparticles were inconclusive of the effects microparticles on macrophage modulation. This was likely due to the lack of IL-4 release past day 4, as shown in section 4.4 where the majority of IL-4 was released between days 1-4.

The effect of the microparticles with direct and in direct cell contact was determined after 3 days for both cell types. It appeared that cellular contact with the microparticles resulted in increased proinflammatory markers but also increased proimmunoregulatory markers, especially when tested on the THP-1 macrophage model. To ensure the effects were resulting from the IL-4 release, blank microparticles were also tested for their effect on macrophage polarisation. When analysing proinflammatory markers the proportion for blank microparticles was greater than for those containing IL-4 suggesting the

proimmunoregulatory effect of the IL-4 particles. A greater proportion of proimmunoregulatory markers was seen for IL-4 particles in comparison to blank particles confirming that the effects were not resulting from the PLGA particle surface.

Overall this suggests that these particles have potential not only as an inflammatory modulation therapy in SCI but with further optimisation could be used for other chronic inflammatory conditions.

Chapter 6: General Discussion, Conclusions, Future Developments and Future Outlook

6.1 General discussion

The main obstacle to spinal cord injury treatment is the chronic inflammatory environment which surrounds the injury site and is detrimental to repair and regeneration (Porcheray *et al.*, 2005; Galdiero and Mantovani, 2015). The result is irreversible loss of function and sensation in the limbs to varying extent (Silva *et al.*, 2014). The current treatments include treating the side effects with anti-inflammatory drugs or the use of physiotherapy, however no current approach is able to return limb function and sensation (Baumann *et al.*, 2009; Kang *et al.*, 2010; McCreedy and Sakiyama-Elbert, 2012; Silva *et al.*, 2014). An understanding of how macrophage cells play a role in inflammation, in particular in spinal cord injury, will provide a new target for spinal cord injury therapeutics and potential alleviation of the chronic inflammatory environment leading to repair and regeneration at the injury site. The modulation of macrophage population from a pro-inflammatory state to a proimmunoregulatory state is not a novel idea, however, the use of microparticle delivered IL-4 for this purpose with the specific application of spinal cord injury is an idea yet to be explored. This thesis aimed to explore the use of a novel IL-4 microparticle delivery system to modulate the inflammatory environment through influencing the macrophage population.

Arguably, the most fundamental step in this project was the optimisation and development of a microparticle formulation able to release protein in a controlled and sustained manner (Chapter 3 and Chapter 4). Variations on the lactide to glycolide ratio in the PLGA polymer used and the addition of F127 P188 were explored as a method to modulate protein release (Chapter 3), however, a suitable release kinetic profile was not obtained and lead to the exploration of different modulation factors. Variations of the total polymer percentage and addition of a triblock (PLGA-PEG-PLGA) copolymer were then explored (Chapter 4) and a suitable formulation resulting in controlled and sustained protein release was discovered. The use of a 20 % *w/v* total polymer microparticle comprised from 85:15 PLGA and 40 % *w/w* PLGA-PEG-PLGA triblock was found to result in a release profile with minimal burst release but sustained release following day 1. This formulation was then tested using encapsulated IL-4 (Chapter 4) to compare the release to that of the model protein, lysozyme, used for optimisation. The results showed that although IL-4 was released from the microparticles, the release was not as sustained as seen for the lysozyme. However, when assessing the release of lysozyme, only the total protein release was determined, this suggesting that the sustained release observed for lysozyme with HSA was a result of the HSA and not the active protein. To confirm this, the total lysozyme would need to be determined rather than the total protein using lysozyme and HSA. When assessing the release of total protein (HSA and IL-4) a similar trend was seen as for HSA and lysozyme. Despite this, the formulation was tested for its efficacy at modulating the macrophage population (Chapter 5).

The next step to this project was to develop two robust *in vitro* cell models to mimic the human macrophage *in vivo* and use them to confirm the modulating ability of IL-4 (Chapter 5). Firstly, exogenous cytokines were used to modulate the macrophage cells towards an $M_{(LPS,\ IFN\gamma)}$ or $M_{(IL\text{-}4)}$ population and cell markers were analysed to characterise this. Using THP-1 cells and iBMDM cells as models, it was shown that the treatment with LPS and IFNγ resulted in increased secretion of proinflammatory marker TNFα and that treatment with IL-4 resulted in increased secretion of proimmunoregulatory marker IL-1ra or IL-10 as was reported in literature (Huleihel *et al.*, 2017). Following on from this, the cell models were treated with IL-4 delivered via microparticles and the cell markers were analysed in comparison to the exogenously treated cells. A similar cellular response was seen for the microparticle delivered IL-4 as for the exogenous IL-4, where increased secretion of proimmunoregulatory markers were seen and decreased secretion of proinflammatory markers.

It was hoped that the analysis of the cell markers would provide distinctive characterisation of the macrophage population, however, it was difficult to obtain results displaying a set $M_{(IL\text{-}4)}$ population. Due to this it may be more beneficial to look at the reduction of proinflammatory markers post-IL-4 treatment rather than looking at increased proimmunoregulatory markers or do further optimisation and explore new techniques and markers as touched on in section 6.3. Despite this, the results shown in this project reiterate the importance of IL-4 as a stimulation factor for the modulation of macrophage phenotype and therefore the inflammatory environment. The results also show, for the first

time, that IL-4 can be encapsulated and released as an active protein from PLGA microparticles in a controlled and sustained manner. Further work needs to be undertaken to further improve the release profile. Finally, the results of this project showed for the first time that the macrophage population could be influenced by treatment with IL-4 containing microparticles. It is hoped that these results will lead to new a new target for inflammation control, not only in the case of spinal cord injury but also adapted into other chronic inflammatory conditions such as rheumatoid arthritis.

6.2 Conclusions

The 85:15 PLGA 40 % *w/w* TB4 microparticle formulation was chosen to be most suitable for controlled sustained release, with release over 20 days. This formulation was repeated with HSA:IL-4 and the release kinetics were compared to that of HSA:Lysozyme. Sustained release of IL-4 was achieved over 4 days which would be suitable to modulate macrophage cells in SCI where the $M_{(LPS,\ IFN\gamma)}$ population is at its most damaging at days 1 - 5 post injury.

A robust cell culture method was established, and it was shown that both cell models could be cultured with microparticles without affecting their growth, providing a suitable in vitro macrophage cell model for the study of macrophage modulation using microparticles.

Polarisation of THP-1 cells and iBMDM cells with LPS, IFNγ and GM-CSF resulted in a distinctive $M_{(LPS, IFN\gamma)}$ population for both cell types. Polarisation with IL-4 and M-CSF also resulted in a distinctive population of $M_{(IL-4)}$ cells in the THP-1 model. The treatment with IL-4 resulted in a reduction in a proinflammatory marker, TNFα for both cell models.

Treatment of both cell types with microparticles containing IL-4 (section 5.2.4) resulted in reduction of TNFα after 3 days in a similar manner to that of the exogenous treatment. The effect following a 7 day treatment was inconclusive and may not be representative due to the lack of IL-4 released from the particles after day 4. However, the effect seen at day 3 was a direct result of the IL-4 release from the microparticles and not from the PLGA microparticle surface by comparison to the effect of a blank microparticle formulation containing water only.

Importantly, this work developed a cytokine delivery system using microparticles that has the potential to modulate macrophage phenotypes towards a pro-immunoregulatory population. As stated in the hypothesis, the application of this drug delivery system was to modulate the highly inflammatory environment in spinal cord injury. This has potential to improve the prognosis of SCI by allowing for repair and therefore improved healing. However, in order to prove the concept, further work needs to be undertaken. Some of these future developments are discussed below.

6.3 Significance and future developments

To achieve a system providing inflammation resolution, further studies are required to confirm the effect of the microparticles and to optimise the therapy further. The microparticle formulation chosen provided the optimal release profile out of the database developed, however, when analysed for IL-4, the sustained release only continued to day 4. With further study this could be improved to ensure sustained release is continuous for a longer period of time, allowing for higher control over cell modulation. To determine the exact time period over which IL-4 release is required, further studies need to be undertaken on the exogenous modulation of macrophage cells past day 3. The use of microparticle delivered IL-4 also has potential for release profile adaptation for different therapies, as changing the microparticle formulation can prolong or shorten the release profile.

It is also important to consider that the work in this project was carried out on two two-dimensional (2D) macrophage cell models *in vitro* and that cells *in vivo* may behave differently. Co-cultured cell models may provide a better representative environment model for SCI as cells are not compartmentalised *in vivo* and the use of single cultures removes the influence of other cells on behaviour and function. The use of a three-dimensional (3D) cell culture may provide a better macrophage model for testing the modulation ability of IL-4 microparticles, due to the influence of the cells on each other as well as use of co-cultures and influence of other cell types. It is also important to consider that culturing the cells on a tissue-culture plastic surface may influence their growth

and function in a way that would not occur in an *in vivo* setting. It would be more beneficial to test the effect of these microparticles on different cell models, for example astrocytes as well as in spinal cord injury models. If tested on SCI animal models, the inflammatory markers can be assessed as well as testing the functional and behavioural recovery post injury at different time points. SCI modulation in literature often make use of animal models, either rat models (Tukmachev *et al.*, 2016) or more commonly murine models (Wang *et al.*, 2014; Jeong *et al.*, 2017). This would be valuable in determining the efficacy of this system as a therapy. This work only analysed the effect of IL-4 on M0 macrophages, an interesting outlook would be to first differentiate to an $M_{(LPS, IFN\gamma)}$ population and then treat with IL-4 and determine if a similar effect is seen. In a therapy setting this scenario would be more likely as the proinflammatory macrophages are required to remove debris on the instance of injury, therefore a treatment would be most effective modulating the already stimulated macrophages.

A further development for this thesis would be to explore various other methods for macrophage characterisation in order to make a more definitive assessment of the cell population. Using additional protein markers for ELISAs such as IL-8 may help to characterise an M2-like predominant population (Parsrinen *et al.*, 2015; Obarzanek-Fojt *et al.*, 2016). Testing multiple gene expression for genes known for each subpopulation would also provide a more robust analysis of the cell populations. For example analysing genes such as iNOS, CXCL9, IRF5 or CD206, IRF4, IL-1ra, IL-12b for $M_{(LPS, IFN\gamma)}$ and $M_{(IL-4)}$ respectively (Maeß *et al.*, 2010; Genin *et al.*, 2015; Parsrinen *et al.*, 2015; Minardi *et al.*, 2016). Further

analysis with immunohistochemistry, flow cytometry, western blots and metabolic analysis as used in literature, would support the ELISA and qPCR results to confirm the cell populations (Barros *et al.*, 2013; Parsrinen *et al.*, 2015; Minardi *et al.*, 2016; Huleihel *et al.*, 2017; Forrester *et al.*, 2018).

Although the results shown in this work provide a novel target for spinal cord injury therapeutic development, these future developments could be used to further test the hypothesis for this thesis. However, it is likely that multiple strategies would be required to use this work in a therapeutic setting, and section 6.4 explores the need for a combination approach.

6.4 Future outlook: Does spinal cord injury require a combinational approach?

As implied by Silva *et al,* an injury as complex as SCI with many biochemical cascades and cellular responses is likely to require a multifaceted approach to a treatment (Silva *et al.*, 2014). As discussed in section 1.3.3, many regenerative strategies have been explored targeting various aspects of SCI but very few have been successful *in vitro* or *in vivo,* and even fewer result in clinical trials. The 'gold standard' for treatment remains the use of physiotherapy, management of the symptoms or treatment with methylprednisolone, a drug with severe side effects and linked to high mortality rates (Hall and Braughler, 1982; Tator, 1998; Short, 2000; Short *et al.*, 2000; Cerqueira *et al.*, 2013; Silva *et al.*, 2014). This highlights the need for research into more effective treatments, possibly into combinations of strategies.

The use of stem cells in regenerative medicine has increased recently and spinal cord injury is one of the many targets being researched. As briefly discussed in section 1.3.3, various stem cells have been used alone, or in combination with biomaterials in the treatment of SCI. These include SCAPs, OECs, DPC, SHEDs, NSC, and MSCs (Teng *et al.*, 2002; Yoon *et al.*, 2007; Silva *et al.*, 2014; Bakopoulou and About, 2016). Although some of these approaches demonstrated slight functional improvements in SCI, they did not lead to a new treatment option. It is possible that the cells are unable to survive the hostile inflammatory environment surrounding the injury site and are therefore unable to differentiate and repair the damaged tissue. This implies that the use of stem cells alone is not sufficient and must therefore be combined with a strategy to reduce hostility at the injury site.

The use of exogenous cytokines, for example IL-4 has been shown, not only in this work but also elsewhere to reduce the proinflammatory environment of macrophages (Huleihel *et al.*, 2017). However, use of exogenous cytokines means daily IV injections for a patient and is therefore not cost effective or practical for patients. This leads on to the use of a delivery system to reduce the need for daily injections and deliver cytokines in a modulated manner. Microparticle use as a sustained delivery system was explored in this project, however, other strategies also have potential such as scaffolds or hydrogels (Shi and Borgens, 1999; Teng *et al.*, 2002). Delivery of cytokines via biomaterial structures provides a method to not only deliver but also to protect the cytokines

from degradation. They also ensure that the cytokines are delivered to the injury site and are more likely to remain at the site.

Biomaterials can also be used for the delivery of cells, more specifically stem cells (Teng *et al.*, 2002; Yoon *et al.*, 2007). The use of a scaffold or hydrogel containing stem cells and microparticles to deliver immune modulating cytokines in a combined therapy would prove an interesting strategy to research. Kirby *et al* showed that microparticles could be attached to a ε-poly-caprolactone scaffold with 20 % *w/w* β-tricalcium phosphate and maintain the particle structural integrity (Kirby *et al.*, 2011), suggesting this as a combined system for drug release. The use of stem cells in a scaffold and microparticle system combines the advantages for each component, using the controlled release cytokines to ensure the environment is suitable for stem cell survival, where they are able to differentiate, initiating repair and regeneration. The use of cytokines to modulate macrophage phenotype, as explored in this work, suggests a method for controlling inflammation. Therefore, controlling the microenvironment in which stem cells could be implanted and aiding their survival.

The work explored in this thesis provides valuable information on the use of a sustained delivery system for IL-4 to modulate macrophage phenotype and provide resolution. With further research and studies the work of this thesis has potential translational applications, possibly in combination with other

technologies, to help in helping to develop an inflammatory targeted SCI therapy in the future.

References

AANS and CNS (2002) ‘Pharmacological therapy after acute cervical spinal cord injury.’, *Neurosurgery*, 50, pp. S63–S72.

Abu-Awwad, H. A. D. M., Thiagarajan, L. and Dixon, J. E. (2017) ‘Controlled release of GAG-binding enhanced transduction (GET) peptides for sustained and highly efficient intracellular delivery’, *Acta Biomaterialia*. Acta Materialia Inc., 57, pp. 225–237. doi: 10.1016/j.actbio.2017.04.028.

Acharya, S. and Sahoo, S. K. (2011) ‘PLGA nanoparticles containing various anticancer agents and tumour delivery by EPR effect’, *Advanced Drug Delivery Reviews*. Elsevier B.V., 63(3), pp. 170–183. doi: 10.1016/j.addr.2010.10.008.

Alvarez, M. . *et al.* (2016) ‘Delivery strategies to control inflammatory response: Modulating M1-M2 polarization in tissue engineering applications’, *J Control Release*, 28(240), pp. 349–363. doi: 10.1016/j.jconrel.2016.01.026. Delivery.

Año, G. *et al.* (2011) ‘A new oral vaccine candidate based on the microencapsulation by spray-drying of inactivated Vibrio cholerae’, *Vaccine*. Elsevier Ltd, 29(34), pp. 5758–5764. doi: 10.1016/j.vaccine.2011.05.098.

Anselmo, A. C. and Mitragotri, S. (2014) ‘An Overview of Clinical and Commercial Impact of Drug Delivery Systems’, *J Control Release*, 28(190), pp. 15–28. doi: 10.1016/j.physbeh.2017.03.040.

Antonios, J. K. *et al.* (2013) ‘Macrophage polarization in response to wear particles in vitro’, *Cellular and Molecular Immunology*. Nature Publishing

Group, 10(6), pp. 471–482. doi: 10.1038/cmi.2013.39.

Armstrong, D. K. and Brady, M. F. (2006) 'Intraperitoneal therapy for ovarian cancer: A treatment ready for prime time', *Journal of Clinical Oncology*, 24(28), pp. 4531–4533. doi: 10.1200/JCO.2006.06.7140.

Arora, S. *et al.* (2017) 'Macrophages: Their role, activation and polarization in pulmonary diseases', *Immunobiology*. Elsevier, 223(4–5), pp. 383–396. doi: 10.1016/j.imbio.2017.11.001.

Atala, A. (2012) 'Regenerative medicine strategies', *Journal of Pediatric Surgery*. Elsevier Inc., 47(1), pp. 17–28. doi: 10.1016/j.jpedsurg.2011.10.013.

Bakopoulou, A. and About, I. (2016) 'Stem Cells of Dental Origin: Current Research Trends and Key Milestones towards Clinical Application', *Stem Cells International*. Hindawi Publishing Corporation, 2016, pp. 1–20. doi: 10.1155/2016/4209891.

Bao, C. *et al.* (2018) 'Blockade of Interleukin-7 Receptor Shapes Macrophage Alternative Activation and Promotes Functional Recovery After Spinal Cord Injury', *Neuroscience*. IBRO, 371, pp. 518–527. doi: 10.1016/j.neuroscience.2017.10.022.

Baptiste, D. C. and Fehlings, M. G. (2006) 'Pharmacological approaches to repair the injured spinal cord', *Journal of Neurotrauma*, 23(3–4), pp. 318–334.

Barros, M. H. M. *et al.* (2013) 'Macrophage polarisation: An immunohistochemical approach for identifying M1 and M2 macrophages', *PLoS ONE*, 8(11), pp. 1–11. doi: 10.1371/journal.pone.0080908.

Batty, C. *et al.* (2018) 'Drug Delivery for Cancer Immunotherapy and

Vaccines', *Pharm Nanotechnol*, 6(4), pp. 232–244. doi: 10.2174/2211738506666180918122337.

Baumann, M. D. *et al.* (2009) 'An injectable drug delivery platform for sustained combination therapy', *Journal of Controlled Release*. Elsevier B.V., 138(3), pp. 205–213. doi: 10.1016/j.jconrel.2009.05.009.

Beck, K. D. *et al.* (2010) 'Quantitative analysis of celular inflammation after traumatic spinal cord injury : evidence for a multiphasic inflammatory response in the acute to chronic environment', *Brain*, 133, pp. 433–447. doi: 10.1093/brain/awp322.

Bethea, J. R. *et al.* (1999) 'Systemically administered interleukin-10 reduces tumor necrosis factor-alpha production and significantly improves functional recovery following traumatic spinal cord injury in rats.', *Journal of Neurotrauma*, 16, pp. 851–863.

Bomstein, Y. *et al.* (2003) 'Features of skin-coincubated macrophages that promote recovery from spinal cord injury', *Journal of Neuroimmunology*, 142(1–2), pp. 10–16. doi: 10.1016/S0165-5728(03)00260-1.

Bosshart, H. and Heinzelmann, M. (2016) 'THP-1 cells as a model for human monocytes', *Annals of Translational Medicine*, 4(21), pp. 438–438. doi: 10.21037/atm.2016.08.53.

Bracken, M. *et al.* (1985) 'Methylprednisolone and neurological function 1 year after spinal cord injury: results of the National Acute Spinal Cord Injury Study', *J Neurosurgery*, 63, pp. 704–713.

Bracken, M. *et al.* (1998) 'Methylprednisolone or tirilizad mesylate

administration after acute spinal cord injury: 1-year follow-up.', *J Neurosurg*, (89), pp. 699–706.

Bracken, M. (2001) 'Methylprednisolone and acute spinal cord injury: an update of the randomized evidence.', *Spine*, 26, pp. 47–54.

Bracken, M. B. *et al.* (1990) 'A Randomised Controlled Trial of Methylprednisolone or Naloxone in the Treatment of Acute Spinal-Cord Injury', *The New English Journal of Medicine*, 323(20), pp. 1120–1123.

Bracken, M. B. *et al.* (1997) 'Administration of methylprednisolone for 24 or 48 hours or tirilizad mesylate for 48 hours in the treatment of acute spinal cord injury.', *JAMA*, (277), pp. 1597–1604.

Branco, F., Cardenas, D. and Svircev, J. (2007) 'Spinal Cord Injury: A Comprehensive Review', *Physical Medicine and Rehabilitation Clinics of North America*, 18(4), pp. 651–679. doi: https://doi.org/10.1016/j.pmr.2007.07.010.

Braughler, J. M. and Hall, E. D. (1984) 'Effects of multi-dose methylprednisolone sodium succinate administration on injured cat spinal cord neurofilament degradation and energy metabolism', *J Neurosurg*, 61, pp. 290–295.

Bregman, B. and Reier, P. (1986) 'Neural tissue transplants rescue axotomized rubrospinal cells from retro-grade death.', *J Comp Neurol*, 244(1), pp. 86–95.

Brenner, D., Blaser, H. and Mak, T. W. (2015) 'Regulation of tumour necrosis factor signalling : live or let die', *Nature Publishing Group*. Nature Publishing Group, 15(6), pp. 362–374. doi: 10.1038/nri3834.

Butovsky, O. *et al.* (2005) 'Activation of microglia by aggregated β-amyloid or lipopolysaccharide impairs MHC-II expression and renders them cytotoxic whereas IFN-γ and IL-4 render them protective', *Molecular and Cellular Neuroscience*, 29(3), pp. 381–393. doi: 10.1016/j.mcn.2005.03.005.

Carvalho, V. *et al.* (2010) 'Biological activity of heterologous murine interleukin-10 and preliminary studies on the use of a dextrin nanogel as a delivery system', *International Journal of Pharmaceutics*, 400, pp. 234–242. doi: 10.1016/j.ijpharm.2010.08.040.

Cerqueira, S. R. *et al.* (2013) 'Microglia Response and In Vivo Therapeutic Potential of Methylprednisolone-Loaded Dendrimer Nanoparticles in Spinal Cord Injury', *Small*, 9, pp. 738–749.

Chanput, W. *et al.* (2010) 'Transcription profiles of LPS-stimulated THP-1 monocytes and macrophages: A tool to study inflammation modulating effects of food-derived compounds', *Food and Function*, 1(3), pp. 254–261. doi: 10.1039/c0fo00113a.

Chanput, W. *et al.* (2013) 'Characterization of polarized THP-1 macrophages and polarizing ability of LPS and food compounds', *Food & Function*, 4, pp. 266–276. doi: 10.1039/c2fo30156c.

Chanput, W., Mes, J. J. and Wichers, H. J. (2014) 'THP-1 cell line: An in vitro cell model for immune modulation approach', *International Immunopharmacology*. Elsevier B.V., 23(1), pp. 37–45. doi: 10.1016/j.intimp.2014.08.002.

Chaubal, M. (2002) 'Polylactides/glycolides-excipients for injectable drug

delivery and beyond.', *Drug Deliv Technol*, 2, pp. 34–36.

Chen, J.-C., Li, L.-M. and Gao, J.-Q. (2019) 'Biomaterials for local drug delivery in central nervous system', *International Journal of Pharmaceutics*. Elsevier, 560(February), pp. 92–100. doi: 10.1016/j.ijpharm.2019.01.071.

Chen, S. *et al.* (2005) 'Triblock copolymers: Synthesis, characterization, and delivery of a model protein', *International Journal of Pharmaceutics*, 288(2), pp. 207–218. doi: 10.1016/j.ijpharm.2004.09.026.

Chen, X. *et al.* (2017) 'PLGA-PEG-PLGA triblock copolymeric micelles as oral drug delivery system: In vitro drug release and in vivo pharmacokinetics assessment', *Journal of Colloid and Interface Science*. Elsevier Inc., 490, pp. 542–552. doi: 10.1016/j.jcis.2016.11.089.

Chen, X. Q. *et al.* (2001) 'Effects of inner water volume on the peculiar surface morphology of microsheres fabricated by double emulsion technique', *Journal of microencapsulation*, 18(5), pp. 637–649.

Chew, S. A., Hinojosa, V. A. and Arriaga, M. A. (2017) *Bioresorbable polymer microparticles in the medical and pharmaceutical fields BT - Bioresorbable Polymers for Biomedical Applications*. doi: http://dx.doi.org/10.1016/B978-0-08-100262-9.00011-2.

Chistiakov, D. A. *et al.* (2017) 'The impact of interferon-regulatory factors to macrophage differentiation and polarization into M1 and M2', *Immunobiology*. Elsevier, 223(1), pp. 101–111. doi: 10.1016/j.imbio.2017.10.005.

Chrapusta, S. J. *et al.* (2015) 'Original article Non-woven nanofiber mats – a new perspective for experimental studies of the central nervous system?',

Folia Neuropathologica, 4, pp. 407–416. doi: 10.5114/fn.2014.47841.

Cozar-Bernal, M. *et al.* (2011) 'Insulin-loaded PLGA microparticles: flow focusing versus double emulsion/solvent evaporation', *Journal of microencapsulation*, 28(5), pp. 430–441.

Crotts, G. and Park, T. G. (1998) 'Protein delivery from poly(lactic-co-glycolic acid) biodegradable microspheres: release kinetics and stability issues', *Journal of microencapsulation*, 15(6), pp. 699–713.

Das, A. *et al.* (2015) 'Monocyte and Macrophage Plasticity in Tissue Repair and Regeneration', *American Journal of Pathology*. Elsevier Inc, 185(10), pp. 2596–2606. doi: 10.1016/j.ajpath.2015.06.001.

Duluc, D. *et al.* (2007) 'Tumor-associated leukemia inhibitory factor and IL-6 skew monocyte differentiation into tumor-associated-macrophage-like cells', *Blood*, 110(13), pp. 4319–4331. doi: 10.1182/blood-2007-02-072587.

Dumont, C. M., Park, J. and Shea, L. D. (2015) 'Controlled release strategies for modulating immune responses to promote tissue regeneration', *Journal of Controlled Release*. Elsevier B.V., 219, pp. 155–166. doi: 10.1016/j.jconrel.2015.08.014.

Emami, J. *et al.* (2009) 'A Novel Approach to Prepare Insulin-Loaded Poly (Lactic-Co-Glycolic Acid) Microcapsules and the Protein Stability Study', *Journal of Pharmaceutical Sciences*, 98(5), pp. 1712–1731.

Esposito, E. and Cuzzocrea, S. (2011) 'Anti-TNF therapy in the injured spinal cord', *Trends in Pharmacological Science*, 32(2), pp. 107–15. doi: 10.1016/j.tips.2010.11.009.

Fehlings, M. and Perrin, R. (2005) 'The role and timing of early decompression for cervical spinal cord injury: update with a review of recent clinical evidence.', *Injury*, 36(46), pp. 13–26.

Festoff, B. W. *et al.* (2006) 'Minocycline neuroprotects, reduces microgliosis, and inhibits caspase protease expression early after spinal cord injury', *Journal of Neurochemistry*, 97(5), pp. 1314–1326. doi: 10.1111/j.1471-4159.2006.03799.x.

Formiga, F. R. *et al.* (2010) 'Sustained release of VEGF through PLGA microparticles improves vasculogenesis and tissue remodeling in an acute myocardial ischemia-reperfusion model', *Journal of Controlled Release*. Elsevier B.V., 147(1), pp. 30–37. doi: 10.1016/j.jconrel.2010.07.097.

Forrester, M. A. *et al.* (2018) 'Similarities and differences in surface receptor expression by THP-1 monocytes and differentiated macrophages polarized using seven different conditioning regimens', *Cellular Immunology*. doi: 10.1016/j.cellimm.2018.07.008.

Fredenberg, S. *et al.* (2011) 'The mechanisms of drug release in poly(lactic-co-glycolic acid)-based drug delivery systems—A review', *International Journal of Pharmaceutics*. Elsevier B.V., 415(1–2), pp. 34–52. doi: 10.1016/j.ijpharm.2011.05.049.

Fu, Q., Hue, J. and Li, S. (2007) 'Nonsteroidal anti-inflammatory drugs promote axon regeneration via RhoA inhibition', *Journal of Neuroscience*, 27(15), pp. 4154–4164. doi: 10.1523/JNEUROSCI.4353-06.2007.

Führmann, T., Anandakumaran, P. N. and Shoichet, M. S. (2017)

'Combinatorial Therapies After Spinal Cord Injury : How Can Biomaterials Help?', *Advanced Healthcare Materials*, 6, pp. 1–21. doi: 10.1002/adhm.201601130.

Galdiero, M. R. and Mantovani, A. (2015) *Macrophage plasticity and polarization: Relevance to Biomaterials*, *Host Response to Biomaterials*. Elsevier Inc. doi: 10.1172/JCI59643.

Gandino, L. and Varesio, L. (1990) 'Immortalization of Macrophages from Mouse Bone Marrow and Fetal Liver', *Experimental Cell Research*, 198, pp. 192–198.

Garlapati, S. *et al.* (2011) 'Immunization with PCEP microparticles containing pertussis toxoid, CpG ODN and a synthetic innate defense regulator peptide induces protective immunity against pertussis', *Vaccine*. Elsevier Ltd, 29(38), pp. 6540–6548. doi: 10.1016/j.vaccine.2011.07.009.

Genin, M. *et al.* (2015) 'M1 and M2 macrophages derived from THP-1 cells differentially modulate the response of cancer cells to etoposide', *BMC Cancer*. BMC Cancer, 15(1), pp. 1–14. doi: 10.1186/s12885-015-1546-9.

Gujral, C. *et al.* (2013) 'Biodegradable microparticles for strictly regulating the release of neurotrophic factors', *Journal of Controlled Release*. Elsevier B.V., 168(3), pp. 307–316. doi: 10.1016/j.jconrel.2013.03.031.

Guo, Y. *et al.* (2013) 'Granulocyte colony-stimulating factor improves alternative activation of microglia under microenvironment of spinal cord injury', *Neuroscience*. IBRO, 238, pp. 1–10. doi: 10.1016/j.neuroscience.2013.01.047.

Gwak, S. J. *et al.* (2016) 'Cationic, amphiphilic copolymer micelles as nucleic acid carriers for enhanced transfection in rat spinal cord', *Acta Biomaterialia*. Acta Materialia Inc., 35, pp. 98–108. doi: 10.1016/j.actbio.2016.02.013.

Hall, E. D. and Braughler, J. M. (1981) 'Acute effects of intravenous glucocorticoid pretreatment on the in vitro peroxidation of cat spinal cord tissue', *Experimental Neurology*, 73(1), pp. 321–324. doi: 10.1016/0014-4886(81)90067-4.

Hall, E. D. and Braughler, J. M. (1982) 'Effects of intravenous methylprednisolone on spinal cord lipid peroxidation and (Na+ + K+)-ATPase activity', *Journal of Neurosurgery*, 57(2), pp. 247–253.

Han, F. Y. *et al.* (2016) 'Bioerodable PLGA-based microparticles for producing sustained-release drug formulations and strategies for improving drug loading', *Frontiers in Pharmacology*, 7(JUN), pp. 1–11. doi: 10.3389/fphar.2016.00185.

Hawryluk, G. W. J. *et al.* (2008) 'Protection and repair of the injured spinal cord: A review of completed, ongoing, and planned clinical trials for acute spinal cord injury', *Neurosurgical Focus*, 25(5). doi: 10.3171/FOC.2008.25.11.E14.

He, C. *et al.* (2016) 'Core-shell nanoscale coordination polymers combine chemotherapy and photodynamic therapy to potentiate checkpoint blockade cancer immunotherapy', *Nature Communications*. Nature Publishing Group, 7, pp. 1–12. doi: 10.1038/ncomms12499.

He, J. *et al.* (2011) 'Stabilization and encapsulation of recombinant human

erythropoietin into PLGA microspheres using human serum albumin as a stabilizer', *International Journal of Pharmaceutics*. Elsevier B.V., 416(1), pp. 69–76. doi: 10.1016/j.ijpharm.2011.06.008.

Hilton, B. J., Moulson, A. J. and Tetzlaff, W. (2016) 'Neuroprotection and secondary damage following spinal cord injury: Concepts and methods', *Neuroscience Letters*. Elsevier Ireland Ltd, 652, pp. 3–10. doi: 10.1016/j.neulet.2016.12.004.

Hombreiro-Pérez, M. *et al.* (2003) 'Non-degradable microparticles containing a hydrophilic and/or a lipophilic drug: Preparation, characterization and drug release modeling', *Journal of Controlled Release*, 88(3), pp. 413–428. doi: 10.1016/S0168-3659(03)00030-0.

Horiuchi, T. *et al.* (2010) 'Transmembrane TNF- a : structure , function and interaction with anti-TNF agents', *Rheumatology*, 49, pp. 1215–1228. doi: 10.1093/rheumatology/keq031.

Hou, Q. *et al.* (2008) 'In Situ Gelling Hydrogels Incorporating Microparticles as Drug Delivery Carriers for Regenerative Medicine', *Journal of pharmaceutical sciences*, 97(9), pp. 3972–3980. doi: 10.1002/jps.

Huang, C. L. *et al.* (2013) 'The influence of additives in modulating drug delivery and degradation of PLGA thin films', *NPG Asia Materials*. Nature Publishing Group, 5(7), p. e54. doi: 10.1038/am.2013.26.

Huleihel, L. *et al.* (2017) 'Macrophage phenotype in response to ECM bioscaffolds', *Seminars in Immunology*, 29(April), pp. 2–13. doi: 10.1016/j.smim.2017.04.004.

Jaguin, M. *et al.* (2013) 'Polarization profiles of human M-CSF-generated macrophages and comparison of M1-markers in classically activated macrophages from GM-CSF and M-CSF origin', *Cellular Immunology*. Elsevier Inc., 281(1), pp. 51–61. doi: 10.1016/j.cellimm.2013.01.010.

Jeong, S. J. *et al.* (2017) 'Intravenous immune-modifying nanoparticles as a therapy for spinal cord injury in mice', *Neurobiology of Disease*. Elsevier Inc., 108, pp. 73–82. doi: 10.1016/j.nbd.2017.08.006.

Jiang, W. *et al.* (2005) 'Biodegradable poly(lactic-co-glycolic acid) microparticles for injectable delivery of vaccine antigens.', *Advanced drug delivery reviews*, 57(3), pp. 391–410.

Johnson, C. D. *et al.* (2018) 'Electrospun fiber surface nanotopography influences astrocyte-mediated neurite outgrowth', *Biomedical Materials (Bristol)*. IOP Publishing, 13(5). doi: 10.1088/1748-605X/aac4de.

Johnson, O. . *et al.* (1996) 'A month-long effect from a single injection of microencapsulated human growth hormone.', *Nature Medical*, 2(7), pp. 795–799.

Jordan, F. *et al.* (2010) 'Sustained release hGH microsphere formulation produced by a novel supercritical fluid technology: In vivo studies.', *J Control Release*, 141(2), pp. 153–60.

Kang, C. E. *et al.* (2010) 'Poly(ethylene glycol) modification enhances penetration of fibroblast growth factor 2 to injured spinal cord tissue from an intrathecal delivery system', *Journal of Controlled Release*. Elsevier B.V., 144(1), pp. 25–31. doi: 10.1016/j.jconrel.2010.01.029.

Kim, H., Cooke, M. J. and Shoichet, M. S. (2012) 'Creating permissive microenvironments for stem cell transplantation into the central nervous system', *Trends in Biotechnology*. Elsevier Ltd, 30(1), pp. 55–63. doi: 10.1016/j.tibtech.2011.07.002.

Kim, M. G. *et al.* (2012) 'In vitro and in vivo metabolism of verproside in rats', *Molecules*, 17(10), pp. 11990–12002. doi: 10.3390/molecules171011990.

Király, M. *et al.* (2009) 'Simultaneous PKC and cAMP activation induces differentiation of human dental pulp stem cells into functionally active neurons', *Neurochemistry International*, 55(5), pp. 323–332. doi: 10.1016/j.neuint.2009.03.017.

Kirby, G. T. S. S. *et al.* (2011) 'PLGA-based microparticles for the sustained release of BMP-2', *European Cells and Materials*, 22(SUPPL.3), p. 24. doi: 10.3390/polym3010571.

Knaus, U. G. (2000) 'Rho GTPase signaling in inflammation and transformation', *Immunologic Research*, 21(2–3), pp. 103–109. doi: 10.1385/ir:21:2-3:103.

Kotwal, G. J. and Chien, S. (2017) 'Macrophage Differentiation in Normal and Accelerated Wound Healing', *Results Probl Cell Differ*, 62, pp. 353–364. doi: 10.1007/978-3-319-54090-0.

Kurtzke, J. (1977) 'Epidemiology of spinal cord injury', *Neurol Neurocir Psiquiatr*, 18, pp. 157–91.

Langer, R. and Folkman, J. (1976) 'Polymers for the sustained release of proteins and other macromolecules.', *Nature*, 263(5580), pp. 797–800.

Lee, J. H. T. *et al.* (2010) 'Lack of neuroprotective effects of simvastatin and minocycline in a model of cervical spinal cord injury', *Experimental Neurology*. Elsevier Inc., 225(1), pp. 219–230. doi: 10.1016/j.expneurol.2010.06.018.

Lee, J. H. and Yeo, Y. (2015) 'Controlled drug release from pharmaceutical nanocarriers', *Chemical Engineering Science*, 125, pp. 75–84. doi: 10.1016/j.ces.2014.08.046.

Lee, S. and Margolin, K. (2011) 'Cytokines in cancer immunotherapy', *Cancers*, 3(4), pp. 3856–3893. doi: 10.3390/cancers3043856.

Lee, Y. B. *et al.* (2000) 'Role of Tumor Necrosis Factor-a in Neuronal and Glial Apoptosis after Spinal Cord Injury', *Experimental Neurology*, 166(5), pp. 190–195. doi: 10.1006/exnr.2000.7494.

Leo, E. *et al.* (2006) 'PLA-microparticles formulated by means a thermoreversible gel able to modify protein encapsulation and release without being co-encapsulated', *International Journal of Pharmaceutics*, 323(1–2), pp. 131–138. doi: 10.1016/j.ijpharm.2006.05.047.

Letellier, E. *et al.* (2010) 'CD95-Ligand on Peripheral Myeloid Cells Activates Syk Kinase to Trigger Their Recruitment to the Inflammatory Site', *Immunity*, 32(2), pp. 240–252. doi: 10.1016/j.immuni.2010.01.011.

Lima, R. *et al.* (2017) 'Systemic Interleukin-4 Administration after Spinal Cord Injury Modulates Inflammation and Promotes Neuroprotection', *Pharmaceuticals*, 10(4), p. 83. doi: 10.3390/ph10040083.

Liu, S. *et al.* (2018) 'Biomaterial-Supported Cell Transplantation Treatments

for Spinal Cord Injury: Challenges and Perspectives', *Frontiers in Cellular Neuroscience*, 11(January), pp. 1–19. doi: 10.3389/fncel.2017.00430.

Lowry, N. *et al.* (2012) 'The effect of long-term release of Shh from implanted biodegradable microspheres on recovery from spinal cord injury in mice', *Biomaterials*. Elsevier Ltd, 33(10), pp. 2892–2901. doi: 10.1016/j.biomaterials.2011.12.048.

Lu, Z. *et al.* (2010) 'Intraperitoneal therapy for peritoneal cancer', *Future Oncology*, 6(10), pp. 1625–1641. doi: 10.2217/fon.10.100.

Ma, G. and Song, C. (2006) 'PCL/Poloxamer 188 Blend Microsphere for Paclitaxel Delivery: Influence of Poloxamer 188 on Morphology and Drug Release Guilei', *Journal of Applied Polymer Science*, 116(5), pp. 1895–1899. doi: 10.1002/app.

Mabon, P. J., Weaver, L. C. and Dekaban, G. A. (2000) 'Inhibition of Monocyte / Macrophage Migration to a Spinal Cord Injury Site by an Antibody to the Integrin aD : A Potential New Anti-inflammatory Treatment', *Experimental Neurology*, 166, pp. 52–64. doi: 10.1006/exnr.2000.7488.

Maciejko, L., Smalley, M. and Goldman, A. (2017) 'Cancer Immunotherapy and Personalized Medicine: Emerging Technologies and Biomarker Based Approaches', *Journal of Molecular Biomarkers & Diagnosis*, 08(05), pp. 1–11. doi: 10.4172/2155-9929.1000350.

Maeda, H. (2012) 'Macromolecular therapeutics in cancer treatment: The EPR effect and beyond', *Journal of Controlled Release*. Elsevier B.V., 164(2), pp. 138–144. doi: 10.1016/j.jconrel.2012.04.038.

Maeda, H., Nakamura, H. and Fang, J. (2013) 'The EPR effect for macromolecular drug delivery to solid tumors: Improvement of tumor uptake, lowering of systemic toxicity, and distinct tumor imaging in vivo', *Advanced Drug Delivery Reviews*. Elsevier B.V., 65(1), pp. 71–79. doi: 10.1016/j.addr.2012.10.002.

Maeß, M. B., Sendelbach, S. and Lorkowski, S. (2010) 'Selection of reliable reference genes during THP-1 monocyte differentiation into macrophages', *BMC Molecular Biology*, 11(90), pp. 1–8. doi: 10.1186/1471-2199-11-90.

Majed, H. H. (2006) 'A Novel Role for Sema3A in Neuroprotection from Injury Mediated by Activated Microglia', *Journal of Neuroscience*, 26(6), pp. 1730–1738. doi: 10.1523/JNEUROSCI.0702-05.2006.

Makadia, H. K. and Siegel, S. J. (2011) 'Poly Lactic-co-Glycolic Acid (PGLA) as Biodegradable Controlled Drug Delivery Carrier', *Polymers*, 3(3), pp. 1377–1397. doi: 10.3390/polym3031377.Poly.

Mantovani, A. *et al.* (2013) 'Macrophage plasticity and polarization in tissue repair and remodelling', *Journal of Pathology*, 229(2), pp. 176–185. doi: 10.1002/path.4133.

Mantovani, A., Vecchi, A. and Allavena, P. (2014) 'Pharmacological modulation of monocytes and macrophages', *Current Opinion in Pharmacology*. Elsevier Ltd, 17(1), pp. 38–44. doi: 10.1016/j.coph.2014.07.004.

Martens, W. *et al.* (2013) 'Dental stem cells and their promising role in neural regeneration: An update', *Clinical Oral Investigations*, 17(9), pp. 1969–1983.

doi: 10.1007/s00784-013-1030-3.

Martinez, F. O. and Gordon, S. (2014) 'The M1 and M2 paradigm of macrophage activation: time for reassessment.', *F1000prime reports*, 6(March), p. 13. doi: 10.12703/P6-13.

McCreedy, D. A. and Sakiyama-Elbert, S. E. (2012) 'Combination therapies in the CNS: Engineering the environment', *Neuroscience Letters*. Elsevier Ireland Ltd, 519(2), pp. 115–121. doi: 10.1016/j.neulet.2012.02.025.

McGuirk, P., McCann, C. and Mills, K. H. G. (2002) 'Pathogen-specific T Regulatory 1 Cells Induced in the Respiratory Tract by a Bacterial Molecule that Stimulates Interleukin 10 Production by Dendritic Cells', *The Journal of Experimental Medicine*, 195(2), pp. 221–231. doi: 10.1084/jem.20011288.

Meda, L. *et al.* (1995) 'Activation of microglial cells by beta-amyloid protein and interferon-gamma', *Nature*, pp. 647–650. doi: 10.1038/374647a0.

Menei, P. *et al.* (2004) 'Stereotaxic implantation of 5-fluorouracil-releasing microspheres in malignant glioma.', *Cancer*, 100, pp. 405–410. doi: doi:10.1002/cncr.11922.

Menei, P. and Benoit, J. P. (2003) 'Implantable drug-releasing biodegradable microspheres for local treatment of brain glioma', *Acta Neurochirurgica, Supplementum*, 88(88), pp. 51–55. doi: 10.1007/978-3-7091-6090-9_9.

Min, Y. *et al.* (2017) 'Antigen-capturing nanoparticles improve the abscopal effect and cancer immunotherapy', *Nat Nanotechnol*, 12(9), pp. 877–882. doi: 10.1038/nnano.2017.113.

Minardi, S. *et al.* (2016) 'IL-4 Release from a Biomimetic Scaffold for the

Temporally Controlled Modulation of Macrophage Response', *Annals of Biomedical Engineering*, 44(6), pp. 2008–2019. doi: 10.1007/s10439-016-1580-z.

Mir, M., Ahmed, N. and Rehman, A. ur (2017) 'Recent applications of PLGA based nanostructures in drug delivery', *Colloids and Surfaces B: Biointerfaces*. Elsevier B.V., 159, pp. 217–231. doi: 10.1016/j.colsurfb.2017.07.038.

Miron, V. E. (2013) 'Dissecting the damaging versus regenerative roles of CNS macrophages: implications for the use of immunomodulatory therapeutics.', *Regenerative medicine*, 8(6), pp. 673–6. doi: 10.2217/rme.13.73.

Moisés Alvarez, M. *et al.* (2016) 'Delivery strategies to control inflammatory response: Modulating M1 – M2 polarization in tissue engineering applications', *Journal of Controlled Release*. Elsevier B.V., 240, pp. 349–363. doi: 10.1016/j.jconrel.2016.01.026.

Molina, E. R. *et al.* (2015) 'Immunomodulatory properties of stem cells and bioactive molecules for tissue engineering.', *Journal of controlled release : official journal of the Controlled Release Society*. Elsevier B.V., 219, pp. 107–18. doi: 10.1016/j.jconrel.2015.08.038.

Mothe, A. J. and Tator, C. H. (2012) 'Advances in stem cell therapy for spinal cord injury', *The Journal of Clinical Investigation*, 122(11), pp. 3824–3834. doi: 10.1172/JCI64124.3824.

Mundargi, R., Rangaswamy, V. and Aminabhavi, T. (2011) 'Poly(N-vinylcaprolactam-co-methacrylic acid) hydro- gel microparticles for oral

insulin delivery', *Journal of microencapsulation*, 28(5), pp. 384–394.

Murray, P. J. *et al.* (2014) 'Macrophage Activation and Polarization: Nomenclature and Experimental Guidelines', *Immunity*. Elsevier, 41(1), pp. 14–20. doi: 10.1016/j.immuni.2014.06.008.

Nair, M. G. *et al.* (2006) 'Novel Effector Molecules in Type 2 Inflammation: Lessons Drawn from Helminth Infection and Allergy', *The Journal of Immunology*, 177, pp. 1393–1399. doi: 10.4049/jimmunol.177.3.1393.

Nakajima, H. *et al.* (2012) 'Transplantation of Mesenchymal Stem Cells Promotes an Alternative Pathway of Macrophage Activation and Functional Recovery after Spinal Cord Injury', *Journal of Neurotrauma*, 29(8), pp. 1614–1625. doi: 10.1089/neu.2011.2109.

NHS and Board, N. H. S. C. (2013) 'NHS Standard Contract For Spinal Cord Injuries (all ages)', *NHS ENGLAND COMMISSIONING BOARD*.

Ning, G. Z. *et al.* (2011) 'Epidemiology of traumatic spinal cord injury in Tianjin, China', *Spine Cord*, 49, pp. 386–390. doi: 10.1097/01.brs.0000207258.80129.03.

O'Brien, F. J. (2011) 'Biomaterials & scaffolds for tissue engineering', *Materials Today*. Elsevier Ltd, 14(3), pp. 88–95. doi: 10.1016/S1369-7021(11)70058-X.

Obarzanek-Fojt, M. *et al.* (2016) 'Tracking immune-related cell responses to drug delivery microparticles in 3D dense collagen matrix', *European Journal of Pharmaceutics and Biopharmaceutics*. Elsevier B.V., 107, pp. 180–190. doi: 10.1016/j.ejpb.2016.06.018.

Otani, K. *et al.* (1994) 'Beneficial effects of methylprednisolone sodium succinate in the treatment of acute spinal cord injury.', *Sekitsy Sekizui*, 7(113), pp. 633–647.

Pajarinen, J *et al.* (2015) 'Modulation of mouse macrophage polarization in vitro using IL-4 delivery by osmotic pumps', *Journal of Biomedical Materials Research - Part A*, 103(4), pp. 1339–1345. doi: 10.1002/jbm.a.35278.

Pannu, R. *et al.* (2005) 'Attenuation of acute inflammatory response by atorvastatin after spinal cord injury in rats', *J Neurosci Res*, 79(3), pp. 340–350. doi: 10.1002/jnr.20345.

Pannu, R. *et al.* (2007) 'Post-trauma Lipitor treatment prevents endothelial dysfunction, facilitates neuroprotection, and promotes locomotor recovery following spinal cord injury', *Journal of Neurochemistry*, 101(1), pp. 182–200. doi: 10.1111/j.1471-4159.2006.04354.x.

Pantović, R. *et al.* (2005) 'Effect of indomethacin on motor activity and spinal cord free fatty acid content after experimental spinal cord injury in rabbits', *Spinal Cord*, 43(9), pp. 519–526. doi: 10.1038/sj.sc.3101763.

Parajó, Y. *et al.* (2010) 'PLGA:poloxamer blend micro- and nanoparticles as controlled release systems for synthetic proangiogenic factors', *European Journal of Pharmaceutical Sciences*, 41(5), pp. 644–649. doi: 10.1016/j.ejps.2010.09.008.

Park, E. K. *et al.* (2007) 'Optimized THP-1 differentiation is required for the detection of responses to weak stimuli', *Inflammation Research*, 56(1), pp. 45–50. doi: 10.1007/s00011-007-6115-5.

Park, H. C. *et al.* (2017) 'The Effects of M1 and M2 Macrophages on Odontogenic Differentiation of Human Dental Pulp Cells', *Journal of Endodontics*. Elsevier Inc, pp. 2–7. doi: 10.1016/j.joen.2016.11.003.

Parsrinen, J. *et al.* (2015) 'Modulation of Mouse Macrophage Polarization in vitro Using IL-4 Delivery by Osmotic Pumps', *J Biomed Mater Res A.*, 103(4), pp. 1339–1345. doi: 10.1002/jbm.a.35278.

Pinzon, A. *et al.* (2008) 'A re-assessment of minocycline as a neuroprotective agent in a rat spinal cord contusion model', *Brain Research*. Elsevier B.V., 1243, pp. 146–151. doi: 10.1016/j.brainres.2008.09.047.

Plemel, J. R., Wee Yong, V. and Stirling, D. P. (2014) 'Immune modulatory therapies for spinal cord injury - Past, present and future', *Experimental Neurology*. Elsevier Inc., 258, pp. 91–104. doi: 10.1016/j.expneurol.2014.01.025.

Pointillart, V. *et al.* (2000) 'Pharmacological therapy of spinal cord injury during the acute phase.', *Spinal Cord*, 38, pp. 71–76.

Popovich, P. G. *et al.* (1999) 'Depletion of Hematogenous Macrophages Promotes Partial Hindlimb Recovery and Neuroanatomical Repair after Experimental Spinal Cord Injury', *Experimental Neurology*, 158(2), pp. 351–365. doi: 10.1006/exnr.1999.7118.

Popovich, P. G. *et al.* (2002) 'The neuropathological and behavioral consequences of intraspinal microglial/macrophage activation.', *Journal of neuropathology and experimental neurology*, 61(7), pp. 623–633. doi: 10.1093/jnen/61.7.623.

Porcheray, F. *et al.* (2005) 'Macrophage activation switching: An asset for the resolution of inflammation', *Clinical and Experimental Immunology*, 142(3), pp. 481–489. doi: 10.1111/j.1365-2249.2005.02934.x.

Qin, Z. (2012) 'The use of THP-1 cells as a model for mimicking the function and regulation of monocytes and macrophages in the vasculature', *Atherosclerosis*. Elsevier Ireland Ltd, 221(1), pp. 2–11. doi: 10.1016/j.atherosclerosis.2011.09.003.

Qutachi, O., Shakesheff, K. M. and Buttery, L. D. K. (2013) 'Delivery of definable number of drug or growth factor loaded poly(dl-lactic acid-co-glycolic acid) microparticles within human embryonic stem cell derived aggregates', *Journal of Controlled Release*. Elsevier B.V., 168(1), pp. 18–27. doi: 10.1016/j.jconrel.2013.02.029.

Rambhia, K. J. and Ma, P. X. (2015) 'Controlled drug release for tissue engineering', *Journal of Controlled Release*. Elsevier B.V., 219, pp. 119–128. doi: 10.1016/j.jconrel.2015.08.049.

Rapalino, O. *et al.* (1998) 'Implantation of stimulated homologous macrophages results in partial recovery of paraplegic rats', *Nature Medical*, 4(7), pp. 814–21.

Reiner, N. (2009) *Macrophages & Dendritic Cells*, *Methods in Molecular Biology*. doi: 10.1007/978-1-59745-396-7_8.

Ren, H. *et al.* (2014) 'Repair of spinal cord injury by inhibition of astrocyte growth and inflammatory factor synthesis through local delivery of flavopiridol in PLGA nanoparticles', *Biomaterials*. Elsevier Ltd, 35(24), pp.

6585–6594. doi: 10.1016/j.biomaterials.2014.04.042.

Richardson, P., McGuinness, U. and Aguayo, A. (1980) ‘Axons from CNS neurons regenerate into PNS grafts.’, *Nature*, 284(5753), pp. 264–265.

Rőszer, T. (2015) ‘Understanding the Mysterious M2 Macrophage through Activation Markers and Effector Mechanisms’, *Mediators of Inflammation*, 2015, pp. 1–16. doi: 10.1155/2015/816460.

Sadler, T. W. (2011) *Central Nervous System*, *Langman’s Medical Embryology*. Elsevier Inc. doi: 10.1007/978-3-642-02824-3_12.

Saganová, K. *et al.* (2008) ‘Limited minocycline neuroprotection after balloon-compression spinal cord injury in the rat’, *Neuroscience Letters*, 433(3), pp. 246–249. doi: 10.1016/j.neulet.2008.01.041.

Sah, H. (1999) ‘Protein behavior at the water/methylene chloride interface’, *Journal of Pharmaceutical Sciences*, 88(12), pp. 1320–1325.

Schwab, J. M. *et al.* (2004) ‘Lesional RhoA+ cell numbers are suppressed by anti-inflammatory, cyclooxygenase-inhibiting treatment following subacute spinal cord injury’, *Glia*, 47(4), pp. 377–386.

Schwartz, M. *et al.* (2006) ‘Microglial phenotype: Is the commitment reversible?’, *Trends in Neurosciences*, 29(2), pp. 68–74. doi: 10.1016/j.tins.2005.12.005.

Schwartz, M. (2010) ‘“Tissue-repairing” blood-derived macrophages are essential for healing of the injured spinal cord: From skin-activated macrophages to infiltrating blood-derived cells?’, *Brain, Behavior, and Immunity*. Elsevier Inc., 24(7), pp. 1054–1057. doi: 10.1016/j.bbi.2010.01.010.

Shaked, I. *et al.* (2004) 'Early activation of microglia as antigen-presenting cells correlates with T cell-mediated protection and repair of the injured central nervous system', *Journal of Neuroimmunology*, 146(1–2), pp. 84–93. doi: 10.1016/j.jneuroim.2003.10.049.

Shechter, R. *et al.* (2009) 'Infiltrating blood-derived macrophages are vital cells playing an anti-inflammatory role in recovery from spinal cord injury in mice', *PLoS Medicine*, 6(7). doi: 10.1371/journal.pmed.1000113.

Shende, P. and Subedi, M. (2017) 'Pathophysiology, mechanisms and applications of mesenchymal stem cells for the treatment of spinal cord injury', *Biomedicine and Pharmacotherapy*. Elsevier Masson SAS, 91, pp. 693–706. doi: 10.1016/j.biopha.2017.04.126.

Shi, R. and Borgens, R. B. (1999) 'Acute repair of crushed guinea pig spinal cord by polyethylene glycol', *Journal of Neurophysiology*, 81(5), pp. 2406–2414. doi: 10.1152/jn.1999.81.5.2406.

Shiratori, H. *et al.* (2017) 'THP-1 and human peripheral blood mononuclear cell-derived macrophages differ in their capacity to polarize in vitro', *Molecular Immunology*. Elsevier, 88(June), pp. 58–68. doi: 10.1016/j.molimm.2017.05.027.

Short, D. (2000) 'Use of steroids for acute spinal cord injury must be reassessed', *British Medical Journal*, 321(7270), p. 1224.

Short, D., El Masry, W. and Jones, P. (2000) 'High dose methylprednisolone in the management of acute spinal cord injury - a systematic review from a clinical perspective', *Spinal Cord*, 38(5), pp. 273–86.

Sierra-Filardi, E. *et al.* (2011) 'Activin A skews macrophage polarization by promoting a proinflammatory phenotype and inhibiting the acquisition of anti-inflammatory macrophage markers', *Blood*, 117(19), pp. 5092–5101. doi: 10.1182/blood-2010-09-306993.

Silva, N. A. *et al.* (2014) 'From basics to clinical: A comprehensive review on spinal cord injury', *Progress in Neurobiology*, 114, pp. 25–57. doi: 10.1016/j.pneurobio.2013.11.002.

Soldano, S. *et al.* (2016) 'Alternatively activated (M2) macrophage phenotype is inducible by endothelin-1 in cultured human macrophages', *PLoS ONE*, 11(11), pp. 1–18. doi: 10.1371/journal.pone.0166433.

Spencer, M. *et al.* (2010) 'Adipose tissue macrophages in insulin-resistant subjects are associated with collagen VI and fibrosis and demonstrate alternative activation', *Am J Physiol Endocrinol Metab*, 299(6), pp. E1016-27. doi: 10.1152/ajpendo.00329.2010.

Spiller, K. L. *et al.* (2015) 'Sequential delivery of immunomodulatory cytokines to facilitate the M1-to-M2 transition of macrophages and enhance vascularization of bone scaffolds', *Biomaterials*, 37, pp. 194–207. doi: 10.1016/j.biomaterials.2014.10.017.Sequential.

Spiller, K. L. and Koh, T. J. (2017) 'Macrophage-based therapeutic strategies in regenerative medicine', *Advanced Drug Delivery Reviews*. Elsevier B.V., 122, pp. 74–83. doi: 10.1016/j.addr.2017.05.010.

Srinivasan, C. *et al.* (2005) 'Effect of additives on encapsulation efficiency, stability and bioactivity of entrapped lysozyme from biodegradable polymer

particles.', *Journal of microencapsulation*, 22(2), pp. 127–138. doi: 10.1080/02652040400026400.

Stirling, D. P. *et al.* (2004) 'Minocycline Treatment Reduces Delayed Oligodendrocyte Death, Attenuates Axonal Dieback, and Improves Functional Outcome after Spinal Cord Injury', *Journal of Neuroscience*, 24(9), pp. 2182–2190. doi: 10.1523/JNEUROSCI.5275-03.2004.

Sykova, E. *et al.* (2006) 'Autologous bone marrow transplan- tation in patients with subacute and chronic spinal cord injury.', *Cell Transplant*, 15(8–9), pp. 675–687.

Tan, E. Y. M. *et al.* (2007) 'Development of a cell transducible RhoA inhibitor TAT-C3 transferase and its encapsulation in biocompatible microspheres to promote survival and enhance regeneration of severed neurons', *Pharmaceutical Research*, 24(12), pp. 2297–2308. doi: 10.1007/s11095-007-9454-6.

Taranejoo, S. *et al.* (2011) 'Chitosan microparticles loaded with exotoxin A subunit antigen for intranasal vaccination against Pseudomonas aeruginosa: An in vitro study', *Carbohydrate Polymers*. Elsevier Ltd., 83(4), pp. 1854–1861. doi: 10.1016/j.carbpol.2010.10.051.

Tardito, S. *et al.* (2019) 'Macrophage M1/M2 polarization and rheumatoid arthritis: A systematic review', *Autoimmunity Reviews*. Elsevier, 18(11), p. 102397. doi: 10.1016/j.autrev.2019.102397.

Tator, C. H. (1998) 'Biology of neurological recovery and functional restoration after spinal cord injury.', *Neurosurgery*, 42(4), pp. 696–707.

Taylor, P. . and Feldmann, M. (2009) ‘Anti-TNF biologic agents: still the therapy of choice for rheumatoid arthritis.’, *Nature Reviews Rheumatology*, 5(10), pp. 578–82. doi: 10.1038/nrrheum.2009.181.

Tedesco, S. *et al.* (2018) ‘Convenience versus biological significance: Are PMA-differentiated THP-1 cells a reliable substitute for blood-derived macrophages when studying in vitro polarization?’, *Frontiers in Pharmacology*, 9(71). doi: 10.3389/fphar.2018.00071.

Teng, Y. D. *et al.* (2002) ‘Functional recovery following traumatic spinal cord injury mediated by a unique polymer scaffold seeded with neural stem cells’, *Proceedings of the National Academy of Sciences of the United States of America*, 99(5), pp. 3024–3029. doi: 10.1073/pnas.052678899.

Teng, Y. D. *et al.* (2004) ‘Minocycline inhibits contusion-triggered mitochondrial cytochrome c release and mitigates functional deficits after spinal cord injury’, *Proceedings of the National Academy of Sciences of the United States of America*, 101(9), pp. 3071–3076. doi: 10.1073/pnas.0306239101.

Tran, V. T. *et al.* (2012) ‘Protein-loaded PLGA-PEG-PLGA microspheres: A tool for cell therapy’, *European Journal of Pharmaceutical Sciences*, 45(1–2), pp. 128–137. doi: 10.1016/j.ejps.2011.10.030.

Tu, B. *et al.* (2015) ‘Macrophages derived from THP-1 promote the osteogenic differentiation of mesenchymal stem cells through the IL-23/IL-23R/??-catenin pathway’, *Experimental Cell Research*. Elsevier, 339(1), pp. 81–89. doi: 10.1016/j.yexcr.2015.10.015.

Tukmachev, D. *et al.* (2016) 'Injectable Extracellular Matrix Hydrogels as Scaffolds for Spinal Cord Injury Repair.', *Tissue engineering. Part A*, 22(3–4), pp. 306–17. doi: 10.1089/ten.TEA.2015.0422.

Tuladhar, A. *et al.* (2015) *Central Nervous System*, *Clinical Aspects of Regenarative Medicine*. Elsevier Inc. doi: 10.1007/978-3-642-02824-3_12.

UniProtKB - P00698 (LYSC-CHICK) (1986). Available at: https://www.uniprot.org/uniprot/P00698 (Accessed: 26 March 2019).

UniProtKB - P05112 (IL4_HUMAN) (1987). Available at: https://www.uniprot.org/uniprot/P05112 (Accessed: 14 December 2018).

Vasconcelos, D. P. *et al.* (2015) 'Development of an immunomodulatory biomaterial : Using resolvin D1 to modulate in fl ammation', *Biomaterials*, 53, pp. 566–573. doi: 10.1016/j.biomaterials.2015.02.120.

Vij, N. *et al.* (2010) 'Development of PEGylated PLGA nanoparticle for controlled and sustained drug delivery in cystic fibrosis.', *Journal of nanobiotechnology*, 8, p. 22. doi: 10.1186/1477-3155-8-22.

Vilos, C. and Velasquez, L. A. (2012) 'Therapeutic strategies based on polymeric microparticles', *Journal of Biomedicine and Biotechnology*, 2012. doi: 10.1155/2012/672760.

Vishwakarma, A. *et al.* (2016) 'Engineering Immunomodulatory Biomaterials To Tune the Inflammatory Response', *Trends in Biotechnology*. Elsevier Ltd, 34(6), pp. 470–482. doi: 10.1016/j.tibtech.2016.03.009.

Viswanath, A. *et al.* (2017) 'Extracellular matrix-derived hydrogels for dental stem cell delivery', *Journal of Biomedical Materials Research - Part A*,

105(1), pp. 319–328. doi: 10.1002/jbm.a.35901.

Vogel, D. Y. S. *et al.* (2014) 'Human macrophage polarization in vitro: Maturation and activation methods compared', *Immunobiology*. Elsevier GmbH., 219(9), pp. 695–703. doi: 10.1016/j.imbio.2014.05.002.

Wang, P. *et al.* (2016) 'Effects of Pluronic F127-PEG multi-gel-core on the release profile and pharmacodynamics of Exenatide loaded in PLGA microspheres', *Colloids and Surfaces B: Biointerfaces*. Elsevier B.V., 147, pp. 360–367. doi: 10.1016/j.colsurfb.2016.08.032.

Wang, X. *et al.* (2009) 'Ibuprofen enhances recovery from spinal cord injury by limiting tissue loss and stimulating axonal growth', *Journal of Neurotrauma*, 26(1), pp. 81–95. doi: 10.1089/neu.2007.0464.

Wang, Y. C. *et al.* (2008) 'Sustained intraspinal delivery of neurotrophic factor encapsulated in biodegradable nanoparticles following contusive spinal cord injury', *Biomaterials*, 29(34), pp. 4546–4553. doi: 10.1016/j.biomaterials.2008.07.050.

Wang, Y. F. *et al.* (2014) 'Curcumin promotes the spinal cord repair via inhibition of glial scar formation and inflammation', *Neuroscience Letters*. Elsevier Ireland Ltd, 560, pp. 51–56. doi: 10.1016/j.neulet.2013.11.050.

Wells, J. E. A. (2003) 'Neuroprotection by minocycline facilitates significant recovery from spinal cord injury in mice', *Brain*, 126(7), pp. 1628–1637. doi: 10.1093/brain/awg178.

White, L. J. *et al.* (2013) 'Accelerating protein release from microparticles for regenerative medicine applications', *Materials Science and Engineering C*.

Elsevier B.V., 33(5), pp. 2578–2583. doi: 10.1016/j.msec.2013.02.020.

Williams, D. F. (2009) 'On the nature of biomaterials', *Biomaterials*. doi: 10.1016/j.biomaterials.2009.07.027.

Winkler, T. *et al.* (1993) 'Indomethacin, an inhibitor of prostaglandin synthesis attenuates alteration in spinal cord evoked potentials and edema formation after trauma to the spinal cord: An experimental study in the rat', *Neuroscience*, 52(4), pp. 1057–1067. doi: 10.1016/0306-4522(93)90552-Q.

Wolf, M. T. *et al.* (2014) 'Macrophage polarization in response to ECM coated polypropylene mesh', *Biomaterials*. Elsevier Ltd, 35(25), pp. 6838–6849. doi: 10.1016/j.biomaterials.2014.04.115.

Yang, Z. *et al.* (2013) 'Macrophages as IL-25 / IL-33-Responsive Cells Play an Important Role in the Induction of Type 2 Immunity', *PLoS ONE*, 8(3), pp. 1–11. doi: 10.1371/journal.pone.0059441.

Yao, L. *et al.* (2013) 'Improved axonal regeneration of transected spinal cord mediated by multichannel collagen conduits functionalized with neurotrophin-3 gene', *Gene Therapy*. Nature Publishing Group, 20(12), pp. 1149–1157. doi: 10.1038/gt.2013.42.

Ye, M., Kim, S. and Park, K. (2010) 'Issues in long-term protein delivery using biodegradable microparticles', *Journal of Controlled Release*, 146(2), pp. 241–260. doi: 10.1016/j.jconrel.2010.05.011.

Yoon, S. H. *et al.* (2007) 'Complete Spinal Cord Injury Treatment Using Autologous Bone Marrow Cell Transplantation and Bone Marrow Stimulation with Granulocyte Macrophage-Colony Stimulating Factor: Phase I/II Clinical

Trial', *Stem Cells*, 25(8), pp. 2066–2073. doi: 10.1634/stemcells.2006-0807.

Zeimet, A. G. *et al.* (2009) 'Pros and cons of intraperitoneal chemotherapy in the treatment of epithelial ovarian cancer', *Anticancer Research*, 29(7), pp. 2803–2808.

Zentner, G. M. *et al.* (2001) 'Biodegradable block copolymers for delivery of proteins and water-insoluble drugs', *Journal of Controlled Release*, 72(1–3), pp. 203–215. doi: 10.1016/S0168-3659(01)00276-0.

Zhao, X. *et al.* (2016) 'Inducing enhanced immunogenic cell death with nanocarrier-based drug delivery systems for pancreatic cancer therapy', *Biomaterials*. Elsevier Ltd, 102, pp. 187–197. doi: 10.1016/j.biomaterials.2016.06.032.

Chapter 7: Supplementary Data and Appendix

7.1 Microparticle supplementary data introduction

This supplementary data provides a more extensive overview of the characterisation data for the microparticle batches manufactured as part of this project. Microparticle batches were made as described in section 2.1.2.

7.1.1 Comparison of the effect of commercial release modifiers on the release of lysozyme from PLGA microparticles

As described in section 3.2, particles were manufactured using 50:50 and 85:15 PLGA with varying percentages of polaxamers F127 or P188. The resulting microparticle batches were characterised for their morphology, size and release kinetics and data is shown in Figures 7.1 – 7.5.

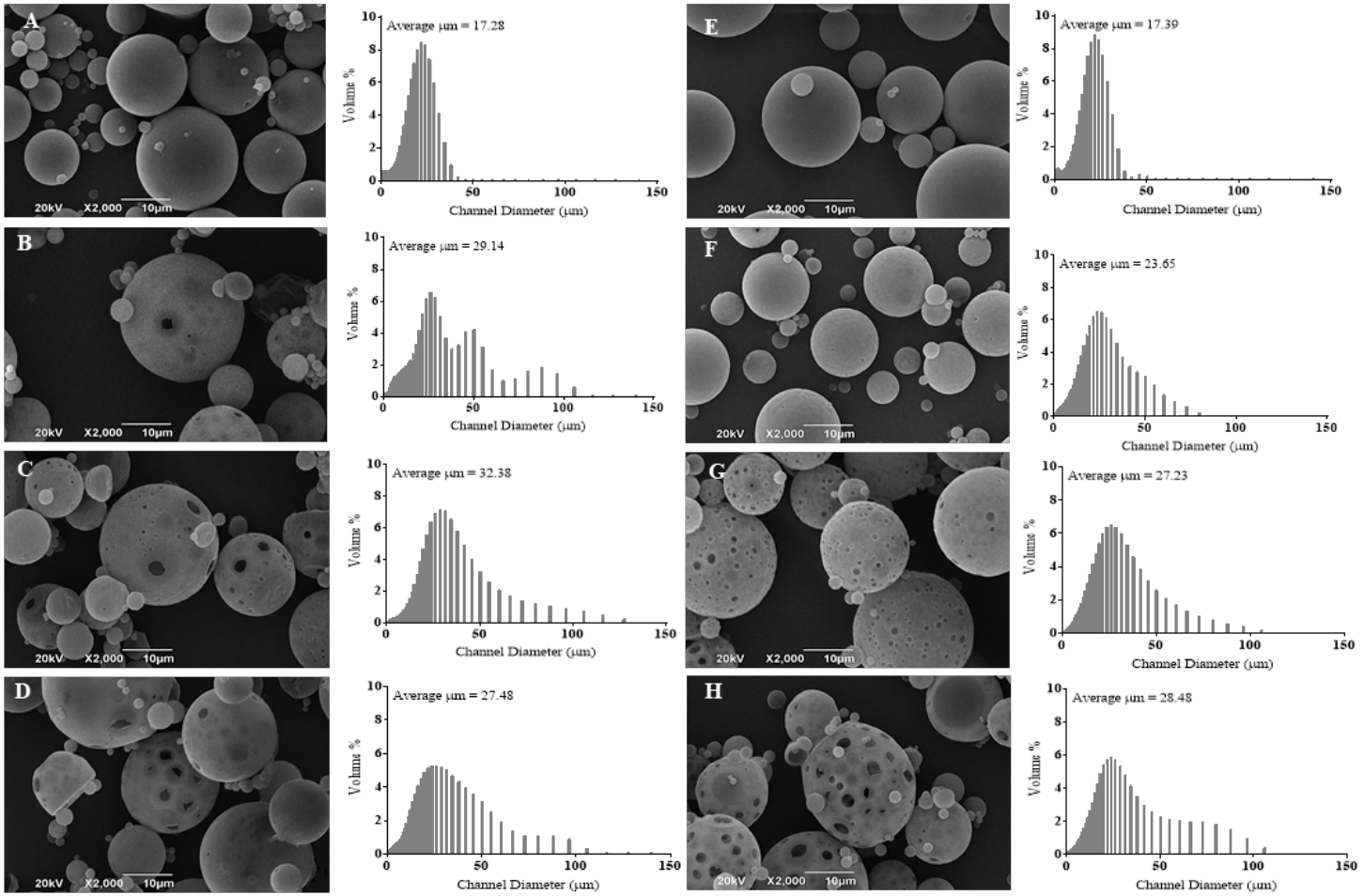

Figure 7.1: Morphology and size distribution of 20 % total polymer particles formed from 50:50 PLGA with different percentages of F127, blank and containing HSA:lysozyme. Formulations: **(A)** 0% F127, HSA:lysozyme. **(B)** 10% F127, HSA:lysozyme. **(C)** 20% F127, HSA:lysozyme. **(D)** 30% F127, HSA:lysozyme loaded. **(E)** 0% F127, water loaded. **(F)** 10% F127, water loaded. **(G)** 20% F127, water loaded. **(H)** 30% F127, water loaded.

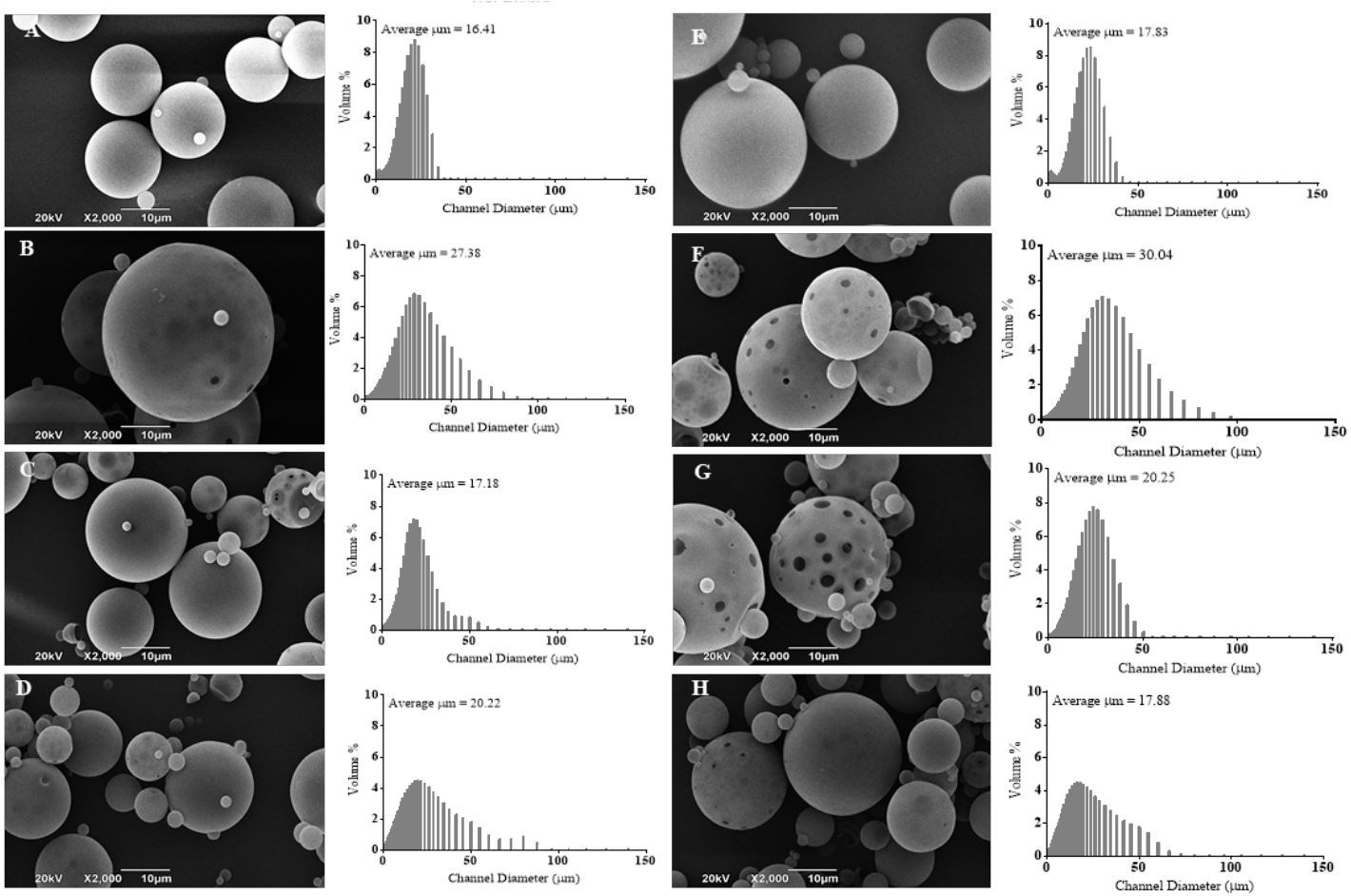

Figure 7.2: Morphology and size distribution of 20 % total polymer particles formed from 85:15 PLGA with different percentages of F127, blank and containing HSA:lysozyme.. Formulations: **(A)** 0% F127, HSA:lysozyme loaded. **(B)** 10% F127, HSA:lysozyme loaded. **(C)** 20% F127, HSA:lysozyme loaded. **(D)** 30% F127, HSA:lysozyme loaded. **(E)** 0% F127, water loaded. **(F)** 10% F127, water loaded. **(G)** 20% F127, water loaded. **(H)** 30% F127, water loaded.

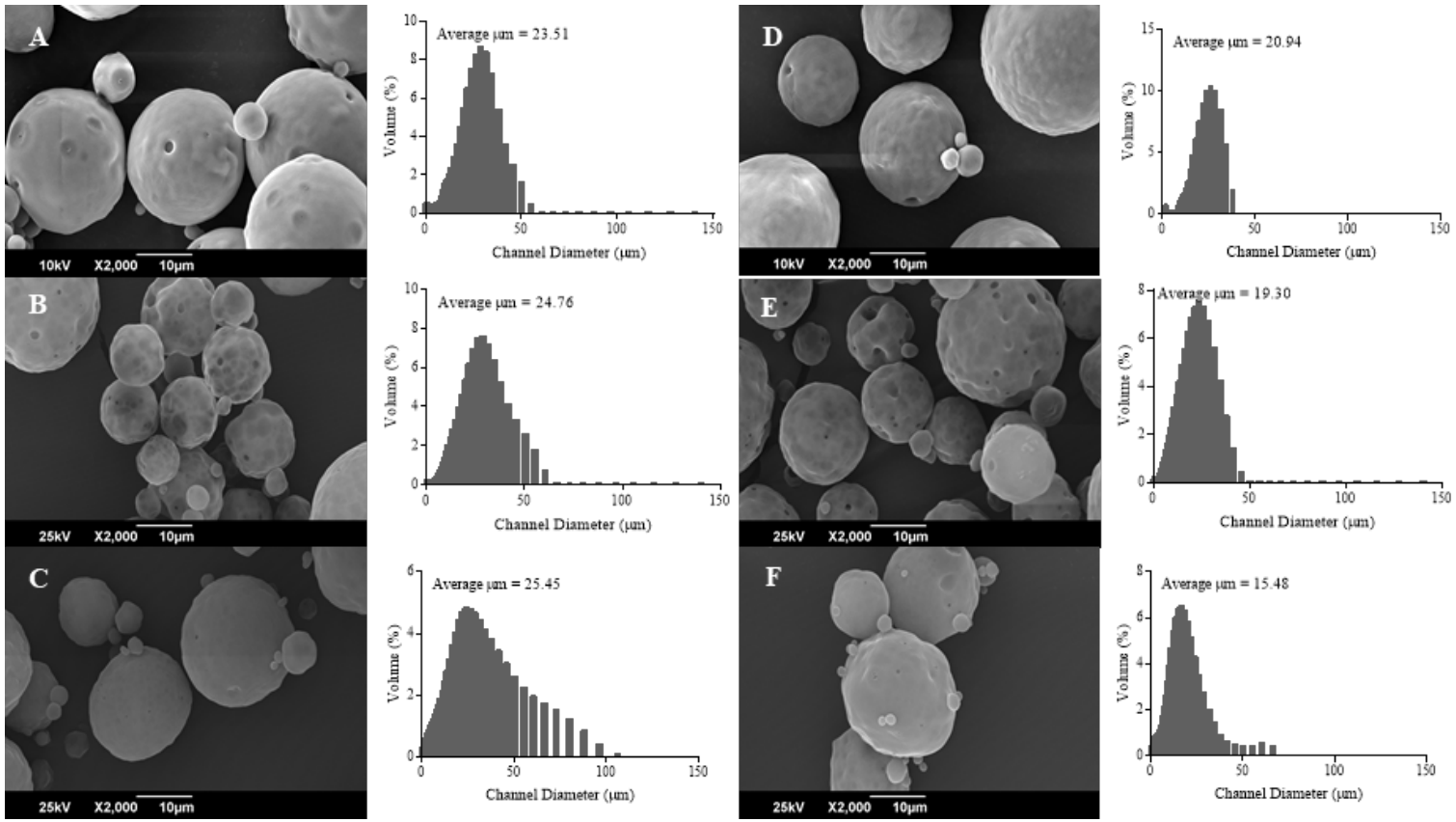

Figure 7.3: Morphology and size distribution of 20 % total polymer particles formed from 50:50 PLGA with different percentages of P188, blank and containing HSA:lysozyme.. Formulation: **(A)** 0% P188, HSA:lysozyme loaded. **(B)** 20% P188, HSA:lysozyme loaded. **(C)** 40% P188, HSA:lysozyme loaded. **(D)** 0% P188, water loaded. **(E)** 20% P188, water loaded. **(F)** 40% P188, water loaded.

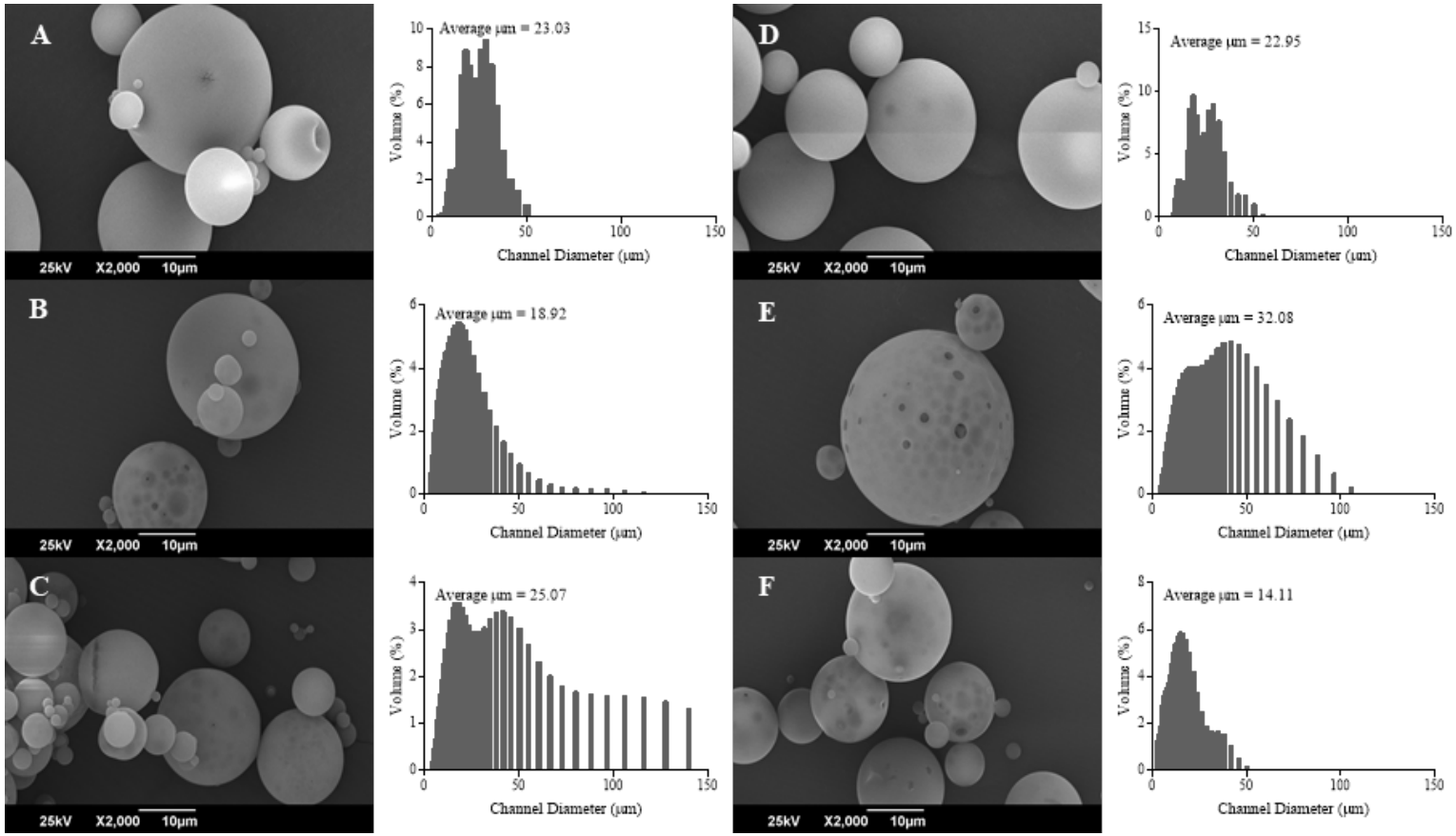

Figure 7.4: Morphology and size distribution of 20 % total polymer particles formed from 85:15 PLGA with different percentages of P188, blank and containing HSA:lysozyme.. Formulation: **(A)** 0% P188, HSA:lysozyme loaded. **(B)** 20% P188, HSA:lysozyme loaded. **(C)** 40% P188, HSA:lysozyme loaded. **(D)** 0% P188, water loaded. **(E)** 20% P188, water loaded. **(F)** 40% P188, water loaded.

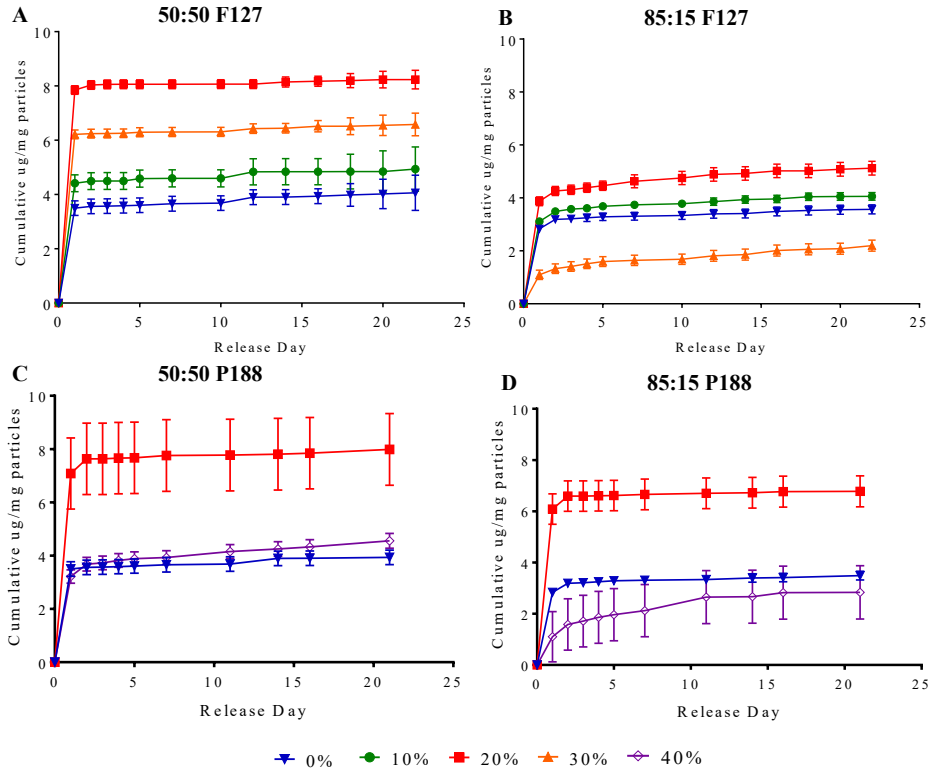

Figure 7.5: Cumulative protein release (µg/mg particles) from 20 % *w/v* total polymer particles from 50:50 or 85:15 PLGA with different percentages of F127 or P188. Formulations: **(A)** 50:50 PLGA with 0, 10, 20 and 30 % *w/w* F127, **(B)** 85:15 PLGA with 0 %, 10 %, 20 % and 30 % *w/w* F127, **(C)** 50:50 PLGA with 0, 20 and 40 % *w/w* P188, **(D)** 85:15 PLGA with 0, 20 and 40 % *w/w* P188**.** All formulations**:** (N1, n3). Results have been adjusted to account for the encapsulation efficiency. Error bars represent cumulative standard deviation.

The microparticles manufactured with F127 and P188 showed more porosity than those made without, also less uniformity in the spherical shape of the particles. The maximum release obtained from the 50:50 particle batches was approximately 80 % *w/w* for 20 % *w/w* F127 (Figure 7.5 (A)) and similar was

seen for 20 % *w/w* P188 (Figure 7.5 (C)), however neither of these resulted in sustained controlled release. The only 50:50 batch from these results producing continuous release was 40 % *w/w* P188 which continued to release past day 20 (Figure 7.5 (C)). In a similar manner to the 50:50 batches, the addition of F127 did not have a release modifying effect on the 85:15 batches (Figure 7.5 (B)). P188 had a more promising effect when used at 40 % *w/w* with 85:15 PLGA however at 20 days the maximum release was only 25 % *w/w.* From this data it is evident that F127 and P188 at 10, 20, 30 and 40 % *w/w* do not have the desired release modifying ability when used with 85:15 and 50:50 PLGA.

7.1.2 Release modifier characterisation: molecular weight

As discussed in section 4.3.1, the in-house made release modifiers were characterised using NMR and GPC to determine the polymer composition, molecular weight and polymer dispersity. The NMR spectra for each polymer are shown in Figure 7.6.

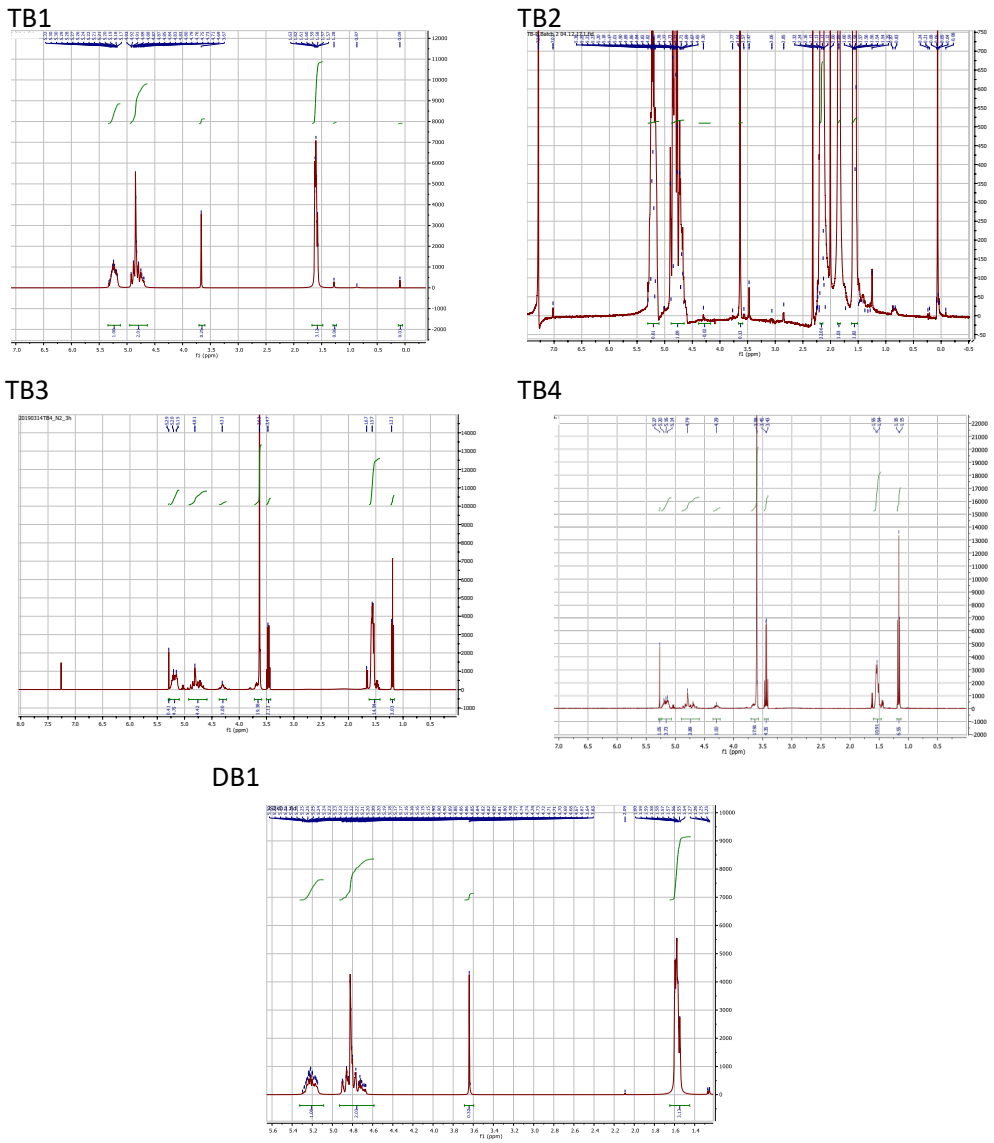

Figure 7.6: Nuclear magnetic resonance spectrum for in-house made release modifiers: TB1, TB2, TB3, TB4 and DB1.

The copolymer composition for TB1, TB2, TB3, TB4 and DB1 were determined as described by Hou *et al,* using proton NMR by integrating the signals relating to each monomer, for example peaks from CH_2 of ethylene glycol and glycolide, and CH and CH_3 from D,L-lactide (Hou *et al.*, 2008). The molecular weight and polymer dispersity was determined using GPC as discussed in section 4.3.1.

7.1.3 Comparison of the effect of triblock on release of lysozyme from 10 % w/v total polymer PLGA microparticles

As described in section 4.2.2, particles were manufactured using 10 % *w/v* total polymer with 50:50 PLGA and varying percentages of TB. The resulting microparticle batches were characterised for their morphology, size and release kinetics and data is shown in Figures 7.7 – 7.8. The cumulative percentage release for microparticles manufactured with 10 and 15 % *w/v* total polymer and 0 % *w/w* TB are also shown for a comparison to 20 % *w/v* total polymer.

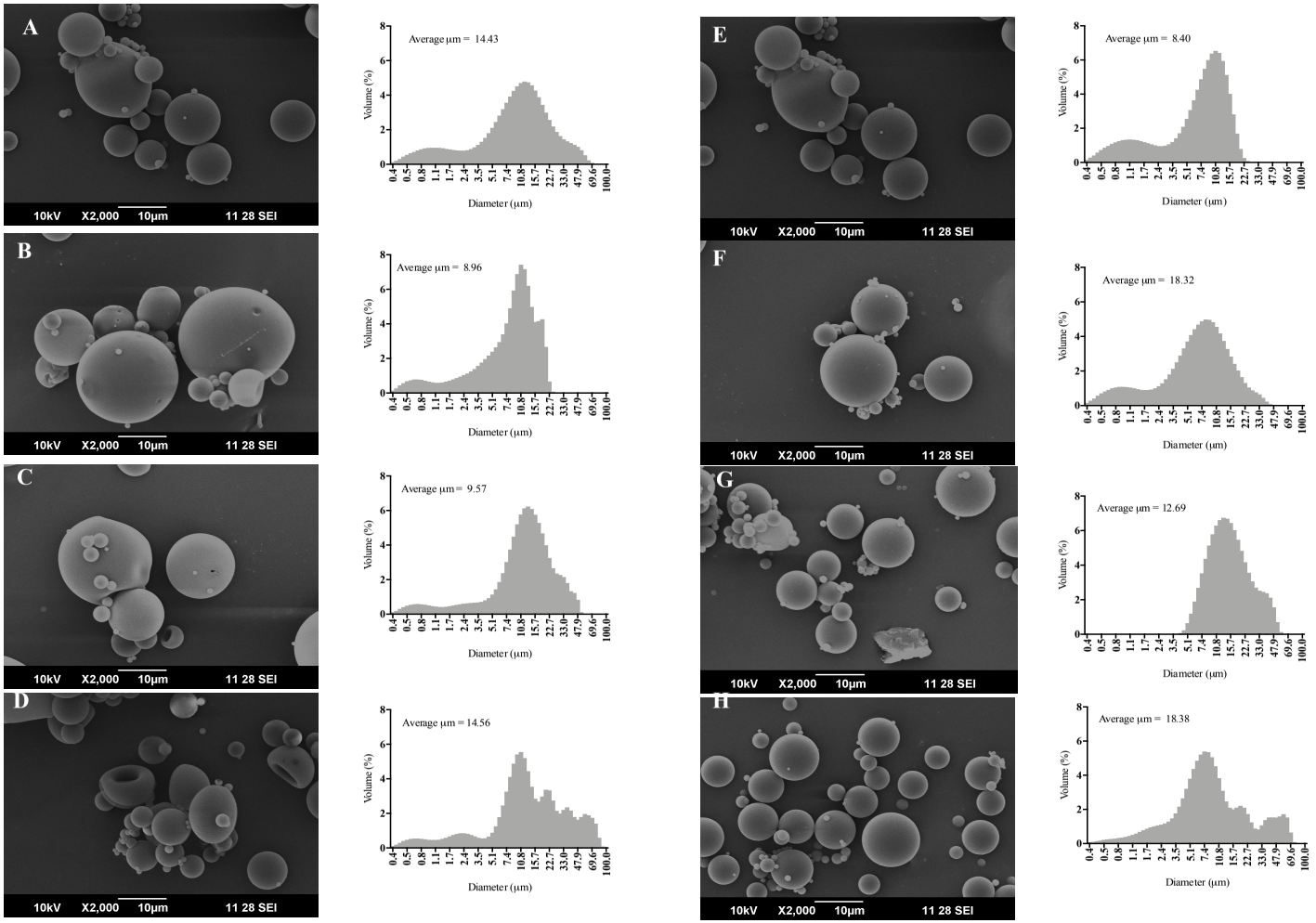

Figure 7.7: Morphology and size distribution of 50:50 PLGA microparticles with different total polymer and TB percentage containing water or HSA:lysozyme. Formulations: **(A)** 10% total polymer, 0% TB2, HSA:lysozyme loaded. **(B)** 10% total polymer, 10% TB2, HSA:lysozyme loaded. **(C)** 10% total polymer, 20% TB2, HSA:lysozyme loaded. **(D)** 10% total polymer, 30% TB2, HSA:lysozyme loaded. **(E)** 10% total polymer, 0% TB2, water loaded. **(F)** 20% total polymer, 10% TB2, water loaded. **(G)** 10% total polymer, 20% TB2, water loaded. **(H)** 10% total polymer, 30% TB2, water loaded.

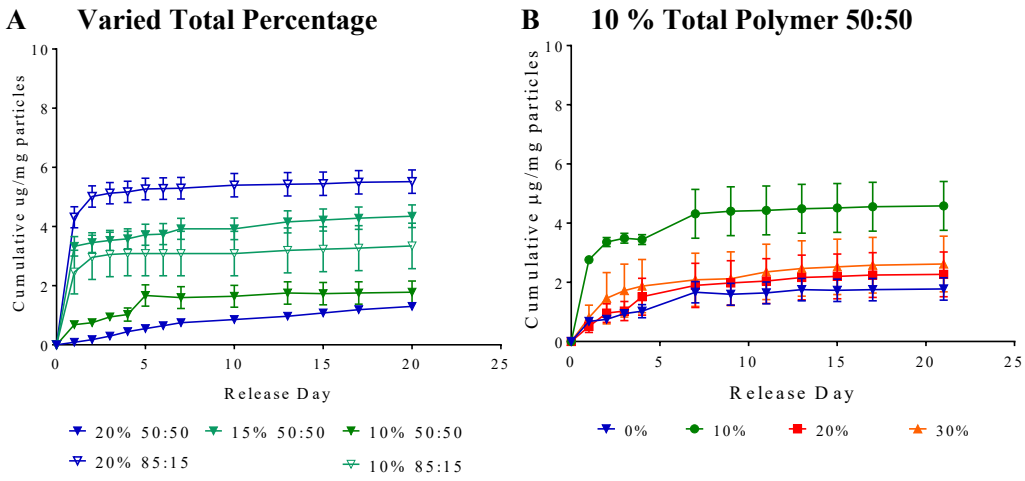

Figure 7.8: Cumulative protein release (µg/mg particles) from different total polymer percentage particles from 50:50 or 85:15 PLGA with different percentages of TB2. **(A)** 10, 15 and 20 % *w/v* total polymer 50:50 and 85:15 PLGA with 0 % *w/w* TB2, **(B)** 10 % *w/v* total polymer, 50:50 PLGA with 0 %, 10 %, 20 % and 30 % *w/w* TB2. (N2, n3). Results have been adjusted to account for the encapsulation efficiency. Error bars represent cumulative standard deviation.

The microparticles fabricated at different total polymer percentages appeared to have less uniform morphology with some particles collapsed or misshapen, unlike those seen for 20 % *w/v* total polymer which appeared spherical and uniform. This may have resulted from a lack of internal structural integrity resulting in particles collapsed or damaged. Despite this the particles remained smooth and non-porous as was seen for 20 % *w/v* total polymer and in literature (White *et al.*, 2013). The particles did appear to have a smaller size distribution with most averaging between 8-18 µm in diameter. This may also have had an

effect on the structural integrity of the particles. As discussed in Chapter 4, the smaller size may also have had an effect on the release kinetics. However, from the release data shown in Figure 7.8, it appears that the release was minimal post-day 1 even on addition of a release modifier (triblock). Therefore, microparticles manufactured using 10-15 % *w/v* total polymer did not obtain controlled and sustained release as required for this project.

7.1.4 Comparison of the effect of PLGA-PEG-PLGA triblock on the release of lysozyme from PLGA microparticles

As described in section 4.2.2, particles were manufactured using 20 % *w/v* total polymer with 50:50 or 85:15 PLGA and varying percentages of TB. The resulting microparticle batches were characterised for their morphology, size and release kinetics and data is shown in Figures 7.9 – 7.13.

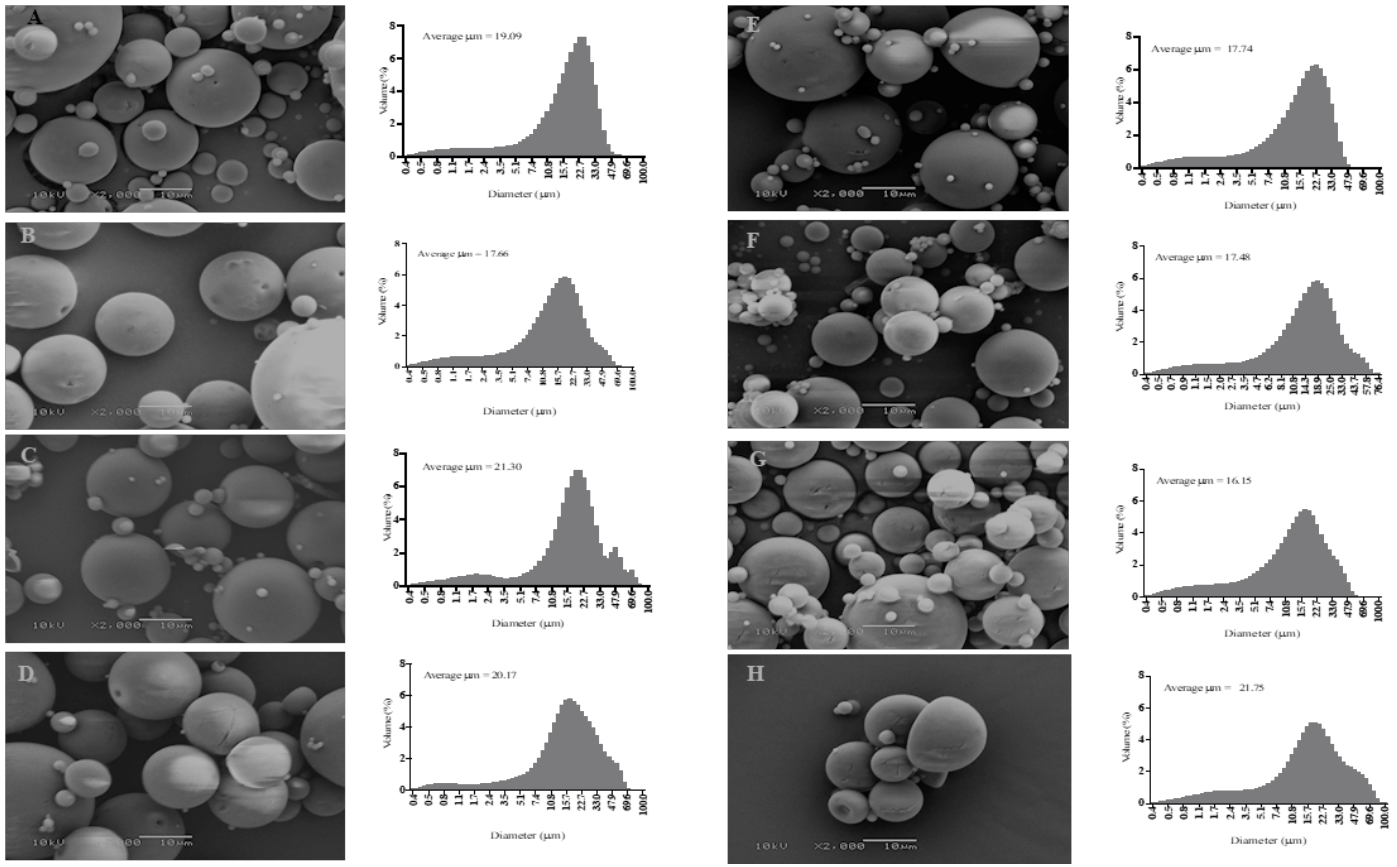

Figure 7.9: Morphology and size distribution of 20 % *w/v* total polymer particles from 50:50 PLGA with different percentages of TB1 containing water or HSA:lysosyme. Formulations: **(A)** 0% *w/w* TB1, HSA:lysozyme loaded. **(B)** 10 % *w/w* TB1, HSA:lysozyme loaded. **(C)** 20 % *w/w* TB1, HSA:lysozyme loaded. **(D)** 30 % *w/w* TB1, HSA:lysozyme loaded. **(E)** 0 % *w/w* TB1, water loaded. **(F)** 10 % *w/w* TB1, water loaded. **(G)** 20 % *w/w* TB1, water loaded. **(H)** 30 % *w/w* TB1, water loaded.

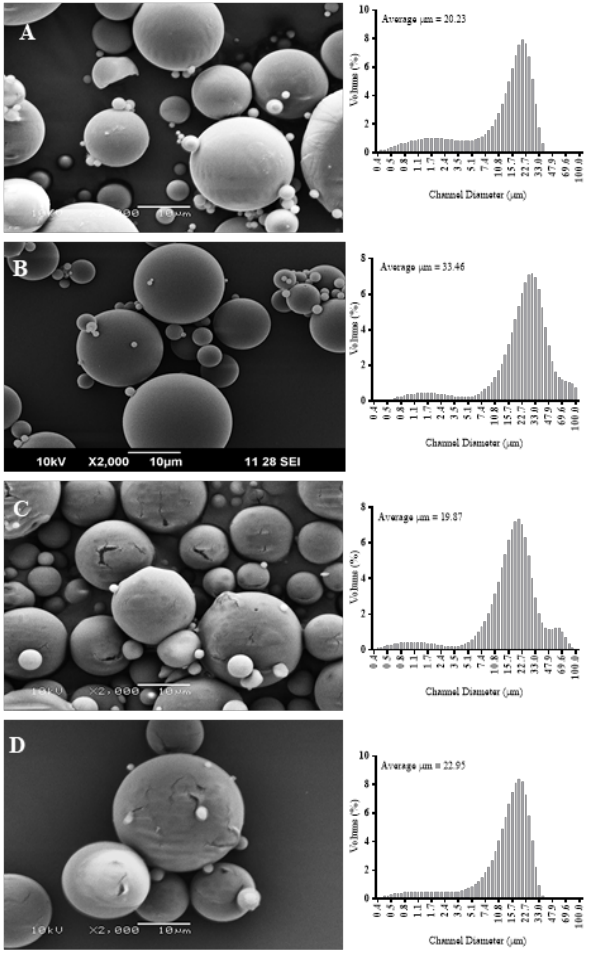

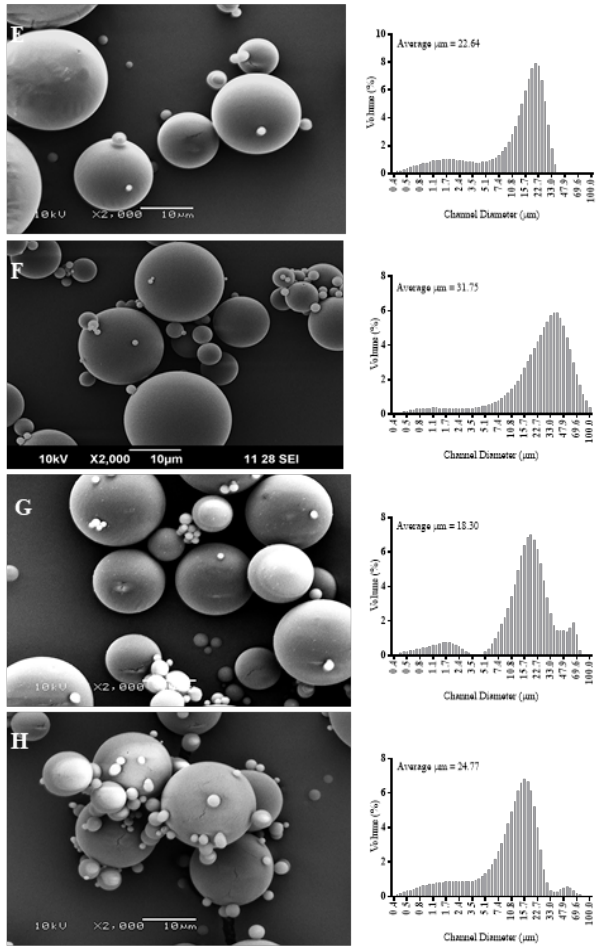

Figure 7.10: Morphology and size distribution of 20 % *w/v* total polymer particles from 85:15 PLGA with different percentages of TB1 containing water or HSA:lysosyme Formulations: **(A)** 0 % *w/w* TB1, HSA:lysozyme loaded. **(B)** 10 % *w/w* TB1, HSA:lysozyme loaded. **(C)** 20 % *w/w* TB1, HSA:lysozyme loaded. **(D)** 30 % *w/w* TB1, HSA:lysozyme loaded. **(E)** 0 % *w/w* TB1, water loaded. **(F)** 10 % *w/w* TB1, water loaded. **(G)** 20 % *w/w* TB1, water loaded. **(H)** 30 % *w/w* TB1, water loaded.

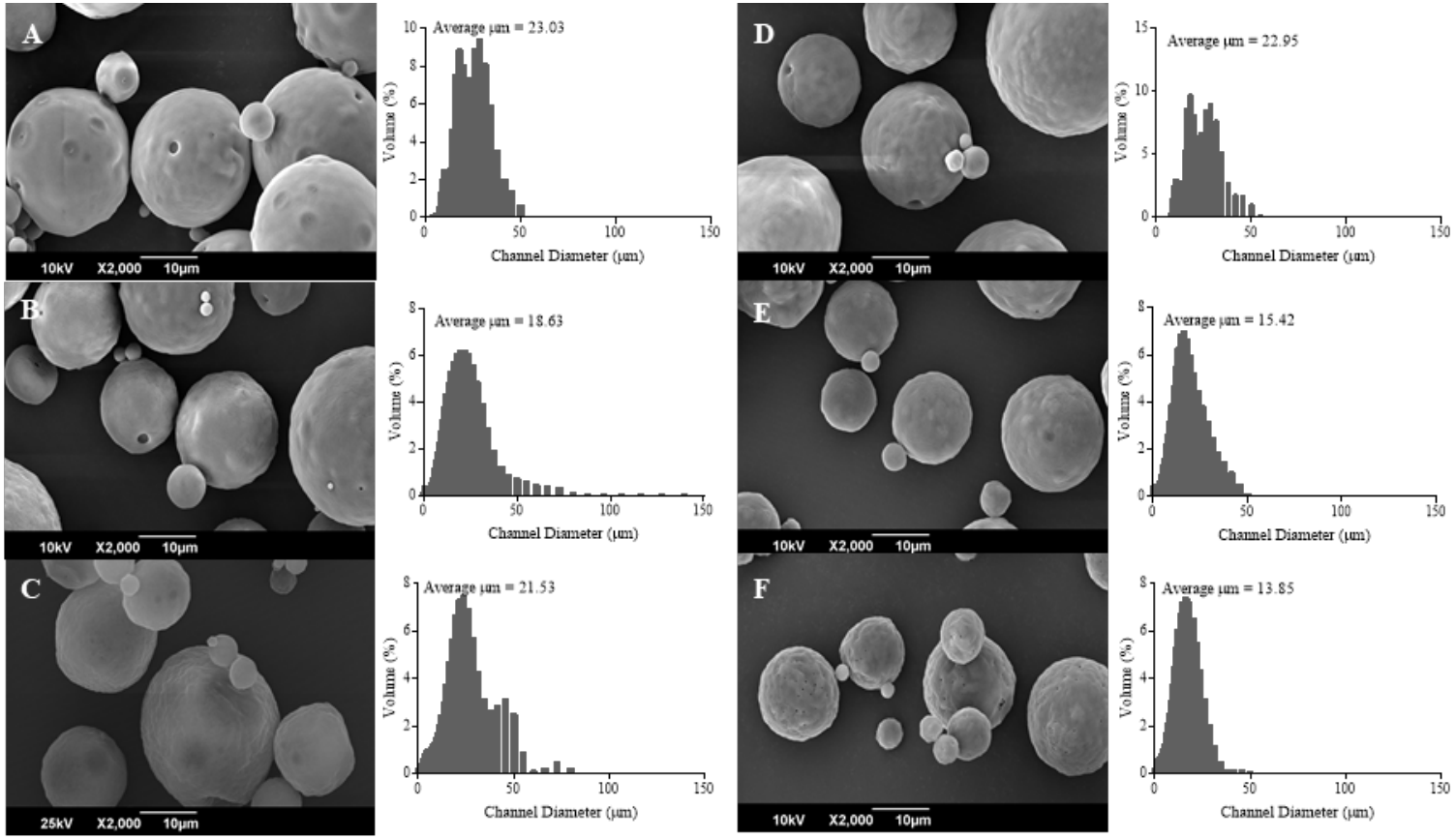

Figure 7.11: Morphology and size distribution of 20 % *w/v* total polymer particles from 50:50 PLGA with different percentages of TB4 containing water or HSA:lysosyme Formulations: **(A)** 0 % *w/w* TB4, HSA:lysozyme loaded. **(B)**, 20 % *w/w* TB4, HSA:lysozyme loaded. **(C)** 40 % *w/w* TB4, HSA:lysozyme loaded. **(D)** 0 % *w/w* TB4, water loaded. **(E)** 20 % *w/w* TB4, water loaded. **(F)** 40 % *w/w* TB4, water loaded.

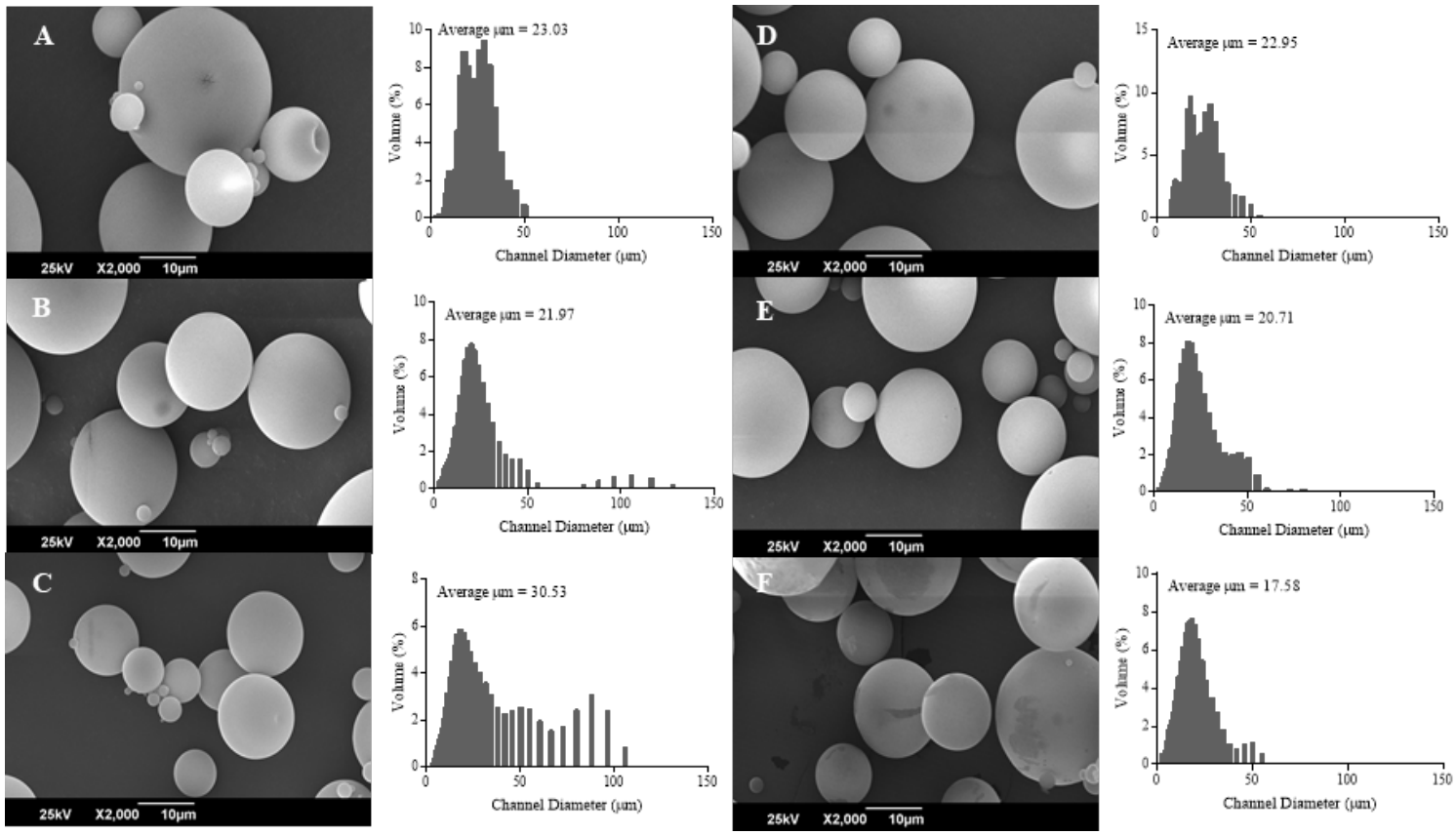

Figure 7.12: Morphology and size distribution of 20 % *w/v* total polymer particles from 85:15 PLGA with different percentages of TB4 containing water or HSA:lysosyme Formulation: **(A)** 0 % *w/w* TB4, HSA:lysozyme loaded. **(B)** 20 % *w/w* TB4, HSA:lysozyme loaded. **(C)** 40 % *w/w* TB4, HSA:lysozyme loaded. **(D)** 0 % *w/w* TB4, water loaded. **(E)** 20 % *w/w* TB4, water loaded. **(F)** 40 % *w/w* TB4, water loaded.

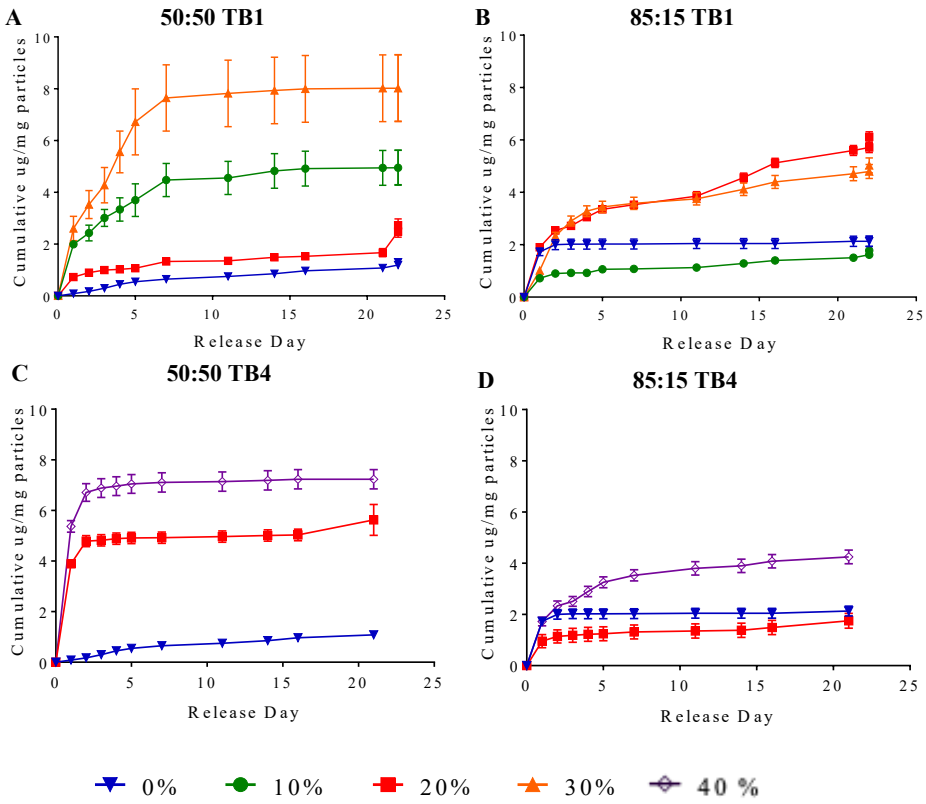

Figure 7.13: Cumulative protein release (µg/mg particles) from 20 % *w/v* total polymer particles from 50:50 or 85:15 PLGA with different percentages of TB. **(A)** 50:50 PLGA with 0, 10, 20 and 30 % *w/w* TB1. **(B)** 85:15 PLGA with 0, 10, 20 and 30 % *w/w* TB1. **(C)** 50:50 PLGA with 0, 20 and 40 % *w/w* TB4. **(D)** 85:15 with 0, 20, 40 % *w/w* TB4. (N2, n3). Results have been adjusted to account for the encapsulation efficiency. Error bars represent cumulative standard deviation.

Microparticles manufactured using 20 % *w/v* total polymer and varying percentages of triblock resulted in more a more uniform spherical shape than those seen for lower total polymer percentages. They also did not appear to be as porous as those made using P188 or F127. However, a few batches did appear

to have dimples or a slightly irregular surface, for example 20 % *w/v* total polymer 50:50 0 % *w/w* TB4 and 20 % *w/w* TB4. This is likely to be a result of the PVA solution used in manufacture step, as a new batch of PVA was made for each fabrication, it is possible that there was a slight difference in concentration of PVA and this may have resulted in the slightly dimpled looking surface. As this was not the desired surface morphology, new PVA was made for subsequent batches and the effect was not explored further.

In a comparison between size distribution of 20 % *w/v* total polymer 50:50 PLGA and 85:15 PLGA with varying percentages of TB1, the average size was around 16-25 μm in diameter. This was the expected sizing for the parameters used in the manufacturing method. There did not appear to be a difference between size distribution of those made with 50:50 PLGA or 85:15, and the addition of TB1 or HSA:Lysozyme also did not appear to affect the sizing. In general the particles manufactured using TB4 had a smaller and more defined size distribution, with the exception of 85:15 40 % *w/w* TB4 HSA:Lysozyme which had a broader size distribution. These factors are suspected to have arisen from the manufacturing method and not as a result of the polymers used, there was also suspected to be some interoperation variability.

The release curves shown in Figure 7.13 display the release of HSA:Lysozyme as a cumulative percentage of the total protein encapsulated. As discussed throughout Chapter 4, the aim was to obtain controlled and sustained release. As is evident from the graphs, the majority of release was below 40 % *w/w* of the

total encapsulated, however, the only formulations resulting in controlled release were 85:15 40 % *w/w* TB4 and 50:50 20 % or 0 % *w/w* TB1. Due to discrepancies with the TB1 batch, the 85:15 40 % *w/w* TB4 were chosen as the formulation to test with IL-4 encapsulation.

The cumulative percentage release of HSA:IL-4 for microparticles formulated from 85:15 40 % *w/w* TB4 is displayed in Figure 7.14.

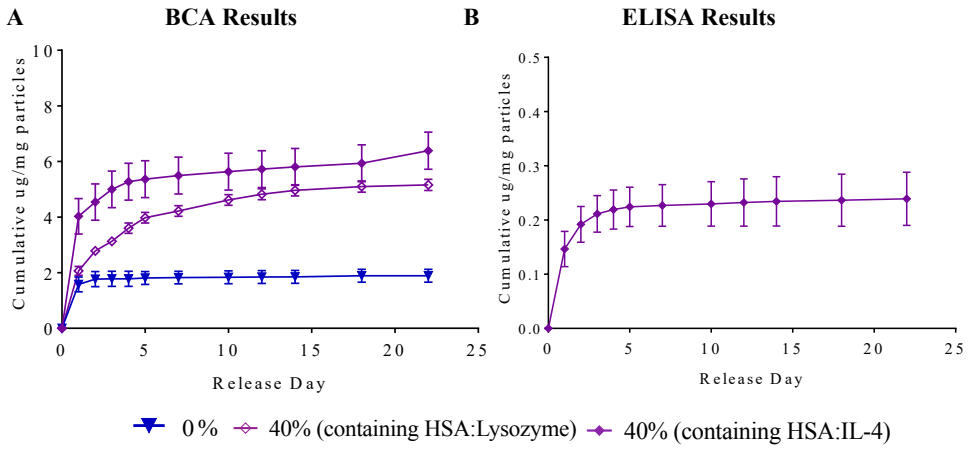

Figure 7.14: Cumulative protein release (µg/mg particles) from 20 % *w/v* total 85:15 PLGA polymer with different percentages of TB4 containing lysozyme or IL-4. **(A)** BCA determined: 40 % *w/w* TB4 containing HSA:lysozyme (◊), 0 % *w/w* TB4 containing HSA:lysozyme (∇) (N3, n3) and containing HSA:IL-4 (♦) (N3, n3). **(B)** ELISA determined: 40 % *w/w* TB4 containing human IL-4 (♦) (N1, n2). Error bars represent cumulative standard deviation.

This shows the continuous and sustained release of protein over the 22 days studied as shown in section 4.3.4. The maximum release after this time period was around 70 % *w/w* of the total protein encapsulated. From the release trend it is suggested that release would continue past this time point. However, as discussed in section 4.3.4, after analysis with an IL-4 ELISA the exact amount of IL-4 in the total protein released was far less than expected.

7.2 Cell culture optimisation methods

7.2.1 THP-1 optimal seeding density

THP-1 cells were cultured and seeded at various densities in tissue culture treated 6-well plates. The cells were then differentiated using PMA as described in section 2.2.1 for 24 hours, before a 48 hour rest in fresh media. An alamar blue assay was used to determine the cell viability. Briefly, alamar blue dye was diluted 1:2 with RMPI-1640 media (containing culture supplements) and 10 % *v/v* of well media volume was added to each well (2 ml media + 200 µl dye) and incubated at 37°C for 1 hour. Media was then removed to 96 well plate and fluorescence read (excitation = 540 nm emission = 580 nm) using a plate reader (Infinite M200, Tecan UK Ltd., Reading, UK). Fluorescence readings for each cell density post-differentiation with PMA and 48 hour rest are displayed in Figure 7.14. Note that an optimal seeding density was not required for the iBMDM cells due to culture optimisation undertaken by Dr Andrew Bennett's lab.

7.2.2 Population doubling: comparison of the effect of PLGA microparticles on cell growth

For differentiated THP-1 cell population growth curve the THP-1 cells were cultured and seeded at 1million in tissue culture treated 12-well plates. The cells were then differentiated to M0 cells using PMA as described in section 2.2.1 for 24 hours, before a 48 hour rest in fresh media. For immortalised bone-marrow derived macrophages (iBMDM) population growth curve the cells were cultured and seeded at 40,000 in tissue culture treated 12-well plates. Images were taken at days 2, 4, 6, 8, 10, 12 and 14 and media was topped up at days 6 and 10 for THP-1 cells and every other day for iBMDMs. ImageJ was used to obtain an average cell count per well.

For both THP-1 and iBMDM population growth with microparticles the cells were seeded and treated as described above. Blank PLGA microparticles (1 mg ± 0.2 mg) were suspended in media and added to transwells (ThinCertsTM, pore size 1.0 μm, Greiner Bio One) in the 12-well plate. At days 2, 4, 6, 8, 10, 12, and 14, the transwells were removed and images taken. Transwells were returned and cells further cultured. An imageJ cell count plugin was used to obtain an average cell count per well. The results for cell population doubling with and without microparticles are displayed in Figure 7.15.

7.3 Cell culture optimisation results

7.3.1 THP-1 optimal seeding density results

THP-1 cells were cultured and differentiated to M0 as described above and seeded at different densities in order to determine the density optimal for experiments with MPs. The results are shown in Figure 7.15.

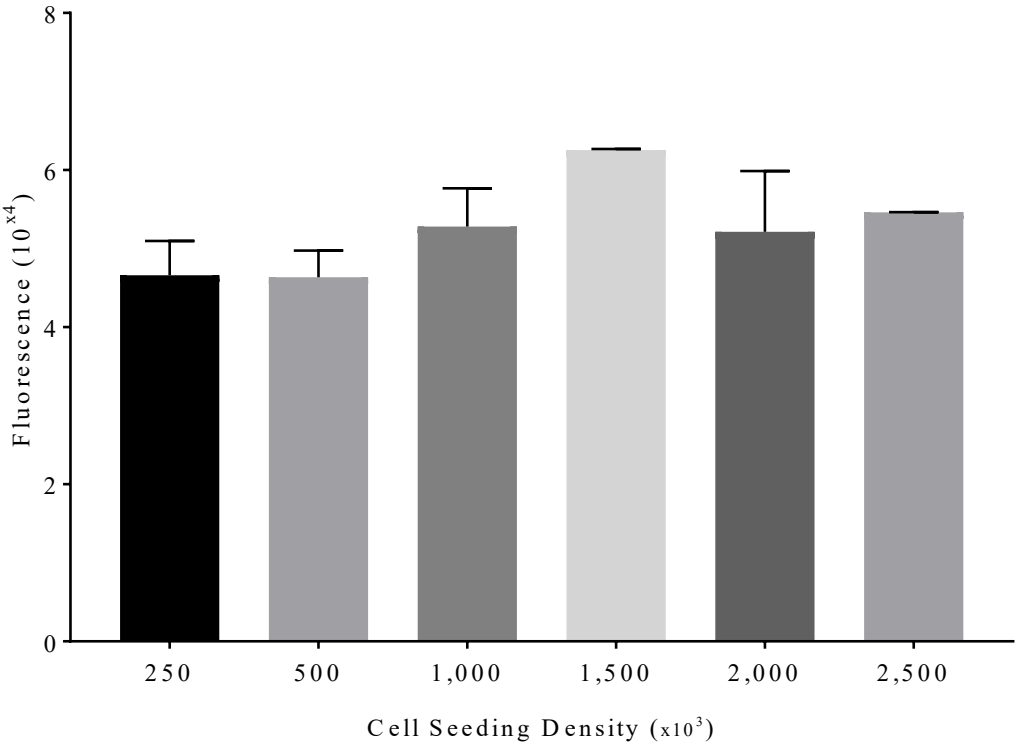

Figure 7.15: Optimal seeding density for differentiated THP-1 cells after 48hour rest post-PMA treatment. (N3, n3) Standard deviation displayed.

The seeding of THP-1s from 250,000 – 2,500,000 cells did result in cell growth, however a density of 1,000,000 was chosen as optimal based on high metabolic activity seen in this assay and literature. 1,500,000 was discarded as although it showed greater metabolic activity at 48 hours post-PMA treatment consideration was made for a 14-day long culture.

7.3.2 Population doubling results: comparison of the effect of PLGA microparticles on cell growth

Cells were cultured as described previously in the presence and absence of blank PLGA microparticles in order to determine if there was an effect of the particles on cell growth. iBMDM as were analysed in their native state and THP-1 cells were analysed once differentiated to M0 macrophages. The results are shown in Figure 7.16.

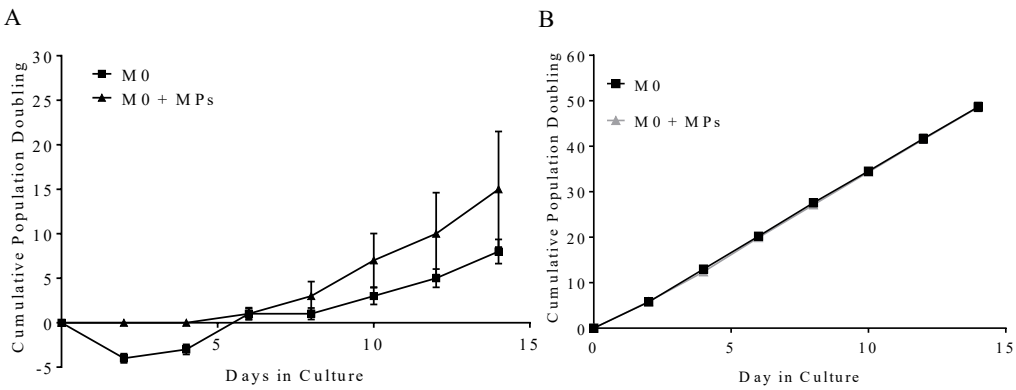

Figure 7.16: Population doubling for **(A)** differentiated THP-1 cells (M0) and **(B)** iBMDM cells with and without the presence of blank PLGA microparticles. (N3, n3) Standard deviation displayed.

The addition of microparticles to the culture of differentiated THP-1 cells did appear to increase the standard deviation between repeats, however it did not appear to affect their population doubling with the trend of growth remaining similar over 14 day's culture. When tested alongside immortalised bone-marrow derived macrophages, microparticles did not affect the population doubling over 14 days and in contrast to THP-1s they did not appear to increase the standard deviation. The large deviation for the THP-1 cells may be due to some cell loss during the treatment process.

THE END